# “Neuronal differentiation and epithelial integrity: The role of *Drosophila* Short Stop”

Dissertation
zur Erlangung des Grades
**Doktor der Naturwissenschaften**

Am Fachbereich Biologie
Der Johannes Gutenberg-Universität Mainz

Wolfgang Bottenberg
Geboren am 06.12.1973
in Wiesbaden, Deutschland

Mainz und Manchester, Juni 2006

# I Chapter Index

# II Figure Index

# III Table Index

# 1. Introduction

## 1.1. The importance and principle features of neuronal growth

The nervous system is the most complex organ in animals. It is composed of two major cell types, neurons and glia cells. Different kinds of neurons are responsible for the major accomplishments of neuronal systems. Sensory neurons perceive external stimuli, interneurons process and integrate these informations and motorneurons or neurosecretory cells mediate reactions or actions by stimulating muscles or glands respectively. Together these cells can build networks with astonishing complexity and capacity (Prokop, 1999).

To build such networks capable of information processing, neurons have to form synaptic connections to other neurons, muscles or gland cells via their lengthy axonal or dendritic processes. During development, the correct growth of neuronal processes towards their target cells occurs often over enormous distances, and is a pivotal prerequisite for neuronal network formation. It is tightly regulated, guided by cellular specialisations on the tips of neuronal processes, called growth cones. Growth cones are highly dynamic cellular compartments, guiding axons through a complex environment, by responding to repulsive and attractive cues in cell-specific manners (e.g. Brose et al., 1999; Kidd et al., 1999). Upon reaching their target cells, cell-cell contacts have to be established, so called synapses (Sherrington, 1906) which are an integral part of neuronal networks enabling information transmission from cell to cell.

Taken together, the formation of complex networks with precisely wired neurons and correctly placed synapses requires reproducibly regulated neuronal growth and differentiation. Any failure to accomplish this task will impair axonal connectivity and have dire consequences for body function and/or behaviour. It is therefore pivotal to get a better understanding of processes such as neuronal growth or synapse formation in health and disease. To this end, my work was dedicated to understanding the molecular function of a *Drosophila* Spectraplakin protein Short stop, which plays a central role in neuronal growth and differentiation.

## 1.2. The cytoskeleton as sub-cellular prerequisite for cellular growth

In order to grow, rearrange or move, cells have to be able to induce shape changes and, vice versa, they have to resist mechanical forces created by their own changes or rearrangements in their surrounding. To this end, all animals contain a set of structural

proteins linked to the plasma membrane which forms a ‘membrane-associated cytoskeleton’, providing protection from mechanical stress and spatially controlling the assembly of signalling molecule or structural molecule complexes (e.g. adhesion molecules, synaptic apparatus). The membrane-associated cytoskeleton links the cell surface with the internal cytoskeleton, which consists of Actin microfilaments, intermediate filaments (IFs) and microtubules (MTs). These filaments are crucial for cells, enabling them to undergo morphogenetic shape changes or retain their shape. Thus, they provide cells with the necessary stability to maintain cell shape and resist mechanical force by connecting the cell surface to other compartments of the cell. Principal cytoskeletal mechanisms are well preserved across species borders and cell-specific processes. Neuronal growth is e.g. very similar to the leading edge of a moving cell (Lambert de Rouvroit and Goffinet, 2001). In order for cells to grow or move in a regulated fashion, cytoskeletal changes have to be tightly controlled. For a long time actin and tubulin have been recognised as major players in both processes. They were seen as distinct players, acting independently but cooperative rather than being physically closely associated or even crosslinked. With the discovery and growing understanding of cytoskeletal crosslinker molecules it became clearer how important the direct crosslinking of different cytoskeletal filaments is for various aspects of animal development. A family of proteins specialised for this task are the Spectraplakins, which share properties with proteins of the Spectrin and Plakin family.

### 1.3. Spectraplakins: Cytoskeletal linker proteins

Cytoskeletal linker molecules of the Plakin family have been known for more than two decades (reviewed in Ruhrberg and Watt, 1997; Jefferson et al., 2004). The Plakins are a family of proteins involved in the organisation of the cytoskeleton. They act as cytolinkers and/or scaffolding proteins, connecting the intermediate filaments (IFs) to other cytoskeletal networks and/or distinct sites at the plasma membrane (Ruhrberg and Watt, 1997; Fuchs and Cleveland, 1998; Leung et al., 2001; Leung et al., 2002). They were first identified as components of desmosomes and hemidesmosomes, connecting the adhesion receptors to intermediate filaments. Prominent members of the Plakin family are desmoplakin, plectin, envoplakin, periplakin and epiplakin (reviewed in Ruhrberg and Watt, 1997; Leung et al., 2002; Jefferson et al., 2004). An interesting feature of Plakins is that its various isoforms perform functions uniquely tailored to suit the cytoskeletal needs of each specialised cell (Yang et al., 1996; Yang et al., 1999). It is becoming increasingly clear that plakins function

as focal points for the assembly of multiprotein complexes at the interface of the cell membrane and the cytoskeleton (Jefferson et al., 2004).

Spectrins are another family of large cytoskeletal crosslinker molecules. The most prominent members of this family are α-Actinin, Dystrophin, Utrophin and α and β-Spectrin (reviewed in Roper et al., 2002). Spectrin superfamily members bind and crosslink Actin filaments and attach these to membrane receptors (e.g. Hirai and Matsuda, 1999). General features of these proteins are that they contain an actin binding domain and several spectrin repeats (also called dystrophin repeats; Roper et al., 2002).

Only recently, the Spektraplakins were discovered (reviewed in Roper et al., 2002). Spectraplakins represent molecules with the ability to crosslink all cytoskeletal elements. Spectraplakins are large cytoskeletal molecules combining properties of both spectrins and plakin family members (Roper et al., 2002). They contain binding domains for all three cytoskeletal filaments, acting as crosslinkers between actin, intermediate filaments and microtubules (Svitkina et al., 1996; Andra et al., 1998; Leung et al., 1999; Yang et al., 1999; Karakesisoglou et al., 2000; Sun et al., 2001; Lee and Kolodziej, 2002). In mammals, two Spectraplakins, Bullous Pemphigoid AntiGene1 (Bpag1/Dystonin) and Microtubule-Actin Crosslinking Factor1 (MACF1) also called ACF7 (Actin Crosslinking Family 7) are known to date (Bernier et al., 1996; Leung et al., 1999 see Fig. 1). BPAG1 was identified as a protein targeted by the autoimmune disease bullous pemphigoid in humans (Minoshima et al., 1991). MACF1 was originally cloned on the basis of sequence homology to the Actin binding domain of Dystrophin (Byers et al., 1995). After the complete cDNA was characterized, MACF1 was found to be the orthologue of Short stop (Shot) the single Spectraplakin present in *Drosophila melanogaster* (Leung et al., 1999; Roper et al., 2002). Short Stop emerged from independent genetic screens (reviewed in Roper et al., 2002) aimed at identifying genes required for integrin-mediated adhesion (Brown and Kafatos, 1988; Prout et al., 1997; Gregory and Brown, 1998) or neuronal growth (Vactor et al., 1993; Prokop et al., 1998; Lee et al., 2000). Also the worm *Caenorhabditis elegans* contains one Spectraplakin, called Vab10. Its two isoforms are expressed in the epidermis and protect it against internal and external forces (Bosher et al., 2003). Spectraplakins have been implicated with and shown to be crucial for various cellular processes.

### 1.4. The Importance of Spectraplakins

As reviewed previously (Roper et al., 2002; Jefferson et al., 2004), Spectraplakins are crucial for epithelial integrity (Guo et al., 1995; Gregory and Brown, 1998; Roper and Brown, 2003), tendon cell stability in *Drosophila* (Prokop et al., 1998), and neuronal development and maintenance (Vactor et al., 1993; Bernier et al., 1995; Brown et al., 1995; Guo et al., 1995; Dowling et al., 1997; Prokop et al., 1998; Lee et al., 2000). On a subcellular level Spectraplakins have been shown to be required for proper cell polarisation (Reuter et al., 2003) and to contribute to the stability of microtubules and regulate their dynamics (Kodama et al., 2003). They also have been shown to regulate actin polymerisation and bundling (Karakesisoglou et al., 2000).

Animals with lacking or mutated Spektraplakins generally display severe phenotypes and often die early (Duchen, 1976; Bernier et al., 1995; Dowling et al., 1997; Prokop et al., 1998; Strumpf and Volk 1998; Lee et al., 2000; Kodama et al., 2003; Jefferson et al., 2004), although the phenotypes of BPAG1 are milder than the ones of MACF1 and Shot.
Bpag1–/– (Plectin) mutant mice display violent jerky movements and abnormal body posture. They develop dystonia musculorum, suffering from dystonia and progressive degeneration of sensory neurons (Bernier et al., 1995; Brown et al., 1995; Guo et al., 1995). They exhibit axonal swellings packed with disorganized IFs and accompanied by gross neuronal degeneration (Yang et al., 1996; Maatta et al., 2001). Beside the effect on IFs there is also gross disorganization of the microtubule network along the axons, which indicates defective axonal transport that could cause the neuronal degeneration (Yang et al., 1999; Liu et al., 2003). The loss of BPAG1 severs keratin IFs from hemidesmosomes and the epithelium can no longer withstand mechanical stress. This is resulting in intraepidermal rupturing and a skin blistering (Guo et al., 1995; Andra et al., 1998). In humans, this condition is known as epidermolysis bullosa simplex (for review see Fuchs and Cleveland, 1998). Similarly to mice, humans defective in the Plectin gene display signs of muscular dystrophy, reflective of Plectin's additional expression in muscles (Andra et al., 1998 and references therein). These findings underscore the importance of Plakins/Spectraplakins for maintaining IF cytoarchitecture.

MACF1 is the mammalian orthologue of Shot. MACF-/- mice die at an early embryonic stage for yet unknown reasons. Endodermal cells derived from these mutant embryos exhibit defects in microtubule (MT) dynamics (Karakesisoglou et al., 2000; Lin et

al., 2005). MTs no longer grow along polarized actin bundles and fail to respond to external cues in polarized cells (Kodama et al., 2003).

Flies carrying mutant alleles of *shot*, the sole Spectraplakin in flies, die at late embryonic stages (Prokop et al., 1998). All known alleles are lethal. Mutant embryos exhibit diverse phenotypes like wing blistering (Prout et al., 1997; Walsh and Brown, 1998), rupture of epidermal tendon cells (Prokop et al., 1998), general dysfunction of epidermal integrity (Gregory and Brown, 1998; Roper and Brown, 2003), disrupted fusion of tracheal branches (anastomosis; Lee and Kolodziej, 2002), disrupted microtubule organisation in the ovary (Roper and Brown, 2004), premature stall of axons (Lee et al., 2000), severe size reduction of dendrites and NMJs (Prokop et al., 1998), and mislocalisation of cell adhesion molecules in *shot* mutant axons (Prokop et al., 1998). Phenotypes analysed in this study are shown in Fig.2. Thus, Shot is crucial for growth related processes as well as for maintaining cellular and tissue stability.

Taken together Spectraplakins are crucial for a variety of cellular and developmental processes from epidermal integrity to neuronal growth and in all these contexts Spectraplakins appear to regulate cytoskeletal growth, polarisation and/or stability. In order to meet the requirement necessary for the different modes of Spectraplakin action, they are composed as modular complex multidomain molecules.

### 1.5. The architecture of Spectraplakins

Reflecting their multi-purpose use, Spectraplakins are large modular multidomain proteins that contain binding sites for all cytoskeletal filaments (see Fig.1). Different promoters and diverse isoforms have been identified for all Spectraplakins (for review see Roper et al., 2002; Jefferson et al., 2004). Alternative start sites define 4 different N-termini in Shot and Bpag1 and 3 in MACF1 (Lee et al., 2000; Roper et al., 2002). At the N-terminus most Spectraplakin isoforms carry an actin binding domain (ABD; see Fig.1). It consists of two so called Calponin homology domains (CH; reviewed in Stradal et al., 1998; Korenbaum and Rivero, 2002). The major determinant for Actin binding is typically in the first of these domains (CH1) rather than the second (CH2; Gimona and Mital, 1998; Gimona and Winder, 1998; Stradal et al., 1998; Yang et al., 1999). Isoforms with only the CH2 domain have been demonstrated to lack high affinity actin binding capabilities (Yang et al., 1996; Leung et al., 1999; Karakesisoglou et al., 2000; Lee and Kolodziej, 2002).

All Spectraplakin isoforms share one domain, the Plakin domain (Young et al., 2003; Fig. 1). The Plakin domain is a protein-protein interaction domain downstream of the ABD which is thought to be responsible for targeting these proteins to the correct cellular destination and imparting specificity to their function (Jefferson et al., 2004). Protein-analysis programmes predict that the Plakin domain comprises a series of spectrin repeats with an embedded putative SH3 domain in some Plakins (Bateman et al., 2002; Letunic et al., 2002; Jefferson et al., 2004). The Plakin domain of BPAG1e targets it to hemidesmosomes, binding to BP180 and ß4 integrin (Hopkinson and Jones, 2000; Koster et al., 2003). A yeast two hybrid screen carried out in our lab revealed several new potential binding partners of the Shot plakin domain (Mende, 2004).

A large portion in the central area of large Spectraplakin isoforms are made of multiple Spectrin/Dystrophin repeats (Fig.1). They were first described in erythrocyte Spectrin as a 106-residue repeating motif (Fontao et al., 2003). It is present in other proteins that are involved in the interaction of Actin with membranes, junctions and the contractile apparatus (Djinovic-Carugo et al., 2002). They occur in large numbers and are thought to give cell membranes elastic properties and to mediate dimerisation and scaffolding (Hartwig, 1994; Gimona et al., 2002; Leung et al., 2002; Roper et al., 2002; Jefferson et al., 2004). The Dynein/Dynactin complex has been shown to interact with a section (ERM) of the BPAG1 Spectrin repeats (Liu et al., 2003; Jefferson et al., 2004). The length of the rod domain can be essential for proper function as few deletions in Dystrophin cause a mild form of muscle dystrophy (Palmucci et al., 1994; Roper et al., 2002).

At the C-terminus, Spectraplakins comprise 3 domains the first of which is a calcium responsive element consisting of two EF-hand motifs (for reviews on EF hands see Kawasaki and Kretsinger, 1995; Lewit-Bentley and Rety, 2000; Bhattacharya et al., 2004; Burgoyne et al., 2004; see Fig.1 and Fig.5). Many cellular processes are regulated by Ca2+ signals, and the EF hand motif is the most common known calcium binding motif (Burgoyne et al., 2004). Astonishingly, relatively little is known about the function of the EF hand in Spectraplakins. First insights on how it might affect Spectraplakin function came from the observation that MACF1 changes its subcellular distribution in the cell upon calcium stimulation (Karakesisoglou et al., 2000). It was not tested whether this is a direct or indirect effect.

Immediately after the EF hand motif several Spectraplakin isoforms contain a bona fide microtubule binding domain, a so called Gas2/GAR domain (Fig.1 and Fig.5). Isolated GAR domains from BPAG1, MACF, GAS2, GAR22 and Shot colocalise with microtubules in transfected cells (Sun et al., 2001; Lee and Kolodziej, 2002; Goriounov et al., 2003). Plakin

isoforms that do not contain the Gas2/GAR domain generally do not interact with microtubules (Jefferson et al., 2004). MACF1 harbours another microtubule binding and stabilising domain downstream of the Gas2 domain, a Glycin Serin Arginin rich (GSR) domain which acts in concert with the Gas2 domain and can induce microtubule bundling (Sun et al., 2001).

At the very C-terminus, Spectraplakins carry an EB1 binding motif, which was described recently (Fig.5). It has been shown to recruit Spectraplakins to the plus ends of Microtubules (Slep et al., 2005). EB1 is a well characterised and highly conserved microtubule plus end tracking protein, which is crucial for processes such as mitotic spindle assembly (Rogers et al., 2002). Shot has been shown to colocalise with EB1 and APC at epidermal tendon cells in *Drosophila* (Subramanian et al., 2003).

### 1.6. Shot function in the nervous system

We are particularly interested in understanding the mechanisms of neuronal growth and differentiation required for the establishment of neuronal networks. In order to build a nervous system pluripotent ectodermal precursor cells (neuroblasts) have to give rise to neurons which, in turn, have to grow neurites and contact target cells with high fidelity. To understand the development of neuronal systems one needs to identify and characterise the involved factors and their modes of function. As described in detail before, Spectraplakins are such molecules and, beside other contexts (see Chapter 1.3.), are essential for a number of aspects of neuronal development and maintenance in vertebrates and invertebrates (Bernier et al., 1995; Yang et al., 1996; Dowling et al., 1997; Prokop et al., 1998; Yang et al., 1999; Maatta et al., 2001; Jefferson et al., 2004). Shot, the single Spectraplakin of *Drosophila melanogaster*, is crucial for neuronal development (Prokop et al., 1998) and it is the only Spectraplakin with a clearly demonstrated role in neuronal growth (Prokop et al., 1998; Lee et al., 2000; Lee and Kolodziej, 2002), whereas BPAG and MACF1 have been demonstrated so far to be involved in neuronal maintenance only (Bernier et al., 1995; Dowling et al., 1997; Yang et al., 1999; Liu et al., 2003).

In *shot* mutant flies, a number of defects of the nervous system have been reported. First, the outgrowth of motorneuronal, sensory and Kenyon cell axons is affected (Lee and Luo, 1999; Lee et al., 2000; Lee and Kolodziej, 2002), but not the growth of all neurons seem to depend on Shot function (Lohr et al., 2002). Second, dendrites of sensory neurons and motorneurons are severely reduced (Fig.2 and Prokop et al., 1998; Gao et al., 1999). Third,

several structural proteins (Futsch, Fasciclin2, Nod-LacZ) fail to compartmentalise properly in axons of *shot* mutant neurons (Prokop et al., 1998; Lee and Luo, 1999, Fig.2.). Fourth, neuromuscular terminals fail to sprout and differentially properly (Prokop et al., 1998, Fig.2). Shot has been demonstrated to act cell autonomously (Lee and Luo, 1999 and this thesis). Accordingly, it is usually present in those neurons requiring Shot activity (Lee and Kolodziej, 2002; Sanchez-Soriano et al., 2005; and unpublished results).

The *shot* mutant phenotypes provide a sound basis from which to explore the molecular details of Spectraplakin functions in neuronal development. It is not understood which type of functions Shot performs during the growth of axons, neuromuscular junctions and dendrites. The fact that Shot functions in other contexts have been partially elucidated, does unfortunately not allow a direct extrapolation into nervous system function. Thus, it has been demonstrated, that different domains of Shot are required in different cellular contexts. For example, the ABD and the Gas2 domain of Shot have to be present in the same Shot molecule to promote proper axonal outgrowth (Lee and Kolodziej, 2002), whilst in the process of tracheal anastomosis either the ABD domain or the Gas2 domain has to be present to fully support the process (Lee and Kolodziej, 2002). Astonishingly, in both cases the large rod-like stretch of spectrin repeats is mostly dispensable, a phenomenon which has been described for MACF7 as well (Karakesisoglou et al., 2000).

The expression of spectraplakins is tissue specific and different isoforms are tailored for specific cellular requirements (Yang et al., 1996; Yang et al., 1999; reviewed in Jefferson et al., 2004). Given the multitude of incorporated domains and known functions it is likely that a number of binding partners or different sets of binding partner exist for different isoforms spectraplakin isoforms. Homo- or hetero-dimerisation of some members of both spectrin and plakin protein families adds another level of complexity (Chan et al., 1998; Geerts et al., 1999 reviewed in Roper et al., 2002). Given the fact that the ectoderm gives rise not only to the skin but also to the entire nervous system, this common embryonic lineage suggests that some molecular isoforms might serve analogous functions in both tissues. Different isoforms are expressed in different tissues (Roper et al., 2002).

## 1.7. *Drosophila melanogaster* as model system to study neuronal growth and the function of Spectraplakins

Many insights into principles and mechanisms of Spectraplakin functions, especially in vertebrates, are derived from a) the analysis of mutant animals (Bernier et al., 1995;

Dowling et al., 1997; Lin et al., 2005) and b) from *in vitro* assays, mostly using cell culture, often using isolated domains to elucidate spectraplakin functions i.e. (Gimona and Mital, 1998; Sun et al., 2001; Liu et al., 2003). Genetic approaches in vertebrates are challenging and time consuming making the *in-situ* study of Spectraplakins difficult.

Studying the function of Spectraplakins in the context of neuronal growth by focussing on *Drosophila* Shot has a number of advantages. Thus, a number of strong phenotypes have been described already (see Chapter 1.5.) demonstrating the relevance of Shot in this natural context and providing read-outs for genetic studies. Furthermore, this work can capitalise on the broad palette of efficient experimental strategies and tools the model system *Drosophila* can offer. First of all, flies are easy and cheap to keep in large numbers and have a short generation time of 10 days (FlyMove). The genome of *D. melanogaster* has been entirely sequenced (Adams et al., 2000) and many genes are homologues or orthologues of vertebrate genes (Jefferson et al., 2004). Thousands of fly stocks carrying identified mutations, transgenes and/or chromosomal aberrations are available (DrosDel; FlyBase 1998). Extensive databases containing up to date information on all known genes of *Drosophila* and related species are available (FlyBase 1998; Matthews et al., 2005). The development of *Drosophila* in general is well documented (Bate and Martínez-Arias, 1993) (Campos-Ortega and Hartenstein, 1997). Efficient genetics can be applied, using high throughput screens (St Johnston, 2002), double and triple mutations and a variety of genetic tricks, allowing the analysis of complex genetic networks and the unravelling of functional interactions between genes (e.g. Entchev et al., 2000). Often, like in the case of Shot, multiple alleles exist deriving from various genetic screens, facilitating the understanding of gene functions. A further powerful experimental tool in *D. melanogaster* is the Gal4/UAS system for targeted gene expression (Brand and Perrimon, 1993; Duffy, 2002). It allows the expression of genes in defined cells or tissues, manipulating gene expression levels in whole animals or single identified cells, expressing genes ectopically or manipulating gene activity via RNA interference, activated or dominant negative constructs. A wide range of cellular markers and antibodies is readily available and can be used to complement genetic approaches, visualising a broad number of proteins to analyse the development of nervous systems (e.g. Landgraf et al., 2003). Furthermore, transgenic fly strains carrying gene constructs can be generated relatively easy, making the fly an ideal test tube for *in-situ* and *in-vivo* assays.

Furthermore, in the context of neuronal growth, *Drosophila* offers the advantage of individually identifiable neurons, typical of all arthropods (Hedwig and Burrows, 1996). This means, that the development of its nervous system can be addressed at the level of single

individual neurons (Thomas et al., 1984; Prokop, 1999; Landgraf et al., 2003). It is for this reason that the *Drosophila* nervous system has become a very well established and efficient model system for the analysis of neuronal development and growth. (Jan and Jan, 1994; Budnik, 1996; Klambt et al., 1996; Brunner and O'Kane, 1997; Hummel et al., 1997; Jefferis et al., 2002; Ishimoto and Tanimura, 2004; Michno et al., 2005).

Taking all these possibilities together, the analysis of *Drosophila* Shot enables us to manipulate and study Spectraplakins *in-situ* in the developing embryo, capitalising on all the advantages *Drosophila* can offer (see above). Given the homology of Shot and MACF1, we believe that insight obtained from Short Stop can, at least partially, be extrapolated to understand vertebrate Spectraplakins.

### 1.8. Aim of this study, experimental approach and brief summary

The large Spectraplakin Shot, a cytoskeletal multi domain protein with demonstrated Actin to microtubule crosslinking activity, is crucial for the development of dendritic structures and neuromuscular junctions in *Drosophila melanogaster* (Fig.2). It is enriched in dendrites and NMJs (Fig.4.) but its mode of activity during the development of these neuronal compartments is unknown. Shot acts differently in different cellular contexts using different domains or domain combinations to exert its function.

In this study, I focussed on one neuronal compartment of neurons, the dendritic side branches of motorneurons, which are easily accessible for experimental manipulation, strongly dependent on Shot function and accumulating high amounts of Shot localisation. Before addressing Shot function in motorneuronal dendrites I addressed their functional and structural nature. Thus, it was speculated previously that these dendritic side branches might represent presynaptic processes (Prokop et al., 1998), in contrast to dendrites of vertebrate neurons. This speculation was deduced from the observation that these dendrites show similar *shot* mutant defects as presynaptic neuromuscular terminals (Prokop et al., 1998). Alternatively, Shot might be multitalented in these neurons and affect different neuronal compartments alike. As explained in detail in Chapter 3.1., my work contributed essentially to the finding that dendrites of *Drosophila* motorneurons are in fact postsynaptic compartments (Sanchez-Soriano et al., 2005). This finding clearly demonstrates that Shot functions in different molecular contexts within the same neuron.

The main aim of my study was to develop a better understanding of how Shot functions during dendrite development. Given the generally accepted view that different combinations

A

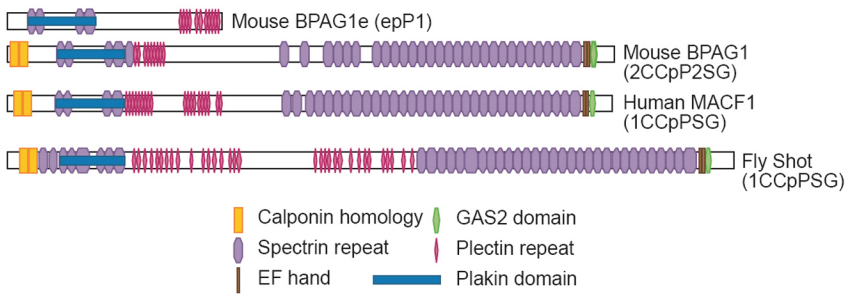
Mouse BPAG1e (epP1)
Mouse BPAG1 (2CCpP2SG)
Human MACF1 (1CCpPSG)
Fly Shot (1CCpPSG)
Calponin homology
Spectrin repeat
EF hand
GAS2 domain
Plectin repeat
Plakin domain

B

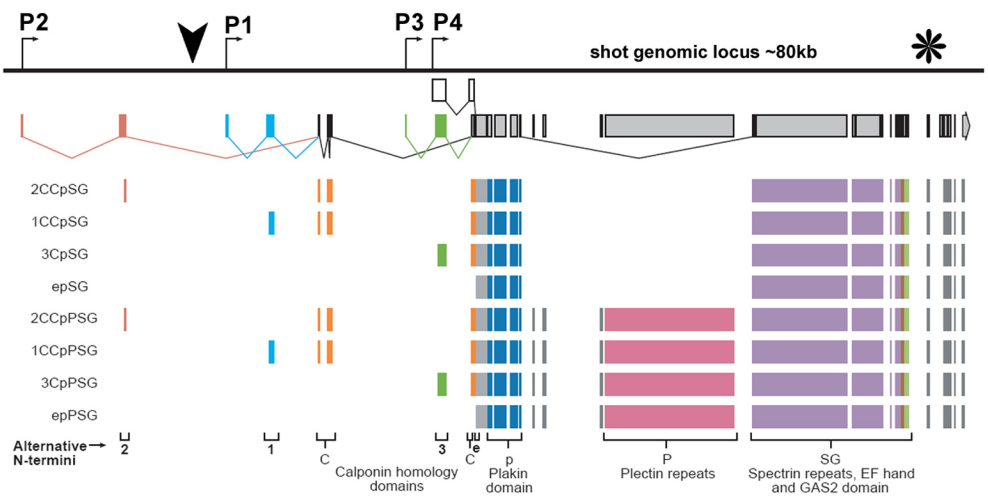
P2
P1
P3 P4
shot genomic locus ~80kb
2CCpSG
1CCpSG
3CpSG
epSG
2CCpPSG
1CCpPSG
3CpPSG
epPSG
Alternative N-termini
2
1
C
3
e
C
p
Plakin domain
Calponin homology domains
P
Plectin repeats
SG
Spectrin repeats, EF hand and GAS2 domain

C


Shot-L(A)
ABD
489
1324
Spectrin repeats
EF
4771-4835
GSR
5039 - 5062
Plakin
150
368
1454
4620
5201
EB1
5145 -5191
Gas2
4847- 4918
Shot-L(B)
32
Shot-L(C)
250
Shot-L(D)
1324

**Fig.1 The Spectraplakin Short Stop: Orthologues, Architecture and Isoforms**

**(A)** The Short Stop protein and its mammalian orthologues (BPAG1 and MACF1) are shown (from Roper et al., 2002). All constitute cytoskeletal crosslinker molecules with the ability to bind all cytoskeletal filaments. Highly conserved domains are depicted in colour. Running from the N to the C terminus spectraplakins harbour an actin binding domain consisting of two Calponin domains, a plakin domain (containing Spectrin repeats), a Spectrin like rod domain made of successive Spectrin repeats, a calcium responsive EF-hand motif, and a Gas2 microtubule binding motif. Different protein isoforms exist for Shot and each orthologue (see B and Roper et al., 2002). **(B)** *Short stop* (Ensembl gene annotation cg18076) has been mapped cytogenetically to position 50C6-11 of chromosome 2R. The organisation of the *shot* genomic locus is shown (~80kb) and four alternative transcriptional start sites are depicted (P1, P2, P3, P4). Coloured boxes represent exons and splicing is only shown for alternative starts or where exons are bypassed. The resulting different transcripts are shown below the gene. The colours of the exons indicate the domain they encode, consistent with A. The nomenclature used is according to (Roper et al., 2002): 1,2,3,4 stands for alternative N termini; C, Calponin homology domain; p, plakin domain; P, the plectin repeat domain; SG, the spectrin repeat domain, EF hands and Gas2. The combination given for each transcript describes their composition. It is not certain that all predicted forms shown are really transcribed. The arrowhead indicates site of P-element insertion in the *shot* mutant allele $shot^{kakp2}$, ***** indicates the position of chromosomal inversion in the *shot* alleles $shot^{V104}$ and $shot^{V168}$. **(C)** Simplified cartoons of some isoforms (Shot long A-D) encoded by the *shot* gene (will be used as reference henceforth). Four different N termini exist and are depicted (see also B). Shot-L(A) which equals Shot-PE (according to Ensembl protein annotation) and (B) contain complete actin binding domains (ABD) shown by red boxes (CH1+CH2). The N terminal sequence preceding the ABD differs in A and B. Isoform C contains only half an actin binding domain (CH2) and harbours an alternative N terminal stretch. Isoform D lacks the complete actin binding domain. The downstream architecture and sequence of the four isoforms is similar.

of Shot domains seem to be required in different cellular or developmental contexts (Chapter 1.5.) I aimed to identify those Shot domains which are required for the proper localisation and function of Shot in dendrites. In comparison to this approach, I studied another cell type, epidermal tendon cells, in which Shot has likewise been shown to be required (Prokop et al., 1998). Whereas Shot function in dendritic growth is likely to be involved in highly dynamic cytoskeletal events (similar to roles described for ACF7; Kodama et al., 2003), its role in tendon cells is likely to be of more static nature: in tendon cells it is required to mediate resistance to mechanical forces by anchoring microtubules at the basal (and perhaps also apical) surface (similar to roles of BPAG1 in hemidesmosomes; Hopkinson and Jones, 2000). Given these potentially very different roles in dendrites and tendon cells, I hoped to find clear differences in the combination of required Shot domains when comparing dendrites and tendon cells.

To this end I used a combination of several cell biological and molecular techniques: I used existing and newly generated *shot* (deletion) constructs and targeted their expression to dendrites of identified neurons, NMJs and tendon cells. First, I studied the subcellular localisation of these constructs. Secondly, I assessed the potential of these Shot isoforms to rescue *shot* mutant phenotypes. To get further support for such findings, I carried out complementary experiments with existing hypomorphic mutant alleles of *shot*, part of which were precisely mapped to find out which of the domains are affected by the respective mutations.

Using the above mentioned strategies, I could pinpoint Shot domains governing localisation in dendrites and tendon cells. Furthermore I could identify domains of Shot required or negligible for the proper formation of dendrites and NMJs. I could show that Shot activity during neuronal development involves more than mere actin microtubule crosslinking. I could furthermore show that the C-terminus of Shot is required for tendon cell integrity but not for neuronal growth. In contrast, I could show that the presence of a full ABD at the N-terminus of Shot is relevant for neuronal development and tendon cell integrity, revealing a context specific N vs. C-terminal requirement of Shot.

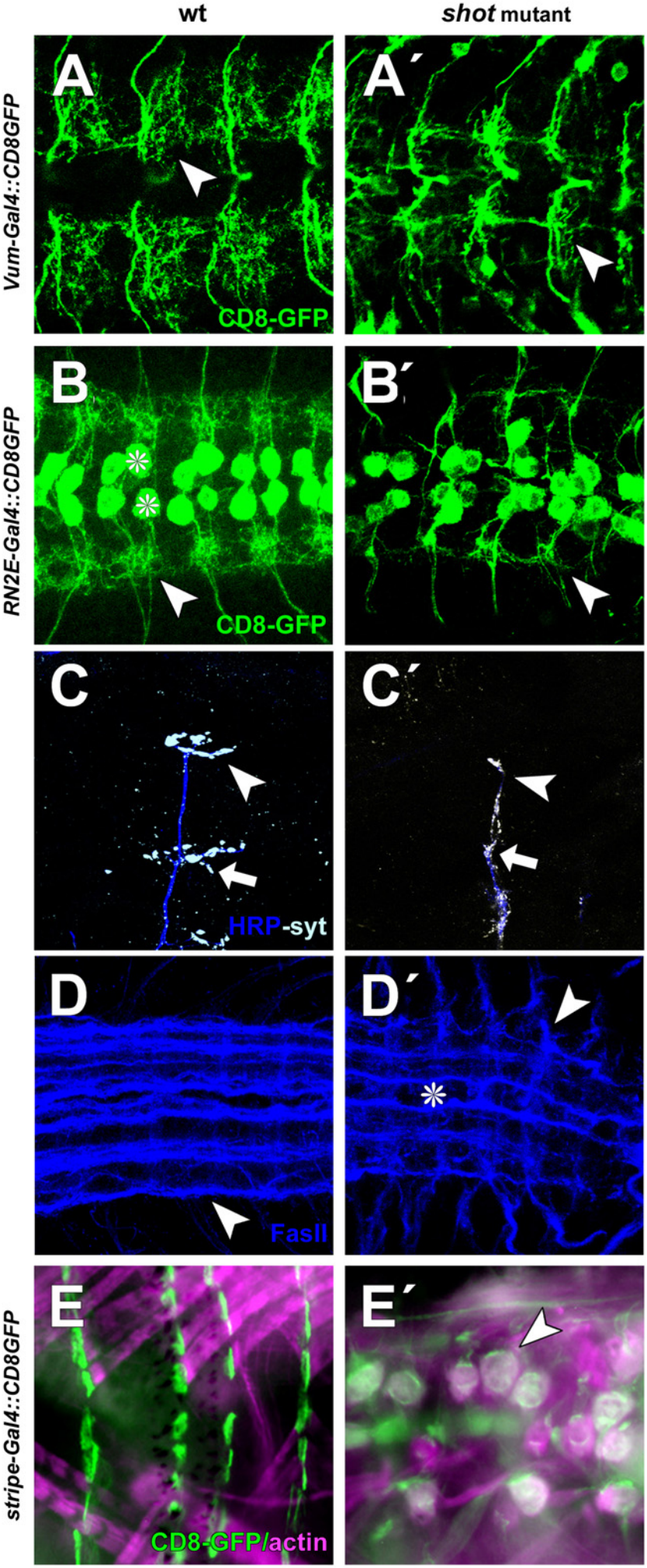
wt
shot mutant
Vum-Gal4::CD8GFP
RN2E-Gal4::CD8GFP
stripe-Gal4::CD8GFP
A
A´
B
B´
C
C´
D
D´
E
E´
CD8-GFP
CD8-GFP
HRP-syt
FasII
CD8-GFP/actin

## Fig.2. *Shot* mutant animals display phenotypes in the nervous system and the epidermis

In this study Shot function was analysed in 3 different neuronal and one epidermal compartment affected by the *shot* mutation: (1) Motorneuronal dendrites (A-B´), (2) neuromuscular junctions (NMJs) (C,C´), (3) the localisation pattern of the neuronal cell adhesion molecule FasciclinII (FasII) (D,D´) and (4) epidermal tendon cells (E,E´). To avoid that unknown mutations on the *shot* mutant chromosomes in homozygosis adulterate our findings, analyses were conducted in transhetrozygous mutant conditions: $shot^{sf20}/shot^{3}$ (both *shot* alleles are null alleles). (A-E´) The *wildtyp*e situation is shown in the left column, the respective *shot* mutant situation is shown on the right. (A-B´and D,D´) Views on the dorsal central nervous system (CNS) of *Drosophila* embryos are shown (confocal images.; see Fig.3). (A-B´) Dendrites of Vum (A,A´) and of aCC/RP2 (B,B´) motorneurons at late stage 17 are visualised via Gal4 driven expression of the cellular marker molecule CD8 coupled to GFP (arrowheads in A and B) Cell bodies are indicated (*). Cell bodies of Vum neurons are positioned in another focal plane. Used Gal4 driver lines are indicated on the left. (C-C´) DO NMJs at the dorsal musculature are shown (confocal images). A schematic representation of the position of DOs in the dorsal muscle field can be found in Fig.15M). NMJ morphology was visualised via FasII antibody staining (blue). In addition the presynaptic marker molecule Synaptotagmin was stained with an antibody (white; arrow in C,C´). (D,D´) FasciclinII localisation in the neuropile of stg.17 embryos was visualised via antibody staining (blue; arrowheads in D,D´). (E,E´) View on the ventral epidermis of stg.17 embryos is shown (normal fluorescence pictures). Muscles (actin) are shown in magenta (phalloidin FITC), tendon cells have been visualised by expressing *CD8GFP* with *stripe-Gal4* (green).

**(A-B´)** Central motorneuronal dendrites are severely affected by the *shot* mutation. Hardly any dendritic branching occurs in the mutant situation **(A´,B´)** as compared to the *wt* situation (A,B). **(C,C´)** Neuromuscular junctions (here DOs) are massively reduced in size and complexity (arrowheads in C *vs.* C´), see also (Prokop et al., 1998). In addition Synaptotagmin (white) mislocalises along the axon (arrow in C´) as compared to wildtype terminals where it is exclusively enriched at terminals (arrow in C). **(D,D`)** The localisation of the neuronal adhesion molecule FasII is altered in the CNS of *shot* mutant animals. FasII normally localises along longitudinal axonal fascicles in the neuropile of the *Drosophila* CNS (arrowhead in D), for details see (Landgraf et al., 2003). In *shot* mutant embryos FasII localises also in nerve roots and commissures (arrowhead and * in D´). **(E,E´)** Shot is essential for the integrity of epidermal tendon cells (see also Prokop et al., 1998). (E) The wildtype muscle pattern of the embryonic ventral musculature is shown in (E) as compared to the *shot* mutant pattern (E´). In the absence of Shot tendon cells are unstable and rupture when muscles start to exert tractive forces at late embryonic stages. Detached muscles round up (arrowhead in E´).

# 2 Materials and methods:

## 2.1. Fly genetics and cell biology:

All materials, items and chemicals used below are listed in the Appendix (Chapter 6).

### 2.1.1. Fly stock maintenance:

Fly stocks were kept at 18°C or 25°C on standard *Drosophila* food medium (Greenspan, 1997) changing the vials every 4 weeks (18°C) or 2 weeks (25°C) respectively.

### 2.1.2. Fly stocks:

Existing and generated *Drosophila* fly stocks used for experiments are listed in Table 1. The genotype, source and reference of these flies are given, and additional information is available on http://flybase.org (Flybase, 2004). Homozygous lethal mutations were kept over balancer chromosomes (Greenspan, 1997; FlyBase, 1998). Stocks were generated using standard *Drosophila* genetics (Fly-Pushing).

| **Genotype** | **Origin** | **Remarks** |
|---|---|---|
| | | |
| **Balancers second chromosome:** | | |
| +;Pin,lobe/CyO twist::GFP;+;+ | Oliver Vef | |
| w-;If/CyO;+;+ | Oliver Vef | |
| | | |
| **Balancer third chromosome:** | | |
| y,w-;+;TM3,Kr::GFP/Dichaete;+ | Oliver Vef | |
| | | |
| Double balancer stocks: | | |
| karussell/FM6,grh-lacZ;CyO,wg-lacZ/ScO | Oliver Vef | |
| If/CyO;TM6b/MKRS | Oliver Vef | |
| w/w;Pm/CyO,twist-lacZ;CXD/TM6b,AbdA-lacZ* | Oliver Vef | |
| | | |
| **Gal4 driver stocks:** | | |
| y,w-;+;eve-Gal4[RN2-E] | N. Sánchez-Soriano | |
| w-;RN2-D+O(eve);+;+ | N. Sánchez-Soriano | |
| UAS-CD8-GFP;RN2E (even-skipped (eve)) | Andreas Prokop | |
| w-;If/CyO;RN2-E | Andreas Prokop | |
| RN2D+O(eve)-Gal4; UAS-homer-myc | generated | |
| w-;shot[3]/CyO;RN2-E | generated | |
| w-;kak[SF20]/CyO;RN2-E | generated | |
| w-;If/CyO;RN2-E | Andreas Prokop | |
| +;shot[sf20],CD8[rec3]/CyO;RN2E;+ | generated | |
| w-;If/CyO;stripe-Gal4/TM6b;+/+ | generated | |
| UAS-CD8-GFP;Stripe-Gal4/TM6b | generated | |
| +;shot[sf20]/CyO;stripe-Gal4/TM6b;+/+ | generated | |
| +;UAS-CD8-GFP;stripe-Gal4/TM6b | generated | |
| Mz-Vum-Gal4;+;+ | Joachim Urban | |
| MzVum-Gal4;shot[SF20]/CyO;+ | generated | |
| Vum-Gal4;CyO/ScO;+;+ | generated | |
| MzVum-Gal4;shot[3]/CyO;+;+ | generated | |
| Vum-Gal4;kak[SF20],CD8(rec3)/CyO;+ | generated | |
| elav-Gal4: P{w[+mW.hs]=GawB}elav[C155] w[*] P{ry[+t7.2]=neoFRT}19A; Bc[1]Egfr[E1]/CyO | Bloomington nr. 5144 | |
| elav-Gal4;+/CyO;CD8 | N. Sánchez-Soriano | |
| elav-Gal4;CyO/ScO;+;+ | generated | |
| elav-Gal4;shot[3]/CyO;+ | generated | |
| +;OK6-Gal4;TM6b/MKRS | Andreas Prokop | |
| D42-Gal4;UAS-CD8-GFP | Andreas Prokop | |

| | | |
|---|---|---|
| **UAS lines:** | | |
| w-;UAS-mCD8-GFP;TM3/TM6b | Andreas Prokop | |
| +;+;UAS-CD8-GFP;+ | N. Sánchez-Soriano | |
| y,w-;pin/CyO;UAS-CD8-GFP | N. Sánchez-Soriano | |
| w-;UAS-actin-GFP;+ | Bloomington/7311 | |
| y[1] w[*];UASp-GFP-C-α-Tubulin-84B;+ | Bloomington/7374 | |
| w-,Rdl-HA;ScO/CyO;+ | generated | generated transgenics |
| w-;RDL-HA(C);MKRS/TM6b | generated | generated transgenics |
| FM6b/M;RDL-HA(C);+ | generated | generated transgenics |
| w-,RDL-HA(2A);ScO/CyO;+ | generated | generated transgenics |
| w-,RDL-HA(2A);RDL-HA(C);+ | generated | generated transgenics |
| | | |
| **Shot mutant allele lines:** | | |
| +;shot[3]/CyO (Kr::GFP);+ | Andreas Prokop | |
| +;kak[V168]/CyO(Kr-Gal4::UAS-GFP);+ | Gregory and Brown, 1998 | |
| +;Shot[3]/CyO (twist::GFP);+ | generated | |
| +;kak[Sf20]/CyO(Kr::GFP);+ | Prokop et al., 1998 | |
| shot[kak-P2]/CyO(Kr::GFP) | Michael Mende | |
| shot-[kak-P2]/CyO(wg-lacZ) | Michael Mende | |
| +;kak[V104]/CyO,Roi,Bl;+ | Prokop et. al.,1998 | |
| +;shot[V104]/CyO(twist::GFP);+;+ | generated | |
| +;kak[V168]/CyO(Kr-Gal4::UAS-GFP);+ | Gregory and Brown, 1998 | |
| +;Shot[V168]/ CyO(twist::GFP);+;+ | generated | |
| +;kak[Sf20],UAS-CD8-GFP(rec1)/CyO;+ | Robert Löhr | |
| +;kak[Sf20],UAS-CD8-GFP(rec4)/CyO;+ | Robert Löhr | |
| +;kak[Sf20],UAS-CD8-GFP(rec0)/CyO;+ | Robert Löhr | |
| +;kak[Sf20],UAS-CD8-GFP(rec3)/CyO;+ | Robert Löhr | |
| w-;shot[3]/CyO;MKRS/TM6b;+/+ | generated | |
| w-;shot[SF20]/Cy0;Mkrs/TM6b;+/+ | generated | |
| w-;kak[V104]/CyO,MKRS/TM6b;+/+ | generated | |
| w-;kak[V168]/CyO;MKRS/TM6b;+/+ | generated | |
| FM6b/karussel;shot[3]/CyO;+;+ | generated | |
| FM6b/karussel;shot[SF20]/CyO;+;+ | generated | |
| FM6b/karussel;kak[V104]/CyO;+;+ | generated | |
| +;kak[SF20](rec3)/CyO;Mkrs/TM6b;+ | generated | |
| +;kak[SF20],CD8(rec4)/CyO;Mkrs/TM6b;+ | generated | |
| FM6b/karussell;kak[SF20],CD8(rec3)/CyO;+ | generated | |
| elav-Gal4;kak[SF20](rec3),UAS-CD8-GFP/CyO | generated | |
| | | |
| **UAS-Shot deletion constructs:** | | |
| Shot full length (A): w-,shot(330-2A)-GFP;Pin/CyO[276];+ | Lee and Kolodziej, 2002 | |
| UAS-shot(full-length-A);shot[3]/CyO;+;+ | generated | |
| UAS-shot(full-length-A);shot[sf20]/CyO;+;+ | generated | |
| w-,shot-ΔGas2(414-A2)-GFP;+;+ | Lee and Kolodziej, 2002 | |
| w-,shot-ΔGas2(414A2)-GFP;shot[3]/CyO;+ | Lee and Kolodziej, 2002 | |
| Shot full length C: w-;shot(C 334)-GFP;+ | Lee and Kolodziej, 2002 | |
| w-;shot(C 334)-GFP,shot[3]/CyO[276];+ | Lee and Kolodziej, 2002 | |
| w-;shotΔEF(415 A2)-GFP;+ | Lee and Kolodziej, 2002 | |
| w-;shot-ΔEF-hand(415A2)-GFP, shot[3]/CyO[276];+ | Lee and Kolodziej, 2002 | |
| w-;shotΔrod(404 M2)-GFP;+ | Lee and Kolodziej, 2002 | |
| +;shot Δrod(404-M2)-GFP,shot[3]/CyO[276];+ | Lee and Kolodziej, 2002 | |
| Shot-L(C)-ΔGas2-GFP | (Lee and Kolodziej, 2002) | |
| shot-L(A)-N´6cmyc-C´GFP | generated | transgenics generated |
| shot-L(A)-N´6cmyc | generated | transgenics generated |
| shot-L(A)-Δ ABD-GFP | generated | transgenics generated |
| shot-L(A)Δ Plakin-GFP | generated | transgenics generated |
| shot-L(A)ΔEB1-GFP | generated | transgenics generated |
| UAS-[$Gas2_{shot}$]-6cmyc | generated | transgenics generated |
| UAS-[$EB1_{shot}$]-2HA | generated | transgenics generated |

**Table 1:** Fly Stocks used in this study. The genotype is given in the first row. The second row states the source of the fly strain or whether it was self established. In the third row it is mentioned when the transgenic flies or the transposition vectors were generated by me.

2.1.3. Virgin collection and genetic crosses:

For genetic crosses it is necessary to use virgin female flies. Upon hatching male and female flies were kept separate. To ensure the virginity of the flies they were collected and separated at least every 6 hours at 25°C or every 12 hours at 18°C. Virgins were identified by their pale appearance and a dark spot on the abdomen (meconium). Collected virgins were used to be crossed them with males of another genotype. To set a cross 10-20 virgins were crossed with 5-10 males of the appropriate genotypes. To analyse embryos or larvae deriving out of a cross male and female flies were left to mate for two days and fed with yeast. After two days they were transferred into cages containing apple juice agar plates to collect eggs. They were constantly fed with yeast. Alternatively the flies were left in normal food vials to grow larvae and finally yield adult fly offspring.

2.1.4. Embryo collection and dechorionisation:

Flies crosses of interest were transferred into cages containing apple juice agar plates (2% Agar agar) and fed with yeast. To synchronise the developmental stages of embryos, plates were exchanged every 1-3h. The plates with collected eggs were stored on 12°C to arrest development (Fly-Pushing) and later transferred to appropriate aging temperatures. Eggs were aged at 18°C, 25°C or 29°C until required stages were reached (aging according to Fly-Pushing). The expression levels of genes under the control of the UAS/Gal4 system (see 2.1.5.) are temperature dependant. Embryos were dechorionated for 90sec in 7.5% bleach, thoroughly washed with tap water and subsequently used for experiments like dissections (see 2.1.7.), molecular biology (2.4.).

2.1.5. Ectopic gene expression in embryos and larvae using the Gal4/UAS system:

The Gal4/UAS System (Brand and Perrimon, 1993; Brand and Dormand, 1995) was used for tissue targeted expression. Two different fly stocks are required. A: a fly (driver) stock carrying an activator (Gal4) under the regulation of an endogenous promoter and b: a fly (responder) stock (UAS stock) carrying a transgene of interest whose expression is regulated by the Gal4 Upstream Activation Sequence (UAS). In the offspring the cross, Gal4 protein expression drives the expression of the UAS transgene in the same pattern. Thus, ectopic expression of the transgene depends on the enhancer that regulates Gal4 expression. The temperature at which flies are kept is crucial, since the expression of Gal4 and thus the target UAS gene increases with rising temperature. To introduce UAS controlled genes or cDNAs into the *Drosophila* genome the *p{UAST}* vector was used (Brand and Perrimon, 1993). For more information on *p{UAST}* see Appendix 6.7.1. and for generation of transgenic flies see 2.2.

2.1.6. Selection of *shot* mutant embryos:

*Shot* embryos are embryonic lethal and die at late stage 17. For stages see http://flymove.uni-muenster.de/. The epidermis and nervous system of mutants is severely affected. They do not hatch. When “hatched” manually by carefully removing them from the vittelin membrane they display a movement phenotype not able to crawl but just “wriggle” their heads and tails. If the genetic condition or balancers did not allow a direct identification, *shot* mutant embryos were selected by using the typical *shot* phenotypes to identify them. At late stage 17 when the mouth-hooks are fully visible *shot* mutant embryos appear shiny and translucent opaque. When developing further they shrink inside the vittelin membrane without being able to escape from it. Tracheal branches which are filled in wt embryos are not filled and the

malphigi tubes appear prominent and white at the posterior pole of the embryos. Often a Fas2 staining was used to make sure that selected embryos are indeed *shot* mutants (Fas2 misloclises in *shot* mutant embryos; see Fig.2.).

2.1.7. Dissection of stage 17 *Drosophila* embryonic brains:

In order to analyse *Drosophila* embryonic brains at stage 17, they were dissected prior to fixation. Often mutant and control embryos could be processed on the same slide.
To dissect embryos, 22mm x 22mm cover slips were coated with a rubber, Sylgard (7:3 Sylgard:polymerising agent) and polymerised over night at 65°C in a hybridisation oven. Sufficient numbers of embryos were collected in a drop of B&B buffer on a Sylgard cover slip. Embryos were glued to the rubber coated cover slips such, that their head region was submersed into a small heap of histoacryl glue. The glue was applied using a pulled out fine glass capillary with an internal filament generated with a vertical pipette puller. The glass capillary was attached to fine tubing with a mouthpiece (blue 1ml pipette tip) and gentle pressure was applied blowing tiny amounts of glue through the needle. Once sufficient numbers of embryos were attached to the cover slip they were gently "pulled" apart, leaving the brain attached to the glued head. To this end tweezers were used to grip the posterior region of the embryos. After the embryos were torn apart and the majority of the body was removed, the brains remained attached to the histoacryl and could be subjected to standard fixation and immunhistochemistry protocols.

2.1.8. Flat preparation of stage 17 mutant *Drosophila* embryos :

The method was modified from (Prokop et al., 1996; Rohrbough et al., 1999; Broadie, 2000). With the formation of the cuticle at late stage 16, early stage 17 embryos do not stick to clean glass surfaces any more. Therefore Histoacryl glue was used to attach the specimen to the surface as described earlier (see 2.1.7). The embryos were attached to the Sylgard surface at their anterior and posterior pole, stretching them slightly. Using sharpened tungsten wires the embryos were cut open. The gut was then carefully removed, and the body walls were folded down and glued to the Sylgard surface. The application of glue was kept to a minimum amount, touching the edges of the body walls only. The dissected embryos were then fixed by exchanging the preparation buffer with fixative solution. Fixation and staining was carried out as described under (2.1.11.). After staining they were cut off the preparation slide with a razor blade splinter, transferred to a clean microscope slide and embedded with VectaShield as normal.

2.1.9. Flat preparation of L2-L3 *Drosophila* larvae:

Fly crosses of interest were kept on standard food vials for 3-5 days until a clear "roughening" of the foods surface as an indicator of the presence of larvae became apparent. Flies were transferred and the larvae were aged on 25°C or 29°C to accelerate development and increase Gal4 expression levels. When appropriate larvae sizes were reached (L2-L3) they were subjected to vivisection. To this end they were transferred into a round plastic dish with a resin of polymerised Sylgard. They were stretched and pinned anterior and posterior with fine tungsten wire needles, the dorsal side facing up not to damage the ventral CNS during the dissection. To avoid tissue rupturing, the needles were stung behind the mouth-hooks at the head and between the main connecting tracheal branch at the posterior end of the larvae. Stretched and pinned larvae were opened with a micro scissor. To this end a small horizontal incision was made at the posterior dorsal epidermis. From there the embryo was carefully cut open longitudinal, always keeping the scissors between the main tracheal branches. Once cut

embryos were opened and the body walls were stretched and fixed with tungsten wires such, that the interior muscles became exposed. The gut and the fat bodies were carefully removed without damaging the muscles or the CNS. The tracheal branches were left in place until after fixation. Such prepared specimen were fixed for 1h with 4% PFA and washed afterwards briefly with PBT. The tungsten wires were pulled and the flat fixed larvae were transferred into Eppendorf caps for further proceedings. They were washed 1h with PBT, renewing it 4 times and subsequently subjected to immunohistochemistry as described in Chapter 2.1.11. After the staining procedures larvae were embedded. To this end the tail and head region were cut off with a razor blade, leaving the CNS in place. If required the CNS was carefully removed and embedded separately. Flat preparations were then aligned on slides, embedded in VectaShield anti quenching medium, covered with a cover slip and sealed with nail varnish.

2.1.10. Whole mount embryo preparation for *in-situ* hybridisation or antibody staining:

Dechorionated embryos were prepared as described above (2.1.4.). They were fixed in a solution of (500µl Heptane + 350µl PBS+150µl formaldehyde: fresh each time) for abt. 25' with constant mild shaking. (PBS: 130mM NaCl, 7mM Na2HPO4, 3mM NaH2PO4). ~500µl of the PBS, formaldehyde mix was removed (lower of the two immiscible phases) and an equal volume of methanol, was added. The cap was rigorously vortexed for 30 s. About 750µl of the lower layer was removed and an equal volume of methanol was added again. The cap was vortexed again for 30s. Embryos were washed twice with Methanol for 15min each time and with constant mild rocking. They were stored at -20°C or directly used for *in-situ* hybrydisations or immunohistochemistry.

2.1.11. Antibody staining:

Fixed whole mount/dissected embryos or larvae were used for antibody stainings. The primary antibody of appropriate dilution (see Table 2) in PBT with 1% Azid was added to the fixed and washed specimens and incubated for 3h at RT or over night/weekend on 4°C. After removal of the primary antibody preparations were washed in PBT 4 times 15´each. To visualise the specifically bound primary antibody an appropriate fluorescence dye coupled, preabsorbed secondary antibody (1:100 in PBT; see Table 2) was added. Preparations were incubated for 3h at RT and subsequently washed 4 times 15´ with PBT. If several primary antibodies were used, they were applied either mixed or sequentially with 4x 15´ PBT washing steps in between. If multiple secondary antibodies were used they were mixed and added together. Specimens were kept in a dark humid chamber. Ready stained and washed specimens were mounted in Vectashield fluorescense mounting medium on standard microscope slides covered, sealed and documented (see Chapter 2.1.19.).

2.1.12. X-Gal staining of unfixed *Drosophila* embryos to select homozygous mutant animals:

Only unfixed tissue can be used to isolate DNA. We used single embryos to map the breakpoints of $shot^{V104}$ and $shot^{V168}$. To be able to isolate DNA from single mutant embryos, they were stained against X-Gal as described earlier (Rastelli et al., 1993; Strumpf and Volk, 1998). Flies carrying the $shot^{V104}$ or $shot^{V168}$ mutation stabilised over a balancer chromosome carrying a reporter gene expressing the lacZ gene under the control of the *wg* regulatory region were used (*shot/CyO wg::lacZ*). Embryos were collected, aged for ~20h (max. late stage 16 because of cuticle), dechorionated 1,5min with 3,5% bleach, rinsed with tap water, permeabilised in Heptane/PBS mixture for 30min and washed with PBS. Embryos were transferred into a BSA (bovine serum albumin) blocked Eppendorf cap. 1ml of X-Gal solution

(prepared from X-Gals stem solution) was added. Incubation was continued until clear staining became apparent. The staining reaction was stopped by washing the embryos repeatedly with PBS. Only white embryos were selected to extract DNA (see 2.1.13).

2.1.13. DNA extraction from unfixed *Drosophila* embryos for "single embryo PCR":

1 to 10 preselected embryos (see 2.1.6.) were squashed in 10µl Gloor and Engel´s buffer with a pipette tip and incubated at 37°C for 40min and at 95°C for 2 min to inactivate the proteinaseK. For each subsequent PCR reaction, 1-2 µl of this lysate was used.

2.1.14. Alkaline Phosphatase staining:

This staining was done when the secondary antibody was coupled to Alkaline Phosphatase, developing a blue/black colour reaction upon staining. After incubation of the secondary antibody the embryos were rinsed with AP detection buffer briefly for two to three times. Then in another Eppendorf cap containing 1ml of AP detection buffer 3µl of BCIP and 6.6µl NBT were added. This constituted the staining solution for the Alkaline Phosphatase reaction. This solution was added to the preparations and allowed to develop for 15-20 minutes depending on the intensity of staining. When the staining was weak, the reaction was prolonged up to 1hour. The reaction was then stopped by rinsing the stained preparations with PBT and then fixed in 10% formaldehyde solution in PBT for 15 minutes. After fixing, the preparations were rinsed in Methanol for 20 minutes followed by a PBT and then a PBS rinse. Stained embryos were then stored in 70% Glycerol in PBS. For double staining procedures, preparations were first subjected to DAB and then Alkaline Phosphatase staining.

2.1.15. *In- situ* hybridisation of whole mount embryos:

*2.1.15.1. General procedures and precautions:*
Due to the environmental abundance of RNAses, RNA *in-situ* hybridisations were done with special precautions. A specific set of pipettes was reserved for RNA use exclusively. Stuffed, RNAse free pipette tips were used. If possible procedures were done under in a sterile bench. All solutions were made RNAse free using DEPC and autoclaved.

*2.1.15.2. RNAse inactivation using DEPC (diethylpyrocarbonate):*
DEPC was added to solutions to inactivated RNA. Solutions with DEPC were incubated over night under the hood and constant stirring with a magnetic follower. On the next day the solutions were autoclaved to inactivate the DEPC. Solutions were only opened under the hood.

*2.1.15.3. In-situ hybridisation:*
Whole embryos in methanol prepared as described above (2.1.10) were used for *in-situ* hybridisation. They were washed with PBT 3 times for 2´. Subsequently they were washed twice in PBT/Hyb. soln. for 5'.

*2.1.15.4.Hybridisation:*
Embryos were prehybridised in 1ml Hyb.soln. complemented with 10µl sonicated salmon sperm DNA (10mg/ml) at 55°C for about 80´. The mixture was removed and the denatured (100°C) anti-*shot* probes (see Chapters 2.6. and 2.7.) were added. Incubation was done over night with low stringency at 45°C. To obtain satisfactory results with probes against *shot* RNA washing steps had to optimised and were finally done extensively for about 2-3h.

*2.1.15.5. Washing:*
All washing steps were done extensively and at stringent 65°C. After hybridisation embryos were washed in Hyb.soln. for 30´ and twice in Hyb.soln./PBT (1:1) for 30´each. Subsequently they were washed 5x in PBT for 20´ each and finally washed in PBT at room temperature for 10´.

*2.1.15.6. Staining:*
Embryos we incubated in PBT/anti-Dig-Ab coupled to Alkaline phosphatase 1:1000 plus Roche Western blotting reagent (10x) to prevent background for 80´. After incubation they were washed five times in PBT for 10´ each. Subsequently they were washed in AP buffer twice for 5´each.

2.1.16. Alkaline Phosphatase staining of whole mount embryos:

Embryos were stained in AP buffer complemented with 3,5ul BCIP plus 4,5µl NBT. Staining progress was monitored under a stereo microscope and stopped by washing 5x in PBT. Depending on the probes it took up to two hours until sufficient staining had developed. To prevent "darkening" of the specimen after the stop of the staining reaction they were fixed in 4% formaldehyde for 10´, washed 3x 10´ in PBT and stored in 70% glycerol at RT, 4°C or on -20°C.

2.1.17. Phalloidin staining of embryonic and larval *Drosophila* flat preps:

Embryonic and larval flat preps were prepped as described earlier (2.1.8. and 2.1.9.). To visualise actin, phalloidin coupled with Cy3 or FITC in a concentration of 1:500 or 1:1000 in PBT (0,3%) was used. If in combination with other antibodies, generally phalloidin staining was done last. The incubation time was between 30min to 90min where staining intensity, especially in tendon cells, became more pronounced with time. Due to the toxicity of phalloidin, work was carried out under a hood with caution. After incubation, the diluted phalloidin was collected and disposed. The flat preps were washed 4x15´with PBT and embedded as described earlier (2.1.8 and 2.1.9.).

2.1.18. Phalloidin injection into stage 17 embryos:

We established a method to visualise muscle patterns in stage 17 embryos where the thick cuticle surrounding the embryos prevents antibody staining. A mixture of phalloidin (coupled to Cy3 or Cy5 1:100- 1:500), formaldehyde (4%) and PBT (0,3%) was injected into the anterior pole of embryos. To this end embryos were dechorionated as described above (2.1.4.) and washed thoroughly with tap water. Embryos of the right stage/phenotype were selected and aligned on an apple juice/agar block. They were then transferred onto a glass microscope cover slip which was coated with Heptane glue. To this end a glue coated coverslip was cautiously pressed onto the aligned embryos on an apple juice agar plate such that the glue side faced the embryos. The embryos stuck to the cover slip. Subsequently the coverslip was attached to a microscope slide with a small drop of water on the opposite, not glue covered side. Embryos were covered in Voltaleff oil to prevent them from falling dry. To inject, pulled out glass capillaries without internal filament were used. Pulling parameters were refined such, that capillaries were stable and pointed. To sharpen the tip further and facilitate the piercing of the embryonic body walls, the tip was carefully broken by touching the side of a glass cover slip. Such prepared capillaries were attached to fine tubing and a 5ml syringe

attached to it. A drop of the injection mixture was applied to a depression slide and the capillaries were filled from this drop. The filled capillaries were clamped into the arm of a micromanipulator. The slide with the aligned embryos in Voltaleff oil (10S) was placed under a microscope and injections were performed using the 10x objective. To inject the filled capillary was placed in a fixed position in the visual field. The force required to pierce the embryos was generated by moving the microscope Table with the embryos towards the tip of the capillary. Once the capillary pierced the embryos they were carefully filled with the injection mixture until they blew up and completely stretched out to full length. The embryos were subsequently embedded in glycerol and imaged using a fluorescence microscope.

2.1.19. Documentation of stained specimens:

After staining and embedding (see above) the specimens were documented. An Olympus BX 50 WI fluorescence microscope with an Olympus U-RFL-T UV-light source was used for standard documentation and to check for staining success. Pictures were taken with a CCD Zeiss Axio Cam (black/white) camera attached to a Macintosh G3 computer. Alternatively specimens were documented using a Leica TCS inverted Confocal microscope attached to a PC. Digital pictures/stacks obtained were processed using Photoshop CS, Leica LCS Lite and Image J software respectively.

| **Antibody** | **Supplier** | **Animal** | **Working concentration** |
|---|---|---|---|
| **Primary antibodies** | | | |
| α-CD8 | Caltech Laboratories | rat | 1:10 |
| α-myc | AbCam | Rabbit | 1:500 |
| α-Haemagglutinin (HA) | Boehringer-Mannheim | Rat | 1:100 |
| α-Green fluorescent protein (GFP) | Invitrogen | Rabbit | 1:200 |
| α-FasciclinII II (FasII) | DSHB (Halpern et al., 1991) | mouse | 1:10 |
| α-Synapsin (Syn) | DSHB (Klagges et al., 1996) | mouse | 1:10 |
| α-Synaptotagmin (Syt) | (Littleton et al., 1993) | rabbit | 1:10000 |
| α- nc82 (Bruchpilot) | DSHB (Wagh et al., 2006) | mouse | 1:100 |
| α-Drab5 | gift of M.Gonzalez-Gaitan | rabbit | 1:50 |
| α-HRS | gift of M.Gonzalez-Gaitan | Guinea pig | 1:500 |
| α- horseradish peroxidase (HRP)-FITC/Cy3/Cy5 | Jackson Immuno Research | goat | 1:200 |
| α-Disc large (Dlg) | DSHB (Budnik et al., 1996) | mouse | 1:10 |
| α-Shot C-terminus (Gas2) | T.Volk (Strumpf and Volk, 1998) | Guinea pig | 1:100 |
| α-Tubulin (Tub) | Sigma Aldrich, Inc | Mouse | 1:500 |
| | | | |
| **Secondary antibodies (preabsorbed):** | | | |
| Cy5 anti rat | Jackson Immuno Research | donkey | 1:200 |
| Cy3 anti rat | Jackson Immuno Research | donkey | 1:200 |
| FITC anti rat | Jackson Immuno Research | donkey | 1:200 |
| Cy3 anti mouse | Jackson Immuno Research | donkey | 1:200 |
| Cy5 anti mouse | Jackson Immuno Research | donkey | 1:200 |
| FITC anti mouse | Jackson Immuno Research | donkey | 1:200 |
| Cy3 anti rabbit | Jackson Immuno Research | donkey | 1:200 |
| Cy5 anti rabbit | Jackson Immuno Research | donkey | 1:200 |
| FITC anti rabbit | Jackson Immuno Research | donkey | 1:200 |
| | | | |
| **Actin staining:** | | | |
| Phalloidin-Cy3 or FITC: | Sigma Aldrich, Inc. | Amanita phalloides | 1:500-1:1000 |

**Table 2**: Antibodies and staining reagents used in this study: The name of the antibody (row1), the supplier (row2), the animal in which the antibody was raised (row3) and the working concentrations (row4) are given.

## 2.2. Generation of transgenic flies:

Transgenic flies were generated through microinjection of plasmid DNA as described earlier (Santamaria, 1986). *p{UAST}-RDL-HA* (see Fig.6) and *p{UAST}-ALS-myc* (not shown) were injected manually. All other constructs were sent to a service company for injection: "BestGene Inc", 2918 Rustic Bridge, Chino Hills, CA 91709, U.S.A. http://www.thebestgene.com/.

### 2.2.1. Preparation of injection plasmids:

Constructs which were to be introduced into the fly genome were subcloned into the *p{UAST}* P-element vector (Brand and Perrimon, 1993). All constructs were verified by restriction digestion and sequencing. Sufficient amounts of high pure plasmids for injection were obtained using the Qiagen Midi or Maxi prep kits. The *p{UAST}* vectors carrying the constructs were co injected together with the "helper plasmid" Δ*(2-3)* coding for transposase (Rubin and Spradling, 1982). Transposase initiates the mobilisation of P-elements mediating germ line transformation.

#### *2.2.1.1. Injection mixture:*

| | |
|---|---|
| *pUAST*-construct: | ~1µg/µl |
| Δ(2-3) transposase helper plasmid: | 0,05µg/µl |
| KCl: | 5mM |
| NaHPO4: | 0,1mM in sterile A. dest (pH 6,8) |

→was centrifuged for 10min at full speed to precipitate possible floating crud and stored at -20°C.

### 2.2.2. Preparation of embryos:

In brief $w^-$ stg.1-3 embryos (syncytial blastoderm) were collected, dechorionated as described earlier and aligned on an apple juice agar block. They were transferred to a Heptane glue coated cover slip as described above (2.1.18.). Embryos were dried for 6-8min to separate the body wall from the vittelin membrane and then covered in a drop of Voltaleff oil (10S) to prevent drying-up.

### 2.2.3. Injection of plasmid DNA:

Pulled out glass capillaries with an internal filament were filled with injection mixture (see above 2.2.1.1.) and attached to a micromanipulator. The capillaries were connected to an air pressure source via a fine tubing system. Pressure could be applied by operating a foot pedal (maximum pressure of 1,2 bar was used). The tip of the capillary was broken by carefully pushing the tip against the side of a cover slip on a slide. DNA was injected into the posterior pole of embryos where the future pole cells (germline cells) develop. DNA injection was continued until a "light cloud" could be spotted in the yolk.

### 2.2.4. Raising of injected embryos:

Injected embryos were raised in humid chambers at 18°C (increasing survival rates). The hatching larvae were collected, counted and transferred to standard fly food where they were raised at 25°C. Each hatched fly was counted and crossed with three flies of the opposite gender. The offspring of these crosses was checked for transformants on a regular basis. Transgenic flies were identified by their red eye colour (from light yellow to dark red) caused by the white-mini-gene included in the P-element on *p{UAST}*. Only transgenic flies were

raised further and brought to homozygosis. Generally P-element construct are less likely to be introduced into the genome the bigger they are. Thus less independent insertion events occur when injecting very big constructs. This is also reflected in the numbers of independent fly stocks obtained (see Appendix 6.8, Table 7). Since the expression strength of P-element constructs crucially depends on the genomic position of the insertion, the strength of several different independent insertions was tested (see Appendix, Table 7). Insertion chromosomes were determined using standard genetic procedures (see below 2.2.5.). All informations regarding the generated transgenic fly strains are combined in the Table 7 (Appendix 6.8).

2.2.5. Determination of the insertion chromosomes of transgenic flies:

Flies with independent P-element insertions were obtained. To determine the insertion chromosomes of transformants, male flies with coloured eyes were crossed to double balancer flies *w-;If/CyO;MKRS/TM6b;+*. F1-virgins with coloured eyes carrying the balancer chromosomes *CyO;TM6b* were selected and crossed with white eyed males carrying *If;MKRS*. F2 flies were analysed upon occurrence of red eye colour in combination with balancers. For example an insertion on the second chromosome was identified when *w-;red/CyO;MKRS/TM6b* occurred whilst insertions on the third chromosome were identified by the occurrence of flies with coloured eyes carrying a balancer combination *w-;If/CyO;red/TM6b*. Insertions were brought to homozygosis. Independent insertions were tested upon expression (levels) of the inserted transgene (see Table 7).

## 2.3. Molecular Biology:

2.3.1. General applied methods:

*2.3.1.1. Sterilisation of solutions and utensils:*
Media, solutions and utensils were autoclaved at 2 bar, 120°C for 20 minutes. Thermolabile solutions were sterilised using Millipore 0,2µm filter cartridges.

*2.3.1.2. Photometric measurements:*
Concentration and purity of dsDNA in solution was assessed by measuring the absorption values at 260nm and 280nm using disposable plastic cuvettes and a photometer. DNA with 260/280 quotient of 1.8-2.0 was regarded as high pure. Alternatively the concentration of PCR products and plasmid DNA solutions was estimated comparing the gel band intensity of different DNA dilutions (1:1, 1:10 and sometimes 1:100) with the band intensity of known DNA ladder mixtures.

*2.3.1.3. Optic density (OD) of bacterial cultures:*
To determine bacterial growth the OD of the cultures was determined. Disposable 2ml cuvettes were used and OD was measured with a Spectrophotometer. Cultures with an OD of 0,5-0,8 were considered optimal as they are in the logarithmic growth phase.

2.3.2. Microbiological methods:

*2.3.2.1. Cultivation of cells:*
*Escherichia coli* were grown at 37°C in liquid culture or on LB-plates and stored at 4°C. Media and Agar contained appropriate concentrations of antibiotics if required. For long term

storage of *E.coli*, 200µl of bacterial culture was added to 800µl 100% sterile glycerol and shock frozen in liquid nitrogen or ethanol in dry ice. Glycerol stocks were stored at -80°C.

*2.3.2.2. Competent cells:*
For specific applications or when high competence was required commercial chemical competent cells were used. Subcloning efficiency cell ($1x10^6$; Invitrogen) were used for normal ligations and standard transformations. Library efficiency cells ($1x10^8$; Invitrogen) were used for ligations of large constructs. In specifically difficult cases like in the final stages of *shot* construct generation, sometimes Maximum efficiency cells ($1x10^9$; Invitrogen) were used. For all other standard subcloning and transformation steps competent cells generated in our lab were used (2.3.2.3.).

*2.3.2.3. Preparation of competent cells:*
*Escherichia coli* DH5a cells from a glycerol stock were plated on a LB plate without antibiotics and grown over night. 2ml LB-Broth (+0,02M $MgSO_4$ + 0,01M KCl) were inoculated with a single fresh colony from the Plate and incubated over night at 37ºC with vigorous shaking. 100ml LB–Broth (+0,02M $MgSO_4$ + 0,01M KCl) in a 100ml Erlenmeyer (conical flask) were inoculated with the overnight culture (dilution: 1:100) and grown at 37ºC with shaking until an OD of approx. 0.3 – 0.55 at 600 nm was reached. The Erlenmeyer flask was transferred to ice and kept there for 10 min gently shaking it now and again. Cells were centrifuged for 10 min at ~6000 rpm in pre-cooled centrifuge at 4ºC. The medium was decanted and the pellet was carefully resuspended in 50 ml TFB-I buffer without generating bubbles. Cells were centrifuged again as above. The pellet was resuspended in 4ml TFB-II 100µl portions were aliquoted into precooled caps (precooled on a mixture of dry ice and acetone under a fume Hood). Cells were stored at -70ºC.

*2.3.2.4. Transformation of chemical competent cells:*
50-100µl of frozen competent cells were thawn on ice. Plasmid DNA or DNA from ligation steps was added and carefully mixed without pipetting. Cells were kept on ice for 30´ , "flicked" every 15min and subsequently heatshocked for 90´´ in a heat block at 42°C. For particularly large constructs heat shock times were sometimes elongated up to 3min. After the heat shock cells were immediately transferred to ice and kept there to recover for 2´. 500-1000µl of 37°C LB or SOC medium without antibiotics was added to the cells and they were incubated at 37°C for 1h with shaking, allowing them to recover and develop antibiotics resistance. After 1h 50µl - 200µl of the cells in LB were plated on a LB plate containing an appropriate antibiotic (see Appendix 6.4.) and incubated over night at 37°C.

2.3.3 Molecular methods:

*2.3.3.1. Generation of Primers:*
Primers were designed manually, using software, Vector NTI Suite 7.1 for Macintosh (Invitrogen) or open source freeware PerlPrimer v.1.1.10 (http://perlprimer.sourceforge.net/). They were analysed upon primer dimer occurrence, secondary structures and melting temperature (Tm) using the same applications. At least one G or C nucleotide was at the 3´end of the primer to ensure a tight binding of the oligo at this crucial point. Stability of primer dimers or secondary structures (ΔG values) were kept at > -3.0 kcal/mol where possible. To prevent the occurrence of primer dimers, annealing at the 3´ends was avoided. Sequencing primers were mostly 16-20bp long with relatively low Tm (~50°C). If primers were designed to introduce restriction sites or other non annealing sequences the Tm of the annealing parts of the primer was generally >/= 60°C (if necessary on both sides of the

sequence introduced).4-6 random bases were always added at the 5´end of an inserted restriction site to facilitate the cutting with restriction endonucleases. Primer sequences were verified using alignment programs and uniqueness was checked using Vector NTI or lalign (http://www.ch.embnet.org/software/LALIGN_form.html). If tags were included in the primers the translation was tested using the sequence utilities of BCM Search Launcher (http://www.searchlauncher.bcm.tmc.edu ). Primers were ordered from BioSpring, Frankfurt, Germany (http://www.biospring.de) or MWG-Biotech, Germany (http://www.mwg-biotech.com). Primers were diluted to 100ng/µl (100µM) and stored at -20°C. Working aliquots with 20ng/µl were used for PCR. The individual primers are listed in the Appendix 6.9.).

*2.3.3.2. Polymerase chain reaction (PCR):*
For PCR reactions the following parameters were used and optimised for the specific need and template/primer combination. Exemplary parameters are given below:

1: 94°C 1min – 10min Initial denaturing
2: 94°C 15´´-1´ denaturing
3: 50-65°C 15´´-45´´ annealing
4: 72°C 15´´- 4´ elongation
5: steps 2-4 were repeated 25-40 times
6: 72°C 8´ final elongation
7: 4°C hold

The annealing temperatures varied depending on the melting temperature (Tm) of the primers. Annealing temperatures were determined using software (see Appendix 6.6.) and the informations supplied by the oligonucleotide manufacturers. In many cases optimal annealing conditions had to be adjusted using gradient PCR, keeping all parameters constant, just altering the annealing temperatures. In general the lower Tm of both primers -3-5°C was a suitable point from where to start optimisation. Analytical PCRs and gradient PCRs to determine the optimal annealing temperatures were always performed using taq polymerase. If maximum proofreading was required, Pfu DNA polymerase was used. If proofreading and high fidelity was required because for example the amplification with Pfu failed (e.g. difficult templates or low DNA concentrations) the Expand High Fidelity PCR System® (Roche) was used. It contains a mixture of taq and proofreading polymerases achieving high yield and high fidelity as compared to Pfu or taq alone. The kit was used following the manufacturers recommendations.

*2.3.3.3. Hot start PCR:*
If necessary and for difficult template DNA (e.g. “dirty” genomic DNA preparations) hot start PCRs were performed to decrease unspecific amplification. To this end the PCR samples were directly put into a preheated (94°C) PCR block and subsequently PCR was done as normal.

*2.3.3.4. Single colony PCR:*
To test ligation success and presence of specific inserts in a DNA construct, single colony PCR was performed. Colonies from a ligation on a LB-plate were picked using a sterile pipette tip or tooth pick. They were first streaked out on a subdivided and numbered LB plate and then dissolved in 30µl or 50µl of PCR master mix (for 30µl see below):
0,1-0,2µl taq polymerase
3µl 10x PCR buffer
1µl $Mg^{2+}$(50mM); 1,5µl dNTPs (2mM)
1µl primer A/B (20pmol/µl)

Primers were chosen such that the presence and orientation of inserts could be determined. Samples were subsequently subjected to PCR using the following protocol:

1: 10min 92°C to crack the bacterial cell walls
2: 2min 92°C to denature DNA
3: 45sec 50-55°C to anneal the primers
4: 45sec- 2min 72°C to elongate
5: steps [2-4] were cycled 40 times
6: 8min 72°C fill up
7: 4°C until used

5µl of the yielded PCR products were analysed on standard 0,7-2,0% agarose gels depending on the size of the predicted amplicon. Positive colonies were identified and could be picked from the plates on which they were streaked out prior to the PCR. Generally 2-4 positive colonies were cultured and plasmid DNA was obtained by standard mini/midi prep procedure.

*2.3.3.5. Agarose gel electrophoresis:*
To separate and visualise DNA samples, standard gel electrophoresis was used (see Sambrook et al., 1989). The size of the DNA samples to separate determined the gel density. Routinely gels containing between 0.3- 2% Agarose were used. Gels contained 0.5µg/ml Ethidiumbromide and were run at 20-100V. DNA samples were mixed with loading dyes, visualised using a UV light benchtop lamp and documented with a gel documentation system. Digital files were stored. DNA concentrations were estimated by comparing the intensity of the sample bands with known concentrations of DNA ladder bands (dilutions of 1:1, 1:10 and if necessary 1:100 were prepared).

*2.3.3.6. Gel purification of DNA fragments:*
DNA in agarose gel slices was cleaned using Qiagen gel elution kits. Fragments up to 9kb were cleaned using the Qiaquick gel elution kit following the manufacturer's protocol. For larger fragments the QiaexII kit from Qiagen was used also following the manufacturers recommendations. Elution efficiency and the concentration of the DNA was tested on a Gel or using a Spectrophotometer.

*2.3.3.7. Isolation of plasmid DNA:*
To obtain highpure plasmid DNA from bacterial cultures QIAprepSpin Miniprep kits were used. The procedures were followed as outlined in the manufacturer's protocol. For large plasmids up to 6ml of bacterial culture were used and the recommended buffer volumes were doubled as suggested by the manufacturer. Fresh colonies were used always. To achieve higher DNA yields when isolating large plasmids (>15kp) the EB buffer for elution was generally heated to ~60°C. To obtain larger amounts of DNA, HiSpeed Plasmid Midi/Maxi kits or Qiafilter Plasmid Midi/Maxi kits from Qiagen were used. DNA concentrations and quality were determined using analytical agarose gels or a spectrophotometer (2.3.1.2.).

*2.3.3.8. DNA isolation from flies:*
To obtain high pure genomic fly DNA the following protocol was used which is adapted from the Qiagen extraction protocol supplied in the Genomic-tip 100/G kit. In brief, 200 flies of the required genotype were collected in an Eppendorf cap and frozen at -80°C as quick as possible. A clean porcelain mortar and the head of a porcelain pestle were precooled by submersing them into liquid nitrogen for about 1 minute. (-80°C gloves, forceps and tongs were used to handle the cold objects !!) They were taken from the liquid nitrogen just prior to use. Liquid $N_2$ was used to transport the flies to the workbench. The cold mortar was filled with a little bit of liquid $N_2$. The flies were taken out of $N_2$ and carefully and swiftly transferred into the mortar with liquid $N_2$. The pestle was taken out of nitrogen and the flies were ground to fine powder. The finer the powder the better the results. The liquid nitrogen was refilled occasionally so that the mortar could not warm up. The mortar may not get wet as

a result of warming. The powder will then stick to the walls and it is impossible to remove it. The fine powder was transferred thoroughly into the prepared dissolving buffer (see the Qiagen extraction protocol for animal tissues). Following procedures were done exactly as described in the Kit's protocol.

*2.3.3.9. Restriction digestion and dephosphorylation of DNA:*
Restriction digestions were carried out as described in (Sambrook et al., 1989). Enzymes were used according to the guidelines given by the manufacturers (Roche or NEB). If double digestion were carried out the buffer recommendations of the manufacturers were followed. Depending on the amounts of DNA, 50µl or 100µl digestion volumes were used. Required plasmid DNA was dephosphorylated (remove the 5´phosphate) subsequently by adding 1µl of Calf Intestine Alkaline phosphatase and incubated at 37°C for 30´ up to 1h. Restriction digestions were cleaned using the Qiaquick PCR Purification Kit or Ethanol precipitation (2.3.4.8.). Millipore DNA cleanup columns were used for large plasmids to prevent high DNA losses. If only specific bands or restriction products were required, they were separated on a gel an excised from it with a clean scalpel. Subsequently the DNA was isolated from the gel as described above (2.3.3.6.).

*2.3.3.10. Ethanol precipitation of DNA:*
In some processes, following enzymatic reactions DNA fragments or plasmids were cleaned using ethanol precipitation. To this end 1/10 Vol of 3M NaAch (pH5.2) and 2,5vol % of ice cold Ethanol or 0,75Vol % room temperature isopropanol were added to the aqueous DNA solution. The solution was mixed thoroughly by inverting it several times and incubated on ice for 10-30´. Depending on the size of the DNA fragments it was subsequently centrifuged between 10´- 30´ at maximum speed in a standard Tabletop centrifuge. For large DNA fragments the centrifugation times were reduced to 5´ - 15´ to facilitate subsequent re-dissolving. The supernatant was carefully discarded and the pellet was washed with 500µl ice cold 70% Ethanol. The sample was centrifuged again for 5´- 10´minutes and as much as possible of the supernatant was carefully removed. The pellet was carefully dried for 10-30´´ at RT or in a Speedvac centrifuge. When large fragments/plasmids were processed, the pellet was not dried too long to facilitate subsequent dissolving. Traces of ethanol were tolerated. The DNA was resuspended in appropriate amounts of dd$H_2O$, TE or EB buffer depending on the downstream applications.

*2.3.3.11. DNA ligation:*
Vector and inserts were prepared according to standard protocols described above. Typically 100ng of linearised and dephosphorylated vector was ligated to a 3-6 molar excess of insert DNA. Vector and insert DNA were mixed in a 20µl volume with 2µl of ligase buffer and 1µl of T4 DNA ligase. Samples were incubated over night at 4°C or 16°C and 1-4µl of the ligation mixture were transformed into competent cells on the next day. For large plasmids and difficult applications like blunt end or triple ligations these standard DNA amounts were exceeded by far, for example 1µg of plasmid with an >10 molar excess of insert was ligated. Alternatively the fast ligation kit from Roche was used according to the manufacturer's protocol.

*2.3.3.12. A-Tailing of DNA for TA ligation and cloning:*
5´A overhangs were added to DNA fragments when using old PCR products or prior to TA cloning of Pfu- PCR fragments.

3-6µl of gel purified PCR product as follows.
1µl of 10xPCR buffer (containing 25mM $Mg^{2+}$)
1µl of 2mM dATP

1µl of taq polymerase.
Xµl A.dest to 10µl

It was vortexed and collected by brief spinning. Subsequently the DNA was incubated for 15´ at 72°C. The sample was placed on ice and used for ligation.

*2.3.3.13. DNA Sequencing:*
Sequencing reactions were set up as follows:

500ng- 1µg of plasmid DNA (depending on the construct size)
5-50ng PCR Frag.
3µl Big dye ™ terminator cycle sequencing kit (Perkin Elmer) v.1.1
2µl Sequencing buffer (Tris/MgCl, see Appendix)
2µl of 2ng/µl sequencing primer
Sterile A.dest. to a final volume of 20µl

Sequencing reactions were done on a "biometra" or "Eppendorf" thermocycler. The cycling parameters used for sequencing were as follows:

1: 96°C 1min
2: 50°C 5 secs
3: 60°C 2-4 min depending on the template length
repeat [1-3] 30 times
4°C hold

The reaction was transferred to a 1,5ml Eppendorf cap and stopped by adding 2µl of 125mM EDTA (pH 8.0); 2µl of 3M NaAcetate (pH 4,5) and 50µl of 95% EtOH. The samples were precipitated for 30´at full speed. Supernatant was removed and the pellet was washed with 500µl 70% EtOH. The sample was spun down for 10´at maximum speed and the supernatant was carefully decanted without dislodging the pellet. The pellet was air dried and handed in for sequencing at the Sequencing facilities of the University of Manchester. Obtained sequences were analysed and verified using Chromas 2.23 (http://www.technelysium.com.au/chromas.html). Alignments were conducted using lalign, VectorNTI suite 7.0, or DNAStar (see Appendix 6.6.).

*2.3.3.14. RNA gel electrophoresis:*
The presence of RNA probes was tested on an RNAsefree agarose gel. RNA electrophoresis under denaturing conditions in 2.2M formaldehyde was performed according to Maniatis et al., (1982) using the MOPS buffer system. RNA under these conditions is fully denatured and migrates according to the $\log_{10}$ of its molecular weight. An RNA agarose gel was prepared by melting the required amount of agarose in distilled water, cooling to approximately 60°C (hand hot) and adding 40% formaldehyde and 10 x MOPS buffer to give 2.2M formaldehyde and 1 x MOPS, respectively. Ethidium bromide was added to visualise RNA. The gel was run in 1x MOPS, 2,2M formaldehyde. RNA samples were prepared by adding 5µl of RNA to 15µl of RNA denaturing buffer. Immediately prior to loading the samples were heated to 65°C for 10min to denature them and transferred to ice for 2min. 2µl of sterile loading buffer was added and the probes were run at 5V/cm. RNA concentrations were compared with standard probes.

## 2.4. Single embryo PCR (sePCR) to confirm and identify chromosomal lesion points of *shot*$^{V104}$ and *shot*$^{V168}$:

Homozygous mutant embryos were identified by the absence of balancer chromosomes which expressed either GFP or lacZ. Genomic DNA was isolated from single mutant embryos as described above (*2.3.3.8*). 2µl of the embryo lysates were used for single PCR reactions. High fidelity PCR kits were used to perform the PCR reactions since the DNA quality and quantities were low. The following optimised PCR protocol was used:

1: 94°C 3´
2: 94°C 45´´
3: 50-60°C 45´´
4: 72°C 1´
repeat [2-4] 39x
5: 72°C 8´´
6: 4°C pause

PCR products were analysed on standard agarose gels.

## 2.5. Inverse PCR (iPCR) to map the precise molecular breakpoints of *shot*$^{V104}$:

2.5.1. Isolation of embryonic DNA:

Genomic DNA of *shot*$^{V104}$ mutant embryos was isolated using a modified protocol from BDGP (Berkley *Drosophila* Genome Project; http://www.fruitfly.org/). Homozygous mutant embryos were identified as described earlier (2.4.). Around 200 mutant embryos were collected in an Eppendorf cap and ground in 200µl buffer A using a disposable tissue grinder. Further 200µl buffer A was added and the grinding continued. The Eppendorf cap with the DNA was incubated on 65°C for 30´´. 800µl of LiCl/KAc solution was added and incubated on ice for at least 10min. Solution was centrifuged for 15min at RT. 1ml of the supernatant was transferred into a new tube, avoiding floating crud. 600µl isopropanol was added, mixed and spun for another 15min at RT. The supernatant was aspirated and the precipitate washed with 70% ethanol then dried. The pellet was resuspended in 100µl TE, used or stored at -20°C.

*2.5.2. Restriction digestion of isolated embryonic DNA:*
To this end adjacent primer pairs were designed such that the downstream primer anneals upstream to the gene fragment and vice versa. This way only ligated DNA would be amplified.
The strategies were designed carefully. The right choice of restriction enzymes and primers is crucial for the success. Digestion: Isolated genomic DNA from homozygous mutant embryos was digested with 1µl of restriction enzymes in 30µl of DNA for 2,5h at 37°C. Cut DNA was cleaned using a Qiaquick PCR product purification kit and eluted in 50µl EB. Ligation: 5µl T4 ligase were added to 45µl digested and cleaned DNA, incubated at 4°C O.N. and subsequently cleaned with the Qiaquick PCR kit and eluted (50µl) again. 10µl out of the 50µl DNA were analysed on a gel.

*2.5.3. Inverse PCR:*
20µl of circularised genomic DNA products described above (2.5.2.) were used as templates for iPCR using specific primer pairs for three parallel approaches. Obtained PCR products were reamplified using a high fidelity PCR kit and subcloned into a pDrive cloning vector for sequencing. The following PCR protocol was used for iPCR:

1: 94°C 2min
2: 94°C 45sec
3: 55°C (for all primer pairs)
4: 72°C 3min
5: [2-4] repeat 35x
6: 72°C 8min
7: 4°C pause

Primers are listed in the Appendix 6.9.

## 2.6. Generation of digoxygenin (DIG) labelled *shot* RNA antisense probes:

Probes against four different *shot* domains were generated. The following anti-*shot* probes were generated: anti-actin binding domain; anti -Plectin repeats (part of the Plakin domain); anti -Spectrin repeats; anti -Gas2 domain. Template: All probes were generated using partial *shot* cDNAs obtained from Talila Volk (Weizmann Institute, Rehovot, Israel) as template. Four different plasmids were obtained, containing different parts of the *shot* cDNA: The complete cDNA is called kak1A (Strumpf and Volk, 1998) and equals cg18076-RE (*shot*-RE identified by alignment performed with Vector NTI). The sequence of cg18076-RE is 17126bp long coding for a long Shot isoform of 5201 residues (Shot-PE). Primer pairs were generated to amplify *shot* domain specific DNA fragments.

### 2.6.1. Primers and probes:

All primers can be found in the Appendix 6.9.14. Actin s & Actin as were used to PCR amplify a 606bp long PCR product comprising a large portion of the first Calponin homology (CH1) domain and the full second CH domain (CH2) (bp 893>1498 in *shot*-RE). The primers Pt-s & Pt-as were used to PCR amplify a 904bp portion of the Plakin domain (Plectin repeats; bp2722-3651). Spectrin-s and Spectrin-as were used to PCR amplify a 926bp part of the rod domain of Shot (bp 11075>11998) and Gas2 s and Gas2 as were used to PCR amplify a 921bp DNA section containing the Gas2 domain (bp14746-15669). All PCR products were cloned into the TOPO vector (Invitrogen) using the 3´A overhang produced by the taq polymerase. The orientation of the inserts was determined by colony PCR using insert specific primer (actin as, plakin as, spectrin as and gas2 as) and M13.

### 2.6.2. Probe synthesis and labelling:

After the orientation of the template inserts was determined I chose those plasmids where the 3´prime end of the partial cDNA sequence (PCR products) was closest to the SP6 promoter of the TOPO plasmid. The plasmids were linearised using EcoRV and used for probe synthesis. All subsequent steps were carried out under sterile conditions and with packaged and protected pipette tips. All reagents were DEPC treated to avoid RNAse contamination.

#### *2.6.2.1. Labelling of probes:*

3µg of linearised template DNA was precipitated with 1/10 volumes of 2M NaCl (DEPC) and 2.5 volumes of 100% Ethanol, incubated on -20°C for 10´and spun down for 45´at full speed. The supernatant was removed carefully and the DNA pellet was washed with 500µl of 70% Ethanol (diluted with DEPC A.dest). The sample was centrifuged for another 10´ at 4°C with full speed. The supernatant was removed and the pellet was carefully dried using a speedvac. The DNA pellet was resuspended in 20ul DEPC treated water and dissolved carefully. The linearization success and the concentration were checked on a standard agarose gel. The DIG RNA Labelling Kit (SP6/T7) from Roche was used to obtain Dig labelled RNA by *in-vitro* transcription. The reaction mix was composed as follows: 14ul of clean DNA template, 2ul

10x transcription buffer, 2ul NTP (Dig) labelling mixture plus 2ul SP6 polymerase. Everything was mixed well, collected at the bottom of the tube by briefly centrifuging it down and incubated at 37°C for 2h. To remove the template DNA 2ul of RNAse free DNAseI was added and the incubation was prolonged for 15´. The reaction was stopped by adding 2ul of 0,2M EDTA solution.

*2.6.2.2. Precipitation of the RNA probe:*
2,5ul 4M LiCl and 70ul 100% Ethanol were added to the Dig labelled RNA (see above) and incubated for at least 30´at -20°C and spun down for 60´at 4°C at full speed. The supernatant was removed and the RNA pellet was washed with 70% Ethanol (diluted with DEPC ddH2O) and spun for another 10´ at 4°C at full speed. The supernatant was removed and the pellet was carefully dried until all Ethanol was evaporated. The RNA probe was finally dissolved in 30ul of DEPC treated water and used or stored at -20°C.

## 2.7. Generation of digoxygenin labelled *shot* domain DNA antisense probes and Dot blot:

2.7.1. Probe generation:

Probes against four different *shot* domains were generated. The sequences of the DNA probes were the same as the ones of the RNA antisense probes, generated using the same primers (see 2.6.1.). The probes were generated by PCR using the PCR DIG Labelling kit from Roche. A normal PCR was done substituting dNTPs with the 5µl of PCR-Dig labelling mix from Roche containing digoxigenen-11-dUTP. The labelled probes were cleaned using a PCR product purification kit (Qiagen) and analysed on an agarose gel.

2.7.2. Dot blot to asses the labelling success of digoxygenin labelled DNA probes:

1µl of Dig labelled probes in three different dilutions (1:1, 1:10 and 1:100) were dropped on a Nylon membrane and dried. 7 dilutions of a labelled control probe were pipetted on the same membrane. Positions and concentrations were indicated using a pencil. The membrane was transferred into a plastic Petri dish and incubated for 10´in a blocking solution. After 10´ anti-Dig-Fab- antibody (1:7500) was added and gently swirled for 15´. The antibody/blocking solution was disposed off and the membrane was washed 2x 5´with P1 buffer. The washing buffer was discarded. 10ml of AP-buffer were added into the plastic dish and 66µl NBT and 33µl BCIP were added to develop the precipitation. The staining progress was monitored and as sufficient staining intensities were achieved the nylon membrane was washed with tap water and dried. Probe staining intensities were compared with the control probe dilutions.

## 2.8. Generation of Shot constructs for Cell culture expression studies:

All primers and vectors described in this section are listed in the Appendix (6.9.). Plasmid sequences can be obtained upon request.

2.8.1. Generation of UAS-coupled expression constructs for S2 cell transfection:

*2.8.1.1. Generation of p{UAST}-Gas2:*
The sequence encoding the Gas2 sequence comprises: 14536bp -14754bp in *shot-RE* and aa4846-aa4918 of Shot-PE respectively. This stretch plus the five flanking residues on either

side of the Gas2 domain was PCR amplified using the primers Gas2-1 and Gas2-2. A *Bgl*II site (Gas2-1) and a *Not*I site (Gas2-2) were introduced 5´ and 3´ by PCR mutagenesis. Using these restriction sites the Gas2 fragment was ligated into *p{UAST}*. Ligation success was checked by colony PCR using the primers Gas2-1 and pUAST 3´. Positive colonies were selected cultured and isolated plasmid DNA was sequenced (wb7-12). The obtained plasmid was named *p{UAST}-Gas2* and used to generate *p{UAST}-Gas2-6xmyc*.

*2.8.1.2. Generation of p{UAST}-Gas2-6cmyc:*
*pCS2+MT*, a plasmid carrying a *6cmyc* repeat epitope tag was kindly obtained from Stefan Thor (Department of Biology, Linköping, Sweden). The *6cmyc* sequence was PCR amplified using the primers Gas2-3v.2 and Gas2-4v.3. A 5´ *Not*I site (Gas2-3v.2) and a 3´ Stop codon plus a 3´ *XhoI* site (Gas2-4v.3) were introduced by PCR mutagenesis. Due to the repetitive sequence of 6-cmyc different primer combinations had to be tried and synthesis of several novel primers was required. The obtained PCR product was introduced into *p{UAST}-Gas2* (see above) using the *Not*I/*Xho*I restriction sites. Ligation success was checked by colony PCR using the primers Gas2-3v.2 and pUAST 3´. Positive colonies were chosen, plasmids were isolated and sequenced using pUAST 5´and pUAST 3´ (wb14-wb18). The vector was used to transfect S2 cells (see 2.9.1.2.) and injected into flies (2.2.3.).

*2.8.1.3. Generation of UAS-EB1aff-2HA:*
The predicted EB1*aff* binding domain comprising aa5145-aa5191 (15432bp- 15573bp) of the *shot-RE* cDNA including the five flanking amino acids was PCR amplified out of *p{UAST}-shot-L(A)-GFP* using the primers EB1-1 and EB1-2v.2. A 5´ *Eco*RI site (EB1-1), a 3´ stop codon and *Bgl*II site after the stop were introduced by PCR mutagenesis (EB1-2v.2) The primer EB1-2v.2 also introduced three *HA* epitope tag repeats with a glycin spacer/joint between each. The obtained product was introduced into *p{UAST}* using EcoRI and BglII. Ligation success was tested by colony PCR using the primers pUAST 5´and pUAST 3´. Plasmid DNA from positive colonies was obtained and sequenced (wb19-24) (wb25-30). Astonishingly, sequencing revealed two insert sizes. Thus two of the sequenced plasmids contained *EB1aff* plus three full copies of HA whilst one only contained *EB1aff* followed by precisely two *HA* repeats. Both contained the Stop and the 3´ *Bgl*II site. The reasons for that can only be speculated. We decided to use the *p(UAST)-EB1aff-2HA* plasmid. The vector was used to transfect S2 cells (see 2.9.1.2.) and injected into flies (2.2.3.).

*2.8.1.4. Generation of p{UAST}-mRFP:*
The *pZsYellow1-C1* vector (Clonetech) in which the *ZsYellow* (yellow fluorescent protein) was exchanged against *mRFP* (monomeric red fluorescent protein, Campbell et al., 2002) was kindly obtained from (Andrew Gilmore, Faculty of Life Sciences). We named the vector *mRFP-C1*. The *mRFP* sequence (including start codon and Kozak sequence) was restricted out of *mRFP-C1* with *Age*I and *Bgl*II and introduced into *p{UAST}*. Ligation success was tested with colony PCR using the primers pUAST 5` and pUAST 3´. The presence of the insert was confirmed by sequencing (Ines 30_01_06). The *p{UAST}-mRFP-C* vector was used to generate the constructs described below *p{UAST}-mRFP-GSR* and *p{UAST}-mRFP-GSR+*.

*2.8.1.5. Generation of p{UAST}-mRFP-GSR:*
The GSR core domain (aa5039 – aa5062) of the Shot-PE (15.115bp - 15.186bp of *shot-RE* cDNA) including 9 and 5 flanking amino acids was amplified out of *p{UAST}-shot-L(A)-GFP* using primers GSR_sense and GSR_as. A 5` *Bgl*II site (GSR_sense) , a stop codon and a 3` *Not*I (GSR_as) site was introduced by mutagenesis. Using the introduced restriction sites (*Bgl*II *and Not*I), the amplicon was restricted and then ligated into *p{UAST}-mRFP* (see above ). Ligation success was tested by colony PCR using the primers seq_GSR and pUAST ´3.

Positive colonies were chosen, plasmids were isolated and sequenced using p{UAST}5´, seq_GSR and p{UAST}3´. The vector was used to transfect S2 cells (see 2.9.1.2.).

*2.8.1.6. Generation of p{UAST}-mRFP-GSR+:*
The GSR+ motif including the GSR core domain (see above) and flanking sequences until 4aa C-terminal to the Gas2 and 5aa N-terminal to the *EB1aff* domain (aa 4926-aa5139) was amplified out of *p{UAST}-shot-L(A)-GFP* (see Fig.8.)using the primers GSR+_sense and GSR+_as. A 5` *Bgl*II site (GSR+_sense) , a stop codon and a 3` *Xho*I (GSR+_as) site was introduced by mutagenesis. Using these introduced restriction sites, the amplified sequence was restricted and then ligated into *p{UAST}-mRFP*. Ligation success was tested by colony PCR using the primers seq_GSR and pUAST´3. Positive colonies were chosen, plasmids were isolated and sequenced using pUAST 5´, seq_GSR and pUAST 3´. The vector was used to transfect S2 cells (see 2.9.1.2.).

2.8.2 Generation of Shot construcst for expression studies in fibroblasts:

The four constructs previously tested in S2 cell culture (see 2.8) were also transferred from *p{UAST}* into the mammalian expression vector *pcDNA3*. To this end they were excised out of *p{UAST*} with *Eco*RI and *Xho*I and transferred into *pcDNA3*. All constructs carry a Kozak consensus sequence. Constructs were subcloned into *pcDNA3* respectively.

*2.8.2.1. Generation of pcDNA3-Gas2/GSR/EB1-GFP:*
The sequence encoding the Shot C-terminus downstream of the EF-hand domain (Gas2, GSR, EB1 domain and GFP, aa4831-5450 of Shot-PE-GFP; see Fig.5) was amplified out of *p{UAST}-shot-L(A)-GFP* (Fig.8) using the primers Gas2/GSR-1fw and Gas2/GSR-4bw. A 5` *Hind*III site (Gas2/GSR-1fw) and a 3´Xho site (Gas2/GSR-4bw) were introduced by mutagenesis. Using the introduced restriction sites, the amplified sequence was restricted and then ligated into *pcDNA3* (*Hind*III and *Xho*I). Ligation success was tested by colony PCR. The vector was used to transfect fibroblasts (see 2.9.2.2.).

*2.8.2.2. Generation of pcDNA3-Gas2/GSR-GFP:*
The construct was generated using a two step PCR strategy. In the first step two PCR fragments with complementary, overlapping 3´ regions were generated. The first PCR amplicon was synthesised using the primers Gas2/GSR-1fw and Gas2/GSR-2bw, amplifying the coding sequence for the Shot peptide stretch between the EF-hand and EB1*aff* domains out of *shot-GFP* (coding for aa4831-5450 of Shot-PE, Fig.5.). In this process a 5`*Hind*III restriction site was inserted and an additional 3´sequence was introduced through the Gas2/GSR-2bw primer, comprising a sequence stretch downstream of the EB1*aff* domain coding sequence (bp16.135-16.152). A second PCR product was generated using the primers Gas2/GSR-3fw and Gas2/GSR-4bw amplifying the C-terminus of *shot* after the EB1*aff* domain (coding for aa5191-aa5201 of Shot-PE) until the end of the eGFP coding sequence. The resulting amplicon contained and additional overhang (introduced by the 3´portion of primer Gas2/GSR-3fw), complementing the 3´overhang from the amplicon generated with Gas2/GSR-1fw and 2bw. In the subsequent step the two yielded PCR products were mixed in one PCR reaction and primed one another by annealing with their overlapping sequences. The resulting PCR product contains the *shot* C-terminal region precisely deleting the EB1*aff* domain coding sequence (coding for aa5145-aa5191, Fig.5.). The introduced restriction sites (*Hind*III and *Xho*I) were used to introduce the yielded amplicon into *pcDNA3*. Ligation success was tested by colony PCR. The vector was used to transfect fibroblasts (see 2.9.2.2.).

*2.8.2.3. Generation of pcDNA3-Gas2/EB1-GFP:*
A construct comprising the C-terminus of Shot (aa5831-aa5450) but lacking the GSR core motif (aa5039-aa5062 of Shot-PE-GFP) was generated. To this end a two step PCR strategy was used. In the first step a PCR product was generated using the primers Gas2/GSR-1fw and Gas2/EB1-2bw. The yielded amplicon contained the sequence stretch downstream of the EF-hand motif to the beginning of the GSR motif (aa 5831-aa5039). In this process a 5` *Hind*III restriction site and a 3` sequence complementary to the sequence downstream of the GSR domain were introduced (through the Gas2/EB1-2bw primer). A second PCR product (coding for aa5063-aa5450 of Shot-PE-GFP) was generated using the primers Gas2/EB1-3fw and Gas2/GSR-4bw. The yielded amplicon contained a sequence (introduced by a 3´ portion of Gas2/GSR-3fw) overlapping with the 3´sequence of the first amplicon. In the subsequent step both yielded PCR fragments were used in a single PCR reaction and primed each other through the overlapping 3´sequences. The introduced restriction sites (*Hind*III and *Xho*I) were used to introduce the yielded PCR fragment into *pcDNA3*. Ligation success was tested by colony PCR. The yielded constructs contains aa4831-5450 of Shot-PE-GFP, lacking the GSR core domain (see above). The vector was used to transfect fibroblasts (see 2.9.2.2.).

## 2.9. Cell culture:

2.9.1. *Drosophila* S2 cell culture:

S2 *Drosophila* cells were a kind gift from Hillary Swank (Manchester University, WTCCMR). S2 cells are derived from embryonic macrophages and are non-polarised and semi-adherent.

*2.9.1.1. S2 cell maintenance:*
The established S2 cell line was maintained in SFM Insect Media supplemented with L-Glutamine (0.6 g/l), 10% heat-inactivated calf serum, Penicillin (50 U/ml) and streptomycin sulphate (50 µg/ml) (complete medium). For general maintenance, S2 cells were sub-cultured to a final density of 2 to 4 x $10^6$ cells/ml. For transformation, S2 cells were maintained in T25 tissue culture flasks with membranous lids in a volume of 6 ml and split every 3days at a 1:5 dilution to keep them in a maximum growth phase (Hillary Swank, personal recommendation). For routine maintenance cells were split every 10 days and kept in tissue culture flask without a membrane in the lid to prevent drying out.

*2.9.1.2. Transient cell transfection:*
DNA was introduced into S2 cells using the Effectene® transfection kit from Qiagen according to the manufacturer's protocol. In brief cells were split 1:5 on day 1 and left to grow and recover over night at 24°C. On day two cells were counted using a cell counting chamber and $2{,}3x10^6$ – $2{,}7x10^6$ cells/ml were transferred into one well of a 6 well tissue plate and diluted to a final volume of 5ml/well culture dish containing a poly lysine coated coverslip prepared as described below (2.9.1.4.). Cells were left to grow and recover over night at 24°C. On day 3, the cells were transfected. In brief the transfection mixture was prepared (1µg DNA, 8µl Enhancer/well), mixed, vortexed briefly and incubated for 5´ at RT. 25µl Effectene transfection Reagent was added, the mixture was vortexed for 10´´ and incubated another 10´at RT to form a precipitate. 1ml of SFM Insect Media with FCS, L-glutamine and antibiotics (penicillin/ streptomycin) was added and mixed by pipetting up and down. The whole precipitate was added drop wise to the cells under constant gentle swirling. The cells were subsequently incubated at 24°C. If possible transfection efficiency was tested

after 24h under a fluorescence microscope, detecting e.g. mRFP (monomeric Red Fluorescent Protein) expression. Alternatively cells were fixed after 24h- 48h incubation and subjected to immunohistochemistry (see 2.9.3.1.). Higher DNA amounts and concentrations were tested according to the manufacturer's protocol but no significant changes of transfection efficiency were achieved.

*2.9.1.3. Transfection plasmids:*
*pUAST + pMT-Gal4:* On day 4 the gene expression of cotransfected cells was induced by adding copper sulfate to the 6 well plates under constant mild swirling to a final concentration of 0,7mM. Copper sulfate induces expression of Gal4 from the promoter of *pMT-Gal4*. Different plasmid concentrations were tested to achieve high transfection rates.

*2.9.1.4. Immobilisation of S2 cells on coverslips:*
So that semiadherent S2 cells could stick on to coverslips, they were first coated with poly-L-lysine. To do so, 22x22mm coverslips were washed in 1% HCl/70% Ethanol for 1hour at room temperature and dried on filterpaper in a laminar flow hood. They were then coated with 0.01% poly-L-lysine in water for 15´ to 1h. The coverslips were dried again and were stored on filterpaper in a Petri dish until needed. To immobilize the cells on a coverslip, 100 to 200 µl of cell suspension was transferred onto the coverslip. After a 15 minutes incubation at room temperature (or 30 min on ice), the coverslip was briefly and carefully rinsed in PBS. The coverslips were then subjected to fixation and immunohistochemistry as described in Chapter 2.9.3.1.

2.9.2. NIH3T3 murine Fibroblast cell culture:

*2.9.2.1. Fibroblast maintenance:*
NIH 3T3 cells (Ref No: 93061524, see Jainchill et al., 1969) were a kind gift from Christof Ballestrem (Faculty of Life Sciences, Manchester). They were cultured in DMEM, supplemented with Penicillin/Streptamycin (50U/ml) and 10% FCS (complete medium). Cells were grown in T75 cell culture flasks. They were split 1:3 every 2-3 days so that they did not get to a point of overconfluence. Transient transfections were performed with LipofectAMINE PLUS (Invitrogen), according to the manufacturer's instructions. Briefly, cells were seeded in 6-well plates at approximately 1 x $10^5$ cells per well and transfected on the next day when they were around 70-80% confluent.

*2.9.2.2. Transfection protocol:*
*F*or each sample two Eppendorf tubes with 100µl of DMEM (transfection medium without antibiotics and without FCS) were prepared. DNA and Plus reagent at the ratio of 4 µl of the Plus reagent per 1µg of DNA were added to tube 1. We used 1.5 µg of plasmid and 6 µl of Plus reagent. The mix was incubated for 15 minutes. Just before the last 5 minutes incubation, Lipofectamine mix was prepared in tube 2: 5 µl of Lipofectamine were diluted to the 100 µl of DMEM. After 5 minutes, it was transferred to the mixture in tube 1. Lipofectamine + Plus reagent + DNA was incubated for additional 15 minutes. Meanwhile the cells were washed once with serum free DMEM (transfection medium). After this 1 ml of DMEM was added to the cells and they were put back into the $CO_2$ incubator. After the 15 minutes incubation period, 800 µl of DMEM was added to the Lipofectamin mix tube and the whole mixture was transferred to the cells. Transfection was performed for 3 to 3.5 hours at $37^OC$ in a $CO_2$ incubator (incubation times were not exceeded too long as these transfection reagents are toxic for the cells) and the transfection mix was removed afterwards. Cells were washed once with PBS, trypsinised and re-plated on 5µg/ml Fibronectin-coated 1-well

chamber glass slide. Coating of the chamber with Fibronectin (Sigma) was done for 3 hours and subsequent wash with PBS. Cells were grown for 24-48 hours and processed, stained or imaged later on.

*2.9.2.3. Vertebrate expression vector:*
Constructs were subcloned into *pcDNA3* (Invitrogen) for transfection into fibroblasts. No induction is required using this vector.

2.9.3. Immunohistocemistry and Life imaging of cell cultures:

*2.9.3.1. Fixation and immunofluorescence of cells:*
Three different fixation methods were used to fix cells on cover slips. Depending on the focus of the experiment on of the three described methods was used.
PFA: Was used when only AB stainings were done and the cytoskeleton needed not to be preserved. Cells on cover slips were fixed with PFA 4% for 8min, washed with PBS for 10´ and 2x with PBT for 10´.
→ Immunohistochemistry was done as normal. Microtubules were badly conserved using this fixation method.
Methanol: To conserve microtubules and combine this with antibody stainings, Methanol fixation was used. Methanol was not used when fluorescent protein expression should be observed. Cells were fixed in ice cold Methanol (-20°C) for 5min´ at -20°C. They were washed 2x with DPBS (Bio Whittaker) for 10´ each
→ Immunohistochemistry was done as normal (antibodies in PBS). Glutaraldehyde: (personal recommendation from Christoph Ballestrem):
To obtain best possible microtubule stainings, Glutaraldehyde fixation with the anti tubulin antibody (see Table 2) was used. 0,5% Glutaraldehyde, 3% PFA, in PBT (0,25% Triton) 15´; 2x10´ DPBS (Bio Whittaker); 15´ incubation in DPBS + 0,01% Sodiumborohydrate; 2x 10´washing in DPBS.
→ Immunohistochemistry was done as normal (antibodies in PBS). Some antibodies did not work well under this fixation condition.

*2.9.3.3. Documentation of stained cells:*
Fixed and stained cells were documented like other fluorescent preparations (2.1.19) but the confocal microscope proofed to be not suitable for documenting cells. Instead pictures were taken with a DeltaVision, microscope (inverted Olympus IX 71 attached).

*2.9.3.4. Life imaging of NIH3T3 Fibroblasts:*
For time-lapse imaging, the experiments with live fibroblasts were conducted in an incubation chamber with the temperature set at 37°C. In order to preserve good envirormental conditions and avoid disturbing the cytoskeleton structure of the cells the DMEM culturing medium was replaced by pre-warmed Ham's F12 (Sigma) medium. An Inverted Axiovert 200 M Carl Zeiss microscope with an Alpha Plan-Fluar 100x/1.45 DICIII oil immersion objective was used, and the pictures were acquired with a CCD CoolSNAP $_{HQ2}$ PVcam coupled to a PC using the IPLab v3.70 software. Digital pictures/stacks were processed using Photoshop CS and Image J software.

# 3. Results

## 3.1. Motorneuronal dendrites of *Drosophila* represent postsynaptic compartments

### 3.1.1. Choice of strategy

As explained in Chapter 1.6, *shot* mutations affect the growth of neuromuscular terminals of *Drosophila* motorneurons as well as their dendritic side branches in the CNS (Fig.2). My first aim was to clarify, whether both structures represent presynaptic cellular compartments, or whether Shot might be required in two qualitatively very different cell compartments (pre- vs. postsynaptic). To this end, I raised transgenic fly strains carrying Gal4-inducible constructs of two different transmitter receptors, the alpha-like subunit gene (ALS) coding for an α-subunit of excitatory acetylcholine-receptors (Bossy et al., 1988) and the *resistance to dieldrien* (*rdl*) gene encoding a subunit of inhibitory GABA-gated postsynaptic chloride channels (Ffrench-Constant and Roush, 1991). I chose these molecules as candidate markers for postsynaptic compartments, because cholinergic synapses are predominant in the insect nervous system and Rdl-containing GABA receptors are likewise abundant (Aronstein et al., 1996). Furthermore, *Drosophila* motorneurons have been reported to be receptive to GABA and acetylcholine (Rohrbough and Broadie, 2002). Unfortunately, the myc-tagged ALS protein, even though it became expressed, did not show any reliable localisation to neuronal processes, and will not be further considered here. However, the HA-tagged Rdl protein displayed very precise localisation, and its cloning and expression pattern are elaborated below.

### 3.1.2. Generation of *p{UAST}-RDL-HA* transgenic flies

*RDL-RC* cDNA inserted into a pNB40 vector was obtained from Martina Grauso (David Sattelle laboratory, Oxford, UK) and was used by me as a starting point to generate the *pUAST-RDL-HA* transposition construct. An HA epitope sequence (influenza Haemagglutinin; YPYDVPDYA; for reference see e.g. Finney et al., 2003) was introduced behind base 135 (aa45) of the coding sequence into the *rdl* cDNA. This insertion point does not lie within any reported structural domain and is therefore less likely to disrupt essential folding or interaction of Rdl. Also, a similar tagging position has been used for tagging of other GABA receptor subunit genes before (Connolly et al., 1996; Connolly et al., 1999;

Bedford et al., 2001; Calver et al., 2001; $GABA_A$-subunit from rat: Lüddens, H., personal communication) or receptor molecules from related receptor-families, such as glycin receptors (Meier et al., 2000; Rosenberg et al., 2001). 5' to the tagging position, lies a predicted N-terminal signal peptide (aa 1-45; Ffrench-Constant, 1993), although my own *in-silico* analyses of the RDL-cDNA sequence with PSORT II, Smart and Expasy (see Appendix 6.6.) did not assign a signal peptide function to this area. By inserting the epitope tag immediately behind the potential signal peptide (at position aa46) I ensured that potential cleavage of the epitope sequence did not remove the tag. Only a single HA-epitope was introduced to interfere with the natural folding and localisation of the receptor protein as little as possible. For details of the cloning procedure see Fig.6. I used the complete *p{UAST}-RDL-HA* construct to generate transgenic flies by injecting DNA into early *Drosophila* embryos following standard procedures (Rubin and Spradling, 1982; see material and methods 2.2.).

### 3.1.3. Analysis of motorneurons using *p{UAST}-RDL-HA* transgenic flies

I used RDL-HA to investigate the molecular nature of dendritic side branches of motorneurons in the CNS of *Drosophila melanogaster*. To this end, I expressed RDL-HA with three different motorneuronal Gal4 driver lines, *even-skipped-Gal4*$^{RN2D+O}$ (in the following abbreviated as *RN2D+O*) targeting embryonic motorneuronal dendrites, and *OK6-Gal4* or *D42-Gal4* expressing in larval motorneurons. In larval motorneurons RDL-HA consistently localised exclusively to dendritic areas in the neuropile (visualised via co-expression of mCD8-GFP) and was completely absent from neuromuscular junctions (Fig. 3.). In contrast, a known presynaptic marker, Synaptotagmin-HA, showed inverse distribution, being absent from dendrites and localising specifically to NMJs (Fig.3.).

When co-expressed in larval dendrites with Actin-GFP, RDL-HA does not localise to puncta of strong Actin-GFP enrichment, indicating that RDL-containing GABAergic receptors suggesting that Rdl-HA might not be localised to the prominent postsynaptic densities of excitatory synapses (Sanchez-Soriano et al., 2005, see Fig.3). Similar observations were made for GABAergic synapses in the calyx area of the cricket brain (Frambach et al., 2004; Frambach and Schurmann, 2004). This might mean that GABAergic synapses in *Drosophila* compare to those of vertebrates which are usually type 2 or symmetric synapses with a sparse PSD (Peters et al., 1991).

To be able to visualise RDL-HA in embryonic dendrites using *RN2D+O-Gal4* it was necessary to combine two independent *UAS-rdl-HA* insertions to increase expression levels.

When using this stock, RDL-HA localised very specifically to sub-regions of dendrites in late stage 17 embryos but seemed not abundant in all dendritic processes (Fig. 3).

Thus, my data with Rdl-HA (together with the data obtained with Syt-HA) clearly indicate that motorneuronal dendrites are mere postsynaptic compartments. These data contributed essentially to work showing that motorneuronal dendrites in *Drosophila* are homologous to vertebrate dendrites (Sanchez-Soriano et al., 2005). RDL-HA is the first specific dendrite marker in *Drosophila* to date and has, since publication, been requested by about a dozen of groups worldwide to be used for work on dendrites. I used Rdl here exclusively with the intention to generate a morphological marker for potential postsynaptic sites of motorneurons, and did not test its physiological function as a $GABA_A$ subunit. However, non-tagged Rdl constructs generated previously were tested and shown to function as GABA-gated chloride channels (N. Sánchez-Soriano, personal communication).

Essential for the work presented here is the conclusion that Shot is crucial for the development of two distinct motorneuronal compartments. Since dendrites in *Drosophila* embryos are experimentally easier accessible than neuromuscular junctions but equally affected morphologically by the *shot* mutation. Therefore, I mainly concentrated on dendrites as model structure to investigate Shot function in neuronal development.

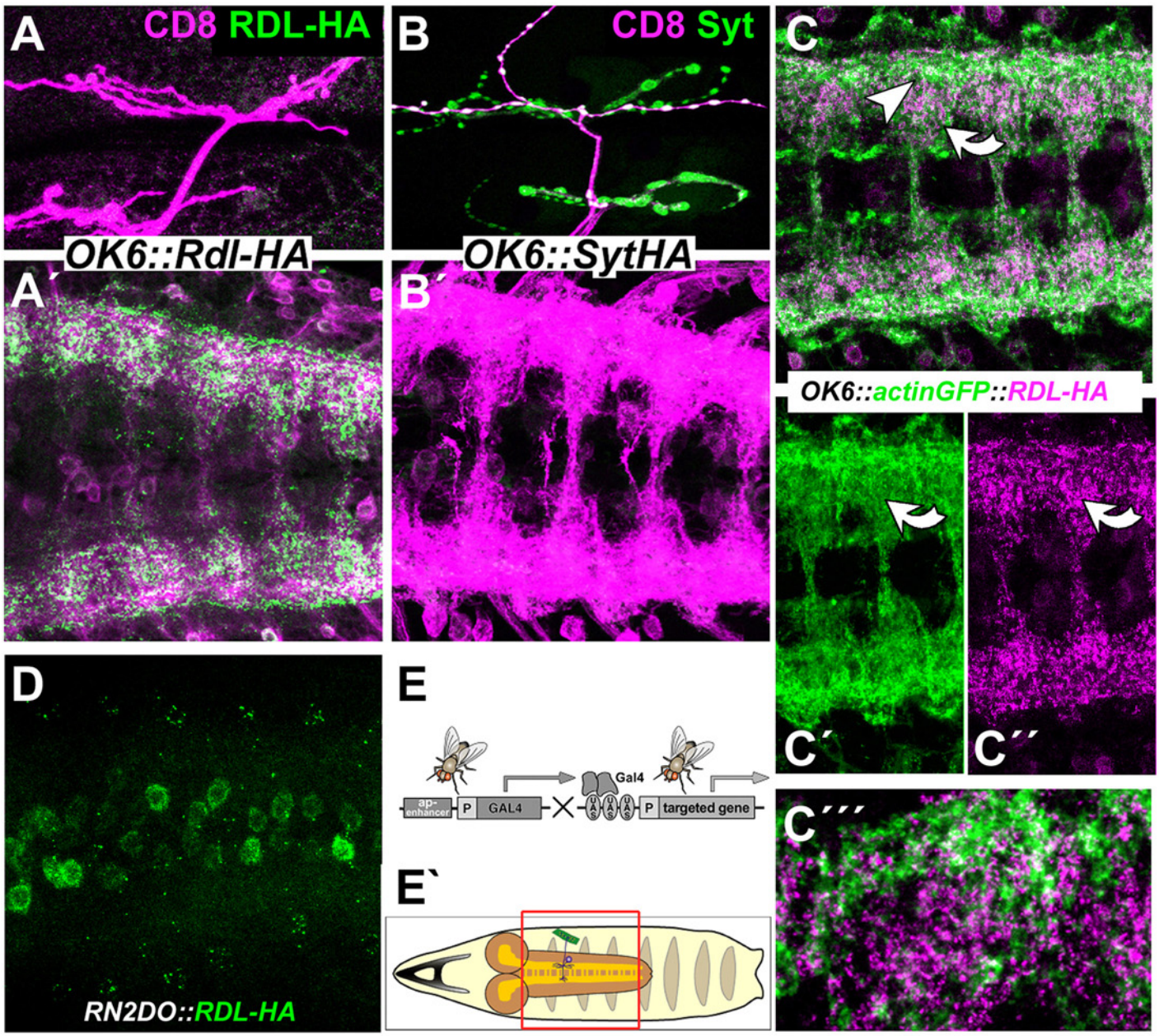
A
CD8 RDL-HA
B
CD8 Syt
C
OK6::Rdl-HA
OK6::SytHA
A´
B´
OK6::actinGFP::RDL-HA
C´
C´´
D
RN2DO::RDL-HA
E
Gal4
ap-enhancer
P
GAL4
P
targeted gene
E`
C´´´

## Fig.3. Motorneuronal side branches represent postsynaptic compartments

To elucidate whether neuromuscular junctions and dendrites of motorneurons represent distinct neuronal compartments, Synaptotagmin-HA (Syt-HA) or $GABA_A$-receptor (Rdl-HA) (both green in A,A´,B,B´,C-C´´´) was targeted to all motorneurons (OK6-Gal4) at larval stages (L3 A-B´) or aCC and RP2 motorneurons (RN2D+O-Gal4 ) at embryonic stages (D). mCD8-GFP was co-expressed as a morphological marker (magenta) and labels motorneuronal dendrites in the CNS (A´,B´) and their terminals at NMJs (A,B). The findings are published in (Sanchez-Soriano et al., 2005). We find that presynaptic Syt-HA exclusively enriches at neuromuscular terminals (B), whilst it is absent from the neuropile (B´). Vice versa postsynaptic RDL-HA exclusively enriches in dendrites in the neuropile (A´) but not in neuromuscular junctions (A). Thus we conclude that the two motorneuronal compartments are of distinct nature: dendrites are exclusively postsynaptic whilst NMJs are exclusively presynaptic. RDL-HA also accumulates in dendrites at embryonic stages (D) but is restricted to a sub fraction of dendritic branch tips (compare with Fig.12A). (C-C´´´) Details of Rdl-HA and Actin-GFP distribution in larval motorneurons. Actin-GFP and HA-tagged GABA receptors (Rdl) targeted to all motorneurons (*OK6-Gal4*) occur in dotted or speckled patterns in dendrites in segmental repeated patterns of distribution; areas of high Rdl-HA (curved arrows) show lower amounts of Actin-GFP (C´*vs.* C´´). Dots of Rdl-HA are restricted to dendrites and do not localise to areas of high Actin-GFP accumulation (C´´) suggesting that they are not situated at postsynaptic densities. Similar observations were made for GABAergic synapses in the calyx area of the cricket brain (Frambach et al., 2004; Frambach and Schurmann, 2004). Note, that also in the mammalian brain GABA receptors are mostly localised at symmetric synapses, which lack pronounced postsynaptic densities (Peters et al., 1991). (E,E´) In this and many other studies presented here we capitalised on the Gal4/UAS system (Brand and Perrimon, 1993). It allows the expression of optional genes in defined cell types. This system requires (1) flies that express the yeast transcriptional activator *Gal4* under the control of an endogenous promoter (driver stock), and (2) flies that carry a transgene of interest whose expression is regulated by the *Gal4* Upstream Activation Sequence (*UAS*; *UAS* stock). When the driver and *UAS* stock are crossed together, the transgene of interest is expressed in the same pattern as the *Gal4* protein. Thus, ectopic expression of the transgene depends on the enhancer that regulates *Gal4* expression. I exclusively used Gal4 driver lines driving expression in the nervous system see red box in E´. (E´) Schematic representation of the *Drosophila* larval/embryonic brain as seen from dorsal. Red box indicates areas depicted in (A´-B´,C-C´´´).

### 3.2. Shot is required and strongly enriched in developing dendrites

As mentioned earlier, Shot severely affects motorneuronal dendrites and neuromuscular junctions (see Fig.2 and Prokop et al., 1998). However, the mechanisms by which Shot exerts its functions are unknown. In order to understand the function of Shot for the development of dendrites it was necessary to clarify, whether Shot is required acutely in growing dendrites or at earlier stages, such as during the compartmentalisation or polarisation of neurons. Since Shot is expressed throughout the synaptic neuropile (Fig.4), I had to choose a mosaic approach to study its sub-cellular localisation. To this end, I targeted GFP-tagged *shot* full length constructs to a subgroup of neurons only. As explained in the introduction, different isoforms of Shot exist. The ones represented by the *UAS-Shot-L(A)-GFP* construct obtained from Peter Kolodziej (Lee and Kolodziej, 2002), contains the full length sequence of Shot isoform E (Shot-PE, formerly referred to as *shot-kak1A*)[1] comprising all but one protein domain encoded by the *shot* genomic locus (Fig.1). Shot-PE was used for historical reasons as it was the first fully sequenced and cloned isoform (Gregory and Brown, 1998; Strumpf and Volk, 1998). However, Shot-PE is lacking a single large plakin repeat domain encoded by a large exon, which was discovered at a later stage (Roper and Brown, 2003, see Fig.1). The respective isoform Shot-PH including this plakin repeat domain is expressed only in the epidermis where it targets Shot to adherens junction maintaining epidermal integrity (Roper and Brown, 2003). Thus, Shot-L(A)-GFP seems appropriate for my studies and has been demonstrated previously to provide wild type function in neurons and tracheae (Lee and Kolodziej, 2002; Lee and Kolodziej, 2002).

When using different Gal4-driver lines, such as *MzVum-Gal4* or *RN2D+O*, to target *UAS-shot-L(A)-GFP* to a subgroup of motorneurons at late embryonic stages, GFP localises and enriches distinctly at dendrites (Fig.4). Dendrites are elaborated and multi-branched terminating in very fine endings, as can be seen when using targeted expression of membrane-bound mCD8-GFP as a neutral morphological marker (Fig.4; Lee and Luo, 1999). Shot does not localise throughout these branches, but is restricted to only the thicker, proximal dendritic branches (Fig.4 and Sanchez-Soriano et al., 2005). Since Shot has been proposed to represent an actin to microtubule cross-linker (Lee and Kolodziej, 2002) we analysed the distribution of these two essential cytoskeletal components. Expression of tubulin-GFP revealed a continuous sharp line reaching from the primary neurites (or axon) into the main dendritic branches but terminating half way (Fig.4 and Sanchez-Soriano et al., 2005). In contrast, actin-

[1] Shot-isoform E: FlyBase reference: FBpp0086744 and cg18076-PE

GFP targeted to dendrites labels dendrites in their whole (Fig.4 and Sanchez-Soriano et al., 2005). These images suggest that Shot seems to localise to the distal end of dendritic microtubules potentially linking them to the actin filaments populating the distal terminals of dendrites. To test this hypothesis and to be able to stain Shot together with either GFP-tagged actin or tubulin via double-staining I first had to generate a differently tagged Shot construct, since all constructs in our hands are GFP-tagged. Based on good experience with other myc-tagged constructs in the laboratory (e.g. homer-myc, Sanchez-Soriano et al., 2005), I generated a Shot-L(A) construct carrying 6cmyc epitopes at its N-terminus (for details of cloning strategy see Fig.8). When expressing the construct with the *RN2D+O-Gal4* driver line in dendrites the construct enriches at proximal thick dendrites in a fashion similar to Shot-L(A)-GFP (Fig.4). Thus, I concluded that the N-terminal tag does not affect the localisation in dendrites and that the construct can be used for localisation studies with other marker molecules in the future. Due to a lack of time the construct has not been used for co-staining studies as yet

Furthermore, if Shot acts as an actin to microtubule cross-linker (Lee and Kolodziej, 2002), this function would require that Shot orientation within dendrites is polarised: the actin-interacting N-terminus outwards, the microtubule-binding C-terminus inward. I tested this prediction by generating a double-tagged Shot construct, bearing a 6cmyc-epitope N-terminally and GFP at the C-terminus (Fig.8). The predicted length of the largest Shot isoform has been estimated to be up to 400nm (isoform H, Roper et al., 2003). Based on this estimation I expected the Shot-PE isoform to be longer than 250nm, i.e. to be able to separate both tags spatially upon confocal microscopy analysis. As shown in Figure 4, the myc-tagged N-terminus of Shot indeed forms a halo surrounding the GFP-labelled microtubule-bound core, strongly supporting our hypothesis of a polarised localisation of Shot in dendrites. However, the construct did not show the same polarised localisation at larval NMJs. From studies with N-terminal constructs (Mende, 2004) we expected a more peripheral position of the myc-tag of 6cmyc-Shot-L(A)-GFP, whereas Shot-L(A)-GFP revealed a microtubule-associated localisation of GFP (Fig.13). However, the double-tag showed a surprising localisation in that the C and N terminus completely overlapped (Fig.13), the C terminus now appeared to localise like the N terminus (Fig.13). We can therefore not exclude that the very N-terminus of Shot preceding the ABD might have an impact on Shot localisation which is impaired by the N-terminal 6cmyc-tag (see Discussion).

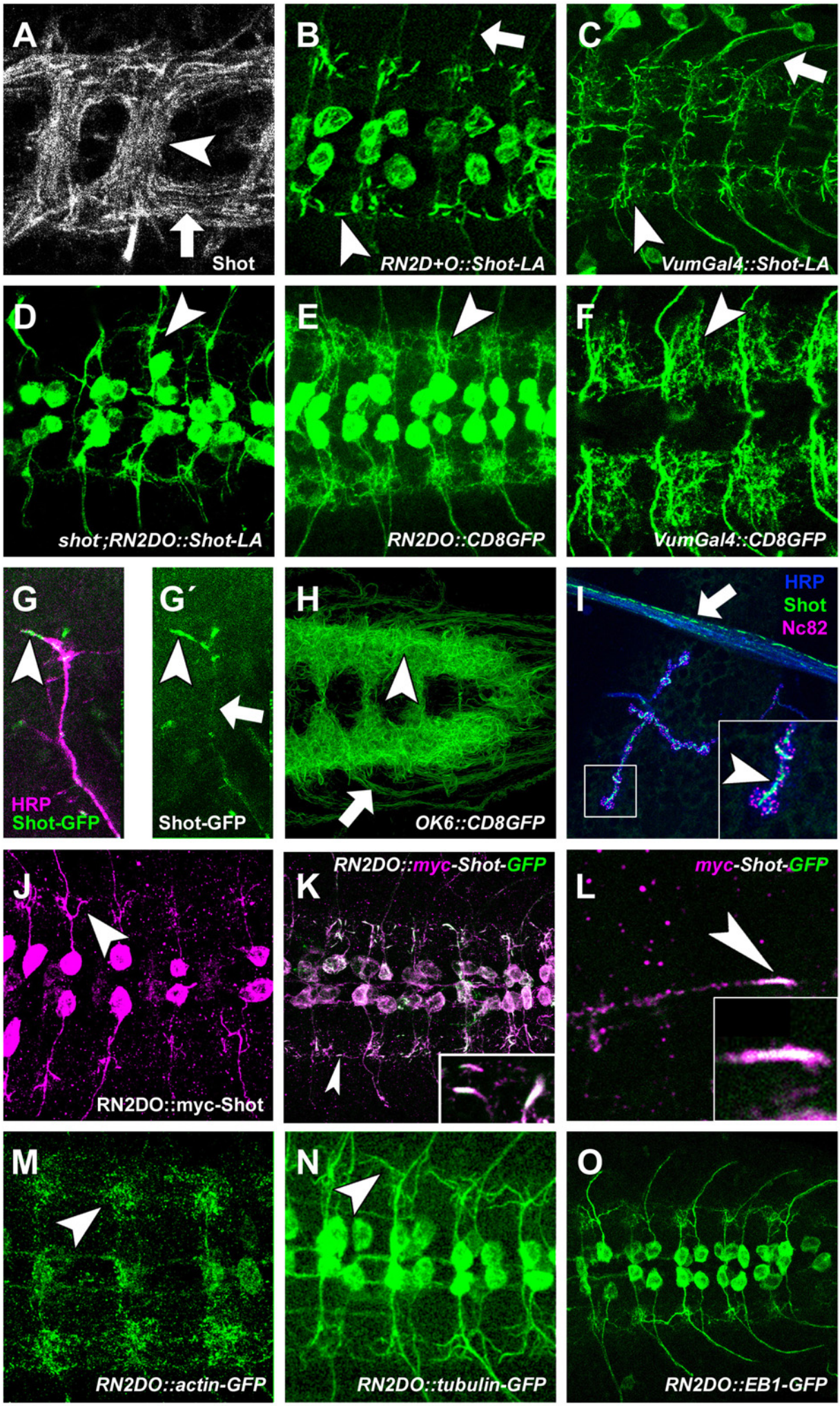
A
Shot
B
RN2D+O::Shot-LA
C
VumGal4::Shot-LA
D
shot;RN2DO::Shot-LA
E
RN2DO::CD8GFP
F
VumGal4::CD8GFP
G
HRP
Shot-GFP
G´
Shot-GFP
H
OK6::CD8GFP
I
HRP
Shot
Nc82
J
RN2DO::myc-Shot
K
RN2DO::myc-Shot-GFP
L
myc-Shot-GFP
M
RN2DO::actin-GFP
N
RN2DO::tubulin-GFP
O
RN2DO::EB1-GFP

## Fig. 4: Short stop localisation in the nervous system of *Drosophila melanogaster*

To understand Shot activity in the nervous system its localisation in different neuronal compartments and stages was analysed. Pictures (except G,G´,I,L) represent dorsal views (confocal images) on the central nerve cord of embryonic (stg.17) or larval (L3; H) *Drosophila* embryos. (G,G´) Shows a neuromuscular terminal at embryonic and (I) at larval stages. (L) Shows an embryonic growth cone of the pCC interneuron. Colours in the figure are coded: GFP (green fluorescent protein), green; FasciclinII (FasII), blue; cmyc, magenta (except I where Nc82 an active site marker is shown in magenta). The *RN2D+O-Gal4* driver line was used for most expression experiments with the exception of (C,F): *Vum-Gal4* and (H,I): *OK6-Gal4*. Anterior is to the left throughout.

**(A)** Anti-Shot staining reveals that Shot is abundant throughout the neuropile within commissures (arrowhead) bridging the midline and connectives (arrow) (with permission from Natalia Sánchez-Soriano). **(B,C)** Shot-GFP driven with *RN2D+O-Gal4* (B) or *Vum-Gal4* (C) enriches in the proximal thick dendritic branches of aCC and RP2 motorneurons and Vum neurons (arrowhead in B and C) but not in the finer branches and at the tips of dendrites (compare with B,C) and only weakly along the primary neurites (arrows in B and C). (*) Cell bodies are indicated. **(D-F)** Morphology of motorneuronal aCC and RP2 (D,E) and Vum (F) dendrites (arrowheads), visualised with the cell surface marker CD8-GFP driven with *RN2D+O-Gal4* (D+E) and Vum-Gal4 (F). Dendrites are massively reduced in *shot* mutants (arrowheads in D *vs.* E). **(G+I)** Shot-GFP localises and enriches at neuromuscular terminals at embryonic stages (arrowheads G,G´) and larval stages (arrowhead I). It also localises along the axons (arrows in G´ and I). In larval NMJs Shot-GFP exclusively localises to the microtubules at the base of boutons but not to the rim of boutons (inset). **(H)** Dorsal view on the CNS of L3 larva. Shot strongly enriches in dendrites (arrowhead) and localises along the nerves (arrow). **(J)** myc-Shot-L(A) enriches in dendrites comparably to Shot-GFP (see B). **(K+L)** myc-Shot-L(A)-GFP enriches at proximal dendrites like Shot-GFP (arrowhead; see B). Anti-myc staining surrounds the C terminal GFP signal like a halo (inset), revealing the polarised localisation of Shot, the C-terminus is microtubule bound whilst the N terminus (with the myc-tag) stretches into the dendritic periphery. **(L)** Shot also enriches at embryonic growth cones (here of interneuron pCC; arrowhead) and localises polarised as well with the N terminus (carrying the myc-tag) stretches into the actin rich periphery (inset). **(M-N)** Localisation of actin-GFP **(M)** and tubulin-GFP (N) reveals the differential distribution in dendrites (Sanchez-Soriano et al., 2005). Whilst tubulin-GFP is exclusively in the thick proximal dendritic branches (arrowhead in N), actin-GFP is localising throughout the dendrites in a dotty pattern (arrowhead in M). (O) EB1-GFP does not show any prominent specific enrichment in dendrites but seems to localise diffused and random.

Thus, Shot accumulates in late embryonic dendrites in a strategically important position at the interface between actin and microtubules. Interestingly, when expressing the same Shot construct at late larval stages, this image is completely changed. At these stages, Shot no longer accumulates but is evenly distributed throughout the neuron, similarly abundant in primary neurite/axon and dendrites (where it now also seems to occupy the finer tips; Fig.13). All along the axon, the C-terminal GFP-tag of Shot-L(A)-GFP localises in "stroke" like fashion, as if Shot has now a strong affinity also to microtubules in the axonal shaft (Fig.13). Thus, Shot accumulation seems to correlate with periods of dendrite growth, whereas at later stages a function in axonal maintenance might predominate. In agreement with such a function in neuronal maintenance, axonal surfaces loose their shape and become vastly undulating in *shot* mutant animals (Prokop et al., 1998). Apart from its mere localisation, I addressed next whether the GFP-tagged full-length construct UAS-Shot-L(A)-GFP is capable to rescue *shot* mutant dendrite phenotypes. This same construct was used successfully to rescue *shot* mutant phenotypes in other cellular contexts, such as axonal outgrowth (Lee and Kolodziej, 2002) and tracheal fusion (Lee and Kolodziej, 2002). By overexpressing Shot-L(A)-GFP in dendrites of *shot* mutant embryos using a motorneuronal driver line (*MzVum-Gal4* and *RN2E-Gal4*) I could rescue dendritic *shot* phenotypes as well. Thus, such specimens show the characteristic mislocalisation of Fasciclin2 in nerve roots, indicating their *shot* mutant nature, whereas dendrites of motorneurons expressing Shot-L(A)-GFP display wildtype morphology, as visualised via co-expression of mCD8-GFP (Fig.14). This proves that the Shot-L(A)-GFP construct is functional in the context of dendrite development. It further clearly demonstrates that Shot is cell-autonomously required in these dendrites, since motorneuron-specific expression of Shot-L(A)-GFP is sufficient to rescue the motorneuronal dendrite phenotypes. Overexpression of Shot-L(A)-GFP does not cause any dominant phenotypes in dendrites as revealed by experiments in which dendrites are visualised with the homer-myc marker in the presence or absence of co-expressed Shot-L(A)-GFP (not shown).

Taken together, my observations clearly demonstrate that *Drosophila* dendrites are a suitable model system for the study of Spectraplakin function in neuronal development. Such work has potential implications for the study of vertebrate dendrites when considering the homology of dendrites between both animal groups (Sanchez-Soriano et al., 2005) and the existence of mammalian orthologues of Shot (see Introduction). Shot localises to dendrites and rescues their *shot* mutant phenotypes. Both these features provide easily assayable read-outs which I capitalised on during the rest of my project. Thus, I used deletion constructs of

Shot and asked whether lack of certain domains would interfere either with Shot localisation and/or with its ability to rescue *shot* mutant phenotypes.

## 3.3. Methodological consideration for the use and generation of constructs for structure-function analysis of Shot

### 3.3.1. Principal strategy and available tools

As discussed earlier, Shot is required for dendrite development and dendritic phenotypes of *shot* mutant embryos and can be rescued via motorneuronal expression of Shot-L(A)-GFP (3.2. and Fig.14). Shot strongly enriches in dendrites at developmental stages and is oriented in a polarised fashion (Fig.4). To understand the localisation and function of Shot in motorneuronal dendrites my first aim was to analyse which domain(s) of Shot are responsible for its high level enrichment to this cellular compartment. To this end, I carried out a structure function analysis capitalising on a number of existing and self-generated deletion constructs of *shot*, using various protein tags as read-outs (Fig.5).

I used the UAS/Gal4 system (Brand and Perrimon, 1993; see Fig.3) to specifically express these deletion constructs of *shot* in identified motorneurons and compared their dendritic localisation with Shot-L(A)-GFP at late stage 17 and at late larval stages, using the driver lines *RN2D+O –Gal4* and *OK6-Gal4*, respectively (Fig.12 and Fig.13). From published work (Lee and Kolodziej, 2002; Subramanian et al., 2003), a number of *shot* deletion constructs were already available and were obtained from the laboratories of Peter Kolodziej (Vanderbilt Medical Centre, Nashville, U.S.A.) and Talila Volk (Weizmann Institute, Rehovot, Israel). At later stages of the project it became necessary to generate additional Shot deletion constructs to complete my studies. Constructs will be described below in detail in the context of the respective expression analysis, but I would like to point out here, that all of them are derivatives of UAS-Shot-L(A)-GFP used for my initial localisation and rescue studies (Chapter 3.2.), and UAS-Shot-L(A)-GFP can therefore be taken as reference. Only the constructs UAS-Shot-L(C)-GFP and Shot-L(C)-ΔGas2-GFP differ slightly from UAS-Shot-L(A)-GFP in that their N-terminal 357 amino acids are taken from isoform C (Lee and Kolodziej, 2002) and not isoform E (equivalent to *shot-kak1A* in Subramanian et al., 2003). An overview over all constructs is given in Fig.5 and Tab.3.

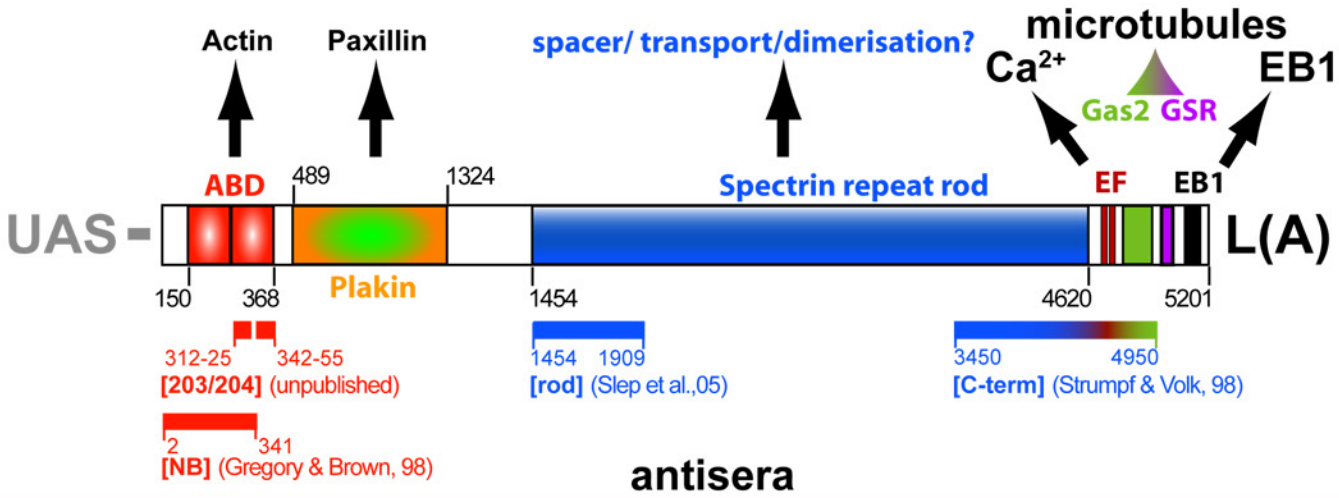


## constructs for targeted expression

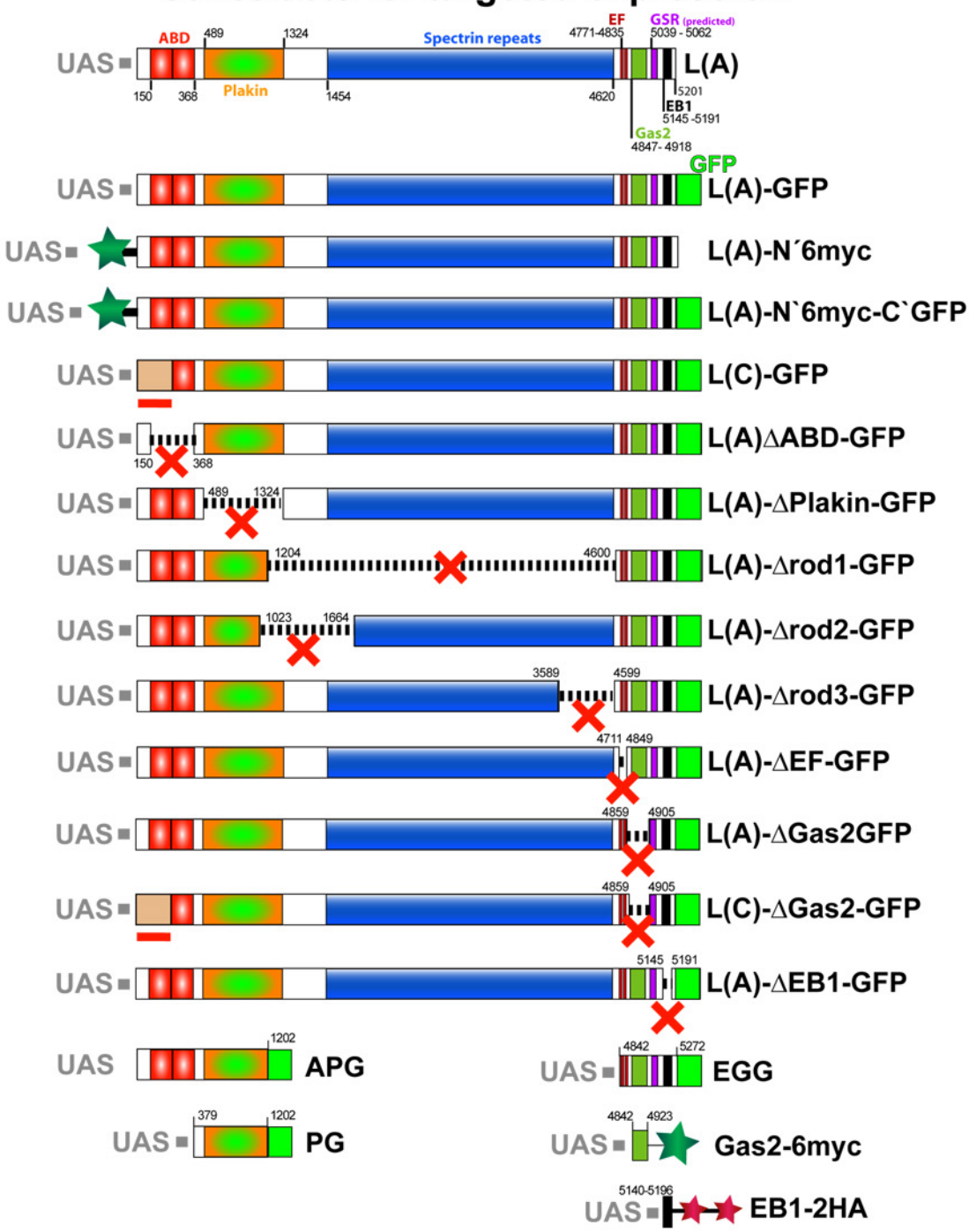

## Fig.5. Short stop domains and expression constructs

**(A)** Short stop is a large Spectraplakin which acts as an act myosin crosslinker. Several isoforms exist (see Fig.1). We used Shot full length isoform L(A) (Shot-RE; 5201aa) and isoform L(C) (Shot-LC; 5160aa) for our expression studies (see below and Fig.1). Shot comprises a whole array of domains which will be listed in the following. Respective domain positions are given and correspond to domains in the Shot-L(A) (Shot-RE) isoform. From the N to the C terminus Shot harbours. An actin binding domain (consisting of two consecutive Calponin homology (CH) domains (CH1 + CH2) (red), a plakin domain (yellow/green), a long spectrin repeat rod domain (blue), two calcium responsive EF-hand domains (red), a microtubule binding Gas2 domain (green) a microtubule binding GSR domain (violet) and an EB1affinity domain (black) at the very C-terminus. Four antibodies against exist which were raised against for different regions of Shot. The borders of the protein portion used to generate the antibodies and the respective source are given. Antibody 203/204 has been raised in our lab (Mende, 2004).

**(B)** A whole array of Shot deletion and expression constructs either existed or was generated by myself (indicated as "*"). I used *shot-L(A)-GFP* as template for the generation of these constructs (see Fig.6-11). Details can be found in the respective results chapters and table 3. They are all under the control of the UAS-sequence (Upstream Activating Sequence) from yeast and thus can be expressed via Gal4 expression (see Fig.3). All constructs are tagged and the respective tags are colour and shape coded: GFP (green fluorescent protein), green square; cmyc-tag, green star; 2xHA, 2 red stars. In brief following constructs are available:

Shot-L(A)-GFP, comprising all domains. 6myc-Shot-L(A) (*), comprising all domains and an N-terminal c-myc tag for co-expression with GFP labelled constructs. 6myc-Shot-L(A)-GFP (*), comprising all domains and carrying an N´terminal 6myc and a C-terminal GFP tag to visualise subcellular localisation of Shot. Shot-L(C)-GFP, lacking the CH1 domain and thus probably actin binding capability. Shot-L(A)ΔABD-GFP (*), lacking the full actin binding domains (CH1+CH2), transgenic flies are pending. Shot-L(A)ΔPlakin-GFP (*) lacking the plakin domain. Shot-L(A)Δrod1-GFP, lacking the whole rod domain. Shot-L(A)Δrod2-GFP lacking an N-terminal portion of the rod domain, the interspersing sequence until the plakin domain and the C terminal part of the plakin domain. Shot-L(A)Δrod3-GFP lacking the C terminal portion of the rod domain. Shot-L(A)ΔEF-hand-GFP lacking the calcium binding EF-hand domains. Shot-L(A)ΔGas2-GFP, lacking the microtubule binding Gas2 domain. Shot-L(A)ΔEB1-GFP lacking the C-terminal EB1 affinity domain. APG (Actin-Plakin-GFP), comprising the N-terminus of Shot including the whole plakin domain. PG (Plakin-GFP), comprising the isolated plakin domain. EGG, comprising the whole C-terminus from the EF-hand downstream. Gas2-6myc (*), comprising the isolated Gas2 domain and finally EB1-2HA, comprising the isolated EB1 affinity domain.

## 3.3.2. Generation of novel Shot constructs

Various questions arising at different stages of my project made it necessary to generate several novel Shot constructs in addition to the already existing ones, as explained later in the respective experimental results Chapters. Constructs generated by myself are listed in Table 3 and indicated as "origin: 3".

| Name | Tag | length of Shot sequence [aa] | Deleted region | isoform | Origin | Comment |
|---|---|---|---|---|---|---|
| **Shot full length/deletion constructs** | | | | | | |
| **UAS-Shot-L(A)-GFP** | eGFP | 5201 | n.a. | E | 1 | full length; control for all experiments |
| **UAS-Shot-L(A)-N´6cmyc** | 6cmyc | 5201 | n.a. | E | 3 | Full length; N instead of C terminal tag |
| **UAS-Shot-L(A)-N´6cmyc-C´GFP** | 6cmyc eGFP | 5201 | n.a. | E | 3 | Full length; N- and C-terminus tagged |
| **UAS-Shot-L(C)-GFP** | eGFP | 5160 | n.a. | C | 1 | Long shot isoform with diverging N-terminus |
| **UAS-Shot-L(A)ΔABD-GFP** | eGFP | 4983 | 150-368 | E | 3 | Full length; ABD (CH1&CH2) deleted |
| **UAS-Shot-L(A)ΔPlakin-GFP** | eGFP | 4364 | 488-1325 | E | 3 | Plakin domain deleted |
| **UAS-Shot-L(A)Δrod1-GFP** | eGFP | 1805 | 1204-4600 | E | 1 | Whole rod domain deleted |
| **UAS-Shot-L(A)Δrod2-GFP** | eGFP | 4560 | 1023-1664 | E | 1 | Part at C-terminus of rod domain deleted |
| **UAS-Shot-L(A)Δrod3-GFP** | eGFP | 4191 | 3589-4599 | E | 1 | Part at N-terminus of rod domain deleted |
| **Shot-L(A)ΔEF-hand-GFP** | eGFP | 5063 | 4711-4849 | E | 1 | Calcium binding motifs deleted |
| **UAS-Shot-L(A)ΔGas2-GFP** | eGFP | 5155 | 4859-4905 | E | 1 | Microtubule binding domain deleted |
| **UAS-Shot-L(A)ΔEB1-GFP** | eGFP | 5164 | 5154-5191 | E | 3 | EB1-binding motif deleted |
| **UAS-Shot-L(C)ΔGas2-GFP** | eGFP | 5114 | 4859-4905 (of Shot-L(A)) | C | 4 | |
| **Isolated Shot domains/fragments** | | | | | | |
| **UAS-APT** | Tap | 1-1202 | n.a. | E | 2 | Isolated Actin & Plakin domains |
| **UAS-PT** | | 379-1202 | n.a. | E | 2 | Isolated Plakin domain |
| **UAS-EGT** | | 4780-5201 | n.a. | E | 2 | Isolated EF-hand, Gas2, GSR & EB1 domains |
| **UAS-[$Gas2_{shot}$]-6cmyc** | 6cmyc | 4841-4923 | n.a. | E | 3 | Isolated Gas2 domain |
| **UAS-[$EB1_{shot}$]-2HA** | 2xHA | 5140-5383 | n.a. | E | 3 | Isolated EB1 domain |

***Table 3***. Summary of all UAS-linked *shot* constructs in transgenic flies used in this study. The following information is given: ***tag****:* Different protein tags were used: eGFP tag of 240aa (Invitrogen, Lee and Kolodziej, 2002), TAP tag of 200aa (Rigaut et al., 1999), 6 copies of c-myc tag (out of pCS2+MT) of together 85aa (Evan et al., 1985), and 2 copies of HA tag linked by a flexible glycin of together 19aa (Keesey, 2000); ***length of Shot sequence****:* Shot isoform E: 5201aa[2]; isoform C:5160aa[3]; ***deleted region****:* indicates the position of left and right break point based on sequence Shot-PE; ***isoform****:* Shot isoform the construct is based on; either Shot-PE (LA) or Shot-PC (LC); ***origin****:* (1) Lee and Kolodziej, 2002; (2) Subramanian et al., 2003 ; (3) generated by me; 4) Lee and Kolodziej, 2002). Further abbreviations used: aa, amino acids; n.a., not applicable.

[2] FlyBase reference: FBpp0086744 and cg18076-PE
[3] FBpp0003325 and Ensembl ref.: cg18076-PC

Due to the enormous length of Shot, cloning procedures were time-consuming and technically difficult. Here, I will briefly provide general background information regarding generation of my constructs, give an overview over the cloning principles and describe some essential guidelines followed for the generation of these large Shot plasmids. Detailed descriptions of the cloning strategies are given in the figure legends of the respective depicted cloning strategies (Fig.7- Fig.11; and in Materials and Methods 2.8).

### 3.3.3. Cloning strategies – general considerations

On the basis of a p{UAST}-Shot-L(A)-GFP construct kindly obtained from Peter Kolodziej (Vanderbilt Medical Centre; Nashville, Tennessee) I developed the cloning strategies to generate the constructs listed in Table 3 and described below (see Fig.5). All primers are shown in the Appendix 6.9. *In-silico* analysis revealed that the Shot cDNA contained in Shot-L(A)-GFP equals Shot-PE (5201aa; Drysdale and Crosby, 2005). Since we could get hardly any information regarding the exact molecular nature of the p{UAST-Shot-L(A)-GFP plasmid (with an overall length of ~25380bp), I initially sequenced the insert (Shot-L(A)-GFP) and the flanking regions of *p{UAST}*. Subsequently I analysed the cDNA to determine restriction sites suitable for my cloning purposes (NEBcutter; see Appendix 6.6.2.). To be able do make precise domain excisions, extensive *in-silico* analyses were conducted, using informations available from various databases such as NCBI, Ensembl, FlyBase, SMART and ProSite (see Appendix 6.6.2.), determining and extracting precise molecular domain positions. These sequence informations were integrated with the restriction analysis to generate cloning strategies. Since p{UAST}-Shot-L(A)-GFP harbours very few unique or suitable restriction sites the development of cloning strategies was lengthy and challenging. It was necessary to disassemble the *shot* cDNA, modify isolated fragments and reassemble it again later. Intermediate products deriving from individual cloning steps can and have been used as components of a construction set, to generate further Shot constructs (see Fig.7-Fig.11).

Next, a number of methodological challenges had to be overcome. Especially, the final cloning steps proved to be particularly tricky due to the enormous construct length and usually hundreds of clones had to be screened. In the following, I will describe some of the procedures which turned out to be helpful during my work with these large plasmids (>15kb). First, to ensure high yields only fresh bacterial colonies were used to inoculate cultures for

plasmid preparations. Second, I generally used midi-plasmid preparations, as mini-preparations did not reliably yield sufficient amounts of DNA. Third, elution buffers (see Materials and Methods) were always preheated to ~60°C to facilitate plasmid elution from Qiagen columns or membranes. Fourth, if several successive restriction or modification steps were necessary, intermediate DNA cleaning steps were carried out via ethanol precipitation or Millipore filter cleaning, rather than on columns (Qiagen or similar) in order to prevent extensive DNA losses. Fifth, for ligation and restriction steps, large amounts of DNA were used, exceeding the amount recommended in standard protocols. Sixth, to ensure the uptake of the low amount of successfully ligated plasmids containing large constructs, highly competent cells with efficiency rates of $10^8$ or $10^9$ were used (see Materials and Methods), whereas less competent cells often failed to take up these plasmids. Further methodical modifications and details are listed in the respective Materials and Methods sections.

Shot constructs were subsequently sent to a service company (BestGene Inc.[4]) for injection and the initial F2 screening for red eyed transformant flies (see materials and methods 2.2.3.). Between 2 and 10 independent transgenic lines were obtained, tested for successful expression by crossing them into suitable Gal4-driver lines and the chromosomes carrying the respective construct insertions were determined using classical genetics (see Materials and Methods 2.2.5. and Appendix 6.8., Table 7).

[4] BestGene Inc; 2918 Rustic Bridge, Chino Hills, CA 91709, U.S.A.

# Fig.6.
## Generation of p{UAST}RDL-HA

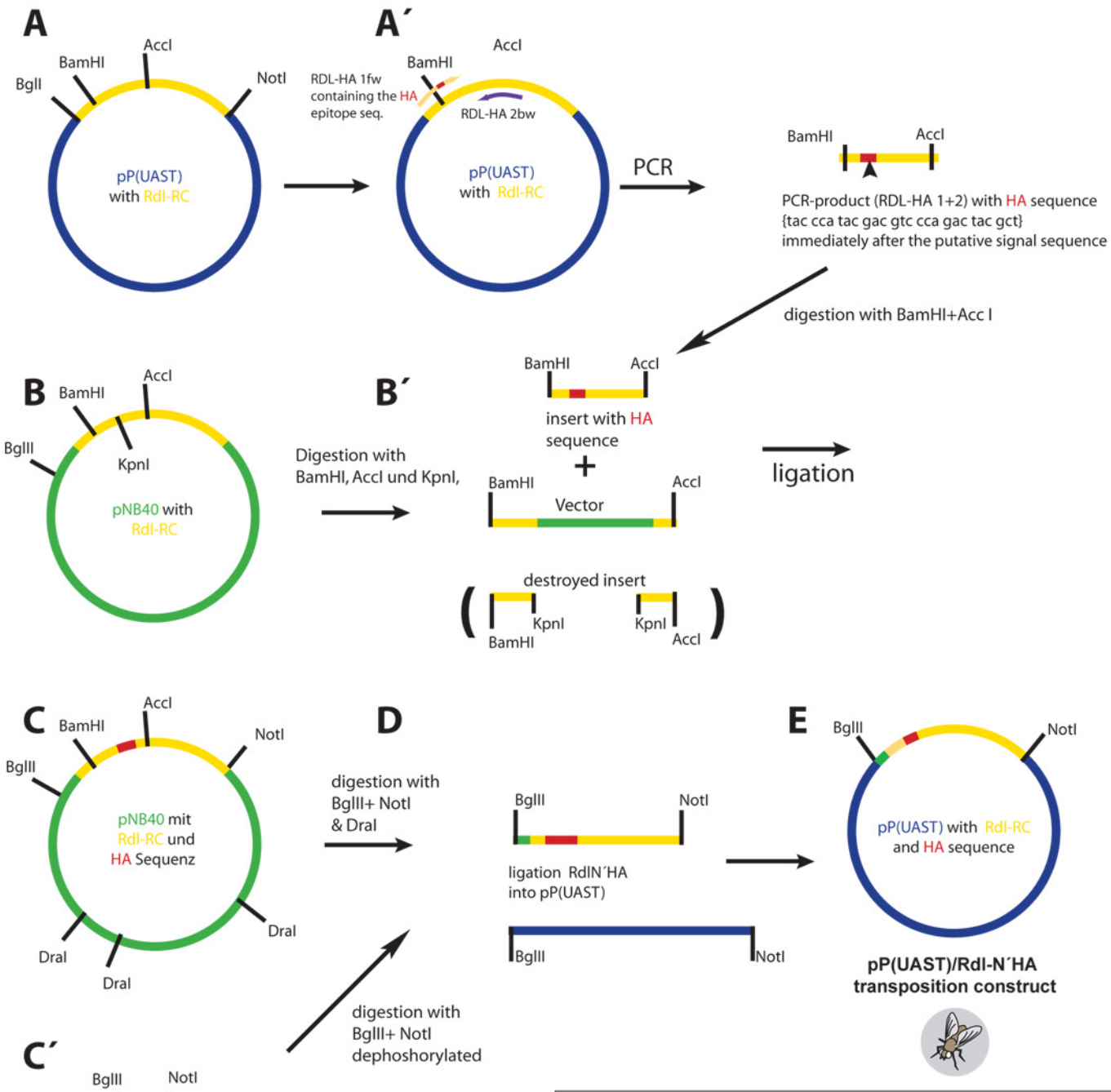


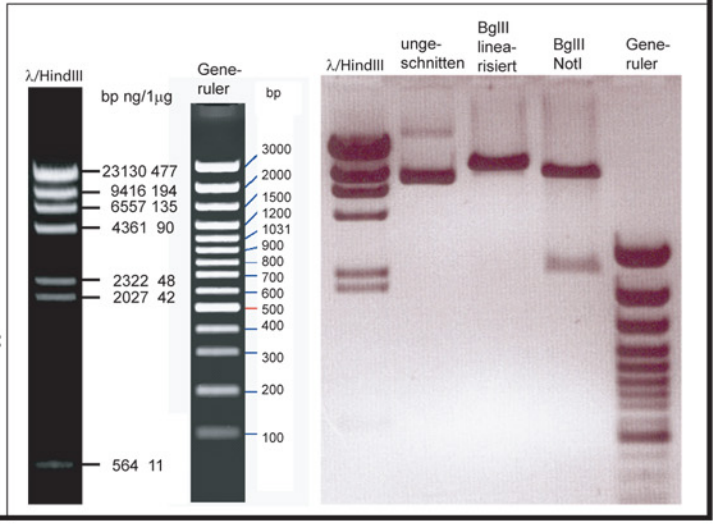


**Control digestion of pPUAST-RDL-HA:**
of sequenced Midiprep DNA.
expected fragment length:
-vector-pP(UAST): ~ 9050bp
-insert: RdI HA: ~ 2300bp

## Fig.6. Generation of *p{UAST}-RDL-HA*

RDL is a postsynaptic $GABA_A$ receptor subunit. *p{UAST}-RDL-HA* was generated to obtain postsynaptic morphological marker molecule carrying an epitope tag (HA). The construct was successfully used to reveal the synaptic nature of motorneuronal dendrites in the CNS of *Drosophila* (see Chapter 3.1 and Sanchez-Soriano et al., 2005). **(A´)** The primers RDL-HA-1fw and RDL-HA-2bw were used to amplify a portion out of the *p{UAST}-RDL-RC* (CG10537-RC)[5] **(A)** obtained from Natalia Sánchez Soriano (Faculty of Life Sciences, Manchester). The primer RDL-HA-1fw contained the HA epitope sequence (influenza Haemagglutinin; YPYDVPDYA (Keesey et al., 2000), such that the sequence was introduced behind base135 (aa45), directly behind a predicted N-terminal signal peptide (at position aa46 Ffrench-Constant, 1993). **(B)** *pNB40-RDL-RC* (kindly obtained from Martina Grauso, Sattele lab, Oxford) was cut with *BamH*I*, Acc*I and *Kpn*I and the amplicon obtained in step (A´) was inserted into the cut *pNB40-RDL-RC* vector backbone **(B´)**. **(C,C´,D)** The *RDL-RC-HA cDNA* (C) and *p{UAST}* (C´) were digested with *Bgl*II and *Not*I (D) and subsequently and ligated. **(E)** The yielded *p{UAST}-RDL-HA* construct was used to generate transgenic flies by injecting DNA into early *Drosophila* embryos following standard procedures (Rubin and Spradling, 1982; see material and methods 2.2.). All primers used can be found in the Appendix and sequences can be obtained upon request.

[5] Flybase ref. number: http://flybase.bio.indiana.edu/.bin/fbidq.html?FBgn0004244&resultlist=/tmp-shared/fbgn1707.data

# Fig.7.
## Generation of p{UAST}$_{mod}$

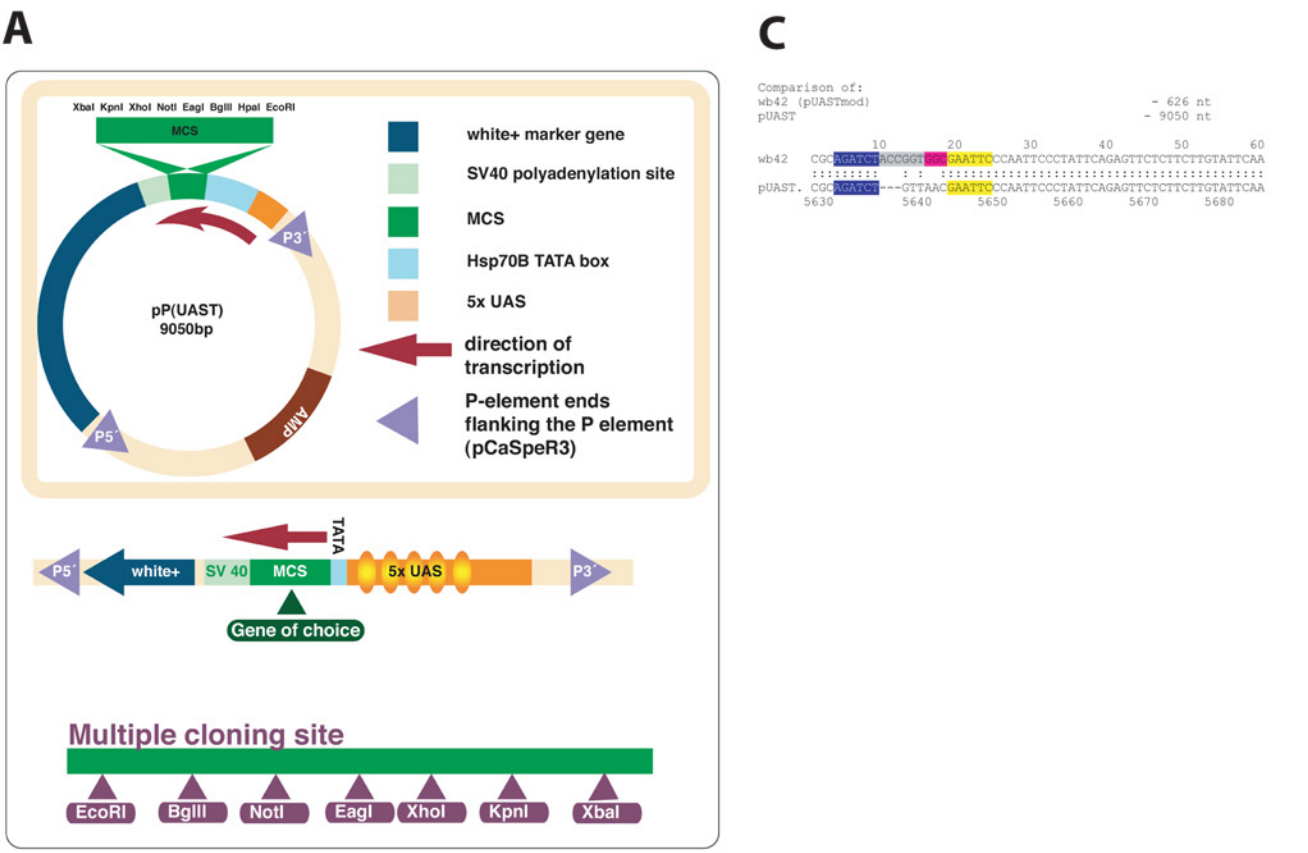


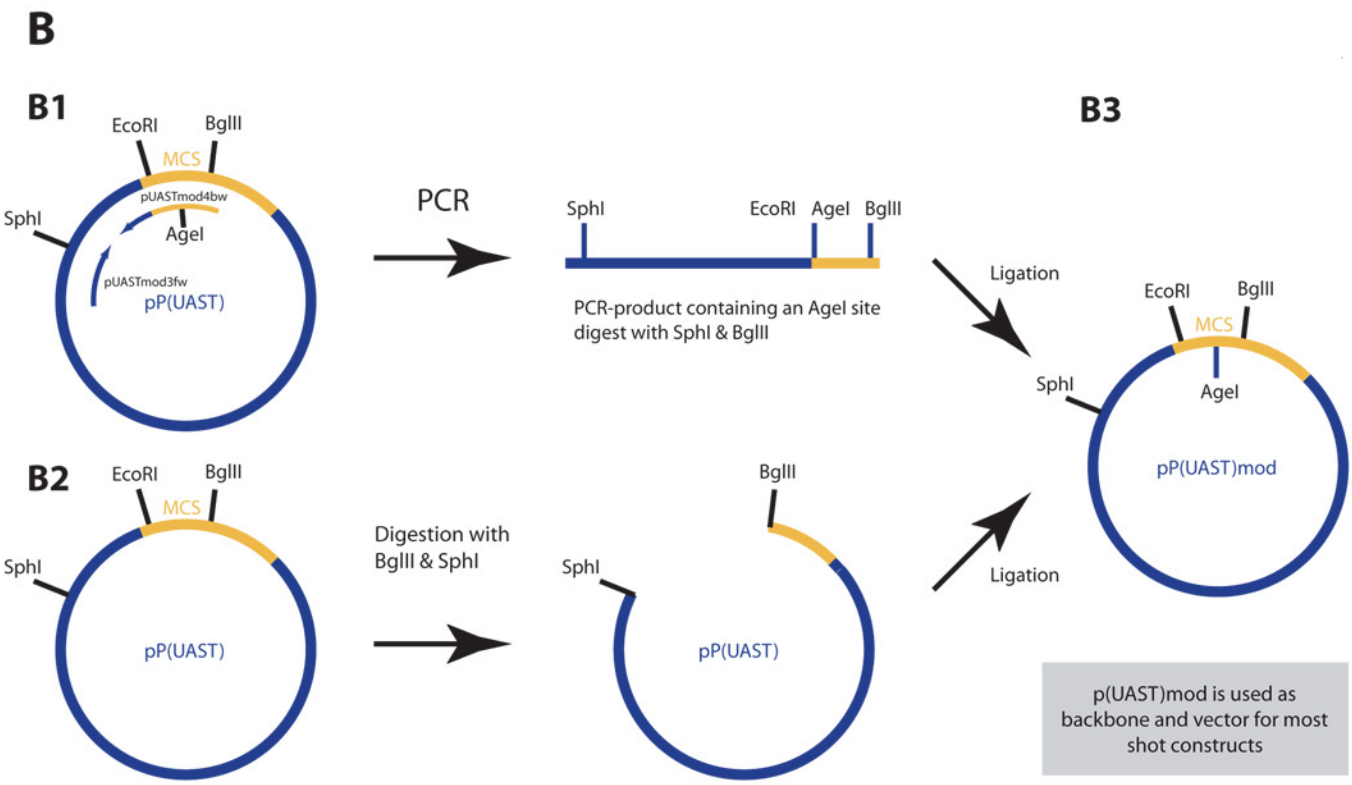

## Fig.7. Generation of *p{UAST}$_{mod}$*

**(A)** The *p{UAST}* vector is a P-element transposition vector (Brand and Perrimon, 1993). It is used to introduce transgenes into the genome of *Drosophila* via P-element mediated germline transformation (Brand and Perrimon, 1993). It is coinjected together with a Δ*2-3* helper plasmid (Rubin and Spradling, 1982) coding for transposase. The plasmids are injected into the posterior pole of early blastoderm stage *Drosophila* embryos (stage 3) where the pole cells (germline cells) develop. The transposase excises the P element with the transgene from *p{UAST}* and randomly inserts it into the genome. We used *p{UAST}* or a variant *p{UAST}mod* (B) as backbone and vector for most of our constructs. **(B)** Cloning strategy of *p{UAST}mod*: An *Age*I restriction site was introduced into the MCS of *p{UAST}* between the *EcoR*I and *Bgl*II sites. To this end a part of *p{UAST}* (bp5462-bp6038) (see flybase for full *p{UAST}* sequence) was PCR amplified using the primers p{UAST}mod3fw, introducing an *Age*I restriction site and p{UAST}mod4 **(B1)**. The *Bgl*II/*Sph*I fragment of *p{UAST}* digested with *Sph*I and *EcoR*I **(B2)** was substituted with the p{UAST}mod3+4 PCR fragment carrying the additional *Age*I site **(B3)**. Ligation success was tested with colony PCR using the primers p{UAST}mod3 and p{UAST}mod4. Positive colonies were cultured and obtained DNA was cut with *Age*I /*Sph*I to test the presence of the new *Age*I site. Positive colonies were sequenced using the primers p{UAST}3´and p{UAST}mod 4bw. The obtained plasmid was named *p{UAST}$_{mod.}$*. It was used as backbone for the generation of *shot* constructs for injection (see Fig.8-11). **(C)** The introduced *Age*I site between *Bgl*II and *EcoR*I is depicted as sequenced. All primers and vectors used can be found in the Appendix and sequences can be obtained upon request.

**Fig.8.**
**Generation p{UAST}-shot-L(A)-N´6cmyc and p{UAST}-shot-L(A)-N´6cmyc-C´GFP**

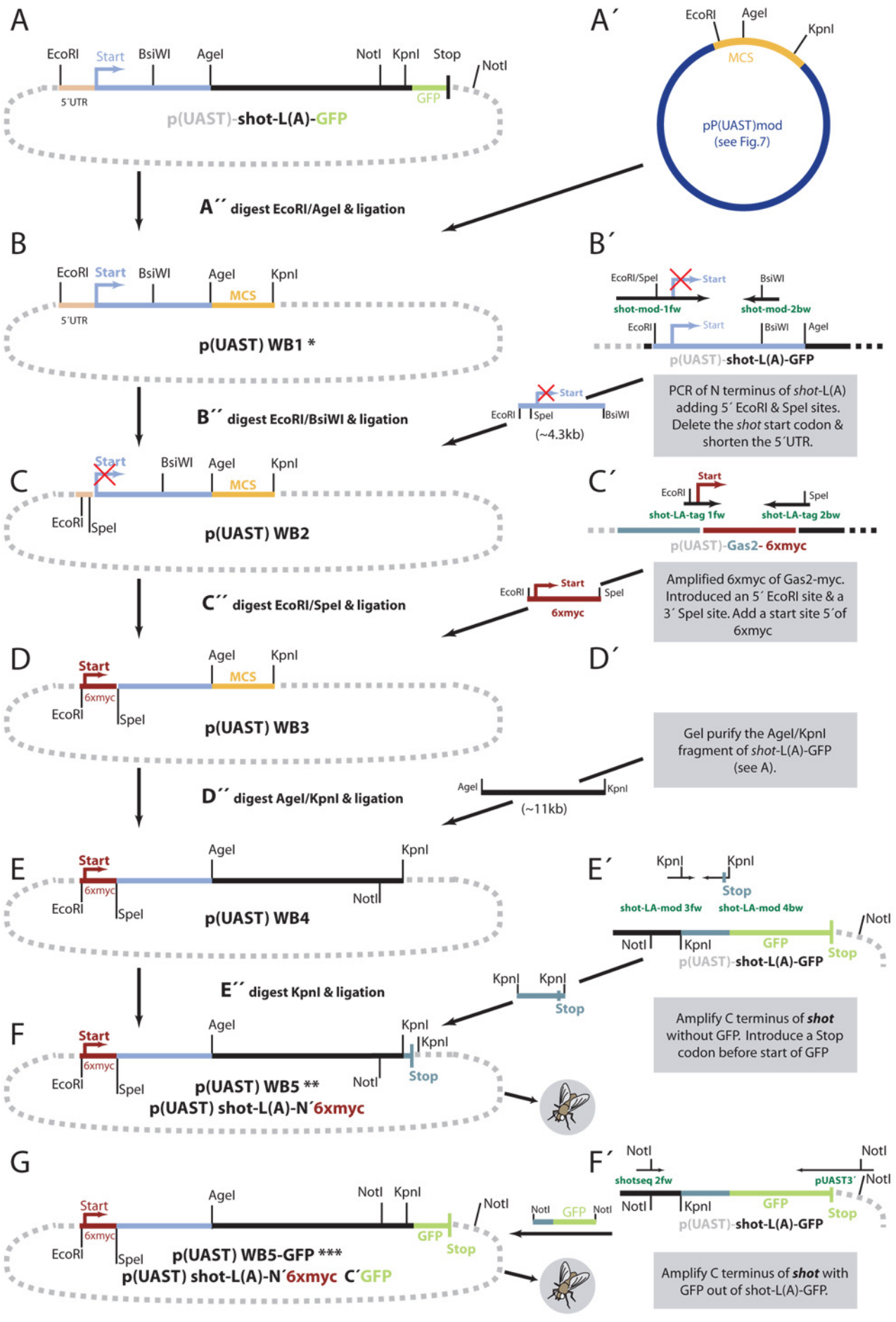

## Fig.8. Generation of *UAS-shot-L(A)-N´6myc (-C´GFP)*

**(A)** Starting point for all cloning strategies was the *p{UAST}-shot-L(A)-GFP* vector kindly obtained from Peter Kolodziej (Vanderbilt Medical Centre, Tennessee, USA). (**B)** Generation of *p{UAST}-WB1*. **(A´´)** To be able to introduce an N´ terminal epitope tag into the *shot* cDNA it was necessary to isolate the *shot* N terminus, such that suitable restriction sites could be used. To this end the N terminal *EcoR*I/*Age*I 4,3kb fragment of *shot* was introduced into *p{UAST}mod* (see Fig.7) using the newly introduced *Age*I site of *p{(UAST}mod*. Ligation success was tested by colony PCR using the primers shotseq1 and p{UAST}5´. Positive colonies were cultured and isolated DNA was sequenced using the primers p{UAST}5´and p{UAST}3´ (see wb45-50). The resulting plasmid was named *p{UAST}-WB1* (B). It was used to generate *p{UAST}-WB2* (C), *p{UAST}-*Δ*actin1* (Fig.9B) and *p{UAST}-* Δ*Plakin2* (Fig.10B). **(C)** Generation of *p{UAST}-WB2* (modifying the N-terminus of *shot* in *p{UAST}-WB1*). **(B´)** To introduce an N terminal tag before *shot*, the N´ terminus of the cDNA had to be modified. The primer shot-mod1fw was designed such, that the Start codon of *shot* was deleted. With the same primer two restriction sites (*EcoR*I/*Spe*I) were introduced 5´ to the start of the *shot* gene. In addition a glycin residue was introduced 5´of the start of the gene (with Shot-mod-1fw). Glycin can rotate freely and thus can operate as a joint and spacer potentially making the epitope tag more accessible for antibodies. To this end a PCR fragment using shot-mod1fw and shot-mod2bw was generated. **(B´´)** The *EcoR*I/*BsiWI* fragment of *p{UAST}-WB1* was substituted with this PCR product. Ligation success was tested by colony PCR using the primers p{UAST}5´and shot-L(A) 2bw. Positive colonies were cultured and obtained DNA was sequenced. The yielded plasmid was named *p{UAST}-WB2*. It was used to generate *p{UAST}-WB3* (D). (**D)** Generation of *p{UAST}-WB3*: introducing an N´ terminal 6xmyc tag into *p{UAST}-WB2*. The *6cmyc* epitope tag coding sequence (6x ATG GAG CAA AAG CTC ATT TCT GAA GAG GAC TTG ATG AAT) coding for the 6x MEQKLISEEDLNE epitope was PCR amplified out of *UAS-Gas2-6cmyc* (materials and methods 2.8.1.2.). To this end the primers shot-LA-tag1fw and shot-LA-tag2bw were used. shot-L(A)tag 1fw was designed Such, that an *EcoR*I site was introduced at the 5´end of 6cmyc. In addition a translation initiation sequence, the Kozak consensus sequence (A/G(-3)xx A(+1)TG-G(+4)) (Kozak, 1987), was added at the Start of the *6cmyc* repeats. The Kozak sequence can increase the translation levels of proteins considerably. shot-L(A)-tag 2bw was designed such that the stop codon 3´of the 6myc epitope tag present in *pUAST-Gas-6cmyc* was deleted. An extra *Spe*I site 3´ of the Stop codon was introduced with the same primer. **(C´´)** The PCR product was introduced into *p{UAST}-WB2* making use of the *EcoR*I/*SpeI* restriction sites. Ligation success was tested by colony PCR using the primers shot- L(A)tag-1fw and shot-L(A)mod2bw. Positive clones were cultured and isolated plasmid DNA was sequenced using the primers p{UAST}5´, shotseq1bw, shotseq5fw, shotseq6fw, shotseq7fw, shotseq8fw, shotseq8fw, shotseq9fw, shotseq10bw, AgeIfw and p{UAST}3´ (see wb67-70 & wb77-84). The yielded plasmid was named *p{UAST}-WB3*. It was used to generate *p{UAST}-WB4* (E). It can be used to generate *shot* constructs carrying an N terminal 6xcmyc epitope tag. **(E)** Generation of *p{UAST}-WB4* (adding the *shot Age*I /*Kpn*I fragment to *p{UAST}-WB3*). After modifying the N-terminus, the rest of the *shot* cDNA was added sequentially. **(D´)** Large amounts of *p{UAST}-shot-L(A)-GFP* plasmid Midiprep DNA were digested with *Age*I and *Kpn*I. The ~11kb *shot* fragment was gel eluted. **(D´´)** The cleaned fragment was introduced into *p{UAST}-WB3* using the *Age*I/*Not*I sites. Ligation success was tested by colony PCR using the primers shotseq2fw and p{UAST}3´. Positive colonies were cultured and isolated DNA was sequenced using the primers shotseqAgeI and p{UAST}3´. The obtained plasmid was named *p{UAST}-WB4* (E). It was used to generate *p{UAST}-WB5* (*p{UAST}-shot-L(A)-N´6xmyc);* (8F) and *p{UAST}-WB5-GFP* (*p{UAST}-shot-L(A)-N´6xmyc-C´GFP),* (G). It can be used to generate *shot* constructs with a N terminal *6xcmyc* epitope tag. **(F)** Generation of *p{UAST}-shot-L(A)-N´6xmyc (p{UAST}-WB5).* **(E´)** The primers shot-L(A) 3fw and -4bw were used to amplify the C terminal fragment of *shot*. shot-L(A) 4bw was designed such that a Stop codon and a *Kpn*I restriction site were introduced at 3´end of the PCR fragment. **(E´´)** The PCR product was introduced into *p{UAST}-WB4* using the *Kpn*I sites. Ligation success and orientation of the insert were tested by colony PCR using shotseq3fw and p{UAST}5´. Positive clones were cultured and isolated plasmid DNA was sequenced (wb120-wb122). The resulting plasmid was named *p{UAST}-shot-L(A)-N´6xmyc* (*p{UAST}-WB5*); (F). The construct was injected and transgenic flies were generated; see materials and methods 2.2.). **(G)** Generation of *p{UAST}-shot-L(A)-N´6xmyc-C´GFP (p{UAST}-WB5-GFP).*The primers shotseq2 and pUAST3´were used to PCR amplify the C terminus of *shot-gfp* **(F´).** The obtained amplicon was *Not*I digested and introduced into *p{UAST}-WB4* which was also cut with *Not*I (F´´). Ligation success and orientation of the insert were tested by colony PCR using shotseq3fw and p{UAST}5´. The resulting plasmid was named *p{UAST}-shot-L(A)-N´6xmyc-C´GFP* (*p{UAST}-WB5-GFP*); **(G)**. The construct was injected and transgenic flies were generated; see materials and methods 2.2.). All primers can be found in the Appendix and all sequences can be obtained upon request.

**Fig.9.**
**Generation of *p{UAST}-shot-L(A)ΔABD* (Actin Binding Domain)**

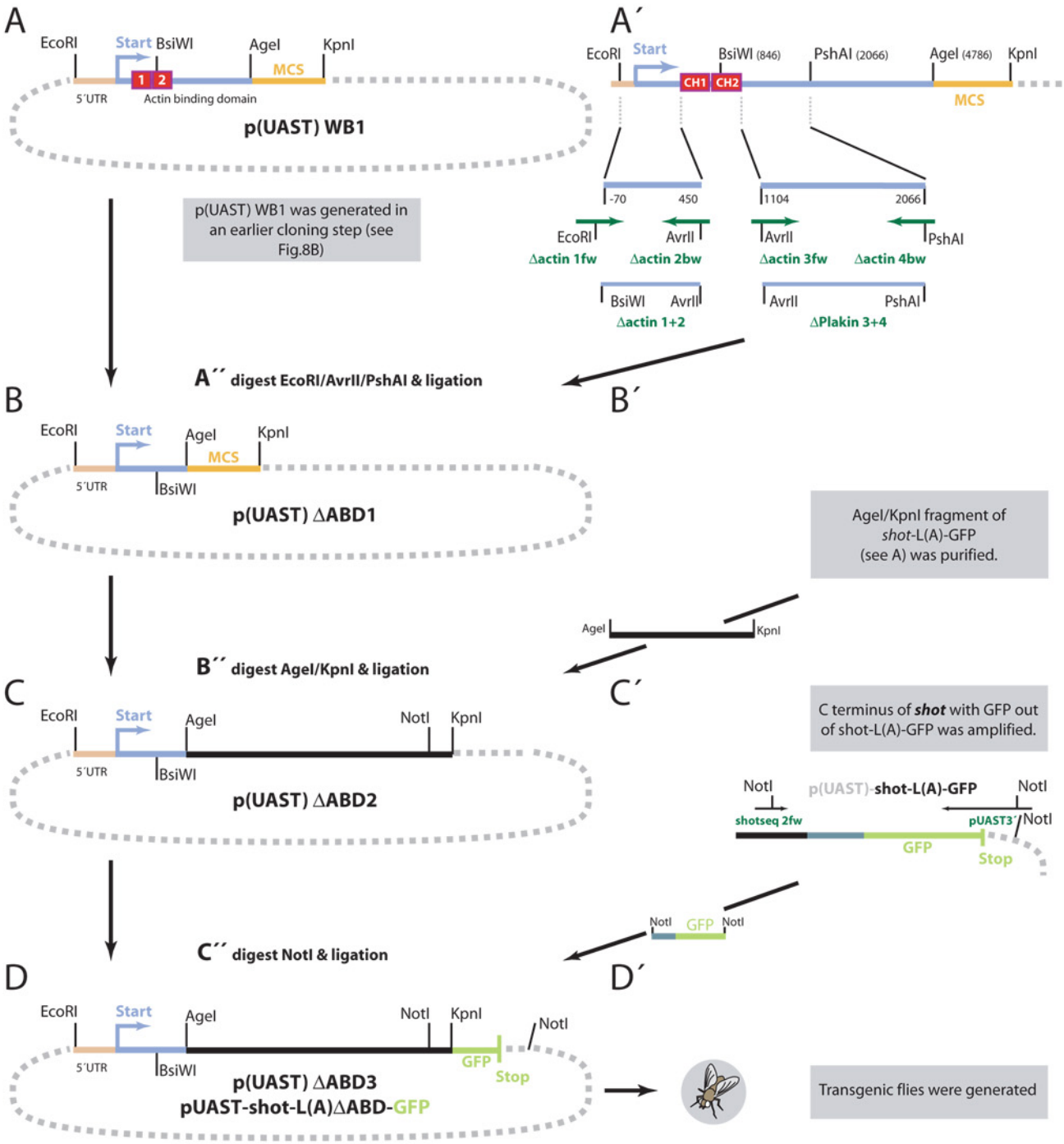

## Fig.9. Generation of *UAS-shot-L(A)-ΔABD-GFP*

To exclude that potential interactions of Shot-L(C) with actin obscure interpretations of our findings we generated a deletion construct lacking both CH domains (Δbp448-1104); *p{UAST}-shot-L(A)Δactin-GFP*. **(A-B)** Generation of *p{UAST}-Δactin1*; deleting the actin binding domain coding sequence from *p{UAST}-WB1* (A). The *EcoRI* (-81) and *PshAI* (2066) fragment of the *shot* 4.3kb cDNA in *p{UAST}-WB1* (A; see Fig.8B) was substituted. The fragment replacing this stretch lacked the actin binding domain coding region (bp448-1104). **(A´)** To this end two Pfu PCR products were generated using the primers Δactin1fw+2bw and Δactin 3fw+4bw. The first primer pair amplified the *shot* fragment preceding the Calponin homology domains out of *p{UAST}-WB1* (Δactin 1+2: bp450-1104). An *Avr*II restriction site (cctagg) and a ½*PshA*I restriction site (gacnn(nngtc)) were added to the 3´ end of the PCR product by mutagenesis. The second PCR product (Δactin 3+4) contained the region after the actin binding domain (from bp1105-2082) including the 3´ *PshA*I restriction site. Δactin 3fw was designed to introduce an *Avr*II restriction site at the 5´end of the PCR fragment Δactin 3+4. **(A´´)** The two PCR products (Δactin 1+2) cut with *Eco*RI/*Avr*II and (Δactin 3+4) cut with *Avr*II/*PshA*I were ligated in a one step triple ligation into *p{UAST}-WB1* cut with *Eco*RI/*PshA*I. Ligation success was checked by colony PCR using the primers Δactin4bw and p{UAST}5´. Positive colonies were cultured and isolated plasmid DNA was sequenced. **(B)** The yielded plasmid was named *p{UAST}-WB-Δactin1*. It was used to generate *p{UAST}-WB-Δactin2*. **(C)** Generation of *p{UAST}-WB-Δactin2*. After deleting the actin binding domain from the N-terminus of the *shot* 4,3kb fragment the cDNA was reassembled successively. To this end a *shot* ~11kb *Age*I/*Kpn*I fragment obtained earlier (Fig.8,D´) was introduced into *pUAST-WBΔactin1* (A´´). Ligation success was tested by colony PCR using the primers shotseq2fw and p{UAST}3´. Positive colonies were cultured and isolated DNA was sequenced using the primers shotseqAgeI and p{UAST}3´. The obtained plasmid was named *pUAST-WBΔactin2*. It was used to generate *pUAST-WBΔactin3* (*pUAST-shot-L(A)ΔABD-GFP*). **(D)** Generation of *pUAST-WBΔactin3* (*pUAST-shot-L(A)ΔABD-GFP*). The last parts of *shot* plus *GFP* were added to *p{UAST}-WBΔactin2* (C). To this end the Pfu PCR amplified C terminal fragment from *shot-L(A)-GFP* (flanked by *Not*I sites) was introduced into the *Not*I site of *p{UAST}-WBΔactin2*. Ligation success and orientation were tested by colony PCR using the primers shotseq3 and pUAST3´. Positive colonies were cultured and isolated DNA was sequenced. The obtained plasmid was named *p{UAST}-shot-L(A)ΔABD-GFP* (*p{UAST}-Δactin-GFP*). Transgenic flies were generated by injection of the plasmid (service by BestGene Inc., Rustic Bridge, Chino Hills, CA, US). For details see materials and methods. All primers can be found in the Appendix and respective sequences can be obtained upon request.

**Fig.10.**
**Generation of p{UAST}-shot-L(A)ΔPlakin**

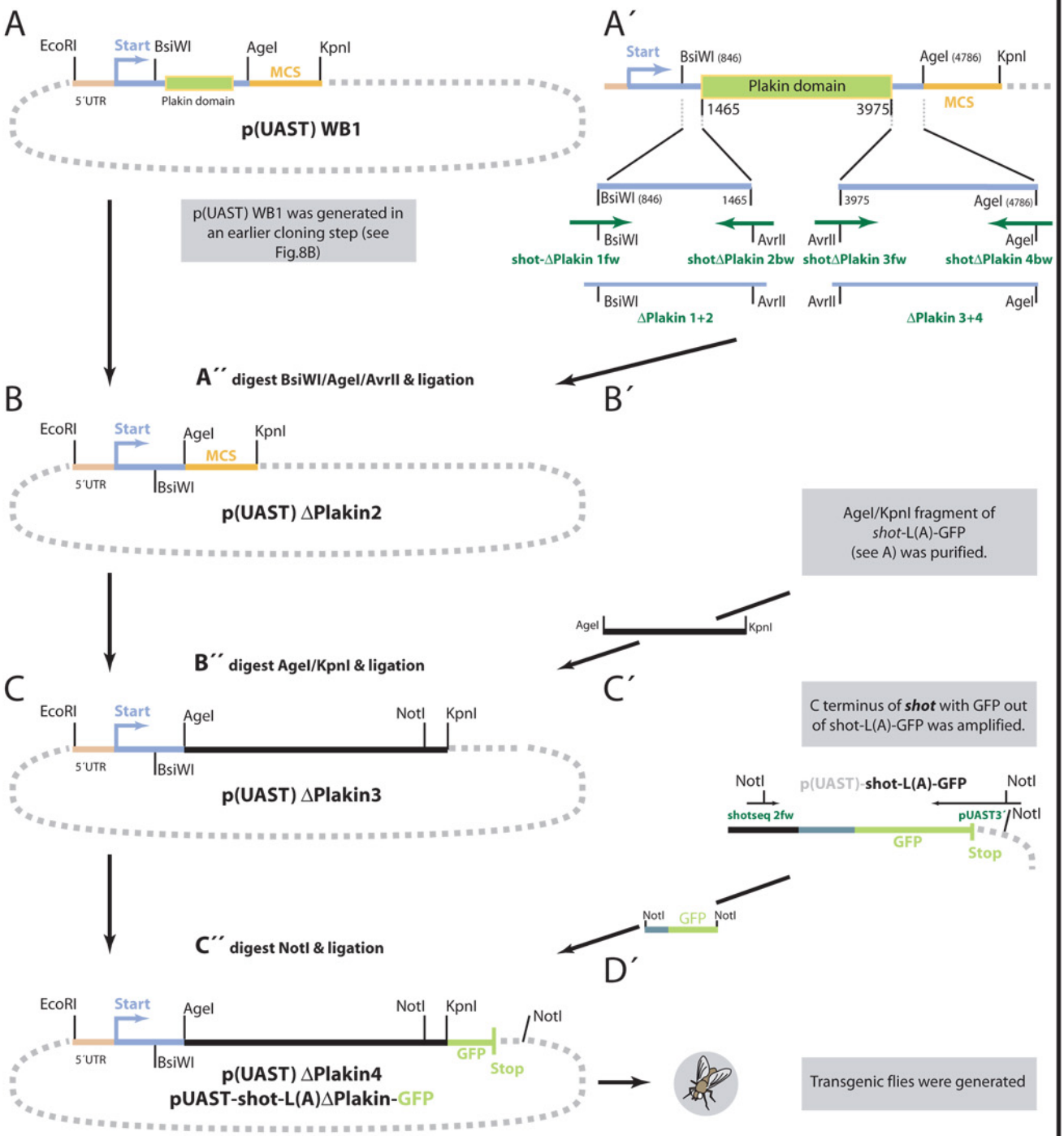


E

```
CLUSTAL W (1.82) multiple sequence alignment

alignment Drosophila Paxillin :: Human Paxillin Isoform A

dros            ---MSSKLISSSFHSSPLS--DCFKVGEFERRLDALLADLQNSVPGQPQQPQPQ------ 49
homo            MDDLDALLADLESTTSHISKRPVFLSEETPYSYPTGNHTYQEIAVPPPVPPPPSSEALNG 60
                   :.: * . .  :* :*    *   *      :     *: .   *  * *.
```

## Fig.10. Generation of *p{UAST}-shot-L(A)ΔPlakin-GFP*

Generation of *p{UAST}*-Δ*Plakin2*. The stretch coding for the plakin domain (1465-3972) was deleted from *p{UAST}-WB.1* **(A)**. The *BsiW*I (846bp) and *Age*I (4786) restriction sites of the *shot* cDNA in *p{UAST}-WB1* were used to substitute the (*BsiW*I/*Age*I) *shot* cDNA fragment with one lacking the plakin domain coding region. **(A´)** To this end two Pfu PCR products were generated using the primers ΔPlakin1fw + 2bw and ΔPlakin 3fw+4bw. The first PCR product (ΔPlakin 1+2) comprised the *shot* fragment preceding the plakin domain (828-1464) adding an *Avr*II restriction site (cctagg) and an *Age*I restriction site (accggt) to the 3´terminal end. The second PCR product ΔPlakin 3+4 comprised the region after the plakin domain (from 3973-4246) including a 3´ *Age*I restriction site, an *Avr*II restriction site included in ΔPlakin 3fw at the 5´end of the PCR fragment. **(A´´,B´)** A triple ligation was conducted, fusing *p{UAST}-WB1* digested with *BsiW*I/*AgeI*, the PCR fragment (ΔPlakin 1+2) cut with *BsiW*I/*Avr*II and the PCR fragment (ΔPlakin 3+4) cut with *Avr*II and *Age*I thus deleting the Plakin domain (1465-3972) from the N terminus. Ligation success was tested by colony PCR using the primers ΔPlakin1fw and ΔPlakin4bw. Positive colonies were cultured, DNA was obtained and sequenced using the primers p{UAST}5´, shotseq5fw, shotseq6fw, shotseq7fw, shotAgeIfw and p{UAST}3´, (see wb71 – wb76). **(B)** The obtained plasmid was named *p{UAST}*-Δ*Plakin2* . It was used to generate *p{UAST}*-Δ*Plakin3*. **(C)** Generation of *p{UAST}*-Δ*Plakin3*: Adding the *Age*I/*Kpn*I fragment to *p{UAST}*-Δ*Plakin2*. After deleting the plakin domain coding region the rest of the *shot* cDNA was added successively. **(C´)** To this end large amounts of *p{UAST}-shot-L(A)-GFP* were digested with *Age*I/*Kpn*I. The ~11kb *AgeI*/*Kpn*I fragment obtained was gel eluted. **(B´´)** The clean fragment was introduced into *p{UAST}*-Δ*Plakin2* using the *Age*I/*Kpn*I restriction sites. Ligation success was tested by colony PCR using shotseq2 and p{UAST}3´. Positive colonies were cultured and DNA was obtained. The plasmid size was checked on an agarose gel after *Kpn*I (unique) digestion. Positive clones were sequenced using the primers p{UAST}5´(wb114), shotseq5fw (wb115), shotseq6fw (wb116), shotseqAgeIfw (wb117), shotseq3fw (wb118) and p{UAST}3´(wb119). **(C)** The obtained plasmid was named *p{UAST}*-Δ*Plakin3*. It was used to generate *p{UAST}*-Δ*Plakin4*. **(D)** Generation of *p{UAST}*-Δ*Plakin4* = *p{UAST}-shot-L(A)*Δ*plakin-GF*: **(D´)** To add the missing C-terminal *shot* fragment and GFP to *p{UAST}*Δ*Plakin3* the *Not*I fragment of the *shot*-cDNA was amplified with Pfu PCR using the primers shotseqfw2 and p{UAST}3´. **(C´´)** The PCR fragment was *Not*I digested and introduced into *p{UAST}*-Δ*Plakin3*. Ligation success was tested by colony PCR using the primers shotseq3 and p{UAST}3´. Positive colonies were cultured, DNA was obtained and sequenced (wb126-wb129). **(D)** The obtained plasmid was named *p{UAST}-shot-L(A)*Δ*Plakin-GFP* or *p{UAST}*-Δ*Plakin4*. Flies carrying this construct were raised. All primers used can be found in the Appendix and sequences can be obtained upon request.

(**E)** Drosophila Paxillin contains a potential SH3 binding motif. *In-silico* analysis reveals the presence of a potential SH3 binding site (PXXP) in Drosophila Paxillin. The site is at a similar position like the SH3 binding site of hPaxillin and depicted in red.

**Fig.11.**
**Generation of p{UAST}-shot-L(A)ΔEB1-GFP**

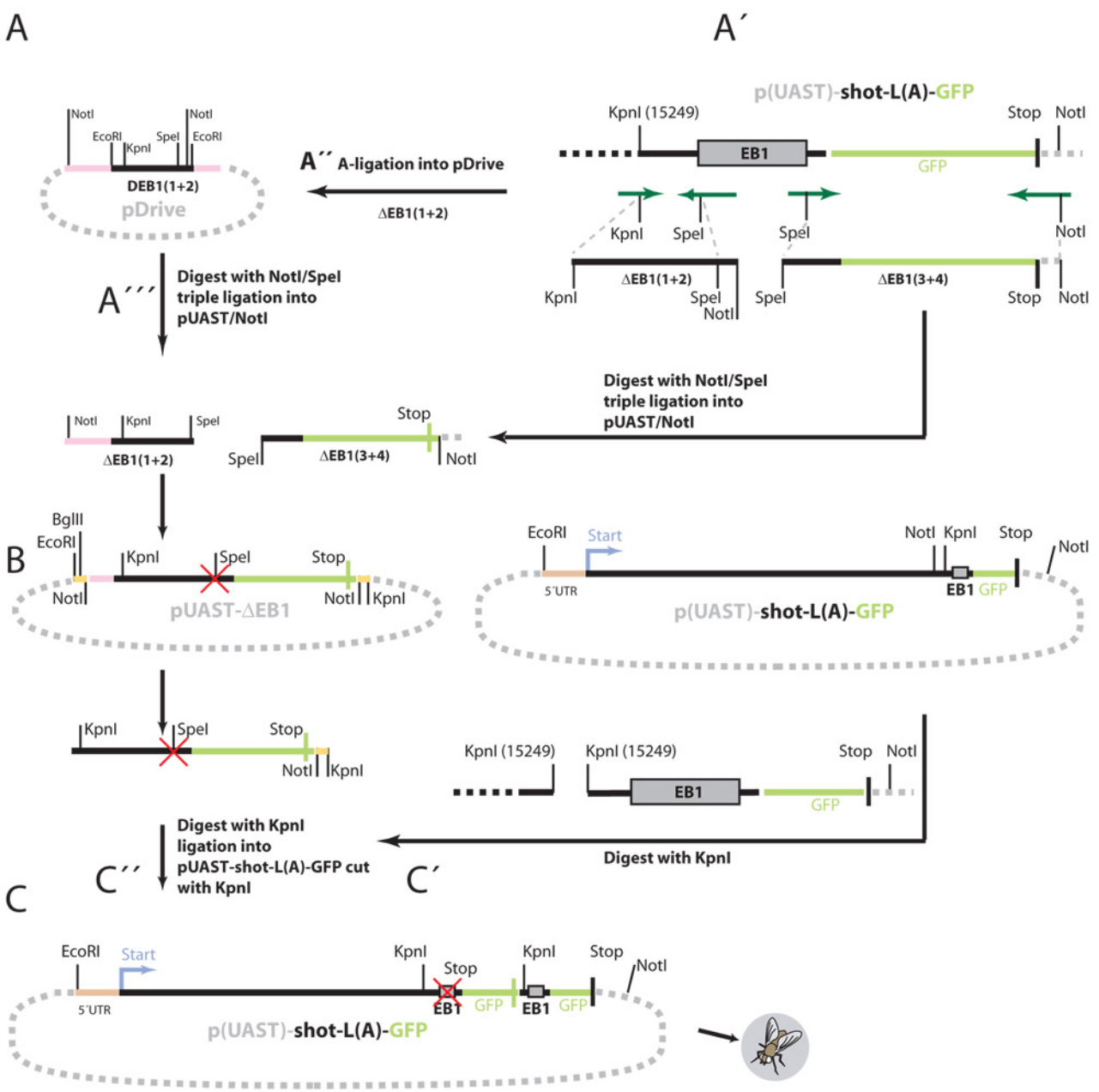

## Fig.11. Generation of *UAS-shot-L(A)-ΔEB1$_{aff}$*

To asses the requirement of the EB1 domain for tendon cell integrity and localisation of Shot I generated a Shot full length construct lacking the EB1affinity domain. **(A)** Generation of *pDrive-ΔEB1* : deleting the EB1 binding domain (15432bp - 15573bp) from *shot-L(A)-GF*P. The *Kpn*I restriction site (15278bp) of the *shot* cDNA– in *p{UAST}-shot-L(A)-GFP* was used to introduce an alternative C terminal end of *shot*, lacking the EB1 binding site (15432bp - 15573bp). **(A)** Generation of *p{UAST}-ΔEB1-GFP*. **(A´)** To this end two Pfu PCR products were generated using the primers Δ-EB1fw+2bw and ΔEB1 3fw+4bw respectively. The first PCR product (ΔEB 1+2) comprised the *shot* fragment preceding the EB1 domain (15249 – 15408) adding a *Spe*I restriction site (actagt) and a *Not*I restriction site (gcggccgc) to the 3´ end. The second PCR product (ΔEB1 3+4) comprised the region after the EB1 domain (15574-16353) including GFP, the Stop of *shot-L(A)-GFP* and a 3´ *Not*I restriction site. ΔEB1-3fw introduced an *Spe*I restriction site at the 5´end end of the PCR fragment allowing ligation with the 3´end of (ΔEB1 1+2). **(A´´)** The ΔEB1(1+2) PCR product was A-tailed and inserted into *pDrive* (Promega). Ligation success and orientation was tested by colony PCR using the primers M13fw-40 + ΔEB1-2bw (for ΔEB1-1+2) and M13fw-40 + ΔEB1-4bw (for ΔEB1-3+4) respectively. Positive colonies of *pDrive-(ΔEB1-1+2)* were sequenced using the primers p{UAST}5´ and p{UAST}3´(wb51-54). *pDrive-(ΔEB1 1+2)* and *PCR* product *ΔEB1-(3+4)* were digested with *Spe*I/*Not*I and the *shot*-fragments were gel eluted. *p{UAST}* was digested with *Not*I. **(A´´´)** The three digested and cleaned fragments were ligated in a one step triple ligation. **(B)** Ligation success was tested by colony PCR using the primers ΔEB1-1fw and ΔEB1-4bw. Positive colonies were cultured and isolated DNA was sequenced (wb85-wb88). Sequencing revealed correct orientation of the insert. A positive colony (wb87+88) was used for further subcloning steps and named *p{UAST}-ΔEB1*. (C) Generation of *p{UAST}-shot-L(A)ΔEB1-GFP*. **(C´&C´´)** The ΔEB1 fragment out of *p{UAST}-ΔEB1* was excised using the flanking *Kpn*I restriction sites and introduced into the *Kpn*I site of *p{UAST}-shot-L(A)-GFP*. Ligation success and orientation was checked by colony PCR using the primers shotseqfw2 and p{UAST}3´. Positive colonies were cultured and isolated DNA was sequenced using the primers shotseq2fw, shotseq3fw and p{UAST}3´, (see wb95-wb100). **(C)** The obtained plasmid was named *p{UAST}-shot-L(A)ΔEB1-GFP* and used to generate transgenic flies (materials and methods 2.2.) All primers used can be found in the Appendix and sequences can be obtained upon request.

## 3.4. Structure-function analyses of Shot localisation and function in motorneuronal dendrites

I capitalised on the existing and newly generated Shot constructs (Tab.3) to conduct a structure function analysis of Shot. My aim was to understand the requirement of Shot domains for the process of dendritic development (see below). I assessed the requirement of different domains for two crucial aspects of Shot function. First, I analysed in how far individual domains are required for the characteristic dendritic localisation of Shot. Second, I tested the requirement of Shot domains for their ability to promote dendritic development. In the following I will describe and discuss the observations made when using the different constructs in my structure function analysis.

### 3.4.1. Shot-L(C)-GFP localises normally and rescues dendrites

Shot contains a high affinity actin-binding domain at its N-terminus. In isolation the actin binding domains of plectin (Fontao et al., 2001), BPAG (Yang et al., 1996), MACF (Leung et al., 1999; Karakesisoglou et al., 2000) and Shot (Lee and Kolodziej, 2002) bind directly to F-actin and co-localise with actin filaments (Jefferson et al., 2004). The actin biding motif of Shot consists of two successive Calponin homology domains (CH1 + CH2) (Roper et al., 2002). CH domains contain 100 residues and are present in both, signalling and cytoskeletal proteins (Jefferson et al., 2004). Although CH1 and CH2 domains are structurally related, their function is most probably distinct (Van Troys et al., 1999). From precedents set by other spectraplakins or spectrins, the major determinant for actin binding is typically in the CH1 domain, whereas CH2 alone binds actin very weakly (Gimona and Mital, 1998; Gimona and Winder, 1998; Stradal et al., 1998; Yang et al., 1999; Fontao et al., 2001). Similar results have been obtained for the ABD of Shot (Lee and Kolodziej, 2002).

In this context it is crucial to understand that Shot displays 4 different N-termini in its various long isoforms (A,B,C,D; see Fig.1 and. Shot-L(C)-GFP represents the long Shot isoform C (Shot-PC, 5160aa) which, endogenously, seems to be expressed in the epidermis but not the CNS (Lee et al., 2000; Roper and Brown, 2003). Isoform C contains only CH2 but lacks CH1 (Fig.1 and Fig.5), and Shot-L(C) has therefore been used to test dependence of Shot function on Actin binding (Lee and Kolodziej, 2002). However, this assumption has to be reconsidered: The absence of CH1 in Shot-L(C) is due to an alternative transcriptional start site which also adds an alternative N-terminal protein stretch upstream of CH2 (see Fig.1). As demonstrated for Plectin and Bpag1, this region seems not to be required for actin binding

*per se*, but seems to be involved in dimerisation and potentially multimerisation of actin filaments, providing a possible mechanism for bundling of microfilaments (Fontao et al., 2001; Young et al., 2003).

With this information in mind, I expressed Shot-L(C)-GFP in embryonic motorneurons and found that it localises to dendrites in a pattern indistinguishable from Shot-L(A)-GFP (Fig.12). Also at late larval stages Shot-L(C)-GFP is indistinguishable from Shot-L(A)-GFP (Fig.13). Proper localisation is a prerequisite for function but not necessarily sufficient. Thus, I assessed the functionality of Shot-L(C)-GFP in the same kind of rescue assay successfully performed with Shot-L(A)-GFP already (see Chapter 3.2. and Fig.14). To this end, I expressed Shot-L(C)-GFP with two motorneuronal driver lines *RN2E-Gal4* and *MzVum-Gal4* in a *shot* loss of function background. Upon overexpression of Shot-L(C)-GFP, dendritic morphology was partially restored (Fig.14). This finding suggests that, although Shot(C) is normally not expressed in the nervous system (Lee et al., 2000), it seems to conduct activity in the context of dendritic development. Interestingly, the same construct completely failed to restore another *shot* phenotype in the nervous system, the mislocalisation of FasciclinII II (FasII) in the CNS (Fig.14). This partial rescue of the dendritic *shot* mutant phenotype with the Shot-L(C) construct is comparable with my analysis of the $shot^{KakP2}$ mutant phenotype (Chapter 3.7.). Since $shot^{KakP2}$ mutant embryos have been suggested to lack the L(A)/Shot-PE and L(B) isoforms and thus express only isoform C and D (Mende, 2004), they confirm my findings with Shot-L(C)-mediated rescue.

Since, I expected that binding to actin would be an essential prerequisite for Shot function (Lee and Kolodziej, 2002), I was surprised to find such a mild phenotype. I can think of two possible explanations. First, actin binding may only be partly required for Shot function and dispensable for its localisation in dendrites. Second, the weak actin binding capability of CH2 (Gimona and Mital, 1998; Gimona and Winder, 1998; Stradal et al., 1998; Yang et al., 1999; Lee and Kolodziej, 2002) may confer some activity to Shot in this particular cellular context. To distinguish between these two possibilities, I decided to generate a Shot-L(A)ΔABD-GFP construct lacking both Calponin domains (Δaa150-368aa; Tab.3; Fig.9), but still containing the N-terminal portion of Shot-PA preceding the ABD. The respective cloning work has been carried out, but the transgenic fly lines could unfortunately no longer be generated in the timeframe of this work (see Fig.9).

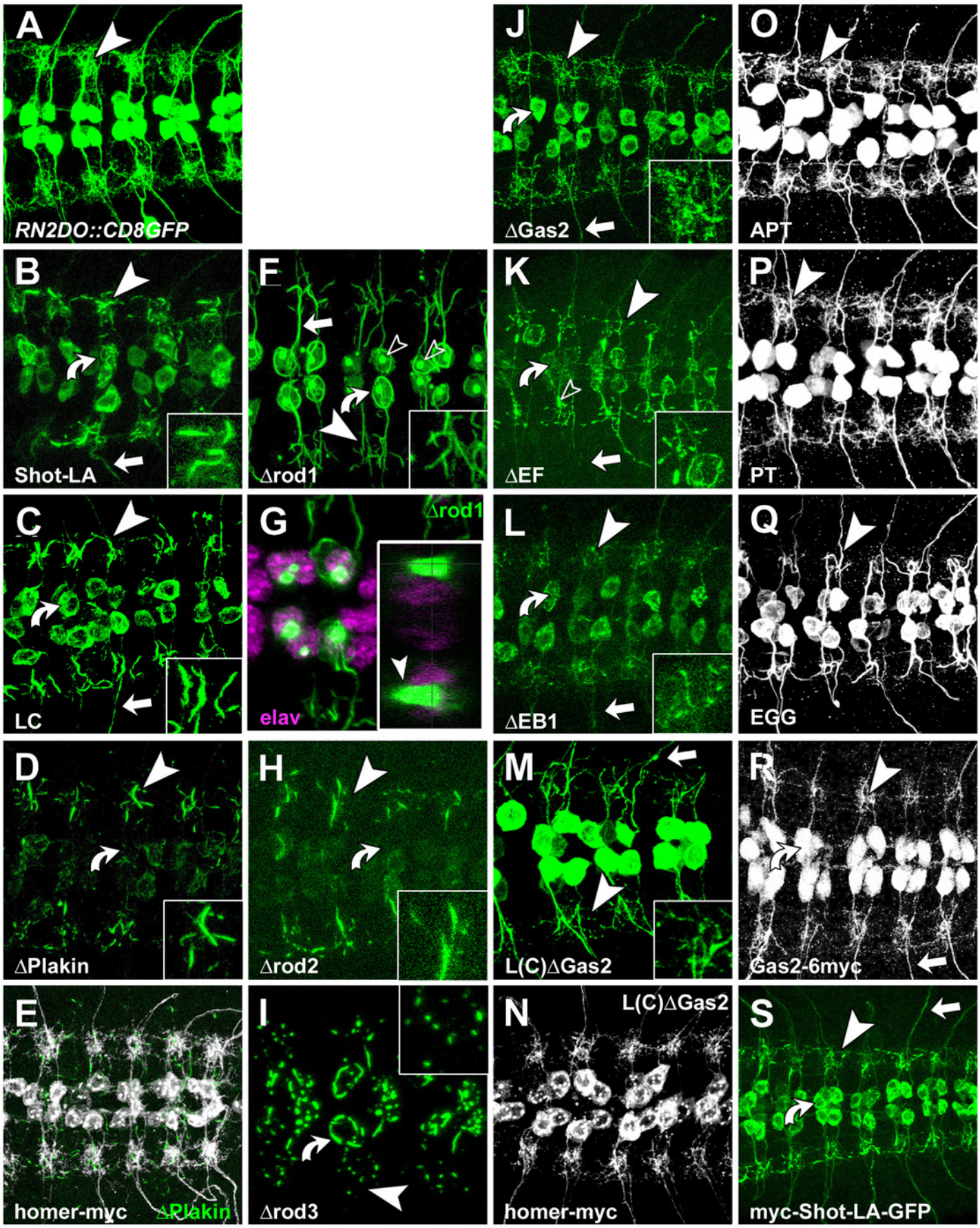
A
RN2DO::CD8GFP
B
Shot-LA
C
LC
D
ΔPlakin
E
homer-myc ΔPlakin
F
Δrod1
G
Δrod1
elav
H
Δrod2
I
Δrod3
J
ΔGas2
K
ΔEF
L
ΔEB1
M
L(C)ΔGas2
N
L(C)ΔGas2
homer-myc
O
APT
P
PT
Q
EGG
R
Gas2-6myc
S
myc-Shot-LA-GFP

**Fig.12: A comparative analysis with Shot deletion constructs reveals differential requirements of individual domains for the localisation of Shot in the CNS and dendrites of late *Drosophila* embryos**

To study the importance of Short stop domains for proper localisation in the CNS, Shot and Shot deletion constructs were expressed in aCC/RP2 motorneurons using the *RN2D+O-Gal4* driver line. Pictures represent a dorsal view on the CNS of stg.17 *Drosophila* embryos (see Fig.13.I) All construct details can be found in Fig.5 and Table 3. If not mentioned otherwise all constructs are GFP (green fluorescent protein) tagged and depicted in green (A-R and S). Stainings against cmyc (P,R) and Tap (C-K) tags are depicted in white. (G) Nuclear elav antibody staining is in magenta. Where sensible a magnification of the dendritic localisation of the respective construct is included in the inset of the figure. Dendritic localisation is generally pointed out with an arrowhead, somatic localisation with a curved arrow, axonal localisation with an arrow.

**(A)** Morphology of aCC/RP2 dendrites in the central nervous system of *Drosophila* visualised with the inert cell surface marker CD8-GFP as reference. **(B)** Shot-L(A)-GFP prominently enriches in the proximal thick dendritic branches but fails to get into the finer branches (compare with A) and only weakly localises in the primary axon. The soma of the neurons is indicated (*). **(C)** Shot-L(C)-GFP (lacking half the ABD domain) localisation is almost distinguishable from Shot-L(A)-GFP with strong dendritic accumulation and normal somatic enrichment. **(D)** The Shot-L(A)ΔPlakin-GFP construct localises to dendrites like Shot-GFP but mostly lacks from the cell body. **(E)** The overexpression of Plakin does not induce a dominant effect as visualised by coexpression of homer-myc (morphological marker comparable to CD8-GFP (see A). **(F)** Shot-L(A)Δrod1-GFP localises to dendrites but fails to enrich prominently in the compartment. On the other hand the enrichment in the primary distal neurite is pronounced as compared to Shot-GFP (F as comp. to B). Shot-L(A)Δrod-GFP associates strongly with microtubules in an @ like shape (curved arrow). Furthermore a prominent somatic GFP enrichment can be observed (open arrowhead), see also (G). **(G)** Antibody staining against the nuclear marker elav (magenta) reveals that the GFP enrichment (green) of Shot-L(A)Δrod1-GFP is pervading the nucleus and partially localises in the perinuclear region (arrowhead). **(H)** Shot-L(A)Δrod2-GFP shows dendritic enrichment but is mostly absent from the soma. **(I)** Shot-L(A)Δrod3-GFP severely mislocalises in dendrites and the soma and it cannot be observed along the axon. The somatic staining pattern slightly resembles the @ like localisation of Shot-L(A)Δrod1-GFP. **(J)** Shot-L(A)ΔGas2-GFP displays a completely altered staining pattern strongly resembling actin-GFP in dendrites (see Fig.4M). It localises speckled along the axon and diffusely at the cell body. **(K)** Shot-L(A)ΔEF-hand-GFP enriches in dendrites and the soma but aggregations form not found in Shot-LA (open arrowhead). **(L)** Shot-L(A)ΔEB1-GFP enriches weakly at dendrites and localises mostly normal at the cell body. **(M)** Shot-L(C)ΔGas2-GFP (pot. lacking actin + MT binding) does enrich in a fashion resembling neither Shot-GFP (B), Actin nor Tubulin (Fig.4M and 4N). **(N)** Unlike in tendon cells the overexpression of Shot-L(C)ΔGas2-GFP does not induce a dominant phenotype in dendrites (visualised with homer-myc, compare with A). **(O, P)** The N terminal APT (ABD + Plakin) and PT (Plakin) constructs localise to dendritic fields but fail to enrich prominently. **(Q)** The C-terminus of Shot strongly associates with microtubules in neurons but fails to enrich in the dendritic areas. **(R)** The isolated Gas2 binding domain (Gas2-6myc) fails to strongly associate with microtubules but localises more diffuse like a general cell marker (e.g. comp. with A). **(S)** The localisation of the double tagged 6myc-Shot-L(A)-GFP construct (here C-terminus in green) seem unaffected at embryonic dendrites.

### 3.4.2. The plakin domain is dispensable for Shot localisation to dendrites

Another N-terminal domain which might confer localisation properties to Shot is a large plakin domain (aa489-aa1324). Plakin domains mediate protein-protein interactions with the potential to impart specificity to protein function and localisation (Jefferson et al., 2004). Even though this domain has the potential to affect Shot activity significantly, it has not been analysed so far. A yeast two-hybrid screen carried out in our lab revealed that Paxillin binds to this domain, and this finding was further supported by genetic and biochemical data suggesting that Paxillin acts upstream of Shot, down-regulating its growth-promoting activity at NMJs (Mende, 2004; A. Prokop, personal communication). My *in-silico* analyses revealed that the Plakin domain of Shot and some other Plakin family member proteins comprises an embedded putative Src-homology 3 (SH3)[6] domain (Bateman et al., 2002; Letunic et al., 2002). Furthermore, I found that *Drosophila* Paxillin[7] harbours a core SH3 binding motif (PXXP[8]) at a similar position (aa43-46 in Pax-PA[9]) as human Paxillin (Turner, 2000) see Fig.10. Thus, there is good reason to believe that the plakin domain of Shot may have important regulatory capabilities.

To test this possibility, I generated a Shot-L(A)ΔPlakin-GFP construct (see Table 3, Fig.10). To this end, I precisely excised the plakin domain (aa489-aa1324; see Fig.5) from Shot-L(A)-GFP (details in Fig.10). Transgenic flies carrying the construct were subsequently used for localisation studies. When targeting Shot-L(A)-ΔPlakin expression to motorneurons via *RN2D+O-Gal4*, it does not induce any dominant effects in dendrites and localisation at dendrites appears perfectly normal (Fig.12). However, in contrast to many other Shot constructs, there is no detectable accumulation in the soma or nuclei of the targeted cells (Fig.12, Fig.13). My *in-silico* analyses revealed that a predicted bipartite nuclear localisation signal (NLS) is present at the Shot N-terminus (aa151 – aa2498)**[10]** with one part of this motif situated at (aa151-aa168) and the other within the Plakin domain (aa984-aa1001). Since this part of the NLS is deleted in the Shot-L(A)ΔPlakin-GFP construct, the whole motif might be disrupted and account for the absence of the construct from the cell body. In agreement with the presence of a predicted NLS, the N-terminal UAS-APT construct (see Fig.5) enriches in the nuclei of neurons (Mende, 2004) and tendon cell (Subramanian et al., 2003 and A.

[6] Ensembl: http://www.ensembl.org/Drosophila_melanogaster/protview?db=core;peptide=CG18076-PE
[7] FlyBase ID: FBgn0041789 and cg31794
[8] The Pawson lab homepage:
http://pawsonlab.mshri.on.ca/index.php?option=com_content&task=view&id=179&Itemid=64
[9] Pax-PA sequence as in Ensembl:
http://www.ensembl.org/*Drosophila*_melanogaster/protview?db=core;peptide=CG31794-PA
[10] Ensembl: http://www.ensembl.org/*Drosophila*_melanogaster/protview?db=core;peptide=CG18076-PE

Prokop, unpublished results). In support of this hypothesis, the presence of a genuine N-terminal NLS has been demonstrated for Shots close orthologue BPAG1 (Young et al., 2003).

Taken together, the Plakin domain is not required for Shot localisation to dendrites but my data strongly suggest that it contains part of a genuine nuclear localisation signal. Due to lack of time, the construct could no longer be used for functional rescue experiments. Thus I cannot comment on the requirement of this domain for Shot function in dendrites. But the *UAS-Shot-L(A)ΔPlakin-GFP* transgenic flies are presently being combined with *shot* mutant strains to prepare such experiments. Since N-terminal domains could so far not be shown to be important for the dendritic accumulation of Shot, I used further deletion constructs uncovering other regions of Shot.

### 3.4.3. Constructs with deletions in the rod domain

#### *3.4.3.1. Shot-L(A)Δrod1-GFP shows abnormal and normal features at dendrites*

The Shot molecule is of extraordinary length (8805aa; up to 400nm according to Roper and Brown, 2003) and a big part is occupied by the central spectrin repeat rod domain, separating the domains at the N- and C terminus. It was therefore thought to serve as spacer. In any case, we would suspect this domain to be of importance, since it is conserved amongst Spectraplakin family member proteins (Roper et al., 2002; Jefferson et al., 2004). Surprisingly, no specific function could be assigned to the rod domain of *Drosophila* Shot so far in other developmental contexts: Shot-L(A)Δrod1-GFP (deleting a large portion of the rod region; Δaa1204-aa4600; see Fig.5) fully rescues axon and sensory axon outgrowth defects and restores tracheal fusion (anastomosis) in *shot* mutant animals (Lee and Kolodziej, 2002; Lee and Kolodziej, 2002). This is paralleled by findings in vertebrate systems, where it has been shown that a mini-gene of vertebrate MACF/ACF7 whose principal architecture is similar to Shot-L(A)Δrod1-GFP could restore microtubule dynamic defects in ACF7 knockout cells (Kodama et al., 2003). Furthermore it has been shown that a similar MACF/ACF7-mini construct can crosslink actin and microtubules (Leung et al., 1999).

In contrast to the above mentioned examples, there are several reports suggesting a function for the rod domain in related molecules. Thus, a few deleted spectrin repeats in mammalian dystrophin cause a mild form of muscle dystrophy (Palmucci et al., 1994; Roper et al., 2002). Furthermore, the rod domain of related spectrins and (spectra)plakins has been implicated to play a role in dimerisation (Plectin; Foisner and Wiche, 1991; Wiche, 1998),

tissue elasticity (Dystrophin; Cross et al., 1990; Kahana et al., 1997) and transport (BPAG1; Liu et al., 2003; for review see Jefferson et al., 2004). Finally, the rod domain of the mammalian neuronal BPAG1n3 isoform has been shown to be crucial for retrograde axonal transport interacting with the dynactin/dynein complex via a so called ERM (ezrin/radixin/moesin) domain (Liu et al., 2003; Jefferson et al., 2004).

Taken together, existing data are contradictory, suggesting that the rod domain of Shot may be dispensable for some cellular processes but might be required for others. Therefore, I tested the capability of Shot-L(A)Δrod1-GFP to localise and execute normal function in the context of dendrites. Localisation studies with the *RN2D+O-Gal4* driver line revealed that Shot-L(A)Δrod1-GFP shows clear abnormalities, but crucial properties of the Shot-L(A)-GFP pattern are nevertheless retained (Fig.12). Unusual features of Shot-L(A)Δrod1-GFP expression are that it aggregates in vesicle-like GFP accumulations in the cell body (Fig.12). Several reasons might account for the formation of these aggregates. First, their formation might be the result of a specific transport failure induced by lacking cues present in the rod domain. Second, it might simply be cleaved GFP or construct fragments, accumulating in the nucleus. Nuclear accumulation of cleaved GFP is a phenomenon observed from time to time when overexpressing GFP tagged constructs. In order to distinguish between these possibilities, I performed double-labelling experiments with the neuronal nucleus marker anti-Elav (Fig. 12), and found that the GFP accumulation is vesicular, aggregating close to the nucleus, probably in the perinuclear region. In many cases the aggregates also reached into the nucleus or even pervaded it fully (Fig.12). Parallel experiments at earlier developmental stages have demonstrated that the GFP-aggregates accumulate over time (N. Sánchez-Soriano, personal communication). I further tried to pinpoint the subcellular compartment in which the aggregate forms. The endosomes appeared to be likely candidate compartments in which proteins with lacking localisation cues might accumulate. Thus, I performed co-labelling experiments using two antibodies against endosomal proteins, α-HRS and α-Drab5 (recommended and kindly obtained by Sean Sweeney, York, UK). However, I could not find any obvious overlap and thus failed to assign the aggregates to a specific sub-cellular compartment at this point. I ceased to further investigate into the nature of this aggregation since it was not of big enough importance to the topic of this paper.

The second unusual feature of the Shot-L(A)Δrod1-GFP staining pattern is a strong localisation along the proximal primary neurite stretching from the soma to the dendritic compartment. This staining extends even into the soma arranging into @-like shapes (Fig.12). Strong staining in the somatodendritic compartment with an abrupt border towards the mostly

unstained axon (i.e. distal neurite) suggests that Shot-L(A)Δrod1-GFP is selectively transported or stabilised within this compartment. Similar spatial distribution in *Drosophila* motorneurons has been found for Bazooka-GFP, indicating that a molecular compartment border exists in the area of dendrites (Sanchez-Soriano et al., 2005). The @-like localisation of Shot-L(A)Δrod1-GFP is most likely representing microtubule-bound construct. From targeted expression experiments with Nod-LacZ, another microtubule-binding protein (Clark et al., 1997), we found comparable @-like structures (N. Sánchez-Soriano, personal communication), suggesting that Shot-L(A)Δrod1-GFP binds microtubules in the soma. At late larval stages (L3) Shot-L(A)Δrod1-GFP shows a similar deviation from the Shot-L(A)-GFP localisation pattern and the same principal properties like at late embryonic stages (stg.17) can be observed: Dendritic enrichment is given but reduced, the aggregation and the @-like enrichment of Shot-L(A)Δrod1-GFP in neuronal cell bodies and the proximal primary neurite can be observed (Fig.13). Whether all aspects of these unusual localisation properties described here represent the intact Shot-L(A)Δrod1-GFP protein remains open. Instead, some elements may represent C-terminal fractions of the fusion protein, perhaps even cleaved GFP (e.g. in somatic aggregates).

However, most importantly, at least two features of the Shot-L(A)Δrod1-GFP pattern carry normal traits. First, the protein retains its microtubule binding capability (see above and Fig.12 and Fig13). Secondly, the construct localises to dendrites at relatively high levels, although the pattern is slightly abnormal. Thus, major prerequisites for proper function are in principle retained in the Shot-L(A)Δrod1-GFP construct. To asses this possibility, I targeted Shot-L(A)Δrod1-GFP to motorneurons of *shot* mutant animals. When expressed with two driver lines (*RN2E-Gal4* and *MzVum-Gal4*), the Shot-L(A)Δrod1-GFP construct could rescue embryonic dendrites to a high degree (Fig.14). This finding is consistent with successful rescue of this construct reported for tracheal fusion and neuronal outgrowth in *Drosophila* embryos (see above and Lee and Kolodziej, 2002; Lee and Kolodziej, 2002), and it is in agreement with the relatively normal dendritic enrichment of Shot-L(A)Δrod1-GFP. As reported later Shot-L(A)Δrod1-GFP could also rescue tendon cell rupture in *shot* mutant animals to a high degree (Chapter 3.6.2.).

Taken together, my findings provide clear evidence that the rod domain is not fully dispensable for dendritic development of embryonic *Drosophila* motorneurons.

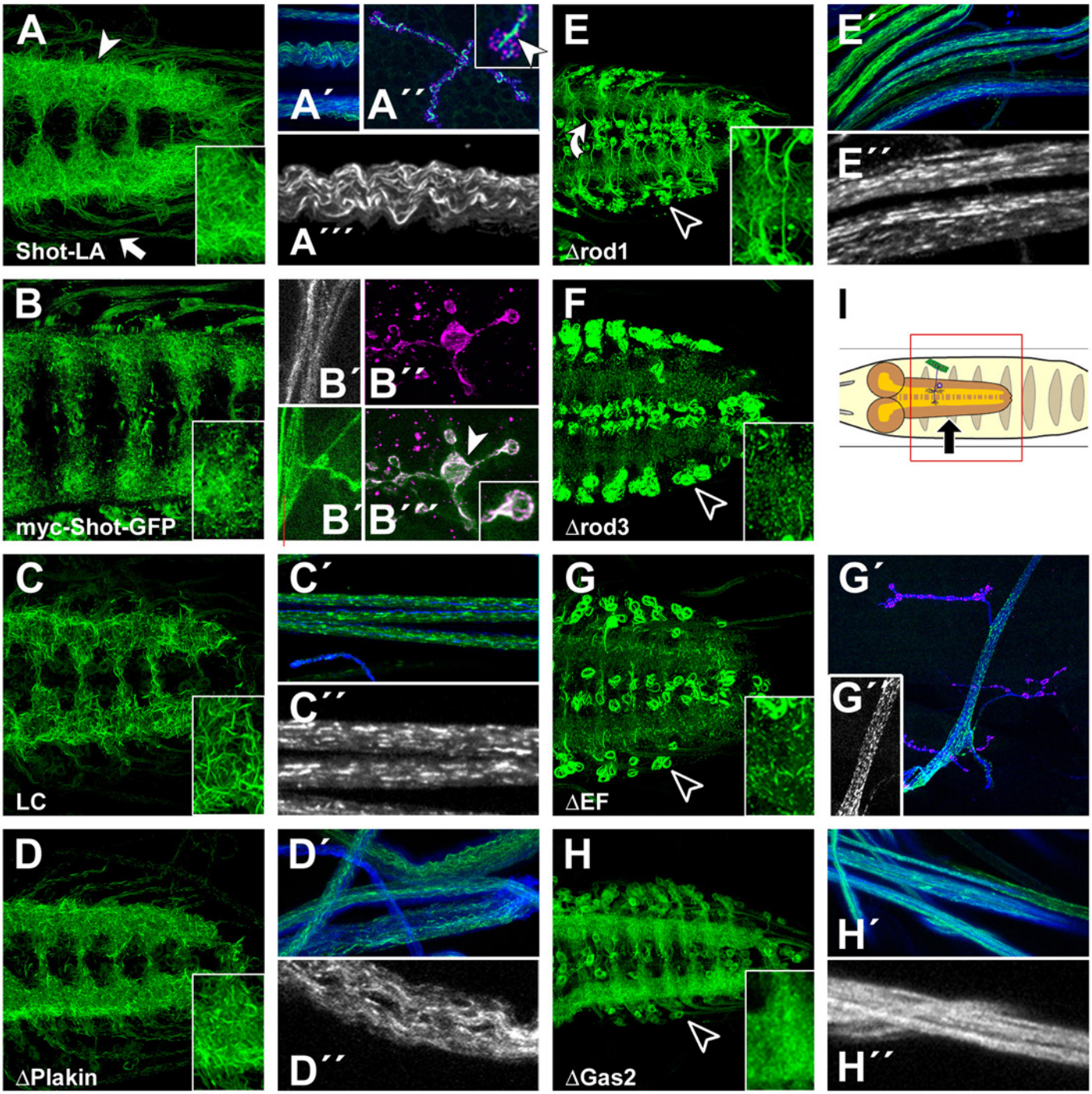
A
A´
A´´
A´´´
Shot-LA
B
B´
B´´
B´B´´´
myc-Shot-GFP
C
C´
C´´
LC
D
D´
D´´
ΔPlakin
E
E´
E´´
Δrod1
F
Δrod3
I
G
G´
G´
ΔEF
H
H´
H´´
ΔGas2

**Fig.13. A comparative expression analysis with Shot deletions constructs reveals the differential importance of Shot domains for the proper localisation of Shot in dendrites, nerves and NMJs of *Drosophila* larvae**

To study the importance of individual Short stop domains for proper localisation in the central nervous system (CNS), UAS-Shot and Shot deletion constructs were expressed in all motorneurons at larval stages (here L3) using the *OK6-Gal4* driver line. Constructs used are given and details about them can be found in Fig.5, Tab.3 and the respective results chapter. If not mentioned otherwise all constructs are GFP (green fluorescent protein) tagged which is shown in green. Stainings against the cmyc tag are depicted in magenta (B´´,B´´´) and HRP staining (neuronal marker) is in blue. **(I)** The CNS is indicated with an arrow. The area seen in (A-H) is indicated by the red box, the yellow neuropile harbours the dendrites and axons, the brown cortex harbours the neuronal cell bodies. A magnification of the dendritic localisation of the respective constructs is shown in the insets of column 1 and 3. Column 2 and 4 show the localisation of the constructs along the axons (magnifications in black and white). In some cases (A´´,B´´,B´´´,G´) the localisation at larval NMJs is shown.

**(A)** Shot-L(A)-GFP strongly enriches in the dorsal neuropile (arrowhead) and accumulates in dendrites (inset). **(A´,A´´´)** It localises along the nerves in a "stroke like" fashion (arrow) and enriches at the microtubule rich base but not the rim of NMJ boutons (arrowhead in A´´ inset). **(B)** Unlike in embryos (see Fig.12S) the localisation of 6cmyc-Shot-L(A)-GFP deviates from the Shot-GFP (A) in the neuropile, dendrites (see inset), along nerves **(B´)** and at the NMJ **(B´´,B´´´)**. Localisation in the CNS appears dottier and is more blurred in dendrites and nerves as compared to Shot-GFP. In NMJs the N-and C terminus (myc and GFP) overlap completely and the C-terminus seems to localise at the rim of boutons unlike Shot-GFP (see A´´). **(C)** Shot-L(C)-GFP localisation appears normal in the CNS and along nerves **(C,C´,C´´)**. **(D, D´,D´´)** The localisation of Shot-L(A)ΔPlakin-GFP appears unaffected (compare with A). **(E)** Shot-L(A)Δrod1-GFP severely mislocalises in the CNS. The construct localises to dendrites but does not enrich as prominently (inset as compared to A inset). It also strongly associates with microtubules (curved arrow) and enriches at the cell body (open arrowhead). On the other hand the localisation along the nerves appears more or less normal (E´,E´´ as compared to A´,A´´´). **(F)** Shot-L(A)Δrod3-GFP displays a strong mislocalisation. Enrichment in dendritic areas is weak and dotty (inset) whilst the construct strongly enriches in the cell bodies (open arrowhead). **(G)** Shot-L(A)ΔEF-hand-GFP strongly mislocalises in the CNS dendrites, (inset). The construct very strongly associates with microtubule like structures at the cell body (arrowhead). On the other hand localisation along nerves and at NMjs appears mostly normal (G´,G´´). **(H)** In accordance with the strong mislocalisation at embryonic stages the Shot-L(A)ΔGas2-GFP construct localises blurred and not concise in the CNS (compare with A and A inset). It also enriches more or less ubiquitous at cell bodies (open arrowhead) and along the nerve (H´,H´´). Thus in the absence of the microtubule Gas2 binding domain Shot fails to localise completely.

*3.4.3.2.. Partial deletions of the rod domain show stronger aberrations*

As explained above, the Shot-L(A)Δrod1-GFP construct shows a complex staining pattern, but maintain some essential features of Shot function. To understand whether aspects of this staining pattern can be mapped to sub-regions of the rod domain, I capitalised on two further existing but unpublished fly lines (*UAS-shot-L(A)Δrod2-GFP* and *UAS-shot-L(A)Δrod3-GFP*; kindly provided by Peter Kolodziej), deleting different parts of the rod domain (Fig.5; Tab.3).

The deletion of Shot-L(A)Δrod2-GFP (deleting aa1023- aa1664; Fig.5) covers a small N-terminal stretch (1204aa-1604aa) of the Shot-L(A)Δrod1-GFP deletion but, in addition, uncovers the C-terminal third of the plakin domain, and the interspersing region between the plakin and rod domains (aa1325-aa1454). Targeted expression with *RN2D+O-Gal4* reveals that dendritic enrichment of the *Shot-L(A)Δrod2-GFP* construct is retained. However, in contrast to the localisation of Shot-L(A)-GFP this dendritic accumulation is less pronounced and appears altered. It is often more interspersed or even like a ball shaped aggregate (Fig.12). Like Shot-L(A)Δrod1-GFP, Shot-L(A)Δrod2-GFP in some cases also enriches prominently at the proximal primary neurite (Fig.12). Besides that no prominent mislocalisation features of the Shot-L(A)Δrod1-GFP construct (see above) could be observed. Hardly any GFP signal can be detected at the soma (Fig.12). This absence from the soma is reminiscent of the Shot-L(A)ΔPlakin-GFP construct. However, the part of the nuclear localisation signal in the Plakin domain (aa984-aa1001, see Chapter 3.4.2) is not deleted in the Shot-L(A)Δrod2-GFP construct (aa1023-aa1664). It might still be possible though that the deletion which starts closely to the NLS still affects the motif in some way. Furthermore, since the true molecular nature of the predicted NLS has not been analysed so far, it could also be possible that other areas in the plakin domain are essential for somatic localisation. Thus at this stage I cannot comment on whether the observed mislocalisation treats are specific consequences of the deletion.

I conclude that the N-terminal area of the rod domain harbours no crucial domains required for Shot localisation to dendrites, which must map therefore to remaining regions of the Shot-L(A)Δrod1-GFP deletion. Furthermore, neither the C-terminal Plakin domain nor the interspersing domain seems important for dendritic localisation. For the plakin domain, this observation was confirmed later on by my Shot-L(A)ΔPlakin-GFP constructs which localise normally at dendrites (Chapter 3.4.2, Fig.12). Having said that it could be possible that cues in this region are crucial for the somatic localisation of Shot.

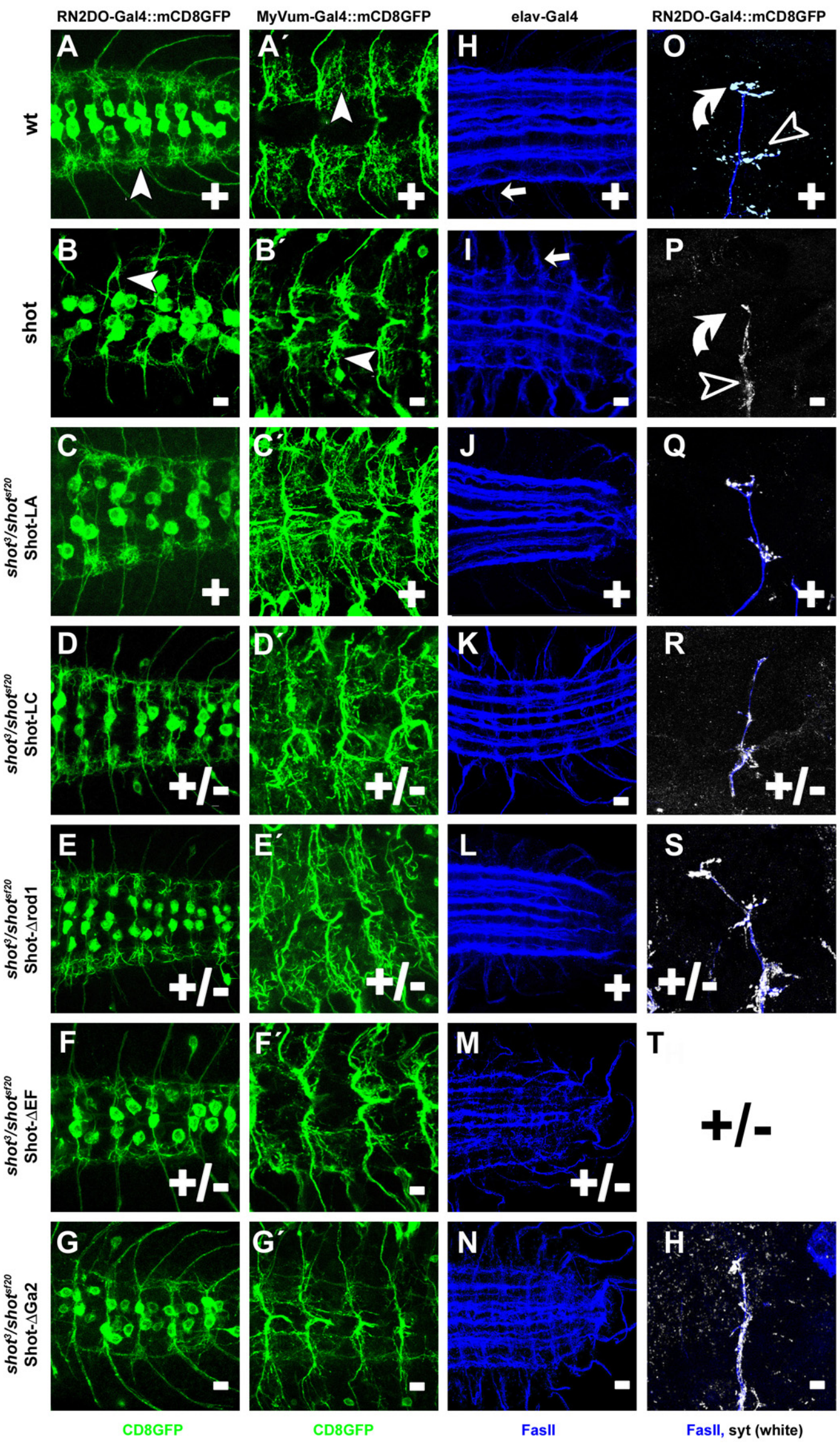
RN2DO-Gal4::mCD8GFP
MyVum-Gal4::mCD8GFP
elav-Gal4
RN2DO-Gal4::mCD8GFP
wt
shot
shot3/shotsf20 Shot-LA
shot3/shotsf20 Shot-LC
shot3/shotsf20 Shot-Δrod1
shot3/shotsf20 Shot-ΔEF
shot3/shotsf20 Shot-ΔGa2
A
A´
H
O
B
B´
I
P
C
C´
J
Q
D
D´
K
R
E
E´
L
S
F
F´
M
T
G
G´
N
H
+
-
+/-
CD8GFP
CD8GFP
FasII
FasII, syt (white)

**Fig.14. Shot domains are of variable importance in different neuronal contexts**

The UAS/Gal4 system was used to rescue different phenotypes in the nervous system of *Drosophila melanogaster* embryos. The top row shows the wildtype, the second row the *shot*$^{3}$/*shot*$^{sf20}$ mutant phenotype, rows 3-7 *shot*$^{3}$/*shot*$^{sf20}$ mutant phenotypes upon attempted rescue with five different Shot deletion constructs, as indicated on the left (for details on the constructs see Fig.5). Stainings used in each column are indicated in colour code at the bottom of the row (FasII, anti-FasciclinII; GFP, green fluorescent protein; Syt, anti-Synaptotagmin). First and second column: horizontal views of ventral nerve cords showing motorneuronal dendrites which are severely reduced in *shot* mutant embryos (white arrow heads in A,A' *vs.* B,B') when visualised in aCC/RP2 motorneurons (targeted mCD8-GFP expression with *RN2D+O-Gal4*; indicated on top) and VUM motorneurons (targeted mCD8-GFP expression with *MzVum-Gal4*). Third column: horizontal views of ventral nerve cords reveal mislocalisation of FasciclinII in motorneuronal nerve roots (white arrows in H vs. I). Fourth column: Images of the dorsal musculature show that NMJs in *shot* mutant embryos (O *vs.* P) are reduced in size (curved arrows) and display mislocalisation of presynaptic Synaptotagmin along the axon (open arrowhead). Details of all phenotypes are illustrated in Fig.2 and elsewhere (Prokop et al., 1998). (C-H) Rescue experiments with the Shot deletion constructs; the degree of rescue is indicated bottom right ("+", full rescue; "+/-", partial rescue; "-", no rescue).

(A and A´ vs. B and B´) Wildtypic dendrite morphologies of aCC/RP2 (A) and Vum (A´) dendrites respectively (arrowheads in A, A´) as compared to severely reduced dendrites in *shot* mutant animals (B-B´). (C, -C´) Expression of Shot-L(A)-GFP (Shot-RE-GFP) in *shot* mutant animals (*Shot-L(A);shot*$^{sf20}$*/shot*$^{3}$*,CD8-GFP;Gal4; shot*$^{3}$ and *shot*$^{sf20}$ are two distinct null alleles) is sufficient to rescue dendritic branching (D, D´), fully restores the FasII pattern (J) and the morphology of NMJs (Q). (D, D´) Expression of Shot-L(C)-GFP (lacking part of the actin binding domain) is only partially sufficient to restore dendritic morphology and NMJ (R) growth but fails to improve the mutant FasII pattern (K). (E, E´) The overexpression of Shot-L(A)Δrod1-GFP can only partially restore dendritic branching and NMJ sprouting (S) but fully restores the mutant FasII pattern (L). The expression of Shot-L(A)ΔEF-hand-GFP is sufficient to initiate dendritic sprouting in aCC/RP2 dendrites (F) but astonishingly not Vum dendrites (F´) and it furthermore improves the mislocalisation of FasII (M). We also have initial findings that the construct partially rescues NMJs (not shown). (G, G´, N, H) Overexpression of shot-L(A)ΔGas2-GFP (lacking the microtubule binding domain) fails to improve the mutant situation in any of the analysed contexts. The overexpression of this construct causes axonal misrouting (white arrows in G; compare with A).

The deletion of Shot-L(A)Δrod3-GFP overlaps with the C-terminal third (Δaa3589-aa4599; see Fig.5) of the Shot-L(A)Δrod1-GFP deletion. A severe mislocalisation could be observed when expressing Shot-L(A)-GFPΔrod3 with *RN2D+O-Gal4* (Fig.12). Instead of localising continuously at dendrites, Shot-L(A)Δrod3-GFP aggregates in round vesicles in the dendritic field (Fig.12). It is difficult to judge in how far the vesicular aggregates are restricted to and possibly associated with the thicker proximal microtubule bundles in dendrites or reaching further into the dendritic branches. Reminding of Shot-L(A)Δrod1-GFP, the typical @ like localisation at the soma can be observed. However, in contrast to Shot-L(A)Δrod1-GFP the Δrod3 construct localises not continuous along these microtubules but localises more interspersed and aggregates in vesicles (Fig.12). The fact that the mislocalisation phenotype of this deletion construct was more severe than that of Shot-L(A)Δrod1-GFP (carrying the far larger deletion) is surprising and might be explained by two potential reasons: First, the construct might be not functional or miss-folded and thus the mislocalisation would merely be a secondary effect. Second, it could be possible that in the absence of one/some domains in the C-terminal rod region remaining domains of the rod express dominant effects on Shot localisation. In agreement with this explanation, the rod domain has been implicated in transport and dimerisation (see above and Jefferson et al., 2004) and isolated portions of the Bpag1n3 rod domain have been demonstrated to cause dominant phenotypes in retrograde axonal transport (Liu et al., 2003).

Taken together localisation patterns of the three Δrod constructs were all aberrant and very different. The patterns of the two partial Δrod domain constructs hardly overlapped with Shot-L(A)Δrod1-GFP and displayed few similarities. Thus, the use of the two constructs did not allow me to allocate different portions of the rod domain to specific ectopic localisation features observed in the absence of the whole rod stretch. I could show though that no critical localisation cue is present in the protein stretch between the Plakin and the rod domain of Shot (see above).

### 3.4.4. The EF hand is required for proper localisation and function of Shot in dendrites

Many aspects of neuronal activity are regulated by $Ca^{2+}$ signals (Bhattacharya et al., 2004; Burgoyne et al., 2004). This requires proteins able to sense $Ca^{2+}$ levels and respond through changes in their activity patterns. The EF-hands are the most common calcium binding domains found in proteins capable of sensing and mediating levels of $Ca^{2+}$ (Lewit-Bentley and Rety, 2000; Bhattacharya et al., 2004). EF-hand calcium sensors family proteins

(e.g. calmodulin) translate the physiological changes in calcium levels into molecular responses by undergoing a large conformational change that exposes or discloses binding sites recognized by interacting proteins (Bhattacharya et al., 2004). The crystal structure of EF-hands is solved and it has been shown that they undergo conformational changes upon $Ca^{2+}$ binding (Bhattacharya et al., 2004). The basic structural/functional unit of EF-hand proteins is a pair of EF-hand motifs (Kretsinger and Nockolds, 1973) that together form a stable four-helix bundle domain (Strynadka and James, 1989; Nelson and Chazin, 1998). As mentioned earlier, Shot contains two highly conserved EF-hand motifs at its C-terminus (Gregory and Brown, 1998; Strumpf and Volk, 1998; Lee et al., 2000). Thus, it appears likely that intracellular free $Ca^{2+}$ levels may regulate Shot activity. Accordingly, it has been shown that Shot EF-hand motifs are required for neuronal outgrowth (Lee and Kolodziej, 2002) whilst they seem to be fully dispensable for tracheal fusion (Lee and Kolodziej, 2002) and Shots principal capability to crosslink microfilaments and microtubules (Lee and Kolodziej, 2002). In vertebrate cells, changes in calcium levels affect the subcellular distribution of MACF/ACF7, demonstrating a direct or indirect dependence of this closely related spectraplakin on $Ca^{2+}$ levels (Karakesisoglou et al., 2000). However, nothing is known about how $Ca^{2+}$ levels might regulate spectraplakin activity.

The Shot-L(A)ΔEF-hand-GFP construct deletes only the predicted 2 EF-hand motives (Fig.5; Table 3). Upon overexpression with *RN2D+O-Gal4*, Shot-L(A)ΔEF-hand-GFP accumulates at dendrites and at the axon (Fig.12). In addition it strongly accumulates at the proximal primary neurite. It still seems to be associated with microtubules but forms aggregates which cannot be observed when expressing Shot-L(A)-GFP (Fig.12). To learn whether these aggregates are also formed at later stages of development, I used the driver *OK6-Gal4* to express Shot-L(A)ΔEF-hand-GFP in larval motorneurons (L3). At these later stages, the localisation features differ significantly from Shot-L(A)-GFP. In L3 larvae the Shot-L(A)ΔEF-hand-GFP construct does not display the prominent sharp and concise dendritic enrichment of the Shot-L(A)-GFP construct but instead localises more “dotty” and throughout the dendritic area (Fig.13). Furthermore, whilst Shot-L(A)-GFP can hardly be detected in the cell bodies at late larval stages, Shot-L(A)ΔEF-hand-GFP strongly enriches at the cell soma (Fig.13) in a pattern reminiscing of the @ like microtubule like localisation which can be observed upon overexpression of Shot-L(A)Δrod1-GFP in embryonic stages (see Fig.12). The finding that mislocalisation defects are stronger at late larval than late embryonic stages might suggest that $Ca^{2+}$ signalling at larval stages might play a more important role.

To understand in how far the EF-hand motifs of Shot are required for dendrite development, I expressed Shot-L(A)ΔEF-hand-GFP in motorneurons of *shot* mutant *Drosophila* embryos using the *RN2E-Gal4* and *MzVum-Gal4* driver lines as above. Astonishingly and unlike in any other rescue experiment I got two contradictory experimental outcomes with the two driver lines. Whilst *RN2E-Gal4* driven Shot-L(A)ΔEF-hand-GFP partially rescued dendrites of the targeted motorneurons aCC and RP2, the same construct driven with MzVum-Gal4 could hardly improve the *shot* mutant situation or failed to rescue dendrites completely (Fig.14). Since expression levels achieved through overexpression with *RN2E-Gal4* are lower than with *MzVum-Gal4* (N. Sánchez-Soriano, personal communication and own observation), I exclude expression levels as explanation for the differential rescue.

I can think of at least two possible explanations which might account for this phenomenon. First, the time at which Shot-L(A)ΔEF-hand-GFP starts to be expressed varies in the two experiments: *RN2E-Gal4*-mediated expression starts at stage10, whilst the onset of *MzVum-Gal4*-mediated expression in VA-motorneurons (contributing to most of the motorneuronal dendrites targeted by that driver line) occurs as late as stage 15/16 (Landgraf et al., 2003 , Fig.4). At first sight, this interpretation contradicts my finding that Shot-L(A)-GFP is able to rescue dendrites when expressed with *MzVum-Gal4* (Chapter 3.2; Fig.14). However, it is not unlikely that the combination of a later onset of expression, expression strength, and the lack of $Ca^{2+}$ responsiveness together account for the failure of VA-dendrite rescue upon Shot-L(A)ΔEF-hand-GFP expression. Second, a recent observation made in our lab provides an alternative explanation. Thus, Shot-L(A)ΔEF-hand-GFP has a strong tendency to restrict to the very proximal primary neurite in all tested neurons (Natalia Sánchez-Soriano and Ulrike Haessler, personal communication). Since the dendrites of VA-motorneurons are considerably more distant from their ventrolateral cell bodies than the dendrites of aCC and RP2 targeted by *RN2E-Gal4* (Fig.4; Landgraf et al., 2003). Thus, a failure of the Shot-L(A)ΔEF-hand-GFP construct to reach the VA-dendrites could account for its inability to rescue. Since these contradictory findings occurred late in my project, I could no longer test this hypothesis. A third possible explanation for differential rescue could be that $Ca^{2+}$-dependent regulation of Shot is less important in aCC/RP2 than it is in VA-motorneurons.

Taken together, the lack of the EF-hand motifs has an influence on the subcellular localisation of Shot, in particular at larval stages. This localisation deficit could be one possible reason for observed differences of the Shot-L(A)ΔEF-hand-GFP rescue capability in different motorneurons. Therefore, even though my findings clearly document that the EF-hand motif is required in dendrites, unfortunately I cannot answer which precise role $Ca^{2+}$-

mediated regulation of Shot plays during dendrite development. This could be solved conclusively, if acute changes of [$Ca^{2+}$] could be shown to have an immediate impact on Shot activity in dendrites.

### 3.4.5. The Gas2 domain is essential for the localisation and function of Shot in dendrites

The Gas2 motif is a high affinity microtubule binding motif present near the carboxy terminus of Shot (aa4847-a4918; Gregory and Brown, 1998; Strumpf and Volk, 1998 and see Fig.5). Isolated Gas2 domains from a number of molecules such as BPAG1, MACF, GAS2, GAR22 and Shot co-localise with microtubules in transfected cells (Sun et al., 2001; Lee and Kolodziej, 2002; Goriounov et al., 2003) but seem not to be functional in isolation (Kodama et al., 2003). Plakin isoforms that do not contain a Gas2 domain generally do not interact with microtubules (Jefferson et al., 2004). The Gas2 domain of Shot is required for neuronal outgrowth (Lee and Kolodziej, 2002) but dispensable for tracheal fusion (Lee and Kolodziej, 2002; Lee and Kolodziej, 2002). This is another striking demonstration of how versatile this large molecule is and how different the domain requirements are in various cellular contexts.

To analyse the requirement of the Gas2 domain for Shot function in dendrites I used the Shot-L(A)ΔGas2-GFP construct lacking the Gas2 domain (aa4859-4905; Tab.3, Fig.5). When expressing this construct with *RN2D+O-Gal4*, it displays a severe mislocalisation (Fig.12). The Shot-typical restriction and enrichment at the proximal thick dendrites is completely abolished and instead the molecule localises similar to actin-GFP (Sanchez-Soriano et al., 2005) throughout the dendrites in a slightly dotty and aggregated fashion entering also the finer distal parts of dendritic protrusions (Fig.12). In contrast to actin-GFP, which localises weaker to primary neurites, the Shot-L(A)ΔGas2-GFP construct localises evenly along the primary neurite at similar strength as in dendrites. Also in larval motorneurons (*OK6-Gal4*) Shot-L(A)ΔGas2-GFP does not occur in stroke- or line-like patterns along the nerves and dendrites but localises more homogeneously like a typical surface marker such as mCD8-GFP (Fig.13H *vs.* Fig.13A; Landgraf et al., 2003; Sanchez-Soriano et al., 2005). This localisation pattern suggests that the Shot-L(A)ΔGas2-GFP protein either tends to diffuse or interacts stronger with the actin cytoskeleton.

Next, I used this construct for motorneuronal rescue experiments as described for the other constructs above. In agreement with the severe mislocalisation of Shot-L(A)ΔGas2-GFP, the construct completely failed to rescue dendrites of *shot* mutant animals regardless whether it was expressed with *RN2E-Gal4* or *Vum-Gal4* (Fig.14). Intriguingly, embryos of

these rescue experiments displayed frequent misrouting of neurites and aberrant projection of axons from the wildtype projection pattern in the area of nerve roots (Fig.14G). This dominant effect suggests that Shot's involvement in neuronal growth seems to have a crucial impact on axonal pathfinding as would be expected from a microtubule-actin cross-linker (Suter and Forscher, 1998). Since I could not observe a similar phenomenon with any other Shot construct, it seems likely that the Gas2 domain is most crucial for this process (see Discussion).

Taken together, my results demonstrate that the Gas2 domain is essential for localisation and function of Shot in dendrites. Furthermore, they suggest that Shot is important for directed neuronal growth.

### 3.4.6. Shot-L(C)ΔGaI2-GFP does not affect dendrites

The Shot-L(C)ΔGas2-GFP construct is a combination of Shot-L(C)-GFP (lacking the first Calponin domain and displaying a different N-terminus) and Shot-L(A)ΔGas2-GFP (Tab.3, Fig.5). Thus, both the actin and microtubule binding capabilities of this construct should be abolished. Indeed it has been shown that it fails to rescue tracheal fusion whilst both, Shot-L(C)-GFP and Shot-L(A)ΔGas2-GFP could rescue tracheae, demonstrating the redundancy of the two domains in this cellular context (Lee and Kolodziej, 2002). Since neither Shot-L(A)ΔGas2-GFP nor Shot-L(C)-GFP (see above) fully rescue dendrites (Chapter 3.4.5. and 3.4.1.; se Fig.14) the domains appear not to be redundant in dendrites and thus it is highly unlikely that Shot-L(C)ΔGas2-GFP can achieve this. Therefore, I initially neglected this construct and only reconsidered it when we made an intriguing discovery in tendon cells where Shot-L(C)ΔGas2-GFP causes a severe dominant phenotype when expressed in wildtype background (Chapter 3.6.3; Fig.15). To test for potential dominant interference during dendrite development, I expressed Shot-L(C)ΔGas2-GFP in dendrites using *RN2D+O-Gal4*. To visualise dendritic morphologies I co-expressed Homer-myc, an inert morphological marker which we have successfully used before (Sanchez-Soriano et al., 2005). However, in contrast to tendon cells, the construct did not induce any visible dominant phenotype in dendrites (Fig.12). This clearly suggests a differential mode of Shot activity in dynamic dendritic growth and robust epidermal tendon cells, a topic which will be addressed in detail later (Chapter 3.6).

However, some conclusions can be drawn from the localisation pattern of Shot-L(C)ΔGas2-GFP which resembles neither the almost normal pattern of Shot-L(C)-GFP nor

the more homogeneous distribution of Shot-L(A)ΔGas2-GFP (Fig.12). Instead it displays an unspecific localisation more reminiscent to an ubiquitously expressed cell marker like CD8 without prominent specific enrichment (Fig.12). In accordance with the lack of actin and microtubule binding capability of the construct its localisation is completely dissimilar to the cytoskeletal markers actin-GFP and tubulin-GFP (Fig.4). This unspecific localisation of Shot-L(C)ΔGas2-GFP suggests that the actin binding capability of Shot-L(C)-GFP is indeed severely reduced.

### 3.4.7. The EB1 domain is not crucial for dendritic enrichment of Shot

Downstream of the Gas2 domain, Shot comprises a C-terminal EB1-binding domain (Slep et al., 2005; aa5145- aa5191; see Fig.5). EB1 is a well characterised microtubule tracking protein conserved from yeast to human (Slep et al., 2005). It has been shown to be essential for *Drosophila* development (Elliott et al., 2005), spindle dynamics (Rogers et al., 2002) and the recruitment of Spectraplakins to microtubule plus-ends (Slep et al., 2005). It was proposed that EB1 may link microtubules to the cell cortex via Short stop (Subramanian et al., 2003; Elliott et al., 2005). Most *EB1* mutant flies die at pupal stages with few escapers and those display severe locomotion and potentially neuromuscular defects (Elliott et al., 2005). Contradictory experimental observations have been published about EB1's requirement to mediate Shot binding to microtubules. Subramanian and co-workers proposed that the association of Shot with microtubules is independent of EB1/APC (Subramanian et al., 2003), whereas Slep and co-workers suggest a direct dependence, and they find that Shot dissociates from microtubules when knocking down *EB1* via *RNAi* in *Drosophila* S2 cells (Slep et al., 2005). The biochemical interaction of Shot with EB1/APC has been demonstrated (Subramanian et al., 2003), the Shot EB1 binding motif was described recently, deduced from sequence homologies with vertebrate BPAG2 (Slep et al., 2005). However, the validity of this domain prediction has not been tested as yet. Taken together, although a lot is known about EB1 and its requirement for isolated cellular processes, it is not understood which biological relevance EB1/Shot interaction has for *Drosophila*.

To address the role of the EB1-binding domain for Shot function, I generated *UAS-shot-L(A)ΔEB1-GFP* constructs lacking this domain (details of the cloning strategy in Fig.11). Respective transgenic fly lines were generated and used for localisation and rescue studies (this Chapter and 3.6.2.).

When expressing the Shot-L(A)ΔEB1-GFP construct in motorneurons using the *RN2D+O-Gal4* driver line, its localisation is altered as compared to Shot-L(A)-GFP (Fig.12). Principal accumulation at dendrites is retained but in comparison far less pronounced (Fig. 12). The Shot-L(A)ΔEB1-GFP construct also localises to the cell body but appears more blurred than Shot-L(A)-GFP and occasional aggregations can be observed (Fig.12). Thus, the EB1 domain as such seems not to be crucially required for dendritic enrichment and the microtubule binding ability of Shot. The comparatively little accumulation of Shot-L(A)ΔEB1-GFP at dendrites might be due to the relatively low expression levels as compared to other *shot* constructs such as Shot-L(A)-GFP. However, so far only two out of six independent transgenic fly lines could be tested (Appendix 6.8., Table 7). Unfortunately, due to lack of time, the transgenic flies carrying Shot-L(A)ΔEB1-GFP could not be used for dendritic rescue experiments any more, but rescue experiments were carried out in tendon cells demonstrating the functionality of the construct (Chapter 3.6.2.).

To further validate my results with the Shot-L(A)ΔEB1-GFP construct, I tried to address the localisation of EB1 in dendrites. To this end, I expressed a *UAS-EB1-GFP* construct in dendrites. The respective transgenic fly line was obtained from Peter Kolodziej (Vanderbilt University, Nashville, Tennessee). The localisation of EB1-GFP revealed no specific localisation except for a few random dots spread throughout dendrites. (Fig.4). This was in agreement with my prediction that EB1 is not required for Shot activity in dendrites (see Chapter 3.5.2). However, we have no positive proof for the ability of this construct to localise like its endogenous counterpart and interpretation has to be taken with care.

### 3.4.8. Localisation studies with isolated Shot domains

Isolated protein domains are widely used for *in-situ* and *in-vitro* experiments and can provide valuable insights into domain functions and properties. Especially when operating with large multi domain proteins, isolated domains or protein fragments can help to unravel complex protein interactions (e.g. Yang et al., 1999; Fontao et al., 2001; Sun et al., 2001; Kodama et al., 2003; Subramanian et al., 2003). Three different UAS-coupled and tagged Shot fragments were available, APT, PT and EGG (Subramanian et al., 2003; Fig.5, Tab.3). Furthermore, I generated two further transgenic fly lines, UAS-EB1*aff*-GFP and UAS-6myc-Gas2 (Fig.20 and Materials and methods 2.8.1). In order to understand the localisation patterns of Shot deletion constructs in more detail, I capitalised on these UAS-coupled Shot fragments and used them for complementary localisation studies.

*3.4.8.1. N-terminal domains seem dispensable for dendritic localisation*

APT (aa1-aa1202) and PT (aa379-aa1202) contain N-terminal Shot portions (A = actin binding domain, P = Plakin domain, T = tap-tag). Thus, APT contains the whole N-terminus of Shot-L(A)-GFP including the ABD (CH1+CH2) and the plakin domain, whilst PT only contains the plakin domain. Plakin domains are protein-protein interaction motifs with the potential to impart specificity to protein function and localisation (Jefferson et al., 2004 ; Chapter 3.4.2). These properties made the plakin domain a promising candidate domain which might be involved in Shot localisation. Upon expression of APT and PT in motorneurons using *RN2D+O-Gal4*, the localisation patterns of both constructs were indistinguishable (Fig.12), resembling no other Shot construct and neither tubulin-GFP nor actin-GFP (Fig.4). Both localise to dendrites but, in contrast to unspecific markers such as mCD8-GFP, fail to reach into the finer dendritic branches suggesting that they are either less well diffusing or transported in dendrites or have some higher affinity for the more proximal dendritic sections (Fig.12). In addition, both constructs clearly fail to enrich at dendrites but localise instead more or less evenly throughout the primary neurite (Fig.12).

*3.4.8.2. C-terminal domains are not sufficient for dendritic localisation*

I speculated that two domains at the C-terminus might be able to target Shot to dendrites: First, the Gas2 domain is a genuine microtubule binding motif demonstrated to bind and stabilise microtubules in isolation (Lee and Kolodziej, 2002), and my experiments with Shot-L(A)ΔGas2-GFP had demonstrated already that the Gas2 domain is absolutely required (Chapter 3.4.5.). Second, published work suggested an important role for the EB1-affinity domain (EB1*aff*) for the recruitment of Shot in S2 cells (Slep et al., 2005), thus it may play a similar role in dendrites (at this stage of my project results with the Shot-L(A)ΔEF-hand-GFP construct were not known yet). Therefore, I wanted to test whether either of these domains might be sufficient for localisation and generated flies bearing *UAS-6myc-Gas2* or *UAS-EB1aff-HA* constructs (see Fig.5 and Materials and methods 2.8.1).

I decided to use the *6myc-tag* out *pCS2+MT* (kindly provided by Stefan Thor, Linköping, Sweden; see Appendix 6.7) for the Gas2 domain in the hope to be able to use this construct in co-expression experiments with GFP-carrying marker molecules. Unfortunately the expression of 6myc-Gas2 with the *RN2D+O-Gal4* driver line revealed a homogeneous

staining throughout the targeted motorneurons, and it appeared not to associate with microtubules but was more reminiscent of cytoplasmatic markers (Fig.12). This failure to bind to microtubules was confirmed by experiments expressing these constructs in fibroblast cells (Chapter 3.9.3) and tendon cells (Chapter 3.6.4). The fact that the transgenic fly line failed to show binding of the Gas2 domain to microtubules came as surprise, especially since in previous experiments a Gas2 domain was successfully tagged with GFP at its C-terminal end and shown to bind microtubules in NIH3T3 fibroblasts (Lee and Kolodziej, 2002). Either, the binding abilities of the Gas2 motif are hampered by the nature of the 6myc-tag, or it is the N-terminal position of the tag which interferes with binding (although five amino acids flank the Gas2 domain to increase the distance between the tag and domain and prevent sterical hindrance; see Materials and Methods 2.8.1.2.)

The second construct, *UAS-EB1aff-HA*, contained the EB1 domain fused to 2 copies of the HA-epitope joined via one glycine, the HA tag has been successfully used for the Rdl-construct (Chapter 3.1.3.). When targeted to motorneurons via the *RN2D+O-Gal4* driver line EB1-HA likewise failed to show any specific localisation. When driving the construct with the *OK6-Gal4* line in all larval motorneurons, the construct could be detected in very few areas of the larval CNS, but no interpretable specific localisation could be observed (not shown). This finding was again confirmed by findings in cell culture (Chapter 3.9.3. and 3.9.4.) and tendon cells (Chapter 3.6.4) where the construct also failed to localise specifically. I can think of at least three possible explanations. Firstly the construct is not functional and the HA tags hamper the proper folding and binding capabilities of the domain. Secondly the expression levels of the single tested independent insertion might be too low to achieve sufficient amounts of expressed construct. However, only one single insertion was tested in dendrites and tendon cells so far. From a second round of injections additional 5 independent insertions were obtained (see Table 7; Appendix 6.8.) but, due to a lack of time, could not be tested as yet. Thus, there is still hope that the construct might proof to be a useful tool to study the properties of the EB1*aff* domain in the future. Thirdly it might be possible that EB1 does not localise prominently in dendrites and thus the construct cannot bind specifically. In favour of this explanation I observed no specific localisation of UAS-EB1-GFP in neurons (Fig.4).

Thus, at the moment there is no positive indication that either Gas2 or EB1*aff* can localise to dendrites. To test, whether their combination might yield better results, I expressed the EGG fragment with *RN2D+O-Gal4*. EGG contains the whole C-terminus, comprising the EF-hand, Gas2, GSR and the EB1 domains, and is tagged with GFP (E = EF-hand domain, 1st G = Gas2 domain, 2nd G = GFP; Tab.3, Fig.5). When expressed in embryonic motorneurons,

the construct binds to microtubules and evenly decorates them throughout the neuron, strongly resembling the pattern of tubulin-GFP but not Shot-L(A)-GFP (Fig.4; Sanchez-Soriano et al., 2005). In dendrites the construct evenly decorates the thick proximal dendritic microtubules and fails to extend further into the finer dendritic branches (Fig.12). It is interesting that EGG fails to enrich specifically at dendrites like Shot-L(A)-GFP but appears to enrich slightly in the somatodendritic segment of the primary neurite (Fig.12). This is probably due to the fact that dendritic and axonal microtubule bundles run together in this section of the primary neurite, adding up to build a thick bundle in the proximal neurite. A further striking localisation feature of EGG is that it reveals the somatic @-like thick microtubule bundles (Fig.12) which was similarly seen with Shot-L(A)Δrod-GFP (Fig.12).

I conclude that, EGG closely binds microtubules, consistent with my finding that the Gas2 domain is crucial for the microtubule binding ability and function of Shot in dendrites. However, the C-terminus does not comprise all domains necessary to enrich Shot specifically at dendrites, although the Gas2 domain is required for this feature (Chapter 3.4.5.).

### 3.4.9. Lessons learned from structure-function analyses of Shot

Taken together, my data suggest that the information required for specific dendritic enrichment of Shot can not be assigned to a single domain at the N- or C-terminus. At first sight, this hypothesis contradicts my finding that deletion of the Gas2 domain completely abolishes accumulation and function of Shot at dendrites (Chapter 3.4.5.), and also in tendon cells displays a mislocalisation phenotype (Chapter 3.6.2.). When seen together, these results suggests that the Gas2 domain is required but not sufficient, i.e. Shot must harbour further domains upstream of the EF-hand motif responsible for dendritic localisation. A potential of the N-terminus to localise specifically has been demonstrated in other cellular contexts: APT and PT enrich at larval NMJs (Mende, 2004), APT enriches in growth cones (N. Sánchez-Soriano, personal communication), and PT and APT also accumulate at actin-rich areas of tendon cells (Subramanian et al., 2003). However, my studies with APT and PT did not reveal convincing accumulation in dendrites. Also, results obtained from N-terminal deletion constructs do not suggest that the Calponin and/or plakin domains are required for dendritic localisation: Deletion of the Plakin domain does not affect dendritic localisation, nor does deletion of the first Calponin domain. However, the full deletion of both Calponin domains (which is underway) needs to be awaited before drawing final conclusions. A potential domain upstream of the EF-hand motif may lie within the central rod domain, and this would

be consistent with observations in other contexts (Liu et al., 2003; Jefferson et al., 2004). In agreement with this possibility, all Shot-L(A)Δrod-GFP constructs (Fig.12, Chapter 3.4.3.) show severely aberrant patterns. I propose therefore that the Gas domain in combination with sequences in the central rod make up the dendritic targeting code.

| construct | Localisation in dendrites | Rescue of dendrites | Rescue FasII | Rescue of NMJs | Localisation at tendon cells | Rescue of tendon cells |
|---|---|---|---|---|---|---|
| **Shot-L(A)-GFP** | + | + | + | + | + | + |
| **Shot-L(C)-GFP** | + | +/- | - | +/-* | + | +/- |
| **Shot-L(A)Δrod-GFP** | +/- | +/- | + | +/- | +/- | + |
| **Shot-L(A)ΔEF-hand-GFP** | +/- | +/- | +/- | +/-* | + | +/- |
| **Shot-L(A)ΔGas2-GFP** | - | - | - | - | - | - |
| **Shot-L(A)ΔPlakin-GFP** | + | n.d. | n.d. | n.d. | +/- | n.d. |
| **Shot-L(A)ΔEB1-GFP** | +/- | n.d | n.d | n.d | + | +* |
| **Shot-L(C)ΔGas2-GFP** | - | n.d. | n.d. | n.d. | -! | n.a. |
| **UAS-[$EB1_{shot}$]-2HA** | -** | n.a. | n.a. | n.a. | -** | n.a. |
| **UAS-[$Gas2_{shot}$]-6myc** | -** | n.a. | n.a. | n.a. | -** | n.a. |

**Table 4.** Summary of results obtained from localisation and rescue experiments: The following information is given: ***construct***: Shot construct used in the study. The ability of the Shot constructs to localise and rescue in a specific context is given: +, similar of equal to *wild type*, +/-, moderate aberration; -, fails to localise or rescue. Further abbreviations used: n.d., not determined; n.a., not applicable, *, preliminary data- needs repetition., **, only one insertion tested so far, analysis has to be continued; !, causes dominant effect.

## 3.5. The F-Actin and microtubule binding capabilities of Shot are essential for the proper development of NMJs and required to organise FasII localisation

### 3.5.1. Motivation and strategy

To learn, whether domain requirements of Shot vary in different cellular or sub-cellular contexts, I analysed Shot function in two further *shot*-dependent neural contexts, FasciclinII (FasII) localisation in nerve roots and NMJ development. The *shot* mutant phenotype at NMJs comprises a significant reduction of the motorneuronal terminal and a severe deposit of presynaptic proteins such as Synaptotagmin along the motornerve (Prokop et al., 1998). The FasII phenotype of *shot* consists in ectopic localisation of FasII in transverse nerve roots, i.e. it fails to restrict to the distal primary neurite (Fig.2 and Prokop et al., 1998). In contrast, in *wildtype* animals, FasII reproducibly localises along longitudinal axonal fascicles in the CNS (e.g. Landgraf et al., 2003), and in motornerves but only outside the CNS (Sanchez-Soriano and Prokop 2005). The *fasII* gene is the orthologue of the mammalian neural cell adhesion molecule N-CAM, member of the transmembrane immunoglobulin superfamily (Goodman and Doe, 1993). It has been hypothesised that Shot, which localises along the length of the primary neurite (Fig.4) is involved in regulating the localisation of membranous Fas2 and 22C10 by linking them to the underlying axonal actin cytoskeleton (Prokop et al., 1998).

To test the requirement of domains for Shot function at NMJs and for Fas2 localisation, I chose similar rescue approaches as applied in the context of dendrite development, and I used the same Shot constructs as mentioned in detail before (Fig.5, Tab.3). For NMJ rescue experiments I used the same Gal4 driver line (*RN2D+O-Gal4*) as employed in the dendritic rescue experiments, but the actual dissections were carried out by colleagues in the laboratory, Mohiddin Lone and Michael Mende. As prerequisite for the structure-function analyses, I demonstrated that Shot-L(A)-GFP enriches in embryonic NMJs like Shot protein in *wildtype* flies (Prokop et al., 1998) and is able to rescue *shot* mutant NMJs (Fig.14). For the FasII rescue experiments, I used the pan-neuronal Gal4-driver line *elav-Gal4* which targets all neurons thus making sure that all those neurons showing the FasciclinII mislocalisation phenotype express the Shot constructs. My control experiments using *elav-Gal4*-mediated panneuronal expression of Shot-L(A)-GFP revealed full restoration of the aberrant localisation pattern of FasII (Fig.14).

3.5.2. The N-terminus of Shot is required in neurons

In accordance with the results from dendrite rescue experiments (Fig.14), the Gas2 domain of Shot proved to be essential for NMJ sprouting and FasII localisation, clearly indicating the dependence of both processes on Shot binding to the microtubule skeleton (Fig.14, Table 4). In further agreement with the results from dendrites, the expression of the Shot-L(A)Δrod-GFP construct mitigated the severity of the NMJ reduction remarkably (Fig.14) and even completely restored the *wildtypic* FasII pattern (Fig.14, Table 4). Thus, the length of the rod domain seems to be of no importance for the organisation of FasII in neuronal membranes and seems to be of minor importance for the development of NMJs. When interpreting the NMJ results one also has to consider the severe restriction of the Shot-L(A)Δrod-GFP construct to the proximal primary neurite, which might suppress proper NMJ rescue due to low local abundance at the terminal. Upon expression of the Shot-L(A)ΔEF-hand-GFP construct, both phenotypes were partially reconstituted but not fully rescued (Fig.14, Table 4) suggesting that, like in dendrites, $Ca^{2+}$ responsiveness of Shot might be required for NMJ sprouting and FasII localisation. However, also in this context, the proximal localisation of the rescue construct (Chapter 3.4.4.) may be a limiting factor for the rescue. The most revealing result was obtained with the Shot-L(C)-GFP construct lacking the first Calponin domain: in contrast to dendrites, the overexpression of Shot-L(C)-GFP did not restore the wildtypic FasII pattern and improved the *shot* mutant situation at NMJs only very mildly (Fig.14). Thus, the presence of the CH1 domain and accordingly most likely F-actin binding ability of Shot (see 3.4.1.) appears to be essential for both processes, consistent with previous reports for rescue of axonal growth cones (Lee and Kolodziej, 2002). All results obtained are summarised in Table 4.

Taken together, I could demonstrate that F-actin and microtubule binding is essential for Shot activity during NMJ development and for the organisation of the FasII membrane localisation. Since both domains are required in the cellular contexts, it is tempting to speculate that cross-linking of both filaments is essentially required for these functions, but of far less important during dendritic growth (see Discussion for details).

## 3.6. A cross tissue comparison highlights specific nervous system requirements only for the EF-hand domain

### 3.6.1. Motivation, strategy and preparational work

As explained in the introduction, Shot carries out very different functions in different tissues. As seen above for different contexts in the nervous system, where Shot has distinct domain requirements, we would expect even more severe differences when comparing less related tissue contexts. Two such examples have been reported already for Shot function in oocyte epithelia (Roper and Brown, 2004) and during tracheal development (Lee and Kolodziej, 2002). Since we have expertise in the laboratory on tendon cells (another cellular context involving Shot function; Prokop et al., 1998; Subramanian et al., 2003), we decided to use our deletion constructs and carry out a comparative structure-function analysis in this context. Tendon cells are specialised epidermal cells which anchor muscles to the cuticle, the exoskeleton of insects (Fig.15; Volk, 1999). Tendon cells achieve this mechanical resistance through linkage of microtubules to the actin-rich junction areas at the apical and basal surfaces of tendon cells (Prokop et al., 1998). Shot is required to mediate this linkage as demonstrated by the fact that loss of Shot function causes rupture of tendon cells (Prokop et al., 1998), comparable to mutant phenotypes of its orthologue BPAG1 at hemidesmosomes (Guo et al., 1995). One would expect that such a static function of Shot would be very different from its dynamic function in neuronal growth.

The most important genetic tool used in our studies on tendon cells was the *stripe-Gal4* driver line, which targets expression predominantly in this cell type (Subramanian et al., 2003). Using this line to drive Shot-L(A)-GFP reveals a apical-basal stretch of GFP-expression coinciding with the arrays of microtubules spanning the tendon cells. Increased intensity of GFP-expression at the apical and basal surfaces of the tendon cells coincides with the apical and basal hemiadherens junctions (Fig.15). We also observed a prominent 400-600nm wide gap between the Shot-L(A)-GFP-signal at the basal junction and the phalloidin-labelled muscles. This gap was not visible when expressing actin-GFP (Fig.15). Therefore, we suspected that, like in dendrites (Chapter 3.2.; Fig.4), Shot is localising in a polarised fashion at the muscle tendon junction (MTJ), with the GFP-tagged C-terminus bound to microtubules at the interior face of the hemiadherens junction density (Fig.15) and the N-terminus anchored deep within the actin rich region of the density. To test the hypothesis, I expressed the Shot-L(A)-N´6cmyc-C´GFP construct (Fig.5) in tendon cells (Fig.15).

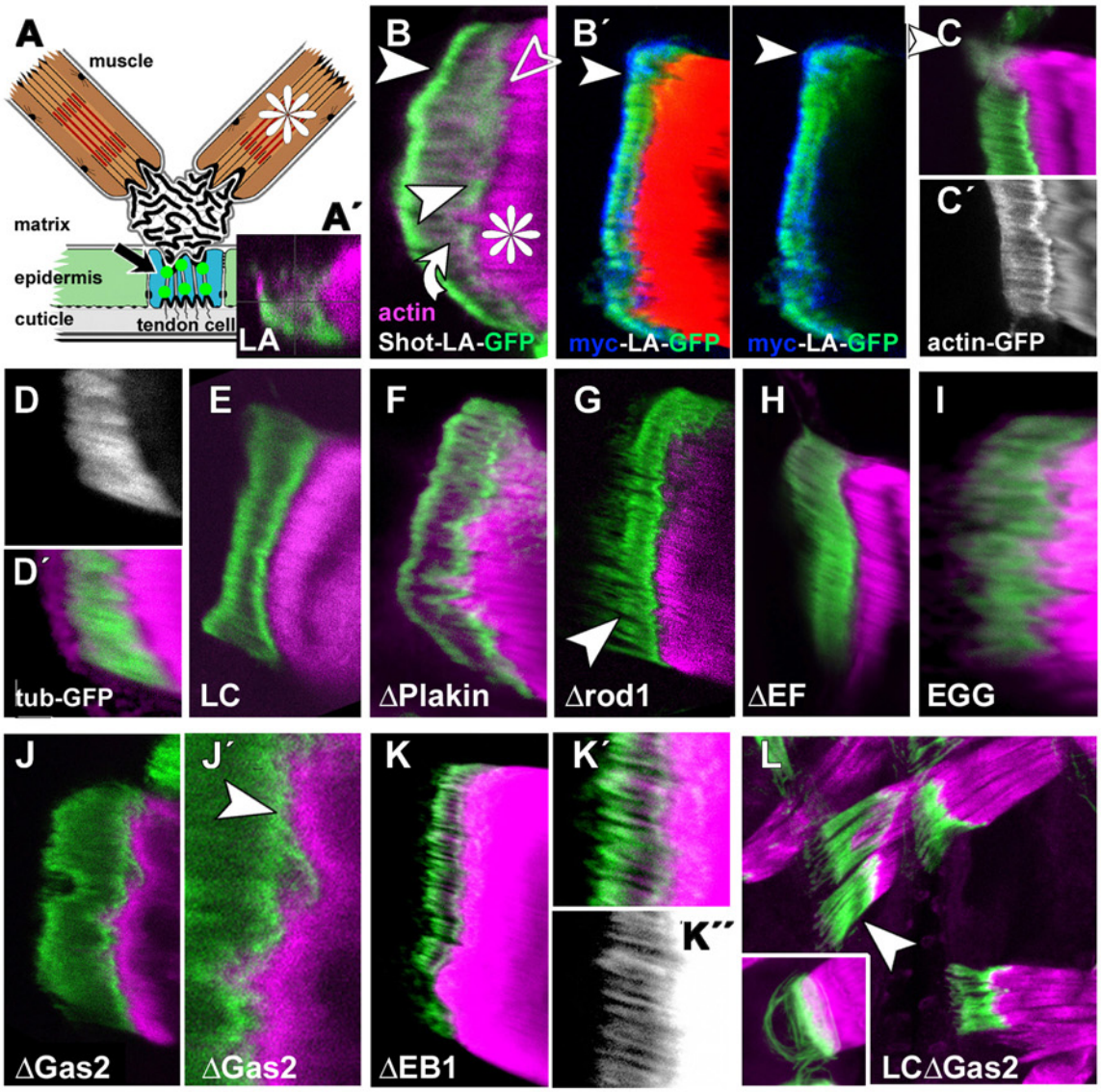
A
muscle
matrix
epidermis
cuticle
tendon cell
A´
LA
B
actin
Shot-LA-GFP
B´
myc-LA-GFP
myc-LA-GFP
C
C´
actin-GFP
D
D´
tub-GFP
E
LC
F
ΔPlakin
G
Δrod1
H
ΔEF
I
EGG
J
ΔGas2
J´
ΔGas2
K
ΔEB1
K´
K´´
L
LCΔGas2

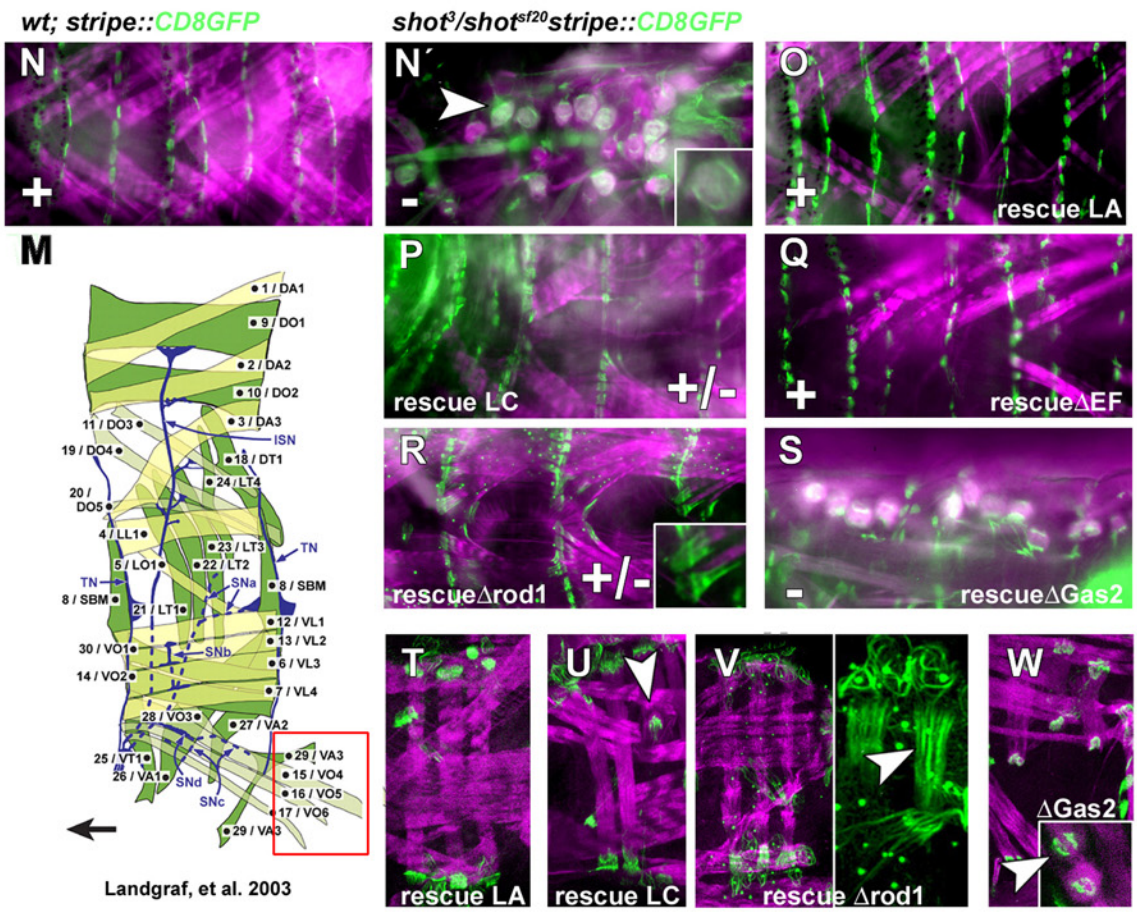
wt; stripe::CD8GFP
shot3/shotsf20stripe::CD8GFP
N
+
N´
-
O
+
rescue LA
M
1 / DA1
9 / DO1
2 / DA2
10 / DO2
11 / DO3
3 / DA3
ISN
19 / DO4
18 / DT1
24 / LT4
20 / DO5
4 / LL1
23 / LT3
TN
5 / LO1
22 / LT2
SNa
8 / SBM
21 / LT1
12 / VL1
13 / VL2
30 / VO1
SNb
6 / VL3
14 / VO2
7 / VL4
28 / VO3
27 / VA2
25 / VT1
29 / VA3
26 / VA1
15 / VO4
SNd
16 / VO5
SNc
17 / VO6
29 / VA3
Landgraf, et al. 2003
P
rescue LC
+/-
Q
+
rescueΔEF
R
rescueΔrod1
+/-
S
-
rescueΔGas2
T
rescue LA
U
rescue LC
V
rescue Δrod1
W
ΔGas2

**Fig.15. Short stop domains are of differential importance for the localisation and function in the epidermal tendon cells**

The UAS/Gal4 system was used (1) to analyses the importance of individual Shot domains for proper localisation and (2) proper function in tendon cells. Accordingly the plate is divided into two sections. The upper panel (row 1-3) shows confocal images of the localisation of different Shot deletion constructs in late larval (B-K´´) or embryonic (L) ventral oblique (VO) tendon cells (see M). Phalloidin FITC stained muscles (actin) are shown in magenta or red (B´), Shot constructs are GFP (green fluorescent protein) tagged and shown in green or cmyc tagged and shown in blue (B,B´). The localisation of actin-GFP (C,C´) and tubulin-GFP (D,D´) in tendon cells is shown. Constructs are indicated at the bottom left. The apical cuticle junction is always to the left, the basal muscle (magenta) tendon junction is to the right. Abbreviations: apical/basal, a/p.

The lower section (row 4-7) shows the muscle pattern of stg.17 animals, in *wt* (N) and *shot* mutant (N´) conditions and upon attempted rescue with five different Shot deletion constructs. (O,P,R,Q,S). The muscle pattern is visualised by injection of phalloidin (magenta) and the pictures shown are fluorescent microscope images taken from VO muscles (red box in M) at the ventral midline of stg.17 *Drosophila* embryos. Anterior is to the left. (T-W) Shows confocal magnifications of lateral transverse muscles 1-3 (LT, see M) in *wt* (T) and upon attempted rescue with different Shot constructs as indicated. The degree of rescue is indicated: "+", full rescue; "+/-", partial recovery; "-", no rescue. The *stripe-Gal4* driver line (see Subramanian et al., 2003) was used in all experiments to express *shot* constructs specifically in tendon cells.

**(A)** Schematic representation of the muscle tendon junction (MTJ). Muscles attach to the exoskeleton (cuticle) via tendon cells which anchor in the cuticle. Tendon cells are microtubule rich (arrow) and also pervaded by actin stress fibres (as shown by us C,C´). Colour codes: Muscles, brown; tendon cell, blue; epidermis, green; cuticle, grey; Shot, bright green; tendon matrix, black lines. **(A´)** Shows a confocal stack crossection of Shot-GFP localisation in a tendon cell (apical, down; basal, up; muscle shown in magenta). **(B)** Shot-L(A)-GFP enriches a/p (arrowheads) and blurred but filamentous throughout the cell (curved arrow). The muscle is indicated (*). A prominent ~400-600nm wide gap can be seen at the MTJ (open arrowhead). **(B´,B´´)** Expression of myc-Shot-L(A)-GFP reveals the subcellular polarised localisation of Shot. The N terminus (cmyc,blue) surrounds the C-terminal staining (GFP, green) and reaches into the actin rich junctional areas (arrowhead in B,B´´) and expands into the gap observed in A. **(C,C´´)** Actin stress fibres pervade the tendon cell and actin is enriched a/p. (C´) phalloidin only. **(D,D´)** Tubulin-GFP labelled microtubules pervade the tendon cell but do not enrich a/p. **(E)** Shot-L(C)-GFP localisation is indistinguishable from Shot-GFP. **(F)** Shot-L(A)ΔPlakin-GFP localisation appears mostly normal. **(G)** Shot-L(A)Δrod1-GFP enriches a/p. It associates concise with cytoskeletal filaments (arrowhead). **(H)** Shot-L(A)ΔEF-hand-GFP a/p enrichment is slightly reduced and localisation appears blurred. **(I)** The Shot C-terminus (EGG) associates with microtubules but fails to enrich a/p. **(J)** Shot-L(A)ΔGas2-GFP enriches a/p but the gap at the MTJ (see A) cannot be observed (arrowhead in J´; magnification of J MTJ). **(K)** Shot-L(A)ΔEB1-GFP enriches a/p. Localisation is slightly altered as it associates with F-actin fibres **(K´,K´´)** and enriches at their tips in a "match like" fashion (arrowhead in K´). **(L)** Overexpression of Shot-L(C)ΔGas2-GFP causes death at early larval stages (L1) and tendon cells are massively elongated (arrowhead in L) as compared to wt cells (inset). Shot-L(A)ΔGas2-GFP enriches a/p and decorates filaments throughout the length of tendon cells.

**(M)** Inside out view onto an abdominal larval hemisegment (from Landgraf et al., 2003). Muscle nomenclature is given and details can be found elsewhere (Landgraf et al., 2003). Note: the red box indicates the position of the VO muscle tendon cells analysed in this study. The wildtypic **(N)** and *shot* mutant muscle pattern **(N´)** is shown. In *shot* mutant animals muscles detach an round up (arrowhead in N´). Shot attachment sites can be seen (inset, green). **(O,T)** Shot-L(A)-GFP overexpression in $shot^{sf20}/shot^{3}$ mutant embryos fully restores the wildtype muscle pattern. **(P,U)** Shot-L(C)-GFP expression can partially restore proper tendon cell integrity. Magnification shows that only two of three muscles attach (arrowhead in U). **(R,V)** Shot-L(A)Δrod-GFP restores the overall muscle pattern but tendon cells are elongated (inset in R and arrowhead in V). **(Q)** Shot-L(A)ΔEF-hand-GFP fully restores tendon cell integrity. **(S,W)** Shot-L(A)ΔGas2-GFP completely fails to restore *shot* mutant phenotype in tendon cell. Muscles round up (S) and detach (W, arrowhead).

Consistent with our hypothesis of polarised Shot localisation, I found that the c-myc labelled N-terminus of Shot precisely fills the gap at the MTJ (Fig.15). Thus, our experiments with the Shot-L(A)-GFP construct provided us with a prominent and reproducible localisation pattern to be used as a reference for our structure-function analysis of Shot in tendon cells.

For the complementary rescue experiments, the *stripe-Gal4* line was used in *shot*$^{3}$ mutant background. For these rescues, a new strategy was developed which involved injection of a mixture of Cy3-coupled phalloidin, Triton-X and paraformaldehyde into late stage 17 embryos. This procedure stretches the young larvae out, fixes them in this position and stains their muscles in red, contrasting nicely against the GFP-tagged Shot constructs in tendon cells. Due to the injection-induced stretch of embryos, the muscles pull hard on tendon cells so that their ruptured mutant phenotype becomes very apparent. Control experiments with Shot-L(A)-GFP clearly showed that the *shot* mutant ruptured tendon cell phenotypes can be rescued, i.e. their resistance to tractive forces can be restored (Fig.15).

Taken together, we were able to demonstrate that Shot-L(A)-GFP in tendon cells localises along the arrays of microtubules and enriches specifically at the apical/basal hemiadherens junctions where it takes on a polarised orientation. Furthermore, we could develop a feasible protocol for rescue experiments. The experiments described here were partly carried out by myself, but in the majority by Ines Hahn, a diploma student in the laboratory, who was co-supervised by me during this period.

### 3.6.2. Structure-function analysis of Shot in tendon cells reveals domain requirements

Most of the deletion constructs described above (Shot-L(A)-GFP, Shot-L(C), Shot-L(A)Δrod1-GFP, Shot-L(A)ΔEF-hand-GFP and Shot-L(A)ΔGas2-GFP; Chapter 3.4.; Fig.5) were targeted to tendon cells in either wild type of *shot* mutant background to assess their localisation and rescue capabilities relative to the results obtained with Shot-L(A)-GFP. Most constructs revealed no or only minor mislocalisation phenotypes (details in Fig.15). Only two constructs will be highlighted here. First, the Shot-L(A)ΔEB1-GFP enriches apical and basal in tendon cells similar to Shot-L(A)-GFP but, in contrast to the Shot-L(A)-GFP construct whose localisation appears to be blurred (Fig.15), Shot-L(A)ΔEB1-GFP seems to be associated with actin fibres spanning the tendon cells in parallel to microtubules and accumulates at their tips in a “match-like” fashion (Fig.15). Second, the Shot-L(A)ΔGas2-GFP construct showed a strong alteration of the GFP pattern. Thus, the gap at the MTJ is completely abolished in the absence of the Gas2 domain, strongly suggesting that microtubule

binding at the hemiadherens junction might be impaired allowing the C-terminus of the Shot-L(A)ΔGas2-GFP molecule to "swing around" freely, localising deeper into the hemiadherens junction density. Consistent with this finding, the Shot-L(A)ΔGas2-GFP construct is the only one failing to rescue the tendon cell phenotype, as best seen in lateral transverse muscles and the ventral tip of ventral oblique muscles (details in Fig.15). Rescue experiments with the other constructs revealed mostly mild phenotypes (Fig.15), suggesting that the respectively deleted domains may play a partial role. Besides Shot-L(A)-GFP only shot-L(A)ΔEF-hand-GFP constructs showed no phenotype at all, ruling out any obvious involvement of the EF-hand domains in the wildtype function of Shot in tendon cells. Rescue experiments with Shot-L(A)ΔEB1-GFP (not shown) are only preliminary and need to be taken with care, whereas rescues with the Shot-L(A)ΔPlakin-GFP constructs were not possible within the time frame of this project.

These results raised a couple of issues briefly addressed in the following. First of all, our results with Shot-L(C)-GFP (lacking the CH1 domain and therefore any essential actin binding; Lee et al., 2000) were surprising at first, since they suggest that N-terminal actin binding of Shot plays only a minor role. As discussed in Chapter 3.4.1., a full deletion of both CH domains is required to strengthen this argument. However, our findings are supported by analyses of the $shot^{kakP2}$ mutant allele which is supposed to mimic the Shot-L(C)-GFP rescue situation and has been reported not to show any tendon cell phenotypes (Mende, 2004; Chapter 3.7.2.). The fact that we found partial failure of the Shot-L(C)-GFP rescue at tendon cells might seem contradictory, but $shot^{kakP2}$ mutant embryos will soon be re-tested with the very sensitive injection-based assay to find out whether minor tendon cell defect might have been missed so far in this mutant background. Interestingly, also the *UAS-Shot-L(A)ΔPlakin-GFP* constructs localised normally at the actin-rich hemiadherens junctions, leaving it open, how the N-terminal localisation of Shot revealed by our myc-tagged construct (see above) is achieved. The C-terminal phenotypes are exciting, since both constructs lacking C-terminal domains showed some aberrations. A clear role of the Gas2 domain is out of question, whereas our results with the Shot-L(A)ΔEB1*aff*-GFP construct have still to be taken with care and will have to be repeated. However, these experiments will be extremely important, since other experimental strategies have revealed that the C-terminal region after the Gas2 domain is crucial for tendon cell integrity and most of our further experiments were focussed on this area (Chapters 3.7., 3.8., 3.9.).

The only construct revealing a real difference between the nervous system and tendon cells was the Shot-L(A)ΔEF-hand-GFP deletion construct. Thus, the rescue in tendon cells

shows principal functionality of this construct. It furthermore reveals that calcium-binding as a potential regulatory element of Shot activity would play a minor role in the rigid context of tendon cells, whereas dynamic action during neuronal growth requires such regulation. Unfortunately, experiments with calcium manipulation during neuronal growth have so far not revealed any data supporting the existence of such a regulation (U. Haessler, L. Ofner and A. Prokop, personal communication).

### 3.6.3. Expression of Shot-L(C)ΔGas2-GFP in tendon cells induces a strong dominant effect

To analyse whether Shot can still bind when binding to both actin and microtubule is affected, we used the Shot-L(C)ΔGas2-GFP construct lacking the CH1 and Gas2 domain at the same time (Fig.15). We found that the expression of the Shot-L(C)ΔGas2-GFP construct in larval tendon cells causes death at early larval stages (L1). The reason for this turned out to be a massive elongation of tendon cells which often even rupture, similar to the situation induced when knocking down *shot* mRNA with RNAi (Subramanian et al., 2003). In stretched and elongated tendon cells, the localisation looked relatively normal with a filamentous appearance throughout and strong accumulations on either side of the tendon cells (Fig.15).

In contrast, expression of Shot-L(C)ΔGas2-GFP in dendrites using *RN2D+O-Gal4* causes no obvious dominant effect (Chapter 3.4.6.; Fig.12), but clear defects were observed in growth cones which enlarged significantly when using exactly the same driver line (N. Sánchez-Soriano, personal communication). Thus, the construct induces a dominant effect which appears context-specific. Sine we haven't observed similar phenotypes with the Shot-L(A)ΔGas2-GFP construct, the combined absence of both cytoskeleton-binding domains seems to be the cause for this phenotype. For example, one could imagine that lack of strong actin binding in Shot-L(C)ΔGas2-GFP enhances interaction of Shot with other proteins of the junctional complex, e.g. via the Plakin domain. In contrast, such interactions would be suppressed in Shot-L(A)ΔGas2-GFP, since tight binding to microtubules reduces the sterical flexibility of the whole molecule.

### 3.6.4. Neither the isolated Gas2 nor the isolated EB1*aff* domain localises specifically in tendon cells

As explained above (Chapter 3.4.8.), a good complementary strategy to the use of deletion constructs is the expression of domain constructs. Therefore, we targeted expression of the self-generated construct *UAS-6myc-Gas2* to tendon cells using the *stripe-Gal4* driver line. Like in dendrites (Chapter 3.4.8.) and S2 cell culture (Chapter 3.9.3.), Gas2-6myc failed to associate with microtubules but it localised throughout the tendon cell's cytoplasm instead (not shown). As mentioned before, it is likely that the architecture of the construct might interfere with the microtubule-binding capability of the isolated Gas2 domain (Lee et al., 1993). Due to lack of time, only one out of ten independent insertions was tested to date (see Table 7, Appendix 6.8.).

Furthermore, I tested the localisation of the other self-generated construct UAS-EB1*aff*-GFP in tendon cells. Like in dendrites (Chapter 3.4.) and S2 cell culture (Chapter3.9.3.), the construct failed to localise specifically (not shown). However, as mentioned earlier, only one single insertion was tested in dendrites and tendon cells so far. From a second round of injections, additional 5 independent insertions were obtained (see Table 7, Appendix 6.8.), but could unfortunately no longer be tested.

## 3.7. Comparative analysis of *shot* phenotypes in different *shot* mutant alleles

### 3.7.1. Strategic considerations for these analyses

Rescue studies with ectopically expressed gene constructs are a powerful tool to investigate the function of genes (Chapters 3.4. and 3.6.). However, results from such invasive genetic experiments become more relevant, if they can be confirmed with mutations of the endogenous gene. Since many different *shot* alleles exist (FlyBase; Drysdale and Crosby, 2005), I decided to capitalise on this fact and conduct an analysis of mutant animals bearing endogenous *shot* gene aberrations. The results from this approach were compared with the results obtained from the rescue experiments. To this end, I used three different mutant alleles described in the literature, of which I already knew that they are of hypomorphic nature (Mende, 2004). I analysed $shot^{kakP2}$ (Gregory and Brown, 1998), $shot^{V104}$ (Strumpf and Volk, 1998) and $shot^{V168}$ (Gregory and Brown, 1998) mutant embryos. Like in the rescue experiments (Chapter 3.5.), the effect of the *shot* mutation on dendrites and on the Fas2 localisation pattern was analysed, complemented by existing data on NMJs and tendon cells (see below).

### 3.7.2. Analyses of $shot^{kakP2}$ confirm results obtained with UAS-Shot-L(C)-GFP

The first allele chosen was $shot^{kakP2}$, an allele affecting the N-terminus of the *shot* gene (Gregory and Brown, 1998). In this allele, a P-element has inserted into the N-terminal promoter region into an N-terminal intron in between the alternative start sites suggesting that only isoforms C and D can be generated (Lee et al., 2000; see Fig.1). This prediction is further supported by the fact that an N-terminal antibody raised against a fragment anterior to the second Calponin domain fails to detect Shot in $shot^{kakP2}$ mutant embryos (Gregory and Brown, 1998), whereas another antibody raised against the second Calponin domain does (Mende, 2004; Fig.5). Therefore, $shot^{kakP2}$ mutant embryos would be expected to show phenotypes to *shot* null mutant embryos rescued with Shot-L(C)-GFP (Chapters 3.4., 3.5., 3.6.).

To avoid that potential additional but unknown mutations on the $shot^{kakP2}$ mutant chromosome cause *shot*-independent phenotypes, I carried out analyses in transhetrozygous mutant animals (e.g. $shot^{kakP2}/shot^{sf20}$). Thus, in a transheterozygous genetic condition in which a weak *shot* allele is over a *shot* null allele, a clean phenotype analysis can be

conducted. To visualise the condition of dendrites and NMJs, the *MzVum-Gal4* driver line was used to drive expression of the cell surface marker mCD8-GFP in motorneurons of $shot^{kakP2}/shot^{sf20}$ transheterozygous mutant animals (Fig.16). Embryos were double-stained with an α-FasII antibody to analyse the FasII mislocalisation phenotype (Fig.16). Tendon cell integrity was analysed with antibody stainings against the C-terminus of Shot in flat dissected embryos (Mende, 2004).

As predicted, the analysis of $shot^{kakP2}$ mutant phenotypes revealed similar results as the Shot-L(C)-GFP rescue experiments. In accordance with the results from the Shot-L(C)-GFP rescue experiments (Chapter 3.5.), the Fas2 pattern in $shot^{kakP2}$ mutant embryos is completely disrupted (Fig.16) whilst the dendrites and NMJs (Fig.16, out of Mende, 2004) are only moderately affected in $shot^{kakP2}$. Thus, the findings from $shot^{kakP2}$ mutant animals and Shot-L(C)-GFP rescue experiments support each other, indicating on the one hand, that Shot-L(C) is the predominant isoforms in $shot^{kakP2}$ mutant animals and, on the other hand, that our results with Shot-L(C) are no artefact.

### 3.7.3. Analyses of $shot^{V168}$ and $shot^{V104}$ suggest a specific requirement of C-terminal Shot sequences in tendon cells

The two other alleles chosen for our analysis were $shot^{V104}$ and $shot^{V168}$ which both affect the C-terminus of *shot* (see below). Both these *shot* alleles are X-ray induced chromosomal inversions. It has been shown that the chromosomal lesion in $shot^{V104}$ mutants lies within a 400bp (373bp) stretch between the position 73.398 to 73.771 of the *shot* locus (Strumpf and Volk, 1998). The mutation leads to the expression of a truncated Shot isoform (Strumpf and Volk, 1998) in which the Gas2 domain is still intact (Strumpf and Volk, 1998 and own findings; see Chapter 3.8.1.2.). However the molecular lesion of $shot^{V168}$ was not exactly mapped and had been narrowed down to the last 10kb of the genomic *shot* locus (T.Volk and A. Subramanian, personal communication).

The phenotypical analysis of the two C-terminal alleles revealed that the situation is inverse to the one in $shot^{kakP2}$ mutant animals. Whilst all analysed neuronal processes (dendrites, NMJs and the FasII pattern) in $shot^{kakP2}$ mutant animals are affected, no neuronal phenotype can be found in both C-terminal alleles. On the other hand and in contrast to the N-terminal $shot^{kakP2}$ allele (in which the tendon cells seem intact), tendon cells in both, $shot^{V104}$ and $shot^{V168}$ are severely affected and rupture (Fig.16). Since the C-terminus is affected in

both these alleles (see above and Chapter 3.8.) our findings strongly suggest that this protein portion is required in tendon cells and probably dispensable in the nervous system.

Taken together, I successfully used an N-terminal endogenous gene aberration to confirm results from our rescue studies with Shot-L(C)-GFP (Chapter 3.4.1. and 3.6.2.). Additionally, I confirmed that Shot activity exhibits tissue-specific differences, where the N- and C-terminal portions of Shot are essential in different cellular contexts. Whilst the N-terminus of Shot is essential in the nervous system and seemingly of minor importance in tendon cells, the C-terminus on the other hand is essential for tendon cells and dispensable in the nervous system.

| ***shot* allele** | **Dendrites** | **NMJs*** | **FasII** | **tendon cells*** |
|---|---|---|---|---|
| | | | | |
| $shot^{kakP2}$ | +/- | +/- | +/- | + |
| $shot^{V104}$ | + | + | + | - |
| $shot^{V168}$ | + | + | + | - |

**Table 5: Effects of different *shot* alleles on the nervous system and tendon cells.** '+' indicates wildtypic phenotype, '-' strong phenotype, '+/-' an intermediate; * taken from Mende, 2004).

anti-FasII, syt
anti-FasII
Vum::CD8GFP
shot V104/V168
ΔGas2
shot kakP2
shot null
wt
+/-
+
-
+/-
NMJs
FasII
dendrites
tendon cells
anti-FasII, syt

**Fig.16. A comparative study of *shot* alleles reveals differential requirements for the N and C terminus of Shot**

*Shot* mutant phenotypes in three different *shot* alleles: $shot^{V104}$ *and* $shot^{V168}$ (C-terminus affected) and $shot^{kakp2}$ (N terminus affected; only isoforms lacking half the actin binding domain are expressed, Gregory et al., 1998) were analysed. The phenotypes were compared with *wt* and mutant situations and related to rescue experiments conducted (see Fig.14 and Fig.15). Four different *shot* phenotypes were compared: **(row1)** The integrity of DO (dorsal oblique) neuromuscular junctions (NMJs) and the localisation of the synaptic marker Synaptotagmin (white) were assessed (NMJs indicated by white arrowheads; see also Fig15M). **(row 2)** the FasII pattern in the CNS of the respective wildtype or allelic condition is shown (white arrows). **(row 3)** The condition of Vum dendrites (open arrowheads), in the CNS were analysed. **(row 4)** The integrity of epidermal tendon cells shown schematic. NMJs, the FasII pattern and tendon cells were visualised by antibody stainings, dendrites were visualised via expression of the cell surface marker CD8-GFP with *MzVum-Gal4*. The condition of $shot^{kakp2}$, $shot^{V104}$/$shot^{V168}$ NMJs and tendon cells was taken from (Mende, 2004; and A. Prokop, unpublished data). Condition of analysed compartments was judged: "wt", wildtypic; "+/-" partially affected; "-" fully penetrant *shot* phenotype. All phenotypes were analysed in late embryonic stages (17) before *shot* mutant animals die. Colour code: Fas2, blue; Synaptic marker Synaptotagmin (Syt), white; CD8-GFP visualising Vum dendrites in (row3), green. Anterior is always to the left.

**(Column 1)** *wild type* and **(Column 2)** *shot* mutant phenotypes are shown. **(Column 3)** The phenotypes of $shot^{kakp2}$ mutants are shown. All neuronal compartments are affected. Whilst NMJs and dendrites are only mildly affected (as compared to row 1), the FasII pattern is completely aberrant. On the other hand tendon cells appear unaffected (see also Fig.15). **(Column 4)** Shows the phenotypes in *shot* mutant animals expressing Shot-L(A)ΔGas2-GFP (see Fig.14,15). None of the assessed phenotypes is soothed proofing that the Gas2 domain is essential in all contexts. **(Column 5)** shows the phenotypes of the C-terminal alleles $shot^{V104}$ and $shot^{V168}$. In both alleles the Gas2 domain is present but the downstream C-terminal portion is lacking. The situation in the nervous system of animal carrying either mutation is perfectly normal whilst the tendon cells are disrupted like in the *shot* minus situation. Thus the situation in the N-terminal $shot^{kakp2}$ allele (nervous system affected, tendon cells intact) is inverse to the situation in the two C-terminal $shot^{V104}$ and $shot^{V168}$ alleles (nervous system intact, tendon cells ruptured).

## 3.8. Molecular mapping of the breakpoint of the *shot* alleles *V104* and *V168*

The molecular lesion of *shot*$^{V104}$ had been narrowed down to a 400bp stretch on chromosome already lying between exons 22 and 23 (Strumpf and Volk, 1998). We concluded from these descriptions that the Gas2 domain should still be intact (Fig.17), consistent with my finding that this domain is absolutely required for nervous system function of Shot. However, we had good reasons to determine the molecular breakpoint more precisely. First, this breakpoint would indicate which sequences downstream of Gas2 are potentially those specifically required in tendon cells. Second, we wished to compare the mutant situation of *shot*$^{V104}$ with the roughly mapped *shot*$^{V168}$ (see below), since both alleles have been reported to show some phenotypic differences outside the nervous system (Gregory and Brown, 1998). A comparison of their molecular constellation might therefore add essential further information. The work involved in the mapping procedures was carried out partly in direct collaboration with Ines Hahn, Diploma student in the group.

### 3.8.1. The Gas2 domain in the *shot*$^{V104}$ allele is not affected

#### *3.8.1.1. Strategy and preparational work*

I firstly determined the position of the known Shot domains on the chromosome using *in-silico* analyses. According to published data (Strumpf and Volk, 1998) the predicted chromosomal breakpoint of *shot*$^{V104}$ lies within a 400bp stretch (bp73.398 to bp73.771), and my analyses revealed that the 5' end of this region falls into the intron between exon 22 and 23. Since the Gas2 domain coding sequence spreads over the exons 21, 22 and 23 (out of 27 reported for Shot-RE covering the region from bp71838 to bp73955 on the *shot* locus)[11], potentially the 3' end of the Gas2 domain encoded by exon 23 is not unlikely to be affected. However, this sequence covers only three amino acids of the Gas2 domain (see Fig.17), and the first of these 9 base pairs is still contained in exon 22 (i.e. the third last amino acid is split between exon 22 and 23). To carry out a detailed mapping of *shot*$^{V104}$, we used a combination of single embryo PCR (sePCR) and inverse PCR (iPCR).

To confirm that the mutant flies stock we worked with was identical to the published stock (Strumpf and Volk, 1998), we repeated the sePCR they had conducted earlier to narrow down the region of the breakpoint. To this end we used the same primers they had used (Volk

[11] Shot genomic locus obtained and annotated through Ensembl: chromosome: http://www.ensembl.org/Drosophila_melanogaster/geneview?gene=CG18076;db=

A-D; see Appendix and Strumpf and Volk, 1998). Unfortunately, the establishment of sePCR posed various problems costing considerable time to solve but, eventually, we were able to confirm the published breakpoint region of *shot*$^{V104}$ (Strumpf and Volk, 1998; details in Materials and Methods 2.4. and Fig.17).

Since the sequence downstream of the chromosomal breakpoint was unknown, no direct PCR could be used to amplify the gene stretch in question to determine the precise breakpoint of the s*hot*$^{V104}$ chromosomal inversion. To circumvent this problem we developed iPCR strategies. To increase the chances for success, we chose to follow three parallel and complementary experimental approaches, each with a different restriction enzyme and a suitable, carefully chosen primer pair (see below). One of these eventually yielded the desired result.

The inverse PCR was conducted accordingly to a modified protocol from the BDGP (Berkley *Drosophila* Genome Project) webpage[12] as detailed in Materials and Methods. To this end, we first isolated sufficient amounts of genomic DNA out of homozygous mutant *shot*$^{V104}$ embryos. To ensure that no wildtype DNA contaminates the mutant DNA, *shot*$^{V104}$ mutant animals were balanced with a chromosome (*CyO,twist::GFP*) which strongly expresses GFP in the body musculature from early developmental stages on. This way, we could easily identify and collect mutant embryos which lacked GFP expression. The isolated mutant DNA was digested with selected restriction enzymes and subsequently re-ligated to obtain circular DNA fragments. In the following steps, these circular fragments were used for inverse PCR. In the following I will describe the criteria for the choice of restriction enzymes and primer pairs.

Restriction enzymes for the digestion of the genomic DNA were chosen thoroughly. First, chosen enzymes did cut in the region between the primers Strumpf A and Strumpf B which precedes the 400bp region containing the *shot*$^{V104}$ breakpoint (Fig.17). Second, enzymes were selected such, that the restriction sites of the enzymes were not too close to the 400bp region containing the breakpoint and therefore potentially unknown DNA sequences in order to have sufficient sequence for proper primer design and annealing (see below). Thus the restriction sites were more than 100bp upstream of Strumpf B (Fig.17). Third, to facilitate subsequent PCR, the size of the randomly cut DNA fragments had to be kept small. Thus, restriction enzymes with recognition sequences of 4bp and 5bp respectively were selected. In average these cut every $4^4$ (256) bases or $4^5$ (1024) bases, respectively. The 3 different

[12] BDGP URL: http://www.fruitfly.org/about/methods/inverse.pcr.html

restriction enzymes which met all requirements were: *Sau3AI* (N/GATC), *Sau96I* (G/GNCC) and *MaeII* (A/CGT; Fig.17).

For each restriction enzyme a primer pair was designed. The primers had to fulfil several basic conditions: First, primers had to be long (~30bp) with melting temperatures higher than 60°C to achieve specific annealing for difficult PCR conditions (see Appendix. 6.9.13.). Second, all primers had to bind in the known chromosome region between the restriction site and primer Strumpf B, i.e. upstream of the 400bp region. Third, the primers were designed such that a maximum distance between the primer ends was achieved. If primers anneal too close, sterical problems may occur and affect the iPCR reaction (B. Altenhein, personal communication). Fourth, the primer with the 3`ends towards the unknown region carrying the breakpoint was customised such that at least 100bp were between the Strumpf B primer and the restriction site of the respective enzyme. This precaution was taken to ensure that subsequent sequencing reactions which are conducted with the same primers have achieved maximum fidelity when reaching the unknown region. The chosen primer sequences are listed in Appendix 6.9.13.

# Fig 17. Determination of the chromosomal breakpoint of *shot[V104]*

## A: Single embryo PCR confirms the chromosmal lesion of *shot[V104]*

### A1: Predicted breakpoint of *shot[V104]*

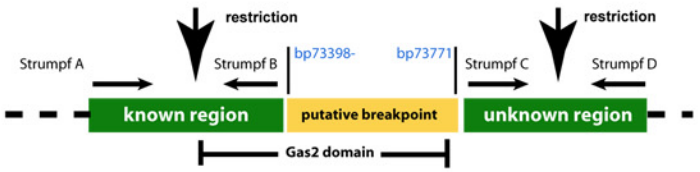


### A2: single embryo PCR confirms the breakpoint of *shot[V104]*

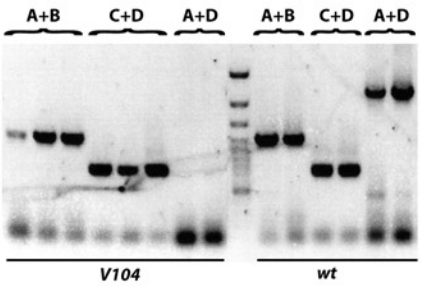


## B: Inverse PCR reveals the precise molecular breakpoint of *shot[V104]*

### B1: Principle of inverse PCR (iPCR)

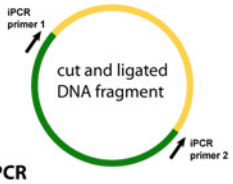


### B2: Restriction enzymes for inverse PCR

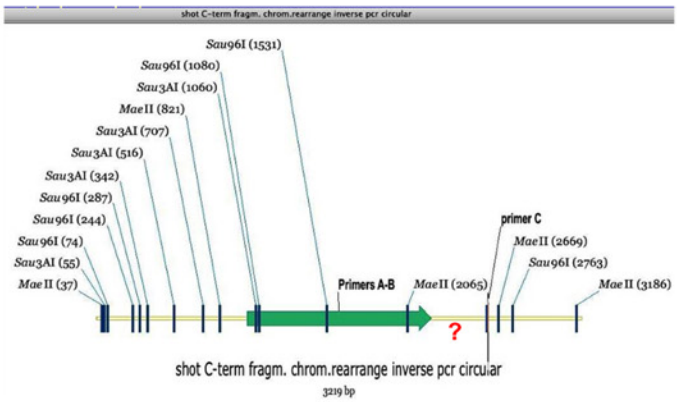


## C: Exact position of chromosomal lesion is revealed through iPCR and confirmed by PCR

### C1: The chromosomal lesion affect intron 22-23 of *shot*

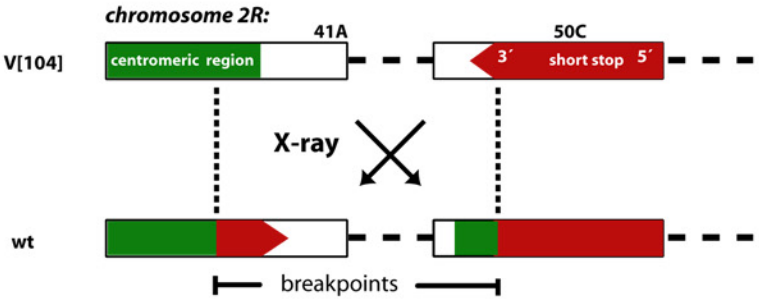


### C2: PCR confirms the chromosomal lesion

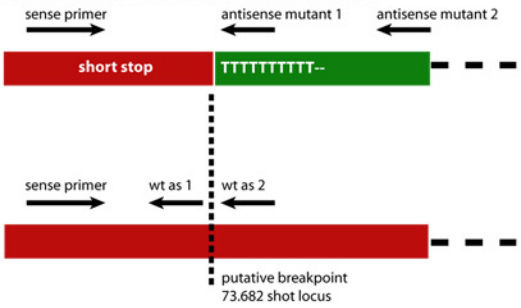


### C1´: Sequence Flanking breakpoint

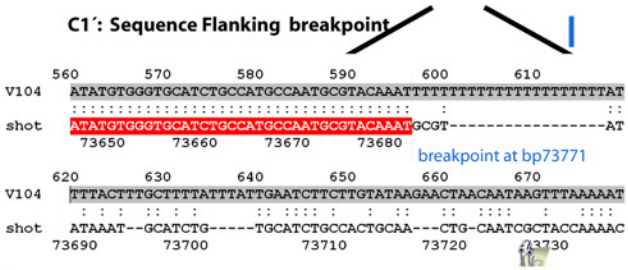


## D: The Gas2 domain of Shot[V104] is modified but stays intact

### D1: Predicted sequence of the truncated Shot[V104] protein until the Stop codon


### D2: Conservation and crystal structure the Gas2 domain strongly suggests that the Gas2 domain of Shot[V104] is intact

D2`: Alignment of the Gas2 N terminus of Shot and orthologues aa71-aa73

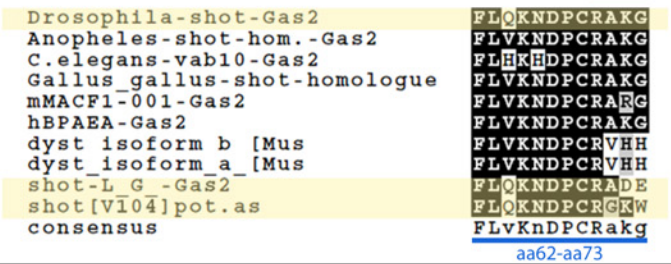


D2`: Structure of the Gas2 domain reveals aa71 as end of domain

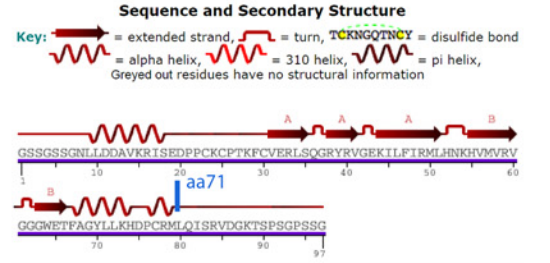

**Fig.17 Determination of the chromosomal breakpoint of the *shot*$^{V104}$ allele**

**(A)** Single embryo PCR confirms the chromosomal lesion of *shot*$^{V104}$**. (A1)** The chromosomal lesion on the *shot*$^{V104}$ chromosome has been shown to lie between bp73.398-bp73.771 of the *shot* locus which means that the C terminus of the Gas2 domain which ends at bp73.769 of the *shot* locus could be affected (Strumpf and Volk, 1998). **(A2)** Single embryo PCR using the published primers (Strumpf A-D; Strumpf and Volk., 1998) confirms that our fly stock is identical with the published stock and carries the same breakpoint. **(B)** Inverse PCR strategy reveals the precise molecular breakpoint of *shot*$^{V104}$. **(B1)** Three parallel iPCR approaches were conducted. **(B2)** To this end three restriction enzymes (*Mae*II, *Sau*96I and *Sau3A*I) were chosen to restrict the *shot*$^{V104}$ mutant DNA. Subsequently the religated, circularised DNA fragments were subjected to iPCR using appropriate inverse primer pairs (For details on the strategy see Chapter 3.8.1.). **(C)** Exact position of chromosomal lesion is revealed through iPCR and confirmed by PCR **(C1)** Sequencing of an obtained amplicon from the inverse PCR described above and in Chapter 3.8.1. reveals the chromosomal breakpoint of *shot*$^{V104}$ at position 73.680bp of the *shot* locus. A Blast search of the obtained downstream sequence of the breakpoint reveals the second chromosomal breakpoint in the centromeric region chromosome 2R which also harbours *shot*. **(C2)** The nature and sequence of the chromosomal breakpoint region was confirmed via a direct PCR approach with primers designed to bind in the novel chromosomal region downstream of the breakpoint (primers: sense, antisense mutant1 and antisense mutant2). All primer pairs used in the procedures described above are listed in the Appendix (6.9.13) and sequences can be obtained upon request. **(D)** The Gas2 domain of the truncated Shot[V104] protein is affected but stays intact. **(D1)** The breakpoint affects intron 22-23 which lies between exon 22 and 23 of the *shot* locus. The last three amino acids of the Shot Gas2 domain (spanning exons 21-23) are encoded by exon 23. The chromosomal lesion results in a termination of the Gas2 domain at position 70 (instead of 73) after the "PCR" amino acids. The chromosomal breakpoint potentially influences proper splicing of the *shot* mRNA such that the usually excised, downstream intronic sequence is now translated. On the basis of this assumption the novel predicted sequence of the truncated Shot[V104] protein is depicted in. This reveals that aa71 (which essentially contributes to the structure of the Gas2 domain; see D2´´) is conservatively exchanged (A vs. G) and thus probably functional and aa 72 is even retained. Only aa73 is exchanged completely (G vs.W). **(D2´)** The C-terminal 3aa of the Gas2 motif are highly conserved across species borders but Shot isoforms and orthologues with different terminal amino acids exist, suggesting that they are not absolutely essential (Shot sequences are shown in colour). **(D2´´)** The solved structure of the Gas2 domain reveals that only aa71 (the first one after the breakpoint) contributes to the structure of the motif, whilst the 2 following ones (aa72 and aa73) are dispensable.

*3.8.1.2. Mapping the break points of inversion V104*

The circular DNA deriving from the restriction and re-ligation was used for iPCR with the respective primer pairs (see Fig.17, materials and methods 2.5.). High Fidelity PCR kits (Eppendorf and Roche) were used to perform polymerase chain reaction as DNA quantity was low and quality was poor. All primers (6.9.13.) and vectors (6.7.) are listed in the Appendix. As expected, the initially obtained PCR products were still "noisy" and unspecific bands were abundant. To identify the specific PCR products, we isolated and cleaned the single amplified bands and used them as templates for a second PCR re-amplification round with the specific pairs used for the initial PCR. All PCRs were conducted under highly stringent conditions (>60°C). Eventually we were able to reduce the background "noise" and identify the specific PCR products. These PCR products were isolated, cleaned and subsequently subcloned into the pDrive vector (Qiagen). Once inside the vector, the obtained PCR fragments could easily be amplified and sequenced.

The sequencing reaction was successful only in the case of the Sau96I restriction enzyme and revealed the chromosomal lesion at position 73.682 of the *shot* genomic locus[13] (Fig.17). This breakpoint lies within the intron 22-23 between exon 22 and 23[14]. As mentioned earlier, the last three amino acids of the annotated Shot Gas2 sequence are coded by exon 23 which lies downstream of the affected intron 22-23. In consequence, this means that the molecular lesion results in an ablation of the last three amino acids of the predicted 73aa long Shot Gas2 domain (aa4846-aa4918 in Shot-PE[15]; discussed below (Chapter 3.8.1.3.). However the obtained sequence not only revealed the first molecular breakpoint of the chromosomal inversion, but also the non-*shot* sequence downstream of the breakpoint. We used this sequence information to identify the second chromosomal breakpoint. Using the blast software[16] we mapped the second X-ray induced chromosomal break point to the centromer region on the right arm of chromosome 2. Centromeric regions are very rich in adenine and thymine (A/T; Fig.17) where successive double hydrogen bonds are weak and particularly prone to mutational events (Juliana Alves da Silva, personal communication). We used this information to confirm our sequencing result from the iPCR. To this end, we generated a backward primer (mutant2) which binds in the centromeric region after the

[13] Shot genomic locus obtained and annotated through Ensembl: chromosome:BDGP4.2:2R:9379532:9458617:-1
[14] Shot genomic locus obtained and annotated through Ensembl: chromosome:BDGP4.2:2R:9379532:9458617:-1
[15] Ensembl ref: http://www.ensembl.org/Drosophila_melanogaster/protview?db=core;peptide=CG18076-PE
[16] NCBI Blast ref: http://www.ncbi.nlm.nih.gov/BLAST/

breakpoint (position +150bp from the breakpoint) and used this primer together with the sensewt-fw primer to amplify the region carrying the breakpoint. The successfully amplified PCR product was sequenced and we could confirm the position of the breakpoint.

### *3.8.1.3. In silico analysis of the shot$^{V104}$ gene product*

Two predictions can be made about the C-terminus of the Shot$^{V104}$ protein. First, the inversion is likely to affect the splicing behind exon 22 allowing translation to extend into the sequence of intron 22-23 until a stop codon occurs. Such a stop codon occurs at bp117-119 of intron 22-23, i.e. 39 amino acids are theoretically added to the truncated protein. The resulting predicted protein sequence is depicted in Fig.17. In this scenario, the three missing amino acids from the C-terminus of the Gas2 domain are replaced, the first of them result in conservative amino acid exchanges which maintains principal properties of this region (A to G; Fig.17; analysed via ClustalW/Boxshade, as listed in Appendix 6.6.2.) and the second one stays a K. Only the last amino acid is altered significantly (G to W exchange). Although one cannot exclude that the added 39 amino acids of the intronic sequence could have an impact on the function of the Shot$^{V104}$ protein, there is no indication in this direction, since the predicted novel sequence does not contain any known protein motifs or structures and does not yield any hit upon a Blast search. Second, the intron could still be spliced and the splicing mechanism recognises another ectopic motif on the novel downstream sequence. In this case the Gas2 domain would also terminate 3 amino acids early, but a random not predictable sequence would follow the truncated Gas2 domain.

Whatever the nature of the last 3 amino acids, they may be of little importance. First, a blast search with the truncated Shot Gas2 domain lacking the last 3aa and still results in a high prediction for an intact Gas2 motif[17]. Second, the Gas2 domain when predicted by smart and pfam protein prediction servers (Appendix 6.6.2.) is very variable with respect to the last three amino acids. Third, alignment of all available Gas2 domains from all Shot isoforms and several other related proteins from other species revealed that the last three amino acids are often highly conserved across species borders (Fig.17), but there are a number of cases in which highly conserved Gas2 motifs show variability for the terminal three amino acids (2 examples in Fig.17; also see Sun et al., 2001). Interestingly, also one Shot isoform (Shot-RG) exists, which contains alternative 3 amino acids at the C-terminus of the Gas2 domain (see

[17] NCBI BlastP: http://www.ncbi.nlm.nih.gov/BLAST/

Fig.17). Perhaps the most important argument is that the solved crystal structure of Gas2 domains (PDB[18]; see Fig.17) includes only the third last amino acid into its most C-terminal helical motif, whereas the last two amino acids seem no longer to contribute to the domain structure (Richard Kammerer, Faculty of Life Sciences, Manchester).

Taken together, the findings from the phenotypic allele study, the molecular mapping and the *in-silico* data strongly suggest, that the function of the Gas2 domain is not essentially impaired by the loss of the last three annotated amino acids. The observed phenotype of *shot*$^{V104}$ mutant animals is very likely to be caused by loss of sequences downstream of the Gas2 domain rather than the small C-terminal truncation of the Gas2 domain *per se*.

### 3.8.2. Mapping the molecular breakpoint of *shot*$^{V168}$

The molecular breakpoint of *shot*$^{V168}$ was unknown but narrowed down to the last 10kb of the *shot* genomic locus using Southern blot experiments (personal communication by Talila Volk and Arul Subramanian, Rehovot, Israel). On the basis of this information, we decided not to use a lengthy Southern blot strategy to further narrow down the region of the chromosomal lesion. Instead we decided to capitalise on our experience gained with single embryo PCR through the mapping of *shot*$^{V104}$. Thus we generated primer pairs covering the last 10kb of the *shot* genomic region (Fig.18). The primers were designed such that the resulting PCR products were approximately 1kb in length and overlapped slightly (Fig.18 and Appendix 6.9.13.3.). We used these primer pairs for single embryo PCRs (Chapter 2.4.) to test the continuity of the mutant chromosomes in *shot*$^{V168}$ embryos in successive steps. By assessing whether or not a specific primer pair is able to amplify the genomic region we were able to narrow down the region of the molecular breakpoint. Since the PCR products overlapped we could exclude that chromosomal inversions or major aberrations escape our attention. The first primer pair which failed to amplify the genomic region was *Gsense* (pos. 73.201 - 73.231) when used together with *Has* (pos. 75.205 - 75.228), whereas normal amplification occurred when the *Gsense* primer was used together with *Gas* (pos. 74.232 - 74.266; Fig.18). Thus, we were able to predict that the Gas2 domain which ends at position 73.769 of the *shot* locus is intact in *shot*$^{V168}$, comparable to the situation found in *shot*$^{V104}$. Unfortunately, lack of time did not allow us to take the next step and subject the already isolated *shot*$^{V168}$ DNA to an inverse PCR approach as carried out successfully for *shot*$^{V104}$ (see Chapter 3.8.1.2.).

[18] PDB: Protein Data Bank: http://www.rcsb.org/pdb/explore/sequence.do

Hence, so far our data suggests that, like in *shot*$^{V104}$, the Gas2 domain of *shot*$^{V168}$ seems to be intact. However, the mapping of the precise molecular breakpoint is still pending. It is likely that *shot*$^{V168}$ lacks DNA portions downstream of Gas2, as is the case for *shot*$^{V104}$.

# Fig 18.

## Determination of the chromosomal breakpoint of *shot[V168]*

**A** schematic representation of sePCR success with *shot[V68]* DNA

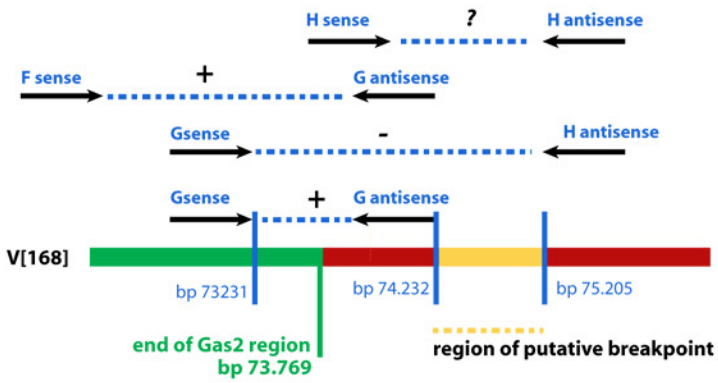


---

**B** Gel picture of sePCR revealing that the chromosmal breakpoint region *shot[V168]* is between bp 74.232 and bp 75.205

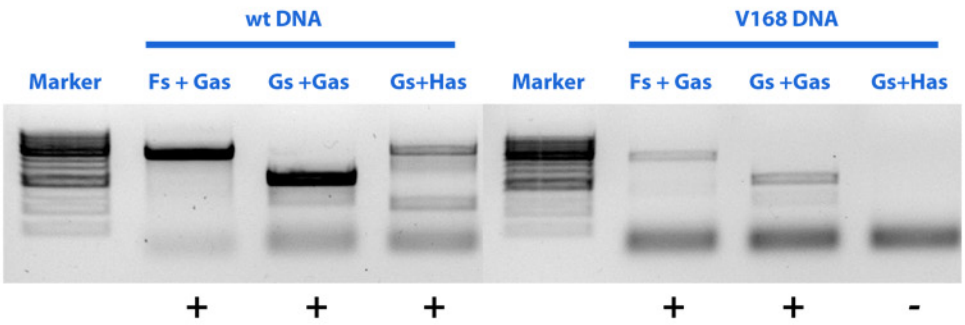

**Fig.18 Single embryo PCR reveals that the Gas2 domain is intact in *shot$^{V168}$* mutant animals**

**(A)** The X-ray induced chromosomal inversion affecting the *shot* gene in the *shot$^{V168}$* mutant allele falls into the last 10kb (of ~78kb) of the *shot* locus (A. Subramanian and T.Volk, personal communication). To understand the precise molecular nature of the *shot$^{V168}$* mutation and to determine the breakpoint, a single embryo PCR (sePCR) strategy was used. To this end primer pairs were generated such, that overlapping PCR products of the 10kb C terminal *shot* gene region could be obtained. By assessing whether a specific primer pair successfully amplifies a part of the genomic region, the breakpoint was narrowed down. The primers used are detailed in the Appendix (6.9.13.3.). PCR success with primers lying close to the identified breakpoint area on the *shot$^{V104}$* chromosome is schematically depicted in : "+", PCR product amplified; "-", no PCR product amplified. *G sense* with *H antisense* failed to generate an amplicon from *shot$^{V168}$* mutant DNA (in contrast to wt DNA) (see gel in **B**). On the other hand *F sen*se with *G antisen*se and *G sense* with *G antisense* generated amplicons (see gel in B). A control amplification carried out with *H sense* and *H antisense* unfortunately did not yield any amplicon in wt and mutant DNA as yet. Novel primers will be generated and used. The findings reveal that the *V168* genomic lesion is lying between *G antisense* and *H antisense* at position bp74.232 and bp75.205 of the *shot* genomic locus. Thus the Gas2 domain coding region which ends at position 73.769 is not affected.

## 3.9. Dissection of the Shot C-terminus: importance of the GSR+ region

### 3.9.1. Strategic considerations

The analysis of the two *shot* mutant alleles *shot*$^{V104}$ and *shot*$^{V168}$ revealed that the C-terminus downstream of the Gas2 domain is likely to be of importance to Shot function in tendon cells but dispensable for its nervous system function (Chapters 3.5 and 3.6.2.). To identify the C-terminal sequences responsible for this context-specific function, I first studied the relevant literature and analysed the C-terminus *in-silico*. On this basis, three hypotheses were formulated which will be explained in the following.

The first hypothesis assumes that the terminal EB1*aff* domain is crucial in tendon cells but not the nervous system. Thus, it was shown that the C-terminus of Shot (also including part of the rod domain, EF-hand and Gas2 domains) strongly co-immunoprecipitate with EB1 (Subramanian et al., 2003). These data do not demonstrate a direct interaction of Shot with EB1 but, since then, the EB1*aff* domain was predicted based on sequence homology to resolved EB1*aff* domains, but this homology is not too stringent (Slep et al., 2005). However, our localisation studies with EB1-HA and Shot-L(A)ΔEB1-GFP and the preliminary rescue experiments with Shot-L(A)ΔEB1-GFP, did not provide any experimental proof that this domain alone might explain the severe tendon cell phenotypes in *shot*$^{V104}$ and *shot*$^{V168}$ mutant embryos (Chapter 3.7.3.).

The second hypothesis assumes a role for the stretch between the Gas2 and EB1*aff* domains in microtubule bundling. Thus, the C-terminus of MACF (the vertebrate orthologue of Shot) contains a Glycin Serin Arginin (GSR) rich domain in this area (Sun et al., 2001). In cultured cells, the GSR construct (after Gas2 to the end of the protein) enhances the Gas2 domain interaction with microtubules, by inducing their bundling. The isolated GSR domain fails to stabilise microtubules but binds and bundles them (Sun et al., 2001). Therefore, this novel domain potentially interacting with microtubules, might be associated with possible mechanisms essential for tendon cell integrity. Since the molecular architecture of Shot and MACF is similar, I searched the C-terminus of Shot for the presence of a potential GSR domain. To this end, I first aligned the published GSR core motif (Sun et al., 2001; Fig.19) with the Shot-PE sequence[19] and could identify a highly homologous sequence stretch in Shot-PE between the Gas2 and the EB1 affinity domains at position aa5039 - aa5062 (Fig.19). Then, I searched the sequences of all Shot isoforms and a number of Shot orthologues–s and

[19] Ensembl: http://www.ensembl.org/*Drosophila*_melanogaster/protview?db=core;peptide=CG18076-PE

aligned known and potential GSR core domains with the help of the ClustalW and Boxshade programmes (see Appendix). Through this alignment it became apparent that the Shot GSR core domain is highly conserved (Fig.19). Therefore, the likelihood that the Shot GSR domain constitutes a genuine motif appeared high. However our *in-silico* analysis of the C terminus did not reveal homologies to other Shot orthologues. The third hypothesis was formulated in discussion with Dr. Richard Kammerer, Structural Biologist at the Faculty of Life Sciences in Manchester. It assumes that the complete C-terminus downstream of the Gas2 domain is composed of three repeats required for microtubule bundling (Fig.19). Bundling is often mediated by repetitive single binding motifs, as exemplified by the microtubule-associated protein Tau which carries successive internal repeats (von Bergen et al., 2005). Therefore, I was advised by Dr. Kammerer to use the repeat prediction server Radar[20] to analyse the whole C-terminus downstream of the Gas2 domain (aa4920-aa5201). This software predicted the presence of three successive repeat regions (based on sequence homology; Fig.19), which will from now on be referred to as "GSR-repeats 1-3". Secondary structure prediction by the Jpred and JUFO servers (Appendix 6.6.2.)[21] failed to recognise any prominent structures for the C-terminus formed by these repeats. However, the same is true for the microtubule-associated protein Tau, which likewise exhibits a strong microtubule affinity through 3-4 repeats without a prominent secondary structure (von Bergen et al., 2005). The GSR-repeat2 of the Shot C-terminus contains the GSR core motif discussed above (Fig.19; Sun et al., 2001), whereas the GSR-repeat3 partially overlaps with the N-terminal half of the predicted EB1*aff* domain (Fig.19). The latter observation tempts to speculate that either the EB1*aff* domain is not valid (see above), or EB1 binding at this site competes with microtubule binding of the whole C-terminus, or the borders of the EB1*aff* domain, as predicted previously (Slep et al., 2005), might not be accurate and it is in fact the whole C-terminus which is required for EB1 interaction. The GSR-repeat theory as formulated here, is based only on the prediction by the Radar server. When running the sequence on three alternative repeat recognition servers (REP, REPRO and TRUST, see Appendix 6.6.2.)[22], no internal repeats are recognised.

Published data on Shot do currently not allow making any statement as to which of the above theories is the most likely. Thus, it has been shown previously that the C-terminal protein stretch downstream of the Gas2 domain (aa4918-aa5201) exhibits moderate

[20] Rapid Automatic Detection and Alignment of Repeats: http://www.ebi.ac.uk/Radar/
[21] Expasy Server: http://www.expasy.ch/tools/
[22] Expasy Server: http://www.expasy.ch/tools/

# Fig.19.

**A**

***In silico* analysis reveals a highly conserved GSR core motif**

```
MACF                          1 GSRAGSRAGSRASSRRGSDASDFD
MACF2-GSR-domain              1 GSRAGSKAGSRASSRRGSDASDFD
GCR-domain-Plectin            1 GSTAGSRTGSRTGSRAGSRRGSFD
GCR-domain-Desmoplakin        1 GSRSGSRSGSRSGSRSGSRRGSFD
hBPAG                         1 GSRAGSKAGSRASSRRGSDASDFD
shot-PE-GSR-domain            1 GSRAGSKPNSRPLSRQGSKPPSRH
A.gambiae_shot_homo           1 GSRANSRPSSRPASRAGSKPPSRH
C.elegans_vob10_1b_GSR        1 NSIVDSSTPSRPESRASSDAGDRQ
consensus                     1 gSragSr gSR  SR gSda  fd
```

**B**

**The C terminus of Shot harbous a predicted EB1*affinity* domain (Slep et al., 2005)**

```
                          *   *                   *
APC III-IV RVTPFNYNPSPRKSSADSTSARPSQIPTPVNNNTKKRDSKTD-STESSGTQSP
hMACF2     ETVPQTHRPTPRAGSRPST-AKPSKIPTP-QRKSPA--SKLDKSSKR
mMACF2     DTS-ESSAAGGQGSSRRGL-TKPSKIPTM-SKKTTT--ASPRTPGKR
Shot       ALTGFGFKPIRRNISGSST---PSGMQTP--RKSSA-EPTFSSTMRRTSRGTT...
```

**Slep, et al. 2005**

**C**

**Jpred predics three consecutive GSR rich repeats at the Shot C-terminus, the third partially overlapping with the EB1*aff* domain**

```
GSR_repeat_1     1 ATASSSPHAHNGGSSNLPPY-MSGQGPIIKVRERSVRSIPMSRPSRSSLSASTPDSLSDNEGSHGGPSGRYTPRKVTYTST
GSR_repeat_2     1 -RTGLTPGGSRAGSKPNSRP-LSRQGSKPPSRHG-------STLSLDSTDDHTPSRIPQRKPSTGSTASGTTPRPARLSVT
GSR_repeat_3     1 --TTTTPGSRLNGTSTITRKTASGSASPATTSNGGMS----RSSSIPALTGFGFKPIRRNISGSSTPSGMQTPRKSSAEPT
consensus        1   tsstPgah gGss lsr  mSgqgs  psr g v     st Sl slsa tp  i  n  stgspsg  TPRk t t T
```

**Jpred prediciton**

**Fig.19. The Shot C-terminus harbours a highly conserved GSR rich domain**

**(A**) *In-silico* analysis reveals that the C terminus of Shot, downstream of the Gas2 domain harbours a highly conserved GSR rich core motif which in MACF1 is essential for microtubule binding and bundling ability (Sun et al., 2001). Other Shot orthologues are aligned with MACF and Shot. Respective MACF and Shot sequences are shown and highlighted in light brown. The position of the GSR motif in Shot-PE (Ensemble protein annotation) is from aa5039 to aa5062 (see also Fig.5). **(B)** The C terminus of Shot harbours a potential $EB1_{affinity}$ motif (Slep et al., 2005). **(C)** *In- silico* analysis of the Shot C terminus reveals that not only a GSR core domain exists (see A and highlighted in light green) but predicts the presence of three successive GSR rich internal repeats (GSR repeat 1-3). Internal repeats often play a role in microtubule bundling like e.g. in the case Tau (e.g. von Bergen et al., 2005). The third GSR repeat partially overlaps with the predicted EB1affinity domain (highlighted in light yellow, see B). Prediction servers predict no secondary structures in the C terminus.

microtubule affinity when expressed in cultured fibroblasts (Lee and Kolodziej, 2002). However, the construct did not single out the GSR or EB1*aff* domains. Furthermore, in contrast to published work on MACF, where the Gas2 domain alone showed clearly distinct properties from the Gas2 domain in conjunction with the C-terminus (Slep et al., 2005), similar constructs of Shot did not reveal such a difference (Lee and Kolodziej, 2002). This is in stark contrast to our observed effects in $shot^{V168}$ or $shot^{V104}$. Thus, we felt that these experiments needed to be repeated and needed to be broken down into constructs addressing subfractions of the C-terminus. To this end, we generated several epitope tagged C-terminal Shot fragments and analysed their properties in cultured cells. In the first step, we analysed localisation properties of 4 constructs comprising isolated C-terminal domains, i.e. the Gas2 domain, the predicted EB1 affinity domain, the GSR domain and of the GSR domain plus its flanking sequences (GSR+). In the next step, we generated constructs comprising the various domains in combination to test for potential synergies (see Tab.6. and Fig.20 for details of all generated constructs).

### 3.9.2. Experimental considerations and details

Details of the generation of constructs are described in the Materials and Methods section 2.8. In general, all amino acid references (aa) are on the basis of the Shot-PE sequence[23]. Constructs of single domains were designed to contain the respective consensus core sequences plus 5 flanking amino acids on either side to facilitate potential folding and to increase the distance to their epitope tags thus avoiding sterical hindrance (see below). *Vice versa*, in deletion constructs lacking single domains, only the consensus core sequences were excised (see Table 6 and Fig.20). All constructs were provided with an N-terminal Kozak consensus sequence (A/G(-3)xx A(+1)TG-G(+4); Kozak, 1987) to increase expression levels. The integrity of all constructs was confirmed through sequencing.

The *UAS-6cmyc-Gas2* construct (aa4842 – aa4923) is the same construct described before for the generation of transgenic flies (Chapter 3.4.8.). It was used in our cell culture experiments as a control, since it has been shown previously to associate with microtubules and stabilise them in culture (Lee and Kolodziej, 2002). Also the *UAS-EB1aff-2HA* construct (aa5140-aa5196 ) is the same construct described before for the generation of transgenic flies (Chapter 3.4.8.). It was used to asses its ability to bind to EB1 and thus microtubule plus ends, since it has never been shown that the EB1 affinity domain of Shot truly harbours a genuine

[23] Ensembl: http://www.ensembl.org/*Drosophila*_melanogaster/protview?db=core;peptide=CG18076-PE

EB1 binding motif (Slep et al., 2005). The *UAS-mRFP-GSR* construct (aa5034-aa5062) was generated to assess whether the GSR core sequence is sufficient to bind to microtubules and potentially even bundle them. Finally, the *UAS-mRFP-GSR+* construct (aa4918-aa5145) was generated to analyse, whether other motifs flanking the GSR core motif (aa5039 aa5062) exhibit microtubule binding and bundling capabilities. The construct is similar to the MACF-GSR construct shown to exhibit microtubule binding and bundling activity (Sun et al., 2001) but lacks the portion from the start of the EB1 domain until the stop of the protein (Δaa5145-aa5201). The composite constructs all contained the Gas2 domain with either the GSR+, the EB1 affinity domain, or in conjunction with both domains.

| Construct | aa of construct | aa of domain | Promoter | MT binding | MT bundling |
|---|---|---|---|---|---|
| | | | | | |
| **Gas2-6cmyc** | 4842 – 4923 | 4847-4918 | UAS*/CMV** | -[$] | n.a |
| **mRFP-GSR** | 5034- 5062 | 5039–5062 | UAS*/CMV** | -[$] | n.a. |
| **mRFP-GSR+** | 4918-5145 | 4918–5145 | UAS*/CMV** | + | - |
| **EB1-2HA** | 5140-5196 | 5145–5191 | UAS*/CMV** | -[$] | n.a. |
| **Gas2/GSR+/EB1-GFP** | 4836-5201 | s.a. | CMV** | no expr.[§] | n.a. |
| **Gas2/GSR+-GFP** | 4836-5145 & 5191-5201 | s.a. | CMV** | + | + |
| **Gas2/EB1-GFP** | 4836-5039 & 5062-5201 | s.a. | CMV** | no expr.[§] | n.a. |

**Table 6: Summary of C-terminal Shot constructs used for expression studies in cell culture:** ***aa of construct:*** amino acids contained in the construct based on the Shot-PE protein sequence[24]; ***aa of domain:*** position of domains in the Shot-PE sequence. ***Promoter*****: *** In *p{UAST}* vector for expression in S2 cells, co-expressed with copper inducible *pMT-Gal4* (Klueg et al., 2002); ** In pcDNA3.1(+) vector (Invitrogen) containing the CMV (CytoMegaloVirus) promoter for expression in vertebrate fibroblasts. ***MT binding***: [$] Expressed but no specific localisation; No expr: Construct became not expressed in cells; [§] Preliminary results which needs to be repeated. Other used abbreviations: s.a., see above; n.a., not addressed.

In order to carry out localisation studies with our constructs, we established cultures of the small semi-adherent *Drosophila* S2 cells in our laboratory (see Materials and Methods 2.9.1.; kindly provided by Hilary Ashe, Faculty of Life Sciences in Manchester) which have been used very successfully for cytoskeletal studies before (e.g. Rogers et al., 2002; Slep et al., 2005). UAS-coupled constructs were driven by the copper-inducible *pMT-Gal4* vector (Klueg et al., 2002) which we kindly obtained from Martin Baron (Faculty of Life Sciences in Manchester). To this end, the *pMT-Gal4* vector was co-transfected with the individual *UAS*

[24] Ensembl: http://www.ensembl.org/*Drosophila*_melanogaster/protview?db=core;peptide=CG18076-PE

constructs. Since the subcellular resolution in S2 cells turned out to be insufficient for our purposes, we turned to NIH3T3 fibroblast at later stages conducting experiments together with Christoph Ballestrem and Juliana Alves-Silva (both Faculty of Life Sciences, Manchester). All work described here was carried out in close collaboration with Ines Hahn, a diploma student in the laboratory who worked under my co-supervision.

### 3.9.3. Properties of isolated C-terminal Shot constructs in cell culture

After successful establishment of the S2 cell cultures, the first four constructs (*UAS-6myc-Gas2*, *UAS-EB1-2HA*, *UAS-mRFP-GSR* and *UAS-mRFP-GSR+*) were tested. All four transfected constructs became strongly expressed as judged by the bright fluorescent signal of the mRFP tag or antibody stainings against the cmyc or HA tags, respectively. We reached good transfection rates of approximately 15-20% for all four constructs. In spite of this fact, we were not able to detect any specific localisation for any of them, and all constructs seemed to localise un-specifically throughout the cells instead (not shown). We tried in vain to optimise the experimental procedure. First, we lowered protein levels by reducing DNA concentrations during the transfection process or protein expression times. Second, we changed fixation methods from paraformaldehyde to methanol and glutaraldehyde. Also, the tiny size and rounded shape of the S2 cells was disadvantageous. It was particularly difficult to visualise microtubules and in general to document sub-cellular features in S2 cells. Potentially, it would have helped to shift to an alternative *Drosophila* cell line, $S2R^+$ cells (Yanagawa et al., 1998), which spread out better than usual S2 cells. However, these cells are more difficult to keep (personal communication by Keith Brennan, Faculty of Life Sciences in Manchester) and we refrained from their use.

Instead, we used vertebrate NIH3T3 fibroblasts for several reasons. First, these cells have been used successfully before to express and analyse Shot constructs (Lee and Kolodziej, 2002). Second, fibroblasts exceed the size of S2 cells, and they are adherent and spread out nicely. Third, fibroblasts display a pronounced cytoskeleton. Fourth, we could capitalise on existing infrastructure and the experience of Christoph Ballestrem (Faculty of Life Sciences in Manchester), who helped us throughout the whole process from the establishment of the cell culture to the interpretation of results facilitating the progress of our analysis. After the four existing UAS-coupled Shot C-terminal constructs were transferred

into the mammalian expression vector pcDNA3 (Invitrogen), fibroblasts were transfected (Materials and Methods 2.9.2.2.).

All four constructs became expressed. Neither the *UAS-6cmyc-Gas2* nor the *UAS-EB1-2HA* construct displayed any specific localisation but occurred evenly distributed in the cytoplasm (Fig.20). This finding is similar to my finding with these constructs when expressing them *in-situ* in neurons or tendon cells of *Drosophila* (Chapters 3.4.8. and 3.6.4.). Thus, the cell culture experiments do not provide any proof for the functionality of these constructs. Especially failure of the tagged Gas2 domain to bind microtubules came as a surprise, since this domain has been shown before to have microtubule binding capabilities (Lee and Kolodziej, 2002). As discussed in Chapter 3.4.8.2. it may either be the nature of the tag (6cmyc *versus* GFP) or its position (N-term *versus* C-term) which may explain this different outcome. Also the *UAS-mRFP-GS*R construct containing the GSR core motif (aa5039-aa5062; see Sun et al., 2001) failed to associate with microtubules and localised un-specifically throughout the cells (not shown). It either means that the GSR domain of *Drosophila* is principally incapable of microtubule binding, or the N-terminal mRFP tag interferes with the short domain motif and hampers its folding or binding capability. Only the GSR+ construct (aa4918-aa5145, Tab.6) displayed a degree of specific localisation (Fig.20). The mRFP signal reveals that the construct is localised throughout the cytoplasm, but in cells which slightly lower expression it can be clearly seen to decorate microtubules (Fig.20). However, in contrast to the *MACF-GSR* construct used by (Sun et al., 2001), we were unable to see bundling of microtubules when expressing the Shot GSR+ domain (Fig.20).

Thus, we were able to identify one further microtubule binding domain at the C-terminus of Shot, the GSR+ domain. This domain might constitute a novel potential player contributing to the stability and thus maintenance of tendon cells. In contrast to experiments with the MACF C-terminus (Sun et al., 2001), we could not detect microtubule bundling with C-terminal sequences alone. However, so far we only used the isolated GSR+ domain. Therefore, it could still be that either protein portions downstream of GSR+ are essential for proper microtubule bundling, or that the whole C-terminus is required. The latter possibility would be in agreement with our GSR-repeat hypothesis.

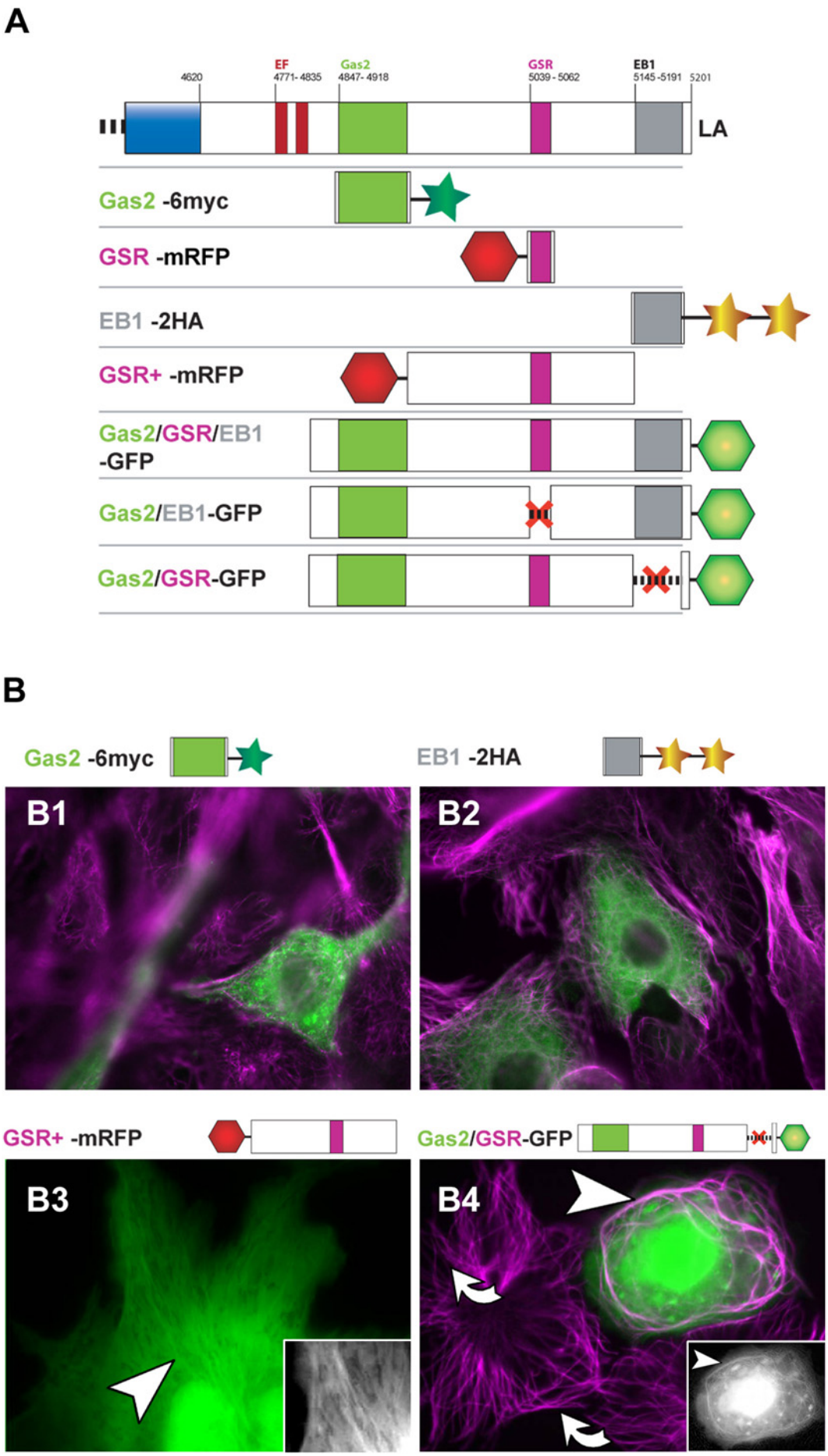
A
EF
4771- 4835
Gas2
4847- 4918
GSR
5039 - 5062
EB1
5145 -5191
4620
5201
LA
Gas2 -6myc
GSR -mRFP
EB1 -2HA
GSR+ -mRFP
Gas2/GSR/EB1
-GFP
Gas2/EB1-GFP
Gas2/GSR-GFP
B
Gas2 -6myc
EB1 -2HA
B1
B2
GSR+ -mRFP
Gas2/GSR-GFP
B3
B4

**Fig.20. Dissection of the Shot C-terminus using cell culture reveals microtubule binding capability of the GSR+ motif**

**(A)** *Drosophila* S2 cells and murine NIH3T3 fibroblast cells were used to identify Shot C terminal domains/motifs which potentially contribute to additional stability required in tendon cells by binding and/or bundling of microtubules. To this end several expression constructs were generated as depicted. More details can be found in Table 6. The Shot C terminus is shown on top. Domains are colour coded and positions are given. Running from N´ to C´ the Shot C terminus comprises two EF-hand motifs (red), a microtubule binding Gas2 domain (green), a GSR (glycine serine arginine rich) core motif (purple) and a predicted $EB1_{affinity}$ domain (grey, Slep et al., 2005). Constructs for expression in S2 cells are under the control of the UAS sequence (UAS/Gal4 system see Fig.3) and constructs for expression in fibroblasts are under control of the CMV (Cytomegalovirus) promoter. All constructs carry an epitope tag and a Kozak consensus motif (Kozak, 1987) to enhance expression levels. The nature and positions of the epitope tags are given: left, N-terminal; right, C-terminal. Used epitope tags are: mRFP (monomeric red fluorescent protein) for GSR and GSR+; eGFP (enhanced green fluorescent protein) for Gas2/GSR/EB1, Gas2/EB1 and Gas2/GSR; 6-cmyc for Gas2; and 2HA (influenza Haemagglutinin) for EB1. The first four constructs, *Gas2-6myc*, *GSR-mRFP*, *EB1-2HA* and *GSR+-mRFP* were successfully expressed in S2 cells but results are not shown as the analysis proofed to be very difficult and no obvious subcellular structures could be visualised. Subsequently fibroblast cells were used for our studies.

**(B)** *The Gas2/GSR/EB1-GFP* and *Gas2/EB1-GFP* constructs failed to express in fibroblasts (not shown) and mRFP-GSR failed to localise specifically (not shown). **(B1, B2)** The *Gas2-myc* and also the *EB1-2HA* constructs were expressed in cells and visualised via antibody staining against the respective tags (green) but also fail to localise specifically. Both induce no obvious microtubule bundling. **(B3)** mRFP-GSR+ (green) clearly associates with microtubules but fails to bundle them (arrowheads in B3 and inset). The localisation of the construct was visualised via the fluorescent signal of the mRFP epitope tag. **(B4)** In contrast the Gas2/GSR-GFP construct (green) strongly associates with microtubules shown in magenta (arrowhead and arrowhead in inset) and induces bundling (arrowhead) as compared to untransfected neighbouring cells (curved arrows). The inset shows only the GFP signal indicating the position of the construct. Clear association with microtubule bundles can be observed (arrowhead inset).

### 3.9.4. The GSR+ domain may explain the differential phenotype of *shot*$^{V104}$ and *shot*$^{V168}$

The next step of our C-terminal analysis strategy was to asses different combinations of the above analysed domains. To this end, three constructs were generated (Tab.6): a *Gas2/GSR+/EB1-GFP* construct (aa4836-aa5201) containing all three domains, a *Gas2/GSR-GFP* (aa4836- aa5201) lacking the EB1 domain (aa5145 - aa5191), and a *Gas2/EB1-GFP* construct (aa4836-aa5039 fused to aa5062-aa5201) lacking the GSR core motif (aa5039 aa5062) were built to asses the microtubule binding and bundling capabilities of the whole Shot C-terminus lacking only this short motif. All constructs were generated (see materials and methods) but, since the cloning work was conducted in the last weeks of this project, they have not been sequenced to confirm their identity. However, we were able to conduct a first transfection round testing all three constructs. Unfortunately, only the Gas2/GSR+-GFP construct became expressed as judged by the GFP signal. Most importantly, this construct exhibited strong microtubule binding, and those microtubules it bound to had a strong tendency to bundle into thick curved structures (Fig.20). This activity was mainly observed in cells with strong expression levels of the construct (Juliana Alves-Silva, personal communication).

Two statements can be deduced from our finding with the Gas2/GSR+-GFP construct. First the EB1 domain seems to be dispensable for the recruitment of the Gas2 and GSR+ domain to microtubules and is not required for the microtubule binding and bundling activity. However, this domain might still enhance the capabilities to do so. Second, the GSR+ domain, when joined to the Gas2 domain, confers essential properties, which may explain the differential phenotypes in *shot*$^{V104}$ and *shot*$^{V168}$ mutant embryos. Thus, tendon cells contain prominent arrays of microtubules, the stability/bundling of which might depend on the C-terminal domains of Shot. Neuronal axons likewise contain bundled microtubules, but factors known to mediate this constellations are other microtubule-associated proteins, such as Tau (e.g. Bettencourt da Cruz et al., 2005). We propose therefore, that Shot is the microtubule stabilising/bundling factor specifically in tendon cells, and that the C-terminal sequences are the mechanistic basis for this property. In the future we will have to assess whether direct binding of EB1 to the C-terminus is required for this activity, or whether mere microtubule-binding through the 3 GSR-repeats is the more likely mechanism.

# 4. Discussion

The aim of this study was to pinpoint context-specific modes of Shot action and the domains required in different cellular contexts. To this end I conducted a comprehensive structure-function analysis and compared Shot activity in the nervous system with tendon cells of *Drosophila melanogaster*. I achieved my goal and successfully elucidated differential domain requirements in dynamic neuronal growth *versus* static resistance in tendon cells. In the following the findings will be summarised and discussed in detail.

## 4.1. Structure-function analyses of Short stop in different developmental and cellular contexts successfully pinpoints context-specific domain requirements

We want to uncover and understand mechanisms of neuronal growth and differentiation, in particular the regulation of the cytoskeleton in this context. To this end, I have focussed on the precise role of one crucial molecule in this context, the large spectraplakin protein Short stop. The overall aim was to understand Shot function by pinpointing specific domain-requirements during neurodevelopment. Comparison of such requirements against developmental or cellular contexts in which the same domains are not required helps to formulate precise and testable hypotheses about the functional roles of such domains and, hence, of Shot in general. Building on known cellular contexts in *Drosophila* and its powerful genetic techniques, I have addressed this question successfully *in-situ*, i.e. in contexts revealing an immediate relevance.

Hence I could show that all domains with the exception of the Gas2 domain show context-specific requirements to different degrees. First, I demonstrated that the first Calponin domain (CH1) is crucial for the sprouting of NMJs and the compartmentalisation of the neuronal adhesion molecule FasciclinII whilst the same domain is of minor importance in dendrites and tendon cells. Second, I was able to demonstrate that the rod domain is only required in processes in which growth is involved or mechanical stress resistance of cells is required. Thus, the rod domain is partially essential in dendrites, NMJs and tendon cells, whilst it is dispensable for the organisation of the membrane molecule FasciclinII. Third, I found that the EF-hand motif is exclusively required in the nervous system where calcium responsiveness of Shot might play a role, whereas it might be of little importance in the epidermal tendon cells. Fourth, I could identify a C-terminal Shot protein stretch potentially

comprising two domains, a predicted EB1 domain and novel GSR rich repeat region. This C-terminal Shot portion is essential only in tendon cells but not in the nervous system.

I propose that the GSR domain supports the Gas2 domain in achieving the high microtubule stability required in tendon cell. Furthermore, I suggest that the EB1 domain has a regulatory function and influences the microtubule binding affinity of Shot. However, we were not able to pinpoint a specific function to the EB1 domain. I propose that Shot may represent the epidermal equivalent to Tau and MAP1 and 2 in neurons.

## 4.2. Manoeuvre debriefing on the methodological approaches used in this project

Several experimental approaches were used to analyse Shot activity in this work. A structure function analysis was conducted to assess the requirement of Shot domains/domain combinations in different neurodevelopmental contexts (such as dynamic dendritic growth, shaping of neuromuscular junctions and compartmentalisation of the transmembrane adhesion molecule FasciclinII) *versus* a very different context, i.e. tissue integrity of tendon cells. These analyses were carried out in 3 different ways: localisation studies and rescue experiments with deletion constructs, analysis of *shot* mutant embryos, and heterologous cell culture experiments.

### 4.2.1. *In-situ* use of deletion constructs

Deletion constructs have successfully been used to analyse Spectraplakin function (e.g. Sun et al., 2001; Lee and Kolodziej, 2002; Lee and Kolodziej, 2002; Subramanian et al., 2003; Slep et al., 2005). The use of deletion constructs in *Drosophila* is a powerful tool in which gene functions can be tested quickly and with a high resolution and the generation of transgenic flies carrying such custom built constructs is comparably easy. I capitalised on this fact by generating several novel transgenic fly strains carrying various new UAS-coupled Shot constructs. I used these and already existing fly lines carrying Shot deletion constructs to conduct my structure function analysis. These generation of fly lines was successful in almost every case and the constructs proofed to be invaluable tools for the analysis and dissection of Shot function.

The use of constructs and deletion constructs offered me various advantages. First, the availability of numerous Gal4 driver lines allowed the expression of UAS-coupled constructs in various tissues, cell types and also at defined time points. Thus they can be used for

localisation studies, dominant-negative effects can be tested and, if desired, genes can be expressed in ectopic contexts and be used for rescue approaches (Duffy, 2002). Furthermore, requirements of certain proteins at given developmental time points can be assessed. Second, constructs/proteins can easily be manipulated and visualised by providing them with various epitope tags.

However, the use of constructs also has its drawbacks. Thus, when constructs are under the control of an extraneous promoter, the native spatiotemporal expression pattern is not given which, in the worst case, may obscure results. The analysis of Shot-L(A)ΔEF-hand-GFP strikingly demonstrated that the right time point of expression may indeed have a massive impact on gene function as the potential of the construct varied when using different Gal4 driver lines (Chapter 3.4.4.). In addition, no protein isoforms are expressed unless the whole gene including all introns is used for construct generation, and even then, the endogenous regulation may not work properly due to temporal or quantitative deviations from endogenous expression patterns. Furthermore, the effect of deletions on the overall folding and function of proteins is difficult to assess. If small domains are used, the chance for miss-folding and failure to function is even higher which was possibly the case for two of the constructs generated by me, *UAS-6myc-Gas2* and *UAS-EB1-HA*. As a result of all these disadvantages, outcomes from ectopic experiments can be doubted if they are negative and often have to be backed by complementary experimental data. A good example for such complementation is the use of the Shot-L(C)-GFP construct in parallel to the analysis of $shot^{kakP2}$ mutant embryos. Whereas the mutant embryos confirmed results from the Shot-L(C)-GFP rescue experiments proving their reliability, the Shot-L(C)-GFP constructs made it possible to study subcellular localisation of this constructs, thus helping to explain the finding with $shot^{kakP2}$ mutant embryos. Another good example is the use of $shot^{V168}$ and $shot^{V104}$ mutant embryos to pinpoint the requirement of the C-terminus in tendon cells, but the use of partial deletion constructs of this area and the use of cell culture experiments in order to dissect this function in greater detail and pinpoint the molecular mechanisms behind this phenomenon.

### 4.2.2. Analyses of mutant embryos

For *Drosophila*, thousands of alleles and genetically manipulated chromosomes can be used to address specific biological questions or the relevance of genes in the whole organism. alleles exist in which not the whole gene but only specific isoforms are affected, whilst others

are Expressed normally. Such alleles allow the assessment of isoform specific requirements, and the *shot*$^{kakP2}$ allele is a good example of this (see also Mende, 2004). However, one major drawback of the mutational analysis was that, unlike in mosaic analysis with targeted expression of epitope-tagged constructs, the subcellular localisation of abundant proteins (like Shot) is more difficult to be visualised and would make it necessary to use other ways of mosaic studies, and suitable transplantation-based strategies have been reported (Lohr et al., 2002). However, such analyses are enormously difficult, and we decided to use a combined approach of allele analysis and ectopic expression studies instead. This proved to be a powerful approach allowing us to combine the advantages of both assays.

In our allele analysis we capitalised on the existence of numerous, publicly available *shot* mutant alleles to complement our result from the structure-function analysis using Shot constructs. Hence, we were abele to relate results obtained through rescue experiments with the situation in the N- and C-terminal *shot* alleles *shot*$^{kakP2}$, *shot*$^{V104}$ and *shot*$^{V168}$. Thus, we learned about the astonishingly low requirement of the CH1 domain from analyses of *shot*$^{kakP2}$ mutant embryos complemented by studies with the Shot-L(C)-GFP constructs. The analysis of the two C-terminal *shot* alleles revealed the relevance of the C-terminus for Shot function in tendon cells. In order to interpret the findings in *shot* mutant embryos and unravel the precise molecular basis underlying the observed phenotypes, we complemented our studies through combined use of transgenic fly lines (*UAS-EGG, UAS-Shot-L(A)-*$\Delta$*EB1*$_{aff}$*-GFP*) *in-situ* and our cell culture approaches. Thus, analyses of *in-situ* situations in the fly tremendously helped to focus our experimental approaches and also to reveal Shot functions which would otherwise have escaped our attention.

### 4.2.3. Use of cell culture for structure-function analyses

The use of cell cultures is a fast and powerful approach to address various cell biological and biochemical questions. It is a is widely used and accepted tool in all model systems (e.g. Karakesisoglou et al., 2000; Thomas et al., 2000; Sun et al., 2001; Lee and Kolodziej, 2002; Lee and Kolodziej, 2002; Kodama et al., 2003; Subramanian et al., 2003; Slep et al., 2005). Several aspects made cell cultures particularly attractive and useful for my work. First, in contrast to the lengthy preparations required when analysing whole animals, cell culture approaches allowed us to analyse numerous constructs quickly and relatively easy. Second, the cytoskeletal context and its molecular players are well described which

facilitated the interpretation of our results. Third, cell cultures allowed a high spatial and, through life imaging, also a high temporal resolution. I profited considerably from these advantages. For example, we could show in culture that GSR+ binds and bundles microtubules, a finding which provides essential mechanistic insights and explanations for the $shot^{V104}$ and $shot^{V168}$ mutant phenotypes. Fourth, it was particular advantageous, that the lengthy process required to generate transgenic fly strains could be substituted by faster experiments in culture. Instead, we could very quickly dissect the C-terminus of Shot and assess the properties of the domains in this portion of the protein. Hence, we were able to analyse properties of Shot and observed effects, such as microtubule binding, which helped to understand Shot activity and transfer these observations into the *in-situ* situation. Insights derived from cell culture experiments were used to decide which constructs to generate and transform into flies, such as a Shot-L(A)ΔGSR+-GFP construct. Thus, results from cell culture were directly translated into the situation in the whole organism.

However, besides all these advantages, cell cultures are also limited with respect to the validity of obtained result. Since we expressed our Shot constructs mostly in a heterologous system, vertebrate fibroblasts, we cannot exclude that observed effects are artificial with little relevance for the situation in flies. In addition, the results obtained in cell culture are not necessarily directly transferable to the situation in living animals. Cells in the organism are exposed to complex signalling events and cross-talk to their immediate environment, as exemplified by the cross-talk of muscles and tendon cells during embryonic development (Volk, 1999). Such interactions with other cell types are impossible to reproduce in culture.

Being aware of the disadvantageous, cell cultures were still a very useful and powerful tool to analyse Shot activity and we will further capitalise on the system in the future. However, the cell culture approach can only be of complementary nature helping to understand phenomena observed in *in-situ* or providing ideas for suitable *in-situ* experiments.

### 4.3. Different domain requirements for Shot in the various cellular contexts

As a result of my analysis I could clearly demonstrate that requirements of Shot domains vary between different neural contexts i.e. dendrites, NMJs and pattern of FasII localisation or the requirements in axonal growth (Lee and Kolodziej, 2002; Lee and Kolodziej, 2002). Furthermore different domains/domain combinations are required in tendon cells as compared to the nervous system. This is in agreement with the requirements in other non-neuronal contexts like oocytes (Roper and Brown, 2004), epithelia (Roper and Brown,

2003) and trachea (Lee and Kolodziej, 2002). Thus, the epidermal function of Shot is clearly distinct form the neuronal function.

In the following my results on the different domains in the different contexts are discussed in detail and related to information existing on these domains from Shot in the other contexts (axonal growth, oocyte epithelia and trachea) and from other related mammalian proteins. Here I will discuss my own insights into each domain in sequence from the N- to the C-terminus, whereas published data will only briefly be mentioned to avoid duplication of information provided already in the introduction and the respective introductory passages of Chapter 3.4.

### 4.3.1. ABD: The CH1 domain reveals surprising context-specific differences

The actin binding domain of Shot consists of two successive Calponin domains (CH1 and CH2) which together account for the actin binding capability of the molecule (Gregory and Brown, 1998; Strumpf and Volk, 1998; Lee and Kolodziej, 2002; Roper et al., 2002). Actin binding is abolished in Shot isoform C and in the Shot-L(C)-GFP constructs where the first CH domain is lacking (Lee and Kolodziej, 2002). However it is important to keep in mind that a residual actin binding of the CH2 domain has been reported for Shot and related proteins (Gimona and Mital, 1998; Gimona and Winder, 1998; Stradal et al., 1998; Yang et al., 1999; Lee and Kolodziej, 2002). The CH1 domain might exert its function through mediating homo- and hetero-dimerisation and thus actin filament organisation (Fontao et al., 2001; Young et al., 2003).

My overexpression studies reveal that the CH1 domain is not crucial for Shot localisation in both, dendrites and tendon cells. Rescue experiments and mutant allele analyses proof that the CH1 domain is only partially required for dendrites and NMJ growth but essential for the compartmentalisation of FasciclinII and, as published earlier, also for the outgrowth of axons (Lee and Kolodziej, 2002). Thus, the CH1 domain is clearly of variable importance in different neuronal processes. Our results also show that Shot functions differently in variable epidermal contexts. The ABD of Shot is not essential for tracheal fusion, where the CH1 domain is redundant with the microtubule binding domain (Lee and Kolodziej, 2002), whilst epidermal integrity and maintenance is dependant on the presence of a complete ABD as shown by the severe phenotypes of $shot^{kakp2}$ mutant animals (Gregory and Brown, 1998; Roper and Brown, 2003). In contrast, our studies show that the CH1 is of moderate importance in epidermal tendon cells where Shot-L(C)-GFP can provide a good

degree of rescue. This finding was also confirmed by analysing *shot*$^{kakP2}$ mutant animals in which the tendon cells appeared unaffected (Mende, 2004). However, it seems that the CH1 domain is more important for other aspects of epidermal cells than mechanical resistance of tendon cells. Thus, Shot has been shown to play a role in organising adherens junctions in epidermal cells (Prokop et al., 1998; Roper and Brown, 2003) . Interestingly, adherens junctions play an important role for epidermal cell polarity, i.e. compartmentalisation of cells (Knust, 2002). Given the fact that *shot*$^{kakP2}$ mutant animals also affects compartmentalisation of FasciclinII, this could mean that Shot's potential role of structuring the submembraneous cortex might in general depend essentially on its ability to effectively interact with actin filaments.

I conclude that the CH1 domain is at least partially required in all analysed processes. However, the absence of the CH1 domain and thus probably of actin binding, does not exhibit the strong phenotypes expected with exception of the severe FasciclinII mislocalisation. Results from ΔABD-construct lacking both CH domains have to be awaited to make sure that actin binding is really abolished and thus accounting for the observed defects/effects. Taken together, the findings suggest that the CH1 domain exhibits context-specific functions of Shot, potentially by organising cortical actin domains.

### 4.3.2. The Plakin domain seems to influence Shot localisation

The plakin domain is a protein-protein interaction domain (Jefferson et al., 2004). Until recently, no insights into the function of the Plakin domain in Shot existed and we were the first to analyse the properties of this large Shot domain. A yeast two-hybrid screen recently carried out in our laboratory revealed an interaction of the Shot plakin domain with the adaptor molecule D-Paxillin and several other proteins (Mende, 2004). Paxillin acts upstream of Shot, down-regulating its growth-promoting activity at NMJs (Mende, 2004; A. Prokop, personal communication). This interaction is probably mediated via the SH3 domain present in the plakin domain (my *in-silico* analysis). The latter hypothesis is presently being tested by Juliana Alves-Silva in our laboratory.

I used my self-generated Shot-L(A)ΔPlakin-GFP construct to reveal that the plakin domain is not essential for the localisation of Shot in dendrites but affects the localisation at the soma of neurons. I suspect that a part of a predicted NLS signal present in the plakin domain might account for the absence of Shot-L(A)ΔPlakin-GFP from the soma. *Vice versa*, APT which contains both, the ABD and the plakin domain localises to the nucleus of

fibroblasts (Juliana Alves-Silva, personal communication), S2 cells (Subramanian et al., 2003) and tendon cells (my findings), whilst PT does not. I conclude that both domains are required to provide a functional NLS. In accordance with this assumption, the first part of the predicted NLS is inside the CH1 domain of Shot (position aa151-aa168; Ensembl; pfscan for Shot-PE)[25].

In tendon cells, the absence of the plakin domain has a very mild effect on the localisation of Shot. The blurred filamentous localisation which normally can be observed throughout the cell when expressing Shot-L(A)-GFP is reduced, but a distinct apical basal accumulation can still be observed. This suggests that the Plakin domain serves a distinct function in tendon cells but, due to a lack of time, the generated Shot-L(A)ΔPlakin-GFP construct could not be tested in functional rescue assays as yet, and functional insights will have to wait. One cause for this delay is the fact that all independent *UAS-shot-L(A)ΔPlakin-GFP* insertions obtained from "The BestGene" are located on the second chromosome (see Tab.7; Appendix 6.8.) which also harbours the *shot* gene. Thus, recombinant chromosomes have to be generated and the required genetics is currently being carried out.

It is difficult to make a prediction about a potential rescue of neuronal or epidermal phenotypes with the Shot-L(A)ΔPlakin-GFP construct. I expect that complex interactions of the plakin domain might be crucial for some aspects of Shot function. Thus, an interaction of Paxillin has been demonstrated and further candidates for interactors of this domain have been named (Mende, 2004). Considering the Shot-Paxillin interaction, I would expect a partial rescue of dendritic *shot* mutant phenotypes or even dendritic overgrowth, since Paxillin counteracts Shots growth promoting behaviour (Mende, 2004). However the overexpression of Shot-L(A)ΔPlakin-GFP in dendrites using the RN2D+O-Gal4 driver line did not induce a dominant phenotype in dendrites. On the other hand it is well possible that other interactions mediated by the plakin domain are crucial to initiate neuronal growth or to maintain the integrity of tissues. Therefore, the lack of Paxillin interaction might be disguised by the complete lack of functionality of Shot-L(A)ΔPlakin-GFP. To address this problem in greater detail, it might become necessary in the future to generate further Shot constructs lacking only portions or few amino acids of the plakin domain.

Taken together, I conclude that the plakin domain is not crucial for dendritic targeting of Shot but influences Shot localisation in the soma and in tendon cells. The plakin domain is probably a domain which is essential for the interaction with other proteins and thus regulates

[25] http://www.ensembl.org/Drosophila_melanogaster/protview?db=core;peptide=CG18076-PE

Shot activity, for example its binding to actin and other proteins localising to actin rich membranous domains.

### 4.3.3. An integrated view of the N-terminus

We found that Shot-L(C)-GFP and Shot-L(A)ΔPlakin-GFP localise normally in dendrites. Thus, I concluded that neither actin binding (CH1) nor the plakin domain is essential for dendritic targeting of Shot. To assess whether a combinatorial requirement in the N-terminus exists, I expressed the whole N-terminus (*UAS-APT*; Subramanian et al., 2003) and the Plakin domain (*UAS-PT*; Subramanian et al., 2003) in dendrites and found that both fail to localise specifically. This indicates that the N-terminus in isolation is not sufficient to induce dendritic targeting. On the other hand, the C-terminus (Gas2 domain) of Shot is essential for localisation. Thus, to test whether the N-terminus together with the C-terminus can provide dendritic targeting cues I expressed the Shot-L(A)Δrod-GFP construct in dendrites. This construct comprises the APT (see above) fused to the C-terminus (EGG, see Fig.5). However, the construct failed to enrich prominently in dendrites. Therefore, I conclude that the whole N-terminus is dispensable for dendritic targeting.

In potential disagreement with this conclusion, the localisation of 6cmyc-Shot-L(A)-GFP at NMJs of late *Drosophila* larvae is affected as compared to Shot-L(A)-GFP (see Chapter 3.2.; Fig.13). At larval NMJs, the GFP signal of Shot-L(A)-GFP (C-terminus) is mostly restricted to the microtubule-rich core of boutons (Fig.13), and the localisation of isolated Shot domains suggests a polarised subcellular orientation of Shot. Thus, the isolated C terminus (EGG) localises to microtubules at the base of boutons and along the axon whilst the N-terminus (APT & PT) localises to the rim of boutons as well (Mende, 2004; Fig.3.13). This suggests a model where Shot is sitting at the base of boutons with its C-terminus, whilst the N-terminus stretches out towards the bouton-periphery. In such a model Shot could act as a spacing molecule, possibly even determining bouton diameters through its length. Surprisingly, the situation was different when overexpressing 6cmyc-Shot-L(A)-GFP in larval NMJs. The 6cmyc- and GFP-tags almost perfectly colocalised and no polarised orientation could be detected (Fig.13). Instead, the C-terminus seems to fail to localise to microtubules, in contrast to our findings in growth cones and dendrites where clear polar orientation is observed in that the C-terminus in localising to the central microtubule rich area and the N-terminus is stretching out into the peripheral actin-rich areas (Fig.4). Hence, the situation at NMJs seems to be the consequence of context-specific molecular interactions. Interestingly,

6cmyc-Shot-L(A)-GFP enriches far stronger at NMJs versus the axon, an effect not observed with Shot-L(A)-GFP. The reason for these differences is unclear but several explanations are thinkable. First it might be that in contrast to embryonic dendrites, Shot is not specifically oriented in larval NMJs. It might be, that Shot orientation is different in growing embryonic dendrites/growth cones as compared to fully grown larval NMJs. However, this would contradict the observations made overexpressing isolated Shot domains (see above and Mende, 2004). Secondly it is possible that the N-terminal 6cmyc-tag interferes with a context specific Shot interaction required at larval stages. In accordance with this explanation a clear localisation effect can also be observed in larval CNS where Shot-L(A)-N´6cmyc-C´GFP displays a clearly altered localisation as compared to Shot-L(A)-GFP (Fig.13), underscoring the potential influences of the N-terminal tag on the proper localisation in the context (Fig.13).

In agreement with our observation a role of the very C terminal region of BPAG1 and Plectin has been demonstrated, where the N-terminal portion preceding the ABD is able to dimerise and potentially multimerise, providing a potential mechanism for actin bundling and thus organisation (Fontao et al., 2001; Young et al., 2003). Thus the very N-terminus of Shot might still play a potential role in the regulation of Shot localisation, although the expression of APT argues against this.

On the basis of existing data, I have to conclude that the N-terminal region is crucial for only some aspects of Shot function in the nervous system, but much less for neuronal growth and tendon cell integrity. However, we still lack a more integrated test of this hypothesis, such as the use of a Shot construct lacking the complete N-terminus (AP). On the basis of my results it has already been decided that such a construct will be generated in the laboratory.

### 4.3.4. The rod domain is involved in Shot targeting and essential for neuronal growth and tendon cell integrity

Published data on Shot function during axonal growth suggest that the rod domain is dispensable (Lee and Kolodziej, 2002). I have shown for the first time that the Shot rod domain is indeed required for various cellular processes in the nervous system and tendon cells. However, even without the rod domain Shot is still able to provide a wide range of functions at embryonic stages.

The three tested Δrod constructs show various degrees of mislocalisation in the nervous system and the localisation of Shot-L(A)Δrod-GFP is also slightly affected in tendon cells. These observations strongly suggest that sequences within the large rod domain are involved in targeting. This assumption is in agreement with a demonstrated function of the BPAG1 rod domain in axonal transport where an ERM (ezrin/radixin/moesin) domain in the rod interacts with the dynactin/dynein complex (Liu et al., 2003) which also exists in *Drosophila*. In contrast to findings in other contexts, the lack of the rod domain has also functional consequences for the growth or integrity of dendrites and NMJs, which are both only partially restored upon expression of Shot-L(A)Δrod-GFP in *shot* mutant animals. The rod domain is also partially essential in tendon cells rescued with Shot-L(A)Δrod-GFP which often display an elongated morphology reminiscent of tendon cells treated with *shot* RNAi (Subramanian et al., 2003). In contrast, the rod domain is not crucial for the compartmentalisation of FasciclinII in motoraxons and for tracheal anastomosis (Lee and Kolodziej, 2002).

A potential requirement of the rod domain for various Shot functions is in agreement with a demonstrated requirement of the rod domain of Shot orthologues for the stability/elasticity of the molecule and thus tissues (Cross et al., 1990; Palmucci et al., 1994; Kahana et al., 1997; Roper et al., 2002; Roper and Brown, 2003).

Taken together, I conclude that the rod domain is involved in Shot targeting. However, it is unlikely that sequences in the rod domain are sufficient for this task. For example, in the context of dendrites, further domains are required, in particular the Gas2 domain. However, the targeting properties of the rod domain do not seem to be as absolutely indispensable since the Shot-L(A)Δrod-GFP construct can rescue *shot* mutant dendrite phenotypes partially. Thus, it seems that the rod domain plays a regulatory role improving Shot performance but not carrying out its actual function. In addition the rod domain seems to provide Shot with additional flexible properties facilitating its role in tissue integrity and stability.

### 4.3.5. The EF-hand domains are specifically required in neuronal but not epidermal cells

Calcium signalling is essential for neuronal growth regulation (Kater 1985; Gomez et al., 2001; Konur and Ghosh, 2005). The EF-hand is a common and highly conserved motif which is always involved in the ability of proteins to sense calcium levels and to alter their activity accordingly (Lewit-Bentley and Rety, 2000; Bhattacharya et al., 2004). In agreement with this notion, I found that the EF-hand domains are specifically required in the CNS and

for dynamic neuronal growth (see also Lee et al., 2000; Lee and Kolodziej, 2002). However, it was observed that Shot-L(A)ΔEF-GFP fails to localise to the distal primary neurite in motorneurons in cell culture and *in-situ* and strongly suggests a function of the EF-motif in neuronal transport of Shot which would argue against acute requirement of EF-hand-mediated regulation during neuronal growth. Unfortunately, the calcium-binding capability of Shot EF-hand domains has never been addressed, and initial attempts to test this possibility by altering the levels of intracellular free $Ca^{2+}$ concentrations in culture have failed so far. On the other hand, we found that the EF-hand motif is not required in the epidermal tendon cells. In agreement with our observation, the EF motif has also been shown to be dispensable in another epidermis-related context, i.e. tracheal fusion (anastomosis; Lee and Kolodziej, 2002). These findings clearly demonstrate that the deletion of the EF-hand domains does not disturb folding of the Shot molecule to a state of non-function, suggesting that further studies into calcium-dependence of Shot regulation during neuronal growth will be sensible.

I conclude that the EF-hand motif is specifically required to regulate Shot activity in neuronal processes but seems not to be required for epidermal functions of Shot. Furthermore, it seems that Shot regulation via this motif is strongly dependant on the specific cell type. However, the mechanism by which the EF-hand domains influence Shot activity are still not understood.

### 4.3.6. The Gas2 domain is essential for all aspects of Shot activity

The Gas2 domain is a highly conserved microtubule binding domain at the C-terminus of Shot. The Gas2 domain of MACF (Sun et al., 2001) and Shot (Lee and Kolodziej, 2002) have been shown to be sufficient to protect microtubules against nocodazole-induced depolymerisation.

I found that the Gas2 domain is essentially required, but not sufficient, for the enrichment of Shot at dendrites and the apical and basal surfaces of tendon cells. In the absence of the Gas2 motif, the Shot molecule mislocalises and displays a more homogeneous distribution in these cells. Complementary to these experiments, the isolated C-terminus of Shot (EGG see Fig.5) is able to bind to microtubules in dendrites and tendon cells but it also fails to enrich specifically in the cellular compartments (own observation and Ines Hahn, personal communication). This clearly indicates that additional factors in the Shot molecule upstream of the Gas2 domain are required for proper targeting in these cells. Our results so far argue against an involvement of the N-terminus in dendritic targeting (discussed in Chapter

4.3.3.). Since all analysed rod deletion constructs failed to localise properly (Fig.12) and thus we propose that the dendritic targeting code is made of the Gas2 domain together with cues in the rod portion. Furthermore, further domains in the very C-terminus might play a role (discussed below). More detailed dissections of Shot would be required to deduce which additional domain/domain combination is responsible for the proper localisation in tendon cells.

Rescue experiments showed that, unlike all other domains, the Gas2 domain proved to be essential in all analysed contexts. The overexpression of Shot-L(A)ΔGas2-GFP in *shot* mutant backgrounds did not improve any of the phenotypes. In this context it is important to recognise that the Shot-L(A)ΔGas2-GFP construct has proven to be functional as it was sufficient to provide *wild type* function in the context of tracheal fusion (Lee and Kolodziej, 2002). However this is the only cellular process analysed so far which seems not to depend on the presence of the microtubule binding domain of Shot.

I conclude that the Gas2 domain is essential for the localisation and function of Shot. I propose that the microtubule binding activity of Shot is the most crucial property of the molecule. I further suggest that the Gas2 domain together with the rod domain makes up for the dendritic targeting code which eventually leads to enrichment of Shot in dendrites. We are currently testing in how far the Gas2 domain cooperates with the GSR+ domain/GSR repeats to stabilise and bundle microtubules in tendon cells.

### 4.3.7. The GSR+ domain can bind but not bundle microtubules and may contribute to tendon cell stability

The GSR+ domain is a glycin serin arginine rich motif which has been shown to be able to bind and bundle microtubules in cultured vertebrate cells. The motif was first identified and characterised in the close Shot orthologue MACF (Sun et al., 2001) and my *in-silico* analysis of Shot revealed that it harbours a highly conserved GSR core domain at the C-terminus between the Gas2 and the EB1 motif (aa5039 - aa5062). Subsequently we identified that the whole C-terminus of Shot comprises three potential successive internal GSR-repeats which might account for the stability of tendon cells microtubule bundles.

The capability of the Shot Gas2 domain to bind and stabilise microtubules has been described before (Lee and Kolodziej, 2002), but the analysis of two C-terminal *shot* alleles $shot^{V104}$ and $shot^{V168}$ revealed that the Gas2 domain alone seems not be sufficient to provide the required stress resistance and microtubule stability in tendon cells (Chapter 3.7.). Initially

we suspected that the EB1*aff* domain of Shot is essentially involved in the process and we did not yet rule out this possibility fully. However we have clear indications that the Shot GSR+ domain has microtubule binding capabilities and, hence, we propose that this Shot domain is essential to establish stable microtubule bundles in tendon cells which are able to withstand tractive forces. We recognised the GSR+ domain as a possible crucial factor for tendon cell stability at a late stage of the project and thus the cloning work to generate the essential Shot-L(A)ΔGSR+-GFP construct started only recently. The construct is being built at present but no insights whether the absence of the GSR+ domain affects the localisation and/or function of Shot as such exist as yet.

Taken together, I conclude that the GSR+ domain in Shot is a highly conserved genuine domain which in isolation has the potential to associate with but not bundle microtubules. Therefore, we propose that the GSR+ domain cooperates with the Gas2 domain to achieve the required stabilisation/anchoring of microtubules in tendon cells where this property may be essential to achieve additional stability against tractive forces. However, at this point we still have to proof our hypothesis and several crucial experiments are pending. These experiments are being prepared at present.

### 4.3.8. The EB1 domain may have a regulatory function for Shot microtubule binding affinity

An interaction of Shot with EB1 has been demonstrated (Subramanian et al., 2003; Slep et al., 2005). Furthermore, localisation studies in S2 cells (Slep et al., 2005) suggest that Shot localisation depends on EB1. This notion is supported by recent observations that microtubule affinity of Shot-L(A)-GFP is strongly increased when EB3, a close homologue of EB1 (Stepanova et al., 2003), is co-transfected into fibroblasts (Juliana Alves-Silva, personal communication). However, it is not clear, if Shot recruitment to microtubules is due to a direct or indirect interaction of Shot with EB1. Thus, it has been shown that the C-terminal portion of Shot co-immunoprecipitates strongly with EB1, but a direct interaction of both proteins has never been addressed (Subramanian et al., 2003). The presence of an EB1*aff* domain at the C-terminus of Shot has been proposed recently (Slep et al., 2005) but was never really tested. From our *in-situ* analyses we know that three predicted C-terminal “GSR repeats” exist which partially overlap with the position of the predicted EB1 domain. Therefore, it needs to be clarified which of these predictions is the essential one, or whether functions exist for both predicted structures acting in a competitive or synergistic manner. The analysis of $shot^{V104}$ and $shot^{V168}$ revealed that all neuronal processes are perfectly normal in

the absence of the complete C-terminus. Therefore, if EB1 interaction with Shot crucially depends on the C-terminus, such interaction would be irrelevant for the nervous system requirement of Shot.

To test the validity, requirement and properties of the EB1*aff* domain, I generated a Shot-L(A)ΔEB1-GFP construct. Expression experiments reveal that the localisation of the Shot-L(A)ΔEB1-GFP construct is only mildly altered in both dendrites and tendon cells, and preliminary rescue studies suggest that this construct might be sufficient to restore Shot function in tendon cells. The F-actin affinity of the Shot-L(A)ΔEB1-GFP construct as compared to Shot-L(A)-GFP appears to be increased (Fig.15), indicating that the EB1*aff* domain might be involved in microtubule association of Shot. I can think of two possible explanations. Either the direct microtubule binding capability of Shot is affected due to the fact that the third GSR-repeat is incomplete, or EB1*aff* indeed binds EB1. Several experiments have been initiated within the framework of this project already to distinguish between these possibilities. First, *UAS-EB1aff-GFP* transgenic flies were generated to analyse the binding capabilities of the isolated EB1*aff* domain *in-situ*. Unfortunately, no specific localisation could be seen. However, there is still hope, since the only construct tested so far did not become expressed in flies at all suggesting principal problems of the construct insertion in this transgenic fly line. A further experiment which we started to prepare is co-transfection of EB3-GFP together with either a *UAS-Gas2/GSR/EB1-GFP* or a *UAS-Gas2/GSR+-GFP* construct (see Fig.20). This experiment should show whether the EB1*aff* domain is genuine and able to increase the EB3-mediated microtubule association of the Shot C-terminus. Unfortunately, although the constructs are existing, a lack of time did not allow us to perform these experiments before the end of this project but they are currently being continued in the laboratory.

Taken together we were not able to proof that the EB1*aff* domain is genuine and we could not identify a specific function of the EB1*aff* domain as yet. We propose however, that the EB1*aff* domain and thus Shot/EB1 interaction has a regulatory function for Shot microtubule affinity and that this regulation depends on EB1 levels. The EB1*aff* motif seems not to be essential in dendrites and apparently is also dispensable in tendon cells. It might well be, that the EB1 domain is crucial at later stages or for higher order functions of Shot. Having said all that we are well aware of the possibility that the predicted EB1*aff* motif may not be genuine and that instead the predicted three successive GSR repeats are required and account for the observed effects and phenotypes. Appropriate studies addressing requirements of the EB1 domain are currently being continued.

4.3.9. An integrated view of C-terminal Shot domains: common and specific requirements

We find that requirements of the C-terminus are context-specific and that different portions of the C-terminus are essential in different contexts. Thus, the potentially calcium-binding EF-hand motifs are exclusively required in the nervous system but within the nervous system they appear essential for all tested functions. We find that the Gas2 is of crucial importance for all analysed aspects of Shot activity.

Binding of Shot to microtubules seems to be required for its dynamic as well as static functions. Whilst the presence of the Gas2 domain is sufficient in neuronal processes, additional downstream protein portions are required for bundling and/or stabilisation of microtubules in tendon cells. Although we could not pinpoint a specific requirement for the EB1*aff* domain, its absence causes slight mislocalisation, and Shot affinity to microtubules is massively enhanced in the presence of EB1. These observations indicate that, as shown previously, Shot can interact with EB1 in some form. Therefore, EB1-binding might regulate Shot activity in a context-specific manner. Even more important seems to be the C-terminal GSR+ region. We could demonstrate and confirm that this portion of Shot exhibits microtubule-binding activity and that the domain in combination with the Gas2 domain strongly bundles and stabilises microtubules. However, at this stage, we cannot comment on whether GSR+ and EB1*aff* domains should be viewed separately, or whether both together act as one entity composed of three GSR-repeats. Additional constructs will have to be built to define domain requirements and borders in more detail.

## 4.4. Pending tasks and work following on from this project

My results clearly elucidate that the Spectraplakin Shot, like its vertebrate orthologues, uses its modular architecture to act as a versatile multi-functional cytoskeletal crosslinker in different cellular contexts. The different Shot domains show clear context-specific requirements and I could pinpoint clear differences of Shot function in the nervous system and epidermis. We demonstrate that a part of the Shot C-terminus is not essential in the nervous system but essential in tendon cells. However, the precise molecular mechanism underlying these differences is yet to be unravelled on the molecular level, building on preliminary results and deduced hypothesis generated through my work.

Thus, future work will have to concentrate on dissections of the Shot C-terminus downstream of the Gas2 domain and its function in epidermal tendon cells. The combined strategy of cell culture experiments, *in-situ* expression and rescue studies and genetic experiments employed in my project needs to be completed as discussed in Chapter 4.3.9. Thus, the molecular borders of the GSR domain required for microtubule binding, bundling and stability (nocodazole resistance) need to be determined. Such studies could be complemented with biochemical assays to verify the ability of the C-terminus to bind EB1 directly.

Besides assessing the properties of the C-terminus in culture, one could make use of the *myospheroid* (*mys*) mutation in *Drosophila* to understand the requirements of the C-terminus *in-situ*. In *mys* mutant embryos, muscles detach from tendon cells. Thus, in *mys*;*shot* double-mutant embryos the tendon cells no longer experience tractive forces, and tendon cells no longer rupture even in the absence of Shot function. Thus the *mys* mutant background allows looking at structurally integer *shot* mutant tendon cells and study the condition of their cytoskeleton, in $shot^{3}$ null mutant embryos *versus* $shot^{V104}$ or $shot^{V168}$ mutant embryos. Such studies would have a high potential to complement our culture assays in answering to which degree microtubules depend on the Shot C-terminus *in-situ*.

Furthermore, the deletion constructs generated by me, i.e. Shot-L(A)ΔABD-GFP, Shot-L(A)ΔPlakin-GFP and Shot-L(A)ΔEB1-GFP will have to be tested in localisation and rescue studies to complete the rescue experiments conducted in this thesis. Such studies should clarify in how far (1) the CH2 domain has an impact on Shot activity, (2) the plakin domain affects Shot function in dendrites or tendon cells, and (3) the EB1*aff* domain of Shot is required in dendrites and possibly tendon cells.

A further intriguing, so far completely neglected, aspect of Shot function which arose from my studies is the potential involvement of Shot in neuronal pathfinding. So far the misrouting was only observed when overexpressing the Shot-L(A)ΔGas2-GFP construct in a *shot* loss-of-function background. The right model system to address such questions is axonal growth cones. Recent findings in our laboratory strongly suggest a function of Shot in this context, where it is crucial for the morphology and thus probably properties of neuronal growth cones (Lisa Ofner, Ulrike Haessler, Natalia Sánchez-Soriano and Andreas Prokop, unpublished results). In addition, Shot localisation at growth cones seems to require N-terminal domains, in contrast to what I found in dendrites. Therefore, all constructs generated in this project will become an asset for the work which is currently being carried out on Shot function in growth cones. Furthermore, growth cones may represent an ideal model to study

the role of the EF-hand motifs, as demonstrated by preliminary experiments manipulating and measuring intracellular free $Ca^{2+}$ levels in growth cones.

# 5. Acknowledgements:

I wish to thank Andreas Prokop who gave me the opportunity to work on this project in Mainz and Manchester and supported me throughout the four years. I am deeply grateful for all the effort and time you invested to teach me and I really appreciated our interesting and challenging discussions. Thank you very much for the excellent training I received, all the help you gave me throughout the project and all the helpful comments on manuscripts applications and on my thesis.

I am grateful to Prof. Gert Pflugfelder, Prof. Gerd Technau and Prof. Rudolf Leube for taking the time to read my thesis and for being my examiners. Thank you Gerd Technau for allowing me to work in your lab for a good part of my project.

My biggest thanks go out to you Nadja Meyer! Thank you very very much for your love and support in all the years. Without you I would not have been able to finish this project and to achieve so much. Thank you for everything!!!

Mein ganz besonderer Dank gilt meinen Eltern Roswitha und Diethelm Bottenberg die mich in all den Jahren nach Kräften unterstützt und ermuntert haben. Ohne Euch hätte ich es nicht geschafft. Vielen vielen Dank!

I also wish to thank all my friends who endured me, visited me in the UK and always supported me. In particular I wish to thank Christian “Wurstebub” Koch and Anna Pitschner, Nina Dietrich and Marc, Martin Klussmann, Niklas Schörnig and Andrea and of cause Christian “OD” Dorner.

Thank you very much Natalia “don’t touch my drawer!” Sànchez-Soriano for being a friend in all the years, for the excellent collaboration which I really enjoyed and for the sharp and very helpful discussions and recommendations at all stages of our projects!

I also wish to thank my little pessimistic and hungry colleague and friend Mohiddin “the time is running out” Lone which went through all good and hard times together with me, providing me with halal food. Remember, “With a little bit of luck” everything will be fine!

Thank you Inezzz! Hahn for being my first and possibly best diploma student ever. I really enjoyed our stay in Manchester and our great collaboration. Thank you Alex Baade for all the fun we had in Manchester.

My special thanks go to you dear Schnuckis (Michael “der Bub” Avermann and Rikki “die Schnucki” Haessler for the good time in the lab and for all the fun we had in England, Manchester and Levenshulme in particular.

Thank you very much Juliana Alves da Silva for helping me, cheering me up and being a friend when things got ugly. Thank you Mauricio for all the fun time in Manchester and Liverpool and for your striking demonstration that one always has a reason to be happy!

Thank you very much indeed Marc Ziegenfuss for giving me a shelter. Thanks to you I did not have to sleep rough under the Mancunian way. I was really happy not to live alone and really liked our shared flat!

Thank you Roger Meadows for giving me insights into the sinister english soul.

Thank you Joe “Josef” Urban for your major contributions to my good times in Mainz! Thank you very much for your excellent help in the lab and for your advice and leadership on the way to become a world class runner. Without you there would be no “Bottenberg” and my name would not be eternal.

Thank you Alex Mauss and thank you Desire for making our life in England even more colourful and pleasant.

Furthermore I wish to thank the Manchester lab: Abduuuuhhhl Al Katheeb, thank you for enduring general abuse and the “Rucksackkontrolle” and for being a huuuuuhhge spiritual leader. Thank you Melanie Klein for sorting us out, organising the lab and in general for being a really nice colleague and collaborator.

I wish to thank all the people from the Technau lab: especially Geo Vogler, for keeping me on my toes, Christoph Rickert, Anna Rogulja Ortman, Christian Berger, Tina Hinkelmann, Benjamin Altenhein, Erika Jost, Karin Luer, Ricki Mettler, Rolf Urbach, Janina Seibert, Ruth Beckervordersandforth, Melli Jawerka, Niko Frank, Diana Cleppien, Tanja Novotny, Thomas Loeffler, Oli Vef (special thanks go out to you for the constant and kind help with all fly problems I encountered), Sebastian Jansen, Michael Mende, Robert Löhr, Ulrike Kalkowski, Barbara Groh-Reichert, Frau Ebenrecht und Frau Kästner. You were really nice colleagues and I really enjoyed the time in Mainz.

This work was funded by: The European Commission; Contract number QLG3-CT-2001-01181 and The Welcome Trust (077748/Z/05/Z).

# 6. Appendix

## 6.1. Chemicals

If not stated differently, chemicals used were purchased from Roth, Karlsruhe, Germany. Sigma-Aldrich Co, UK. or Fluka, UK.: Chemicals obtained there and not mentioned elsewhere: Ethanol, Methanol, Heptane and Isopropanol.

## 6.2. Kits

**QIAquick Gel extraction Kit** (Qiagen, Hilden, Germany)
**QiaexII Gel extraction Kit** (Qiagen, Hilden, Germany)
**Qiaquick PCR purification kit** (Qiagen, Hilden, Germany)
**Qiaprep Spin Miniprep kit** (Qiagen, Hilden, Germany)
**HighSpeed Plasmid Midi kit** (Qiagen, Hilden, Germany)
**HighSpeed Plasmid Maxi kit** (Qiagen, Hilden, Germany)
**Qiagen Plasmid midi kit** (Qiagen, Hilden, Germany)
**Qiagen PCR cloning kit** (with pDrive) (Qiagen, Hilden, Germany)
**Fastplasmid kit** (Eppendorf, Germany)
**TOPO TA Cloning Kit** (with TOPO) (Invitrogen, Carlsbad, USA)
**Effectene**® transfection kit (Qiagen, Hilden, Germany)
**LipofectAMINE PLUS** (Invitrogen, Carlsbad, CA)
**Rapid DNA ligation kit** (Roche, Lewes, UK)

## 6.3. Enzymes and implements for molecular biology

### 6.3.1. Restriction enzymes

Restriction enzymes were obtained from three different manufacturers and used according to their recommendations:

**New England Biolabs**, Ipswich, MA, U.S.A.: http://www.neb.com/nebecomm/default.asp
**Roche Applied Science,** Lewes, UK: https://www.roche-applied-science.com
**Fermentas MBI**, St. Leon-Rot, Germany: http://www.fermentas.de/

### 6.3.2. Polymerases

**Biotaq DNA polymerase**, (Bioline Ltd., London, UK.)
**Native Pfu DNA polymerase**, (Stratagene, La Jolla, CA, U.S.A.)
**Expand High Fidelity PCR System**, (Roche, Lewes, UK.)
**TripleMaster PCR System**, (Eppendorf, Hamburg, Germany)
**Dig RNA labelling mix,** (Roche, Lewes, UK)
**PCR Dig Probe Synthesis Kit,** (Roche, Lewes, UK)

### 6.3.3. DNA modifying enzymes

**Calf Intestine Alkaline Phosphatase**, (Roche, Lewes, UK.)
**T4 DNA Ligase**, (Roche, Lewes, UK.)

### 6.3.4. Other relevant reagents

**dNTP set (4x25µg)** (Bioline Ltd., London, UK.)
***Hyperladder VI*** (Bioline Ltd., London, UK.)
***Roche molecular weight marker II*** (Roche, Lewes, UK)
***Roche molecular weight marker XVI*** (Roche, Lewes, UK)
***Big dye*** ™ terminator cycle sequencing kit v.3.1 (Perkin Elmer, MA, USA)
***6x loading dye*** (Fermentas, St.Leon Rot, Germany)

## 6.4. Buffers, media and others

***A&B phosphate Buffer:*** *S*olution A: 28.39g Na2HPO4 in 1L H2O; Solution B: 27.6g NaH2PO4 in 1L H2O. A mixture of 36ml solution A and 14 ml solution B is filled up to 100ml with H2O. The resulting buffer is set to pH 7.2

***Agar Agar*** (König & Wiegand, Düsseldorf, Germany)

***Agarose*** (Melford Labs LTD., UK.)

***Alkaline phosphatase (AP) detection buffer*****:** 10ml 5M NaCl, 25ml 1M MgCl2, 50ml 1M Tris (pH9.5), 0.5ml Tween20, 412ml H2O, pH set to 9.5

***Apple-agar*** **:** 27-28g of agar are dissolved in 1L commercially available apple juice. Mixture is poured into petridishes, which are stored upside down at 4°C

***Apple juice agar plates for egg collections:*** 21g Agar Agar; 1l commercially available apple juice; → cooked until the Agar Agar dissolved completely and poured into plastic dishes. Plates were stored at 4°C and used for up to 3 weeks.

***Bleach:*** (ADOCO Ltd., Bright Mills, Bolton, UK)

***5-Bromo-4-chloro-3-indolyl phosphate (BCIP)***: solution for AP-staining: 50mg/ml BCIP in 100% N,N-Dimethylformamide

***BSA*** Bovine serum albumine 96% (Sigma, Steinheim, Germany)

***Bouin's fixative solution*** *(Featherstone et al., 2002)*: 7.5ml saturated picrinic acid, 2.5ml formaldehyde (37%), 0.5ml glacial acetic acid.

***Broadie and Bate buffer (B&B)*****:** 135mM NaCl, 5mM KCl, 4mM MgCl2, 0.5mM CaCl2, 5mM TES – N-tris[Hydroxymethyl]methyl-2-aminoethansulfonic acid, 36mM sucrose, pH is set with NaOH to 7.15

**BufferA:** 100mM Tris-HCl (pH7.5), 100mM EDTA, 100mM NaCl and 0,5% SDS.

***DAB-Solution*****:** 10mg 3,3'-Diaminobenzidine Tetrahydrochloride are dissolved in 30ml PBT and subsequently aliquoted in volumes of 1ml and stored at -20°C.

***DEPC 97%*** (diethylpyrocarbonate) (Sigma, Steinheim, Germany)

***DMEM*** Dulbecco´s modified Eagles medium (Sigma, Irvine, UK)

***DPBS*** Dulbecco´s phosphate buffered saline (Bio Whittaker, Verviers, Belgium)

***Embedding Oil:*** 70% glycerol in 1x PBS

***Ethidium Bromide*** 95% (Sigma, Irvine, UK)

***FCS*** fetale calf serum (Biochrom KG, Berlin, Germany)

***Fibronectin*** (Sigma, Irvine, UK)

***Glutaraldehyde:*** (Sigma, Irvine, UK)

***Gloor and Engel´s buffer (Squishing buffer):*** 10 mM Tris HCl (pH 8.2); 1 mM EDTA; 25 mM NaCl; 200mg/ml proteinase K (always fresh from 20mg/ml stock solution)

***Glycerol*** (VWR International Ltd., UK)

***Heptane glue (coated coverslips)***: Sticky tape was submerged in Heptane to dissolve the glue from the tape. The obtained glue was spread on 22x22mm cover slips and they were dried until the Heptane evaporated. Cover slips were used to attach dechorionated embryos for injection.

***Histoacryl glue*** (B/Braun, Melsungen, Germany)

***Hybridisation solution (Hyb soln.):*** 12.5 ml 20xSSC; 25 ml formamide;12.5 ml DEPC water
50µl tween20

***LB agar:*** 0.17M NaCl, 1.0% (w/v) Tryptone, 0.5% (w/v) Yeast extract, 2.0% (w/v) Agar

***LB agar and ampicillin plates*:** add 15g/L agar to freshly prepared LB broth (see below), autoclave and cool to 50°C, add ampicillin to 100µg/ml, pour plates and store at 4°C

***LB-Broth with MgSO4 and KCl (250 ml:)*** MgSO4 (0,02M); KCl (0.01M); in LB-Broth.

***LB agar and chloramphenicol plates****:* add 15g/L agar to freshly prepared LB broth, autoclave and cool down to 50°C, add chloramphenicol 30µg/ml. pour plates and store at 4°C

## 6.4.1. Concentrations of antibiotics stock solutions used for liquid culture (according to Maniatis):

***Ampicillin*** (sodium salt); 50 mg/ml, in water; ***Kanamycin*** in water, 10mg/ml; ***Tetracyclin HCl***, 5mg/ml in ethanol; ***Chloramphenicol***, 34mg/ml, in ethanol. → Stock solutions of antibiotics were prepared, sterile filtrated and aliquoted and stored -20°C.

*Concentrations of antibiotics used on selective plates or liquid culture (according to Maniatis):*
***Ampicillin*** (1:500) from stock ,100 µg/ml; ***Kanamycin*** (1:200) from stock, 50µg/ml; ***Tetracyclin*** (1:100) from stock, 50µg/ml; ***Chloramphenicol*** (1:200) from stock, 170µg/ml. → Before adding antibiotics to freshly autoclaved medium, the medium was cooled to below 50°C.

***LB Broth*:** 0.17M NaCl, 0.8% (w/v)Tryptone, 1.0% (w/v) Yeast extract

***L-glutamine*** (Bio Whittaker, Verviers, Belgium)

***Lithium Cl*** (VWR International, Poole, England)

***MgCl2 stock solution:*** 0,2mg MgCl2 in 50ml A.dest; store at 4°C.

***MOPS buffer 10 x****:* 0.2M MOPS (morpholinopropanesulphonic acid); 50mM sodium acetate; 5mM EDTA. The buffer is adjusted to pH 7.0 with 1M NaOH and sterilised by autoclaving.

***NaAch*** Potassium Acetate (BDH Laboratory Supplies, Poole, UK)

***Nitro-blue-tetrazolium (NBT)***: 50mg/ml NBT in 70% N,NDimethylformamide

***Phosphate-buffered saline (PBS)***: 137mM NaCl, 2.7mM KCl, 4.3mM Na2HPO4 .7H2O, 1.4mM KH2PO4, pH 7.3; autoclaved

***PBS with Tween detergent (PBT)***: 0.3% Tween-20 in PBS

***PBT-DEPC***: 50µl tween in 50ml 1X PBS-DEPC

***Paraformaldehyde 4%***: 4% paraformaldehyde is dissolved in A&B phosphate buffer. The solution was stored at -20°C. Before using, the solution is thawed at room temperature.

***Penicillin/Streptomycin*** (GIBCO, Paisley, Scotland)

***Phenol-Chloroform-Isoamyl alcohol*:** Phenol, chloroform and isoamyl alcohol are added together in a ratio of 25:24:1 (v/v)

***Potassiumhexacyanoferrate solution:***3mM K4FeII(CN)6; 3mM K3FeII(CN)6 (Ferrocyanate) in A.dest. Store in the dark at 4°C.

***Proteinase K*** (Promega, Southampton, UK)

***Resuspension buffer*** for DNA Miniplasmid preparation: 50mM Glucose, 10mM EDTA (pH8.0), 25mM Tris (pH 8.0), autoclaved, stored at 4°C

***RNA denaturing buffer:*** 10ml 100% deionized formamide; 3.5ml 40% formaldehyde; 1.5ml 10 x MOPS buffer, Formamide is deionized by stirring 100ml with approximately 20g of Amberlite MB3 (or MB1) ion exchange resin for 15 minutes.

***Sequencing buffer*** (Tris HCl pH9, 175mM; MgCl, 1.25mM)

***SFM*** *Drosophila* Insect Media (Gibco, Paisley, Scotland)

***Sylgard*** (Dow Corning, Wiesbaden, Germany)

***SOC medium***: 0.5% Yeast extract, 2.0% tryptone, 10mM NaCl, 2.5mM KCl, 10mM $MgCl_2$ , 20mM $MgSO_4$, 20mM glucose**.**

***Sodium Azide*** (Sigma, Steinheim, Germany)

***Sodiumborohydrate*** (Sigma, Steinheim, Germany)

***Sonicated salmon sperm DNA:*** (10mg/ml) in Hyb. Soln (Invitrogen, Paisley, UK).

***TFB – I (200ml):*** KAcetat (30mM)***;*** Mn2Cl (50mM); RbCl (100mM); CaCl2 (10mM); Glycerine 15%. Fill up with A.dest; pH 5,8 adjusted with Acetic Acid.Filter sterile and store at 4ºC.

***TFB – II (200ml):*** MOPS (1M). Adjust pH to 7.0 with NaOH. CaCl2 (75mM); RbCl (10mM); Glycerine 15% in A.dest. Sterile filtrate and store at 4°C. → filter Sterile and store at 4ºC.

***Triton X100*** (Sigma, Steinheim, Germany)

***Tris-Acetate buffer (50x)***: 2M Tris Base, 1M Glacial acetic acid, 0.5M EDTA pH8.0

***Tris-EDTA (TE)-buffer*** (pH 7.4): 10mM Tris-HCL (pH 7.4), 1mM EDTA (pH 8.0)

***Tris buffered saline (TBS)***: 37.5ml 2M Tris-HCl (pH9.5), 2.9g NaCl, 25ml 1M MgCl2 in a total volume of 500ml

***Tween 20*** (Sigma, Steinheim, Germany)

***Vectashield*** (Vector Laboratories, Burlingame, CA, USA)

***Voiltalef Oil (10S)*** (kind Gift of Karin Luer, University of Mainz, Mainz, Germany)

***Western blotting reagent (10x)*** (Roche, Mannheim, Germany)

***X-Gal (5-bromo-4-chloro-3-indolyl-b-D-galactopyranoside) staining solution:*** 670µl PBS (pH 6,5); 100µl MgCl2 stock solution; 200µl Ferrocyanate solution.→ heat to 70°C and add 30µl of X-Gal stock solution, vortex and cool to RT.

***X-Gal stock solution:*** 16mg 5-Bromo-4-Chloro-3Indolyl-b-d-Galaktosid (X-Gal) in 184µl of N,N-Dimethylformamid

## 6.5. Equipment

## 6.5.1. General equipment

Accurate scale Mettler PM4600 Delta Range (Mettler Instruments, Giessen, Germany)
Agarose Gel Unit Jencons (Jencons, Leighton Buzzard, UK)
Balance OHAUS Explorer finebalance (Fisher Scientific, Leistershire, UK)
CCD video camera Sony 3 CCD colour (Olympus, Hamburg, Germany)
Centrifuge Eppendorf 5417R (Eppendorf, Hamburg, Germany)
Centrifuge Eppendorf 5410 (Eppendorf, Hamburg, Germany)
Centrifuge Sigma 1-15 (Sigma, Osterode, Germany)
Centrifuge Sigma 4K15 (Sigma, Osterode, Germany)
Camera Zeiss AxioCam (Zeiss, Jena, Germany)
CO2 incubator, Galaxy R (Wolf Laboratories, Ltd. Pocklington, York, UK)
Confocal Microscope Leica TCS (Leica, Bensheim, Germany)
Dissecting Microscope Leica MZ FLIII (Leica, Bensheim, Germany)
EasyjecT Prima Electroporator (peqlab, Erlangen, Germany)
Fridges and Freezers Liebherr (Fisher Scientific, Leistershire, UK)
Gel documentation system, Gel Logic 100 (Kodak, Herts, UK)
Heat plate and stirrer MB 3001 (Heidolph, Germany)
Hybridisation Hybaid Oven "Shake´n´Stack" (Fisher Scientific, Leistershire, UK)
Incubator WTB Binder (VWR, Darmstadt, Germany)
Light Source Zeiss KL1500LCD (Schott, Mainz, Germany)
Macintosh Powermac G-4 (Apple)
Microscope Olympus BX50WI (Olympus, Hamburg, Germany)
Microwave
Monitor Monacor B+W video monitor (Intermercador GmbH+co, Bremen, Germany)
Millipore MiliQ Q Guard1 waterfilter (Fisher Scientific, Leicestershire, UK)
Millipore Steriflip 50ml (Fisher Scientific, Leicestershire, UK)
Millipore 0,2 µm filter cartridges (Fisher Scientific, Leicestershire, UK)
Micromanipulator , manual (Olympus, Hamburg, Germany)
pH-meter CG840 (Schott, Mainz, Germany)
Photometer Eppendorf Biophotometer RS232C (Eppendorf, Hamburg, Germany)
Pipettes Eppendorf (Eppendorf, Hamburg, Germany)
Pipettes StarLab (Milton Keynes, UK)
Power supply Biometra Power Pack P25 (Biotron, Göttingen, Germany)
Power supply Olymus TH3 (Olympus, Germany)
Printer DPU-414 Seico Thermal printer (Eppendorf, Hamburg, Germany)
Printer Mitsubishi p91 video copy processor (VWR, Darmstadt, Germany)
Puller P-97 Sutter micropipette puller (Science Product GmbH, Hofheim, Germany)
Puller Kopf vertical puller Model 270, David Kopf Instruments, Jujunga, CA, U.S.A.
Pump ILMVAC LVS301 (Ilmvac, Ilmenau, Germany)
Shaker GFL3015 (Gesellschaft für Labortechnik, Burgwedel, Germany)
Shaker thermo Grant Bio (Boekel Scientific, Jencons, Leighton Buzzard, UK)
Speedvac Savant (Thermo Life Sciences, Egelsbach, Germany)
Sterile banch Steril-VBH (Mahl Labortechnik, Kaarst. Germany)
Thermoblock Biometra TB1 (Biotron, Göttingen, Germany)
Thermocycler Biometra T-Gradient (Biotron, Göttingen, Germany)
Thermocycler Eppendorf Mastercycler gradient (Eppendorf, Germany)
Transilluminator MS Laborgeräte (Benda, Wiesloch, Germany)
UV bench Bio viewer (Fisher Scientific, Leicestershire, UK)
Vortexer Clifton Cyclone (Jencons, Leighton Buzzard, UK)
Waterbath Certomat WR (Braun Biotech, Melsungen, Germany)
Waterbath GFL1002 (Gesellschaft für Labortechnik, Burgwedel, Germany)

## 6.5.2. Additional items

Cell counting chamber, Improved Neubauer double cell, Standard (Weber Scientific Ltd; West Sussex, UK)
Forceps, DUMONT 55 (FST, Fine Science Tools, Heidelberg, Germany)
Glass capillaries, GB 100T-8P (Science Products, Hofheim, Germany)
Glass capillaries, GB 100TF-8P (Science Products, Hofheim, Germany)
Micro scissor (FST, Fine Science Tools, Heidelberg, Germany)

Millipore DNA cleanup columns (Fisher, Scientific Ltd., UK)
T25 Cell culture chambers (Fisher Scientific Ltd.; UK)
T75 cell culture flasks (Fisher Scientific Ltd.; UK)
Tungsten wires Nr. 260002-10 (FST, Fine Science Tools, Heidelberg, Germany)

## 6.6. Bioinformatics and data processing

### 6.6.1. Software

**Adobe Acrobat 6.0 Professional** was used to process and generate PDF documents.
**Adobe Photoshop CS** pictures processing and fluorescence data.
**Adobe Illustator CS** figures generation and schemes.
**Chromas 2.31** was used to display sequence data files http://www.technelysium.com.au/chromas.html.
**EndNote 7** archiving of publications and sources.
**Microsoft Office XP** was used to write this thesis.
**Vector NTI suite 7.0** for Mac, **DNA Star** and **Perl Primer** (http://perlprimer.sourceforge.net/) were used to perform diverse operations like primer design and analysis, restriction analysis, sequence alignments etc.
**Windows Editor** was used to save and modify sequences.

### 6.6.2. Online tools

**NEBcutter V.2.0** was used to identify restriction sites in DNA sequences: http://tools.neb.com/NEBcutter2/index.php.
**BCM Search Launcher** tools were used for all kinds of sequence operations like cleaning, formatting, translation or (inverse) reverting sequences http://searchlauncher.bcm.tmc.edu/.
**Lalign** (http://www.ch.embnet.org/software/LALIGN_form.html) was used for two sequence alignments.
**ClustalW** was used for multiple sequence alignments http://www.ch.embnet.org/software/ClustalW.html.
**Boxshade 3.21** was used for shading and visualising ClustalW multiple alignment files http://www.ch.embnet.org/software/BOX_form.html.
**PSORT II** was used to cellular protein localisation sites
http://psort.nibb.ac.jp/.
**NetPhos 2.0** Server was used to identify potential phosphorylation sites in proteins
http://www.cbs.dtu.dk/services/NetPhos/.
**Radar, REP, REPRO and TRUST** were used to predict internal repeats: http://www.expasy.ch/tools/
**Jpred and JUFO** were used to predict secondary structures of protein sequences:
http://www.expasy.ch/tools/
[1] **PDB: Protein Data Bank:** http://www.rcsb.org/pdb/explore/sequence.do

### 6.6.3. Data bases

**ENSEMBL:** a joint project between EMBL – EBI and the Sanger Institute: URL: http://www.ensembl.org/index.html.
**NCBI (National Centre for Biotechnology Information):** URL: http://www.ncbi.nlm.nih.gov/.
**DSHB (Developmental Studies Hybridoma Bank):** URL: http://www.uiowa.edu/~dshbwww/
**FlyBase** (1998) Fly Base: A comprehensive database of the *Drosophila* genome: Nucleic Acid Res. 26, 85-88. URL: http://flybase.org/
**FlyMine:** An integrated database for *Drosophila* and Anopheles genomics. URL: http://www.flymine.org/
**Bloomington *Drosophila* Stock Centre at Indiana University**: URL: http://flystocks.bio.indiana.edu/
**Flybrain** An Online Atlas and Database of the *Drosophila* Nervous System. URL:http://flybrain.org oder http://flybrain.neurobio.arizona.edu.
**The interactive fly** A Cyberspace Guide to *Drosophila* genes and their roles in development. URL: http://sdb.bio.purdue.edu/fly/aimain/1aahome.htm.
***Drosophila* Genomic Resource Centre- DGRC**: resource on vectors, cell lines DNA clones
http://dgrc.cgb.indiana.edu/
**Expasy Proteomics Server:**
http://www.expasy.org/

## 6.7. Vectors

### 6.7.1. *p{UAST}*

For a vector map see Fig.7.General information of the vector can be found here: http://www.gurdon.cam.ac.uk/~brandlab/reagents/pUAST.html

The full sequence can be obtained here:
http://flybase.bio.indiana.edu/.bin/fbidq.html?FBmc0000383

### 6.7.2. *p{UAST}$_{mod}$*

*p{UAST]$_{mod}$* is based on *p{UAST}* (see 6.7.1). An *AgeI* restriction site was inserted in between the *EcoRI* and *BglII* restriction site of the MCS of *p{UAST}*. The vector was generated in the context of the Shot construct cloning strategies (see Fig.7-11).

```
Comparison of:
wb42 (pUASTmod)                                    - 626 nt
pUAST                                             - 9050 nt

               10         20         30         40         50         60
wb42    CGCCCGGTACCGGTGGCGAATTCCCAATTCCCTATTCAGAGTTCTCTTCTTGTATTCAA
       :::::::::   : :  ::::::::::::::::::::::::::::::::::::::::::
pUAST. CGCAGATCT---GTTAACGAATTCCCAATTCCCTATTCAGAGTTCTCTTCTTGTATTCAA
      5630         5640       5650       5660       5670       5680
```

**Fig.21 MCS of *p{UAST}mod*:** Alignment of *p{UAST}*mod (5.6.1.1.) vs. *p{UAST}* (5.6.1.). *AgeI* restriction site (grey) was introduced between the *BglII* restriction site (blue) and the *EcoRI* restriction site (yellow). A glycin spacer was introduced between *AgeI* and *EcoRI*. Sequences (wb-41 and wb42) can be found on a CD available in the Prokop lab.

### 6.7.3. Δ*2-3- helper plasmid (pπ25.7 Δ2-3*

The vector was kindly obtained from Joachim Urban (Institute of Genetics, University of Mainz, Germany). The plasmid harbours a *transposase* cDNA. It was used to generate transgenic flies. For details of this vector see (Rubin and Spradling, 1982).

### 6.7.4. pNB40

For details of this vector see (Brown and Kafatos, 1988).

### 6.7.5. *pMT-GAL4*

The *pMT-Gal4* vector was kindly obtained from Martin Baron (Faculty of Life Sciences, Universtiy of Manchester). It harbours a Methalloprotein promoter *Gal4* gene to induce expression of UAS-coupled constructs in culture (Klueg et al., 2002). Sequence can be obtained on the DGRC website; URL: http://dgrc.cgb.indiana.edu/vectors/store/vectors.html?action=view&id=85

6.7.6. pCR2.1 (TOPO cloning kit, Invitrogen, Carlsbad, USA)

*pCRII TOPO* was used to subclone PCR fragments into, using the 3´A-overhangs produced by taq DNA-polymerase. All information regarding the TOPO cloning kit and the *pCR 2.1.* vector can be found on the Invitrogen webpage; URL: http://www.invitrogen.com/content/sfs/manuals/topota_man.pdf.

6.7.7. pDrive (PCR cloning kit, Qiagen)

*pDrive* was used to subclone PCR fragments into, using the 3´ A-overhangs produced by taq DNA-polymerase. All information regarding the *pDrive* PCR cloning kit can be found in the Qiagen manual which can be obtained here: http://www1.qiagen.com/literature/handbooks/PDF/Cloning/PCR_Cloning/1016726HBDNYPCRCloning401WW.pdf

6.7.8. *pcDNA3 (Invitrogen)*

The *pcDNA3* vector was kindly obtained from Christof Ballestrem Faculty of Life Sciences, Universtiy of Manchester). *pcDNA3* is a expression vector for vertebrate culture carrying a CMV promoter.Full informations regarding the vector including the full sequence can be found here: http://www.invitrogen.com/content/sfs/manuals/pcdna3.1_man.pdf

6.7.9. *pCS2+MT (with 6xcmyc tag)*

*pCS2+MT* was kindly obtained from Stefan Thor, Linköping, Sweden. All information on the MCS and the properties of *pCS2+MT* and all derivatives can be found here: www.xenbase.org/WWW/Marker_pages/PlasMaps/CS2.word

6.7.10. *mRFP-C1 based on pZsYellow1-C1*

*mRFP-C1* was kindly obtained from Andrew Gilmore (Faculty of Life Sciences, Universtiy of Manchester). *mRFP-C1* is based on *pZsYellow1-C1* vector (Clonetech) the yellow fluorescent protein *ZsYellow* was exchanged against *mRFP* (Campbell et al., 2002) using the *Age*I and *Bgl*II restriction sites. The sequence information of *mRFP* can be found under the Genbank, accession number: AF506027 (Campbell et al., 2002; Campbell et al., 2002). For sequence information of *pZsYellow1-C1* see: http://www.clontech.com/clontech/techinfo/vectors/vectorsT-Z/pZsYellow1-C1.shtml

## 6.8 Generated fly strains

| Construct injected | Independent insertions | Expression strength (1/no- 3/strong) | Chromosome | Homozygous viable |
|---|---|---|---|---|
| ***UAS-Shot-L(A)-N´6cmyc*** | Total of 3 | | | |
| | 1M | 2-3 | X[§] | yes[§] |
| | 2M=3M | 2-3 | 4[§] | no[§] |
| | 4M | n.d. | X[§] | yes[§] |
| ***UAS-Shot-L(A)-N´6cmyc-C´GFP*** | Total of 2 | | | |
| | 1M = 2M | 2-3 | 2 | yes[§] |
| | 3M | 1-2 | 2 | yes[§] |
| ***UAS-Shot-L(A)ΔABD-GFP*** | Sent for injection no flies obtained | - | - | - |
| ***UAS-Shot-L(A)ΔPlakin-GFP*** | Total of 4 | | | |
| | 1M* | 1* | n.d. | n.d. |
| | 2M = 3M | 2-3 | 2 | yes[§] |
| | 4M = 5M | 2-3 | 2 | yes[§] |
| | 6M = 7M | n.d. | 2 | yes[§] |
| ***UAS-Shot-L(A)ΔEB1-GFP*** | Total of 6 | | | |
| | 1M | 2 | 2 | yes[§] |
| | 2M | 2 | 3 | yes[§] |
| | 3M | n.d. | 2 | yes[§] |
| | 4M | n.d. | 2 | yes[§] |
| | 5M | n.d. | 2 | yes[§] |
| | 6M | n.d. | n.d. | yes[§] |
| ***UAS-[Gas2$_{shot}$]-6cmyc*** | Total of 10 | | | |
| | 1M | 1-2 | n.d. | n.d. |
| | 2M | n.d. | n.d. | n.d. |
| | 3M | n.d. | n.d. | n.d. |
| | 4M | n.d. | n.d. | n.d. |
| | 5M | n.d. | n.d. | n.d. |
| | 6M | n.d. | n.d. | n.d. |
| | 7M | n.d. | n.d. | n.d. |
| | 8M | n.d. | n.d. | n.d. |
| | 9M | n.d. | n.d. | n.d. |
| | 10M | n.d. | n.d. | n.d. |
| ***UAS-[EB1$_{aff}$]-2HA*** | Total of 6 | | | |
| | 1M | 1 | n.d. | n.d. |
| | 2M | n.d. | n.d. | n.d. |
| | 3M | n.d. | n.d. | n.d. |
| | 4M | n.d. | n.d. | n.d. |
| | 5M | n.d. | n.d. | n.d. |
| | 6M | n.d. | n.d. | n.d. |

**Table7:** List of all injected **Shot constructs** and the obtained fly stocks carrying **independent insertions**. The ***expression strength*** of the individual insertions was determined by expressing them with RN2D+O-Gal4 and judged according to the following guidelines: 1, no expression; 2, medium expressing strength; 3, strong expression. ***Insertion chromosome*** of the P-element were determined by standard genetically methods. ***Further abbreviations:*** n.d. not determined; [§] not finally determined; * discarded because expression levels are not sufficient. Injections and the initial screening was done by a company: BestGene Inc", 2918 Rustic Bridge, Chino Hills, CA 91709, U.S.A. http://www.thebestgene.com/.

## 6.9. Primers

All primers sequences are stored on a CD "*shot* cloning" available in the lab. Reverse complement always means that it is the 5´→ 3´sequence of a backward primer. Small letters indicate changes as compared to the original sequence. Abbreviations used: r.c.: reverse complement; nt: nucleotide; aa: amino acid.

### 6.9.1. General sequencing primers

**pUAST 3'**, 18 bases; CATCAGTTCCATAGGTTG
**pUAST 5'**, 18 bases; GCATGTCCGTGGGGTTTG
**T3**, 19 bases; ATTAACCCTCACTAAAGGG
**T7**, 19 bases; TAATACGACTCACTATAGG
**M13** forward (–20), 17 bases; GTAAAACGACGGCCAGT
**M13 forward (–40),** 17 bases; GTTTTCCCAGTCACGAC
**M13 reverse**, 16 bases; AACAGCTATGACCATG
**SP6 promoter**, 19 bases; CATTTAGGTGACACTATAG
**T7 promoter**, 19 bases; GTAATACGACTCACTATAG 3'

### 6.9.2. *shot* sequencing primers

**shotseq.1bw**, 24 bases; GGTGCGTCGTCTGGCGGGAGC
**shotseq.2fw**, 23bp; GCCGATTTGTTCGATCGCAATGG
**shotseq.3fw**, 23bp; CGAGCACGCGCACGGGTCTCACGC
**shotseq.4fw**, 22bp; CTGCTGCCCGACAACCACTACC
**shotseq5-fw**, 18 bases; GACGGGCAGTGCATCATC
**shotseq6-fw**, 18 bases; CTTTACGTCGTCGTGGCG
**shotseq7-fw**, 18 bases; CCGGATGCCATCGAGAAG
**shotseq8-fw**, 18 bases; CAATTGCTTGCCGCTGAC
**shotseq9-fw**, 18 bases; CTGCAGCTAACACTCTGC
**shotseq10bw**, 18 bases; TGCAGCATATGGAAACGC
**shotseq11bw**, 18 bases; GGATAGAGGGTGGCTCCG
**shotseq12bw**, 18 bases; CATGTCCTGGATGGGTTC
**shotseq-AgeIfw** (covering the AgeI restr.site), 18 bases; CTTCGGCATACGAACTAG
**shotseq13fw**, 18 bases; GCACCAGCACCATTAC

#### *6.9.2.1. shot sequencing primers ordered by position on shot-L(A)-GFP*

```
shot-L(A)-GFP-ATG-Stop.SEQ(1_16353) _ at offset       0, len 16353
shotseq.primer1bw.SEQ(1_21)         _ at offset      88, len   21
shotseq5-fw.SEQ(1_18)               _ at offset     302, len   18
shotseq10bw.SEQ(1_18)               _ at offset     602, len   18
shotseq6-fw.SEQ(1_18)               _ at offset     860, len   18
shotseq11bw.SEQ(1_18)               _ at offset    1102, len   18
shotseq7-fw.SEQ(1_18)               _ at offset    1401, len   18
shotseq12bw.SEQ(1_18)               _ at offset    1662, len   18
shotseq8-fw.SEQ(1_18)               _ at offset    1950, len   18
shotseq9-fw.SEQ(1_18)               _ at offset    2460, len   18
shotseq-AgeIfw.SEQ(1_18)            _ at offset    3982, len   18
shotseq. Primer 2fw.SEQ(1_23)       _ at offset   14433, len   23
shotseqpr.3fw.SEQ(1_24)             _ at offset   15085, len   24
shotseqpri.4fw.SEQ(1_22)            _ at offset   16215, len   22
```

**Alignment of all shotseq primers:** Generated with SeqMan (from DNA Star software package). Sings used: _ backward primer; _ forward primer.

#### *6.9.2.2. Shot sequencing primers relative to shot-L(A)-GFP*

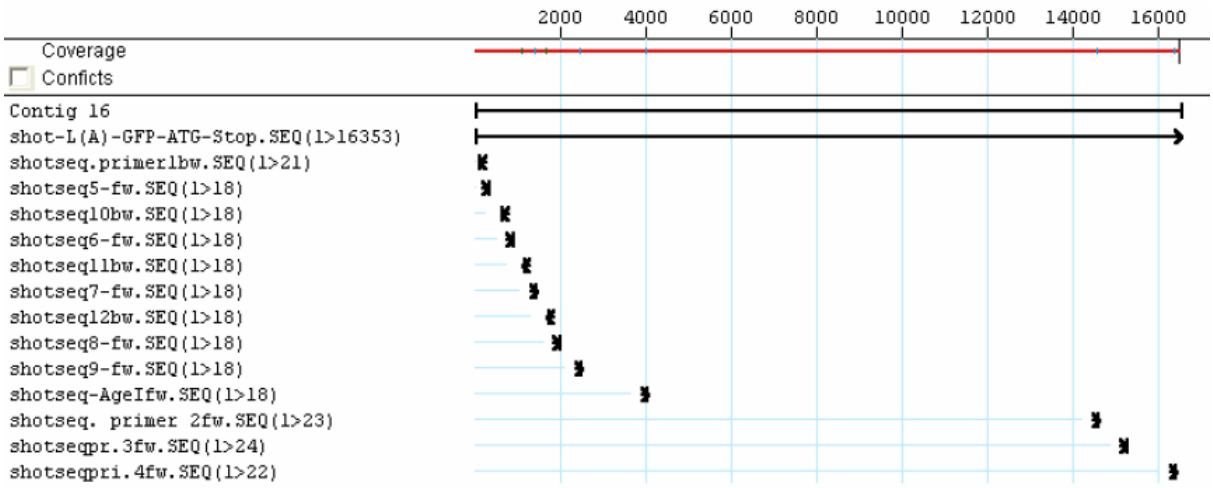


**Fig.22.** Graphical representation of *shot* sequencing primer positions relative to *shot-L(A)-GFP*. Generated with SeqMan from the DNA Star package.

6.9.3. Primers for the generation of *p{UAST}mod*

>**pUASTmod3fw (1fw)**,45 bases; TACTACAGATCTACCGGTGGCGAATTCCCAATTCCCTATTCAGAG

```
signal  AGA TCT acc ggt ggc GAATTCCCAATTCCCTATTCAGAG
------- ------- ------- --- ------------------------
spacer   BglII   AgeI   gly  EcoRI and neighbouring region
```

>**pUASTmod4bw (2bw)**, reverse complement, 21 bases; GATCCAAGCTTGCATGCCTGC

Primer to modify *p{UAST}* (together with pUASTmod3fw) and add an *Age*I restriction site to the MCS.

6.9.4. Primers fort the generation of *UAS-shot-L(A)-6´cmyc* and *shot-L(A)-N´6cmyc-C´GFP*

>**shot-LA-tag(6myc)1fw**, 35 bases; GCCGCGCAGAATTCCATCGATTTAAAACTATGGAG

```
GC CGC GCA GAA TTC CAT CGA TTT AAA aCT ATGG AG
---------- ------- --------------- -------- --
           EcoRI                   Kozak
```

Primer to introduce *EcoR*I 5´of 6xmyc to tag *shot-L(A)* with *6xcmyc* N´terminal. To amplify 6xmyc out of *Gas2-6xmyc*.

>**Shot-LA-tag(6xmyc)3bw**, rev. complement; GTACCCTCGAGTTCAGGACTAGTATTCAAGTC

>**Shot-LA-tag(6xmyc)3bw**, wrong orientation;

```
GAC TTG AAT  aCt Agt CCT gaa ctc gag GGT ACC TCT AGA GGA
-----------  -------------- --------------------------
bind.inside  3´bind;stop-del       binding 3´
             EcoRI deleted
```

Primer to delete *EcoR*I & introd. *Spe*I 3´ of *6xcmyc* to tag *shot-L(A)*

>**I-1-fw**, 49 bases; ATCGGCGAATTCACTAGTGGCACATCGCATTCCTACTATAAAGACCGCC

```
atc ggc gaa ttc act agt ggc ACATCGCATTCCTACTATAAAGACCGCC
------- ------- ------- --- ----------------------------
spacer       EcoRI      SpeI   binding sequence 28bp (ATG deleted)
```

Primer to modify the N terminus of *shot.* ATG deleted and *Spe*I and *EcoR*I sites 3´inserted.

>**I-2bw**, reverse complement, 23 bases; CTCGCCACGACGACGTAAAGTCG

Primer to modify the N-terminus of shot-L(A) antisense

>**shot-L(A)mod3-fw**, 20 bases; ACGGGCAGCACAGCCAGCGG

Binds 5´of *Kpn*I splice site at the C-terminus of *UAS-shot-L(A)-GFP* (p330)

>**shot-L(A)mod4-bw**, reverse complement, 42 bases;
GATGCCGGTACCGCCTTATAGCCGGAATGGCTCACGCTTCTC

>**shot-L(A)mod4-bw** (wrong orientation)
GAGAAGCGTGAGCCATTCCGGCTA taa ggc ggtacc ggc atc
------------------------ --- --- ------ -------
annealing seq stop gly KpnI spacer

Primer to amplify the C´terminus of Shot without GFP out of *shot-L(A)-GFP (p330).* Together with Shot-L(A)mod3-fw. For N´terminal tagged *shot-L(A).*

6.9.5. Primers fort the generation of *UAS-shot-L(A)ΔABD-GFP*

>**delta-actin-1fw**, 23bp; GGGAATTGGGAATTCCGGTGAGG.

Primer to amplify delta-actin fragment I out of *p{PUAST}-WB1*

>**delta-Actin-2bw**, 33 bases; ATCATCCCTAGGCTGAATGGCATCGCGTTCGTC

>**delta-Actin-2bw**, (wrong orientation)
GACGAACGCGATGCCATTCAG cct agg gacga
---------------------- ------- -----
binding region AvrII ½-PshAI

Primer to amplify delta actin fragment I out of *p{UAST}* together with delta-Actin-1fw. Carries ½ *Psh*AI sequence in case triple ligation does not work.

>**delta-Actin-3fw**, 34 bases; AGTAGTCCTAGGGAGCCACCCTCTATCCATCCAC

agt agt cct agg GAGCCACCCTCTATCCATCCAC
------- ------- ----------------------
spacer AvrII annealing region

Primer to amplify delta actin fragment II out of *p{UAST}* together with delta action 4bw.

>**delta-Actin-4bw**, reverse complement, 22 bases; CTTGGTCTGCTGACGTTCGTCG

Primer to amplify delta actin fragment II out of *p{UAST}* together with delta action 3fw. PCR fragment obtained with delta-Actin-3fw includes *Psh*AI restriction site

6.9.6. Primers for the generation of *UAS-shot-L(A)ΔPlakin-GFP*

>**delta-Plakin 1fw**, 20bases; CACTGCTCGGTATCCGGGCG

Primer to amplify s*hot* portion 5´of the Plakin domain together with delta-Plakin-2bw.

>delta-plakin-2bw, reverse complement, 42 bases;
AGTGATACCGGTGATCCTAGGGATAACCTCGCGATCCTGCAG

Primer to amplify *shot* portion 5´of the Plakin domain together with delta-Plakin-1fw.

>**delta-plakin-2bw**, wrong orientation;
GCTGCAGGATCGCGAGGTTATC cct agg atc acc ggt atc act
---------------------- ------- --- ------- -------
annealing region AvrII PinAI spacer

Primer to amplify *shot* portion 3´of the Plakin domain together with delta-Plakin-1fw.

>**delta-Plakin-3fw.**, 33 bases, ATCATCCCTAGGCCCACCGCCACTTCGGCATAC

atc atc cct agg CCCACCGCCACTTCGGCATAC
------- ------- --------------------
spacer AvrII binding portion

Primer to amplify second part for plakin deletion construct together with delta-plakin-4bw.

>**delta-plakin-4bw**, reverse complement, 23 bases; CAGACAAAACATCACCACCGGTG

Primer to amplify second part for plakin deletion construct together with delta-plakin-3fw.

6.9.7. Primers for the generation of *UAS-shot-L(A)ΔEB1*

>**deltaEB1-fw**, 18 bases; GCCTTCAACGGGCAGCAC

To amplify *shot* portion 5´of the EB1 domain together with deltaEB1-2bw

>**delta-EB1-2bw**, rev. compl, 49 bases;
GATACCGCGGCCGCCGCCACTAGTTGGTATACTGGATGATCTACTCATG

>**delta-EB1-2bw**, wrong orientation;
CATGAGTAGATCATCCAGTATACCA act agt ggc g gcggccgc ggt atc
------------------------ ------- --- - -------- -------
binding seq. SpeI gly NotI spacer

Primer to delete EB1 binding seq. out *of shot-L(A)-GFP*. Introduces *Spe*I and *Not*I splice sites. Together with primer deltaEB1-fw. To amplify seq. 5´of EB1 domain.

>**delta-EB1-3fw**, 30 bases; ACTTACACTAGTCCGACGGAGAAGCGTGAG

act tac act agt CCGACGGAGAAGCGTGAG
------- ------- ------------------
spacer SpeI binding portion

Primer to delete the EB1-binding motif out of *shot-L(A) (RE)*. Amplifies together with deltaEB1-4bw the terminus of shot + GFP out of *pSBL(330) (shot-L(A)-GFP).*

>**delta-EB1-4bw**, reverse complement, 20 bases; TCACAAAGATCCTCTAGGCG

Primer to amplify (with deltaEB1-3fw) the C-terminus of shot+GFP out of pSBL(330)=UAS-Shot-L(A)-GFP.

6.9.8. Primers for the generation of *UAS-Gas2-6cmyc*

>**Gas2-1**, 18 bases; AGGCTGAGATCTATGCCAGCCAATGATTCGGAC

```
agg-ctg-AGATCT-atg-CCA-GCC-AAT-GAT-TCG-GAC
------- ------ --- ------------------  \
spacer  BglII  start   5xflanking aa     first codon of Gas2 seq.
```

5´primer to amplify Gas2 out of *UAS-shot-L(A)-GFP* and introduce it into *p{UAST}.*

>**Gas2-2** reverse complement, 33 bases; GCTGCTGCGGCCGCTCTCTATGTTAGTGCGTCC

```
>Gas2-2, wrong orientation;
GGA-CGC-ACT-AAC-ATA-GAG-agc-ggc-cgc-agc-agc
    ------------------  ---------- -------
       5x flanking aa       NotI    spacer
```

Primer to introduce *Not*I site 3´of Gas2seq and subclone it into *p{UAST}*.

>**Gas2-3v.2**, 42 bases; ATCGTCTGCGGCCGCGCAGGATCCCATCGATTTAAAGCTATG

```
atc gtc TGCGGCCGC GCAGGATCCCATCGATTTAAAGCTATG
------- --------- --------------------------
spacer        NotI            5´sequence
```

Primer to amplify *6cmyc* out of *pCS2+MT* and to introducing *Not*I 5´ of *6xcmyc*

>**Gas2-4v.3**,rev. comp, 42 bases; CTATAGTTCTAGAGGCTCGAGTTAAGGCCTTGAATTCAAGTC

```
>Gas2-4v.3, wrong orientation;
GAC TTG AAT  TCA AGG CCT taa CTC GAG CCT CTA GAA CTA TAG
-----------  ----------- --- ------- -------------------
bind.inside  binding 3´  stop xhoI   binding 3´
```

Primer to amplify *6cmyc* out of *pCS2+MT* together with Gas2-3v.2. Introduces stop codon and *Xho*I site at the C´terminus of *6cmyc*.

6.9.9. Primers to generate *UAS-EB1-2HA*

>**EB1-1**, 42 bases; AGTAGAgaattcatgTCATCCAGTATACCAGCACTAACAGGC

```
AGT AGA gaa ttc atg TCATCCAGTATACCA GCA CTA ACA GGC
------- ------- --- -------------- --- --- --- ---
spacer  EcoRI   sta.5xflanking aa   4 codons of EB1
```

Primer to amplify the pot. EB1 domain out of *shot-L(A)-GFP*. Introduces an *EcoR*I site N´terminal to subclone into *p{UAST}* MCS.

>**EB1-2v.2**, reverse complement, 132 bases.
GTATAGAGATCTTTAAGCGTAGTCTGGGACGTCGTATGGGTAGCCAGCGT
AGTCTGGGACGTCGTATGGGTAGCCAGCGTAGTCTGGGACGTCGTATGGG
TAGCCCACGCTTCTCCGTCGGTGTGGTTCCCC

>**EB1-2v.2**, wrong orientation; introduces 3xHA.

```
Ggg GAA cca cac CGA CGG AGA AGC GTG ggc TACCCATACGACGTCCCAGACTACGCT ggc
--------------- ------------------     --------------------------
                  5xaa after EB1                    HA1

TACCCATACGACGTCCCAGACTACGCT ggc TACCCATACGACGTCCCAGACTACGCT taa aga tct
--------------------------     -------------------------- --- ------- --
```

```
            HA2                         HA3                  stop BglII
cta tac
--- ---
 spacer
```

Introduces 3x*HA*, a Stop and an *Bgl*II site after the EB1 sequence together with EB1-4v.

6.9.10. Primer for the generation of *p{UAST}/pcDNA3-Gas2/GSR+-GFP*

>**Gas2/GSR-1fw**, 36 bases; GGCGGAAAGCTTGGCATGGCCCTTCGTCCCGATTGG

```
GGC GGA AAGCTT GGC ATG GCCCTTCGTCCCGATTGG
------- ------ --- --- ------------------
spacer  HindIII start     binding seq.
```

Primer to amplify together with Gas2/GSR-2bw Gas2 and GSR+ out of *shot-L(A)-GFP*,15aa away from Gas2 and 1aa away from EF-hand; exact excision of EB1 (no aa space)

>**Gas2/GSR-2bw**, 43 bases, reverse complement;
CTCACGCTTCTCCGTCGGTGGTATACTGGATGATCTACTCATG

>**Gas2/GSR-2bw**, wrong orientation;

```
CATGAGTAGATCATCCAGTATACCA CCGACGGAGAAGCGTGAG
------------------------- ------------------
     binding seq.         binds seq after EB1
```

Amplifies with Gas2/GSR-1fw Gas2 and GSR out of *shot*-cDNA,(derived from delta-EB1-2bw)

>**Gas2/GSR-3fw**, 43 bases ; CATGAGTAGATCATCCAGTATACCACCGACGGAGAAGCGTGAG

```
CATGAGTAGATCATCCAGTATACCA CCGACGGAGAAGCGTGAG
------------------------- ------------------
     binds before EB1      binding sequence
```

Amplifies together with Gas2/GSR-4bw *shot* C-terminus after EB1 + GFP (derived from delta-EB1-3fw).

>**Gas2/GSR-4bw primer**, reverse complement, 30 bases;
GCCGCCCTCGAGTCACAAAGATCCTCTAGGCG

>**Gas2/GSR-4bw**; wrong orientation;

```
CGCCTAGAGGATCTTTGTGA CTCGAG GGC GGC
------------------- ------ -------
 binding sequence     XhoI   spacer
```

Amplifies together with Gas2/GSR-3fw Shot C-terminus after EB1 + GFP (derived from delta-EB1-4bw).

6.9.11. Primer for the generation of *p{UAST}/pcDNA3-Gas2/EB1-GFP*

**>Gas2/EB1-2fw**, 44 bases; CGCACGGGTCTCACGCCAGGAGGCTCCACGCTGTCGCTAGATAG

Amplifies EB1 + c-term + GFP if used with Gas2/GSR-4bw primer
(= Gas2/EB1-1bw reverse complement)

>**Gas2/EB1-1bw**, reverse complement, 44 bases;
CTATCTAGCGACAGCGTGGAGCCTCCTGGCGTGAGACCCGTGCG

>**Gas2/EB1-1bw**, wrong orientation;
CGCACGGGTCTCACGCCAGGA GGCTCCACGCTGTCGCTAGATAG

```
--------------------- -----------------------
  binding sequence      sequence next to GSR
```

Amplifies Gas2 domain together with Gas2/GSR-1fw

6.9.12. Primers for the generation of *p{UAST}-mRFP-GSR and GSR+*

>**GSRsense**, 38bp.
AGGTACAGATCTGGCGGCCGCACGGGTCTCACGCCAGG

```
AGGTAC AGATCT GGCGGCCGCACGGGTCTCACGCCAGG
------ ------ --------------------------
spacer  BglII       annealing portion
```

To insert GSR into *p{UAST}*together with GSRas. Inserts a *Bgl*II restricton site 5´of the domain.

>**GSRas**, rev. comp, 36b bases:
AGGTACGCGGCCGCTTACTACAGCGACAGCGTGGAG

>**GSRas**, wrong orientation.

```
CTCCACGCTGTCGCTGTAGTAA GCGGCCGC GTACCT
---------------------- -------- ------
   annealing portion     NotI   spacer
```

To insert GSR into *p{UAST}*together with GSRs. Adds a *Not*I site 3´of the domain.

>**GSR+ sense**, 36 bases.
AGGTACAGATCTGGCGGCGAGCTACGCGAGCAATTC

```
AGGTAC AGATCT GGC GGC GAGCTACGCGAGCAATTC
------ ------ --- --- ------------------
spacer  BglII   gly   annealing portion
```

To insert GSR+ into *p{UAST}*together with GSR+as. Adds a *Bgl*II site 5´of the domain.

>**GSR+as**, reverse complement.
AGGTACCTCGAGCTATCTACTCATGCCTCCGTTGC

**>GSR+as,** wrong orientation.

```
GCAACGGAGGCATGAGTAGA TAG CTCGAG GTACCT
-------------------- --- ------ ------
annealing portion   stop  XhoI  spacer
```

To insert GSR+ into *p{UAST}*together with GSR+s. Adds an *Xho*I site 3´of the domain.

6.9.13. Primers used for the inverse PCR mapping of *shot*$^{V104}$ and *shot*$^{V168}$

| | Position on shot genomic locus (nt) |
|---|---|

*6.9.13.1. Single embryo PCR V104*

| | |
|---|---|
| Strumpf A, 18nt: CTGTTATGGTGCGCGTGG | 72.188-72.205 |
| Strumpf B, 18nt (r.c.): CGGGTTCGGTTTATCAAG | 73.389-73.406 |
| Strumpf C, 18nt: CACTAACATAGAGCTACG | 73.780-73.797 |
| Strumpf D, 18nt (r.c.): CAGTGTGTTGTTGGATGAC | 74.975-74.993 |

*6.9.13.2. Inverse PCR V104*

| | |
|---|---|
| MaeII sense, 27bp: TTACTAATCAAACTTTATGTTTACCCC | 73.301 – 73.327 |
| MaeII as, 25bp: AAACGAAAAACAAATAACACAAATT | 73.275 – 73.299 |
| Sau96I sense, 24bp: CCTGCTTTCAAACTAACATCCTGC | 73.115 – 73.138 |
| Sau96I as, 22bp: CTGGCTGAATGGCAATTAAAGG | 72.771 – 72.792 |
| Sau3AI as, 22bp: GGAATTTATGTGGCTGGTATGG | 72.354 – 72375 |
| mutant1, 38bp: TGTTAGTTCTTATACAAGAAGATTCAATAAATAAAAGC | directly after tttt-region (as) |
| mutant2, 32: GCAATTAAAGGTAAAATTCGCCCTAAGGCACA | 150bp after breakpoint(as) |
| wt1, 25bp: TTTGTACGCATTGGCATGGCAGATG | 73.656 -73.680 |
| wt2, 29bp: GGCAGATGCACAGATGCATTTATATACGC | 73.681 – 73709 |
| sense-wt-fw, 25bp: TCTACGCTTGCGCTGCCCGCTCGCC | 73.421 – 73.445 |

*6.9.13.3. Single embryo PCR V168*

| | |
|---|---|
| Primer A sense, 34nt: GAGAGAAACCCAAATCATTTTCCATTATGTAAAC | 67.903 – 67936 |
| Primer A as, 27nt: TGTGGCTTCCTCGATAATTTGATCCAG | 68.915 – 68.941 |
| Primer B sense, 28nt: TGATCTTGATTAAGAACCTGCTCGTGTC | 68.748 – 68.775 |
| Primer B as, 27nt: AATCGAAAGCCAGTTCTTGATGATCGG | 69.731 – 69.757 |
| Primer C sense, 27nt: AGACTTTTGAGTACGCCGAGGACATTA | 69.678 – 69.704 |
| Primer C as, 29nt : AATAGGTTAAGCGGCAGTGATTAAGCAGG | 70.679 – 70.707 |
| Primer D sense, 28nt: ACATCTGATATACCGAAACCATACCAAG | 70.555 – 70.582 |
| Primer D as, 32nt: TTCAGATACAGAAGATGATCGTTAAGCAGCCG | 71.509 – 71.540 |
| Primer E sense, 31nt: AATATCACATTTTAATATAGCACCTCGGGAC | 71.395 – 71.425 |
| Primer E as, 33nt: TGATTTGGGTGGAATATTAAAAATGTGAACTAC | 72.412 – 72.444 |
| Primer F sense, 30nt: ACATCCATACCAGCCACATAAATTCCATAC | 72.350 – 72.379 |
| Primer F as, 33nt: GGGGTAAACATAAAGTTTGATTAGTAAAAAACG | 73.295 – 73.327 |
| Primer G sense, 31nt: ATGTCACCCATTTTATGTTTGAATCCTCATC | 73.201 – 73.231 |
| Primer G as, 35nt: GAACCTCTTTTTAAAATACTTTTTGGATATTATAG | 74.232 – 74.266 |
| Primer H sense, 32nt: CATTTCAACTAACCTATTATATTTCTGTTTGC | 74.170 – 74.201 |
| Primer H as, 24nt: CTCGTTGTCGCTCAGGGAGTCGGG | 75.205 – 75.228 |
| Primer I sense, 37nt: ATAATATTTGTTTATTTATTTTTCTGTAAAGGTACGC | 75.105 – 75.141 |
| Primer I as, 27nt: TACAACGATAGTTAGCAAAGATAAACC | 76.150 – 76.176 |
| Primer J sense, 32nt: CGTAACATAAATACATACTCATAAGTTTAGGC | 76.079 – 76.110 |
| Primer J as, 33nt: AGTTGAGTGTTTTGTATGTGGTTTAAATATTGG | 76.808 – 76840 |
| Primer K sense, 31nt: ATGCTTAAGTTCGATTACCAGATTACAATAC | 76501 – 76.531 |
| Primer K as, 23nt: GTTCGATTTCTTTCGCCCTTCTG | 77.722 – 77.744 |

| 6.9.14. Primers used to generate Dig-labelled RNA and DNA probes against *shot* domains | Ampified piece out of Shot-RE (cDNA) |
|---|---|
| >***Actin s***,22bp.<br>CGTCGTGTGGTGGACTTGTTCG | 893>1498 |
| ***>Actin as***,20bp.<br>CGGGAACACATCGTACAGCG | |
| >***Pt s***,20bp.<br>TATGTCCGAACTGGAGAAGC | 2722>3651 |
| >***Pt as***,20bp.<br>CCTGTTTGCTCTCCTCTTCG | |
| >***Spectrin s***, 24bp.<br>GCTAGACAAACTGAACAAGACTGG | 11075>11998 |

>***Spectrin as***, 20bp.
Tcaatgtccgaacccacagc
>***Gas2 s***, 24bp. 14746>15669
Agtacatgaaccacaagaagtcgc
>***Gas2 as***, 20bp,
tgtgatcgtccgtgctatcc

6.9.15. Primers for the generation of *p{UAST}-RDL-HA*

>**RDL-HAfw**, 74 bases:
CAAACGGATCCATACAGTGCAATACCCATACGACGTCCCAGACTACGCTG
CGGCGACTGGCGGTGGCAGCATGC

```
C AAA CGG ATC CAT ACA GTG CAA
       BamHI    3´binding
tacccatacgacgtcccagactacgct GCGGCGACTGgcggtggcagcatgc
--------------------------- -------------------------
     HA-epitope seq.           5´binding

ggt ggc agc atgc
-----------------
```

>**RDL-HA-2bw**, 20bp
AATAGTTGCCTGTGGTTAGG

## 6.10. Position and sequences of Shot domains in shot-RE and Shot-PE

This is a comprehensive list of all domains and domain positions in *shot-RE* and Shot-PE (Ensembl Gene Report CG18076). Shot-PE is the Shot isoform most of the constructs (besides Shot-L(C)-GFP and Shot-L(C)ΔGas-GFP) are based on. The sequences are deduced from predictions and papers. All sequences are in plain FASTA format. The list was generated as template to access domain sequences as easy as possible. The annotation in this list was the base for the now generally used annotated Shot-RE(-PE) sequence in the Vector NTI software. Abbreviations used: nt: nucleotide; aa: amino acid(s).

### 6.10.1 Actin binding domain (CH1 and CH2)

#### *6.10.1.1. CH1 domain*

```
>CH1 domain seq., 306nt,  from 448nt-753nt of shot-RE.
CAGAAGAAGACTTTCACAAAATGGGTTAACAAACATCTGAAAAAGGCCAA
TCGTCGTGTGGTGGACTTGTTCGAAGATCTGCGCGATGGTCACAATTTAC
TTTCACTCCTGGAGGTGCTATCTGGCGAACACCTGCCACGCGAGAAGGGT
AAAATGCGTTTCCATATGCTGCAGAATGCACAAATGGCTCTGGACTTTTT
GCGCTACAAGAAGATCAAACTGGTCAACATACGCGCCGAGGATATTGTGG
ATGGCAATCCAAAGTTAACCCTGGGCCTGATCTGGACCATCATATTGCAC
TTCCAG

Comparison of:
CH1                                                306 nt vs.
shot-RE(ATG-STOP)                                 15606 nt

                                        10        20        30
./wwwt ---------------------------CAGAAGAAGACTTTCACAAAATGGGTTAACAAA
                                   :::::::::::::::::::::::::::::::
shot-P CAGTTTAAAGACGAACGCGATGCCATTCAGAAGAAGACTTTCACAAAATGGGTTAACAAA
              430       440       450       460       470       480
 ........to……..
            280       290       300
./wwwt GGCCTGATCTGGACCATCATATTGCACTTCCAG---------------------------
       ::::::::::::::::::::::::::::::
shot-P GGCCTGATCTGGACCATCATATTGCACTTCCAGATCTCCGATATTGTTGTGGGCAAAGAG
              730       740       750       760       770       780
```

---

```
>CH1 domain peptide, 102aa from  aa150-aa251 of Shot-PE.
QKKTFTKWVNKHLKKANRRVVDLFEDLRDGHNLLSLLEVLSGEHLPREKG
KMRFHMLQNAQMALDFLRYKKIKLVNIRAEDIVDGNPKLTLGLIWTIILH
FQ

Comparison of:
CH1                                                 102 aa vs.
shot-PE                                            5201 aa

                                          10        20        30
./wwwt ----------------------------QKKTFTKWVNKHLKKANRRVVDLFEDLRDGH
                                    ::::::::::::::::::::::::::::::
shot-P KAKHSSTQAQPQGGYEDALTQFKDERDAIQKKTFTKWVNKHLKKANRRVVDLFEDLRDGH
              130       140       150       160       170       180

              40        50        60        70        80        90
./wwwt NLLSLLEVLSGEHLPREKGKMRFHMLQNAQMALDFLRYKKIKLVNIRAEDIVDGNPKLTL
       ::::::::::::::::::::::::::::::::::::::::::::::::::::::::::::::
shot-P NLLSLLEVLSGEHLPREKGKMRFHMLQNAQMALDFLRYKKIKLVNIRAEDIVDGNPKLTL
              190       200       210       220       230       240

             100
./wwwt GLIWTIILHFQ-------------------------------------------------
       ::::::::::::
shot-P GLIWTIILHFQISDIVVGKEDNVSAREALLRWARRSTARYPGVRVNDFTSSWRDGLAFSA
              250       260       270       280       290       300
```

***6.10.1.2. CH2 domain***

```
>CH2-domain seq., 312 bases from 793nt-1104nt of Shot-RE.
GCTCGGGAGGCTCTGCTGCGCTGGGCACGTCGCTCCACTGCTCGGTATCC
GGGCGTACGTGTCAACGACTTTACGTCGTCGTGGCGAGATGGATTGGCTT
TCTCGGCGTTGGTGCACCGCAACCGACCGGACTTGCTTGACTGGCGAAAG
GCAAGGAACGATCGGCCACGGGAGCGCCTGGAGACGGCCTTCCACATTGT
GGAGAAGGAGTACGGAGTTACGCGTCTGTTGGATCCTGAGGATGTGGATA
CCAACGAGCCGGATGAGAAGTCCCTTATCACGTACATTTCATCGCTGTAC
GATGTGTTCCCG

Comparison of:
CH2                                                312 nt vs.
shot-R(E)-ATG_Stop                                15606 nt

                           10        20        30        40
./wwwt ------------GCTCGGGAGGCTCTGCTGCGCTGGGCACGTCGCTCCACTGCTCGGTAT
                   ::::::::::::::::::::::::::::::::::::::::::::::::::
shot-R GACAACGTATCCGCTCGGGAGGCTCTGCTGCGCTGGGCACGTCGCTCCACTGCTCGGTAT
              790       800       810       820       830       840
........to

      290       300       310
./wwwt TCATCGCTGTACGATGTGTTCCCG-----------------------------------
       :::::::::::::::::::::::
shot-R TCATCGCTGTACGATGTGTTCCCGGAGCCACCCTCTATCCATCCACTCTTTGACATGGAG
             1090      1100      1110      1120      1130      1140
```

```
>CH2-domain peptide, 104aa from aa265-aa368 of Shot-PE.
AREALLRWARRSTARYPGVRVNDFTSSWRDGLAFSALVHRNRPDLLDWRK
ARNDRPRERLETAFHIVEKEYGVTRLLDPEDVDTNEPDEKSLITYISSLY
DVFP

Comparison of:
CH2                                                 104 aa vs.
shot-PE                                            5201 aa


                                      10        20        30
./wwwt ------------------------AREALLRWARRSTARYPGVRVNDFTSSWRDGLAFSA
                               :::::::::::::::::::::::::::::::::
shot-P GLIWTIILHFQISDIVVGKEDNVSAREALLRWARRSTARYPGVRVNDFTSSWRDGLAFSA
              250       260       270       280       290       300

         40        50        60        70        80        90
./wwwt LVHRNRPDLLDWRKARNDRPRERLETAFHIVEKEYGVTRLLDPEDVDTNEPDEKSLITYI
       ::::::::::::::::::::::::::::::::::::::::::::::::::::::::::::::
shot-P LVHRNRPDLLDWRKARNDRPRERLETAFHIVEKEYGVTRLLDPEDVDTNEPDEKSLITYI
              310       320       330       340       350       360

        100
./wwwt SSLYDVFP-------------------------------------------------
       ::::::::
shot-P SSLYDVFPEPPSIHPLFDMESQRRVHEYRDLAQQFIYWCREKTAYLQERSFPPTLIEMKR
              370       380       390       400       410       420
```

**6.10.2. Plakin domain (Lee and Kolodziej, 2002)**

```
>Plakin like domain, 2508 bases from nt1465-nt3972 of Shot-RE.
CTTCAGCAGGAAATTGAGCGACTAGAACGGCTGCAACGACTGGCCGATAA
GGTTCAGCGCGAGATCAAGCATGTAGATCAGAAGCTTACCGATCTTGAGG
GCCGAATTGGCGAGGAAGGTCGCCGCATCGAGCGACTACATCCCGTGGAC
GCTAAGAGCATTGTCGAGGCGCTTGAAACCGAGATCCGGCACCTGGAGGA
ACCCATCCAGGACATGAACCAGGACTGCCACGTGCTCAACGAGGGTCGCT
ATCCTCATGTCAGTGAGCTGCACAAGAAGGTCAACAAATTGCACCAGCGT
TGGGCTCAACTGCGCACCAATTTCCACACGAACCTGGTACAGAAGCTGTC
CGGTTTGAAGTATCCCGTCCACGAGACCACGGTGACGCGTCAAACGCGCA
TGGTGGTCGAGTCCCGTCAGATCGACACGAATCCCCATTTCCGCGATCTG
CAGGAGCACATTGAGTGGTGCCAAAACAAGTTGAAACAATTGCTTGCCGC
TGACTATGGCAGTGACCTGCCGTCGGTCAAGGAGGAACTGGATCGCCAAC
AGCACGAGCACAAGATCATTGATCAGTTCCACACGAAAATACTCAACGAC
GAACGTCAGCAGACCAAGTTCTCTGGAGATGAGCTGGCTTTGTACCAACA
```

```
GCGTCTCAATCAGCTGCAGAAGGTGTATGCCGAGTTGCTTAGCACCTCGA
CGAAGCGTCTGTCCGATTTGGATTCGCTGCAGCACTTCCTGGGACAGGCC
TCGGCGGAACTGCAATGGCTTAACGAAAAGGAGCAGGTGGAGATTACGCG
CGACTGGGCGGACAAACAACTCGATCTTCCCTCCGTGCACAGATACTACG
AGAACCTTATGTCCGAACTGGAGAAGCGTGAGATGCACTTTGCCACCATC
CTGGATCGTGGAGAGGCACTGCTGAACCAGCAGCATCCGGCCTCCAAGTG
CATCGAAGCCCATCTGACAGCCCTGCAACAGCAATGGGCGTGGCTGCTGC
AGCTAACACTCTGCTTGGAGGTTCATTTGAAACACGCCACGGAGTACCAT
CAGTTCTTTGGCGAGATCAAGGATGCCGAGCAGTGGCTGGCCAAGCGTGA
CGAAATACTCAACAGCAAGTTCTCACAGTCAGACTTTGGCTTGGACCAGG
GTGAAACTCTACTCAGGGGAATGCAGGATTTGCGCGAGGAACTGAATGCC
TTTGGCGAGACAGTGGCCACACTGCAGCGAAGAGCCCAGACAGTGGTGCC
TCTAAACAAGCGACGACAGCCGGTAAATCGACAAGGACCCGTGCAGGCCA
TTTGTGCCTACAAACAACAGGGTCAACTGCAGATCGAAAAGGGCGAGACT
GTTACGCTGCTGGACAACTCGGGACGTGTGAAGTGGCGCGTGCGCACTGC
TAAGGGGCAGGAAGGACCCATACCGGGCGCTTGCCTGCTATTGCCACCTC
CTGACCAGGAGGCTATCGATGCCGCCGAACGTCTGAAGCGTCTGTTCGAT
CGATCAGTAGCTCTTTGGCAGAAGAAGCATCTGCGACTGCGCCAGAACAT
GATCTTCGCCACCATTCGTGTGGTTAAGGGCTGGGACTTTGACCAGTTCT
TGGCCATGGGTCCTGAGCAGCGCACGGCCATCCGGCGTGCCCTCAACGAC
GATGCCGACAAATTGCTGAGCGAGGGTGATCCAAACGATCCGCAGCTGCG
ACGCCTGCGCCGTGAAATGGACGAGGTCAATCGCTTGTTCGATGAGTTCG
AGAAGCGTGCGCGCGCCGAAGAGGAGAGCAAACAGGCCAGTCGCATCTTC
ACCGAGGAATGCCTTGCCATCAAGAGCAAACTGGAGGACATGGCCCGTGA
GCTGGATCAGATTATACTGGCTCCGTTGCCACGTGATTTGGACTCTTTGG
AGCATGTGCTGGAAATTCATTCGGACTACGAGCGCAGGTTGCACCTGTTG
GAGCCTGAGTTGAAACACCTGCAGGAAACATTCCGCACGATTGCGTTGAA
GACGCCAGTGCTGAAGAAGAGCCTGGACAATCTAATGGAGCTGTGGAAGG
AGCTGAACACTCAAAGTGGCCTGCACAAGGACCGTCTGAAGTTGCTTGAG
GCTTCGCTGGCTGGTCTGGAGGACAATGAGCATGTGATTTCCGAACTCGA
GAACGAGCTGGCCAGGCACCAGGATCTGCCATCGACCGCTGAGGGCCTGC
AGCAAGTGTTTAAGCAACTGAACCACATGCAGGACATCATTACACAACAG
CAGCCGCAAATGGATAAGATGAACGATGCGGCCGATCAGCTGGGACGCAT
GGGAGTGCCCACCAAGGTGCTCGGCGACCTCAAGAGACTGCACTCGAACG
TGGAGCGCCTGAACACGCGCTGGAGTGCGGTGTGCAACCAATTGGGTGAA
AGAATGCGCTCATGCGAGACGGCTATCGGGCTTATGAAGAATCTCCAGTC
GAGCGTGCAAGTGGAGGAATCATGGGTGGATGGCACCACGGAGCGACTGT
CTGCCATG
```

```
Comparison of:
Plakin domain                                        - 2508 nt
shot(ATG-Stop)                                       - 15606 nt

               10        20        30        40        50        60
Plakin CTTCAGCAGGAAATTGAGCGACTAGAACGGCTGCAACGACTGGCCGATAAGGTTCAGCGC
       ::::::::::::::::::::::::::::::::::::::::::::::::::::::::::::
shot(A CTTCAGCAGGAAATTGAGCGACTAGAACGGCTGCAACGACTGGCCGATAAGGTTCAGCGC
         1470      1480      1490      1500      1510      1520
.....to....
             2470      2480      2490      2500
Plakin GTGGAGGAATCATGGGTGGATGGCACCACGGAGCGACTGTCTGCCATG
       :::::::::::::::::::::::::::::::::::::::::::::
shot(A GTGGAGGAATCATGGGTGGATGGCACCACGGAGCGACTGTCTGCCATG
         3930      3940      3950      3960      3970
```

---

```
>Plakin domain peptide, 83aa from aa489-1324aa of Shot-PE.
LQQEIERLERLQRLADKVQREIKHVDQKLTDLEGRIGEEGRRIERLHPVD
AKSIVEALETEIRHLEEPIQDMNQDCHVLNEGRYPHVSELHKKVNKLHQR
WAQLRTNFHTNLVQKLSGLKYPVHETTVTRQTRMVVESRQIDTNPHFRDL
QEHIEWCQNKLKQLLAADYGSDLPSVKEELDRQQHEHKIIDQFHTKILND
ERQQTKFSGDELALYQQRLNQLQKVYAELLSTSTKRLSDLDSLQHFLGQA
SAELQWLNEKEQVEITRDWADKQLDLPSVHRYYENLMSELEKREMHFATI
LDRGEALLNQQHPASKCIEAHLTALQQQWAWLLQLTLCLEVHLKHATEYH
QFFGEIKDAEQWLAKRDEILNSKFSQSDFGLDQGETLLRGMQDLREELNA
FGETVATLQRRAQTVVPLNKRRQPVNRQGPVQAICAYKQQGQLQIEKGET
VTLLDNSGRVKWRVRTAKGQEGPIPGACLLLPPPDQEAIDAAERLKRLFD
RSVALWQKKHLRLRQNMIFATIRVVKGWDFDQFLAMGPEQRTAIRRALND
DADKLLSEGDPNDPQLRRLRREMDEVNRLFDEFEKRARAEEESKQASRIF
TEECLAIKSKLEDMARELDQIILAPLPRDLDSLEHVLEIHSDYERRLHLL
EPELKHLQETFRTIALKTPVLKKSLDNLMELWKELNTQSGLHKDRLKLLE
ASLAGLEDNEHVISELENELARHQDLPSTAEGLQQVFKQLNHMQDIITQQ
QPQMDKMNDAADQLGRMGVPTKVLGDLKRLHSNVERLNTRWSAVCNQLGE
RMRSCETAIGLMKNLQSSVQVEESWVDGTTERLSAM

Comparison of:
Plakin like domain                                    - 836 aa
```

```
shot-PE                                                 - 5201 aa

               10        20        30        40        50        60
Plakin LQQEIERLERLQRLADKVQREIKHVDQKLTDLEGRIGEEGRRIERLHPVDAKSIVEALET
       ::::::::::::::::::::::::::::::::::::::::::::::::::::::::::::
shot-P LQQEIERLERLQRLADKVQREIKHVDQKLTDLEGRIGEEGRRIERLHPVDAKSIVEALET
      490       500       510       520       530       540

....to.......
              790       800       810       820       830
Plakin HSNVERLNTRWSAVCNQLGERMRSCETAIGLMKNLQSSVQVEESWVDGTTERLSAM
       ::::::::::::::::::::::::::::::::::::::::::::::::::::::::::::
shot-P HSNVERLNTRWSAVCNQLGERMRSCETAIGLMKNLQSSVQVEESWVDGTTERLSAM
     1270      1280      1290      1300      1310      1320
```

---

**6.10.3. SH3 binding domain**

```
>SH3 domain seq., 162nt from 2749nt-2910nt of Shot-RE.
GGACCCGTGCAGGCCATTTGTGCCTACAAACAACAGGGTCAACTGCAGAT
CGAAAAGGGCGAGACTGTTACGCTGCTGGACAACTCGGGACGTGTGAAGT
GGCGCGTGCGCACTGCTAAGGGGCAGGAAGGACCCATACCGGGCGCTTGC
CTGCTATTGCCA

Comparison of:
SH3 domain                                              - 162 nt
shot(ATG-Stop)                                          - 15606 nt
100.0% identity in 162 nt overlap; score:  810 E(10,000): 9.6e-59

               10        20        30        40        50        60
SH3    GGACCCGTGCAGGCCATTTGTGCCTACAAACAACAGGGTCAACTGCAGATCGAAAAGGGC
       ::::::::::::::::::::::::::::::::::::::::::::::::::::::::::::
shot(A GGACCCGTGCAGGCCATTTGTGCCTACAAACAACAGGGTCAACTGCAGATCGAAAAGGGC
     2750      2760      2770      2780      2790      2800

               70        80        90       100       110       120
SH3    GAGACTGTTACGCTGCTGGACAACTCGGGACGTGTGAAGTGGCGCGTGCGCACTGCTAAG
       ::::::::::::::::::::::::::::::::::::::::::::::::::::::::::::
shot(A GAGACTGTTACGCTGCTGGACAACTCGGGACGTGTGAAGTGGCGCGTGCGCACTGCTAAG
     2810      2820      2830      2840      2850      2860

              130       140       150       160
SH3    GGGCAGGAAGGACCCATACCGGGCGCTTGCCTGCTATTGCCA
       ::::::::::::::::::::::::::::::::::::::::
shot(A GGGCAGGAAGGACCCATACCGGGCGCTTGCCTGCTATTGCCA
     2870      2880      2890      2900      2910
```

---

```
>SH3 domain peptide, 54aa from aa917-aa970 of Shot-RE.
GPVQAICAYKQQGQLQIEKGETVTLLDNSGRVKWRVRTAKGQEGPIPGAC
LLLP

Comparison of:
SH3 domain                                              - 54 aa
shot-PE                                                 - 5201 aa
100.0% identity in 54 aa overlap

               10        20        30        40        50
SH3    GPVQAICAYKQQGQLQIEKGETVTLLDNSGRVKWRVRTAKGQEGPIPGACLLLP
       ::::::::::::::::::::::::::::::::::::::::::::::::::::::
shot-P GPVQAICAYKQQGQLQIEKGETVTLLDNSGRVKWRVRTAKGQEGPIPGACLLLP
        920       930       940       950       960       970
```

---

**6.10.4. The Calcium binding EF-hand motifs**

The predictions for the exact position of the EF-hand motifs vary (see ENSEMBL). Thus the sequence below gives the earliest predicted startpoint and latest predicted endpoint.

```
>EF hand seq., 219 bases from 14287nt-14505nt of Shot-RE.
AAGTACATGAACCACAAGAAGTCGCGCTTGACGGATCTGTTCCGGAAAAT
GGATAAGGATAACAATGGCATGATTCCGCGCGATGTCTTCATCGATGGCA
TACTCAATACGAAATTCGATACATCTGGCTTGGAAATGAAGGCTGTAGCC
GATTTGTTCGATCGCAATGGCGAAGGCCTCATCGACTGGCAAGAGTTCAT
TGCTGCCCTTCGTCCCGAT

(A) EF-hands                                            - 219 nt
```

```
(B) Shot-PE                                                    - 15606 nt

               10        20        30        40        50        60
EF-han AAGTACATGAACCACAAGAAGTCGCGCTTGACGGATCTGTTCCGGAAAATGGATAAGGAT
       ::::::::::::::::::::::::::::::::::::::::::::::::::::::::::::
Shot-P AAGTACATGAACCACAAGAAGTCGCGCTTGACGGATCTGTTCCGGAAAATGGATAAGGAT
      14290     14300     14310     14320     14330     14340

------to-------
              190       200       210
EF-han ATCGACTGGCAAGAGTTCATTGCTGCCCTTCGTCCCGAT
       :::::::::::::::::::::::::::::::::::::
Shot-P ATCGACTGGCAAGAGTTCATTGCTGCCCTTCGTCCCGAT
      14470     14480     14490     14500
```

---

```
>EF-hand peptide, 73 bases from aa4763-aa4835 in Shot-PE.
KYMNHKKSRLTDLFRKMDKDNNGMIPRDVFIDGILNTKFDTSGLEMKAVA
DLFDRNGEGLIDWQEFIAALRPD

Comparison of:
(A) EF-hands                                                   - 73 aa
(B) Shot-PE                                                    - 5201 aa

               10        20        30        40        50        60
EF-han KYMNHKKSRLTDLFRKMDKDNNGMIPRDVFIDGILNTKFDTSGLEMKAVADLFDRNGEGL
       ::::::::::::::::::::::::::::::::::::::::::::::::::::::::::::::
Shot-P KYMNHKKSRLTDLFRKMDKDNNGMIPRDVFIDGILNTKFDTSGLEMKAVADLFDRNGEGL
           4770      4780      4790      4800      4810      4820

------- to ----------

EF-han IDWQEFIAALRPD
       :::::::::::::
Shot-P IDWQEFIAALRPD
           4830
```

---

**6.10.5. Gas2 domain**

```
>Gas2 domain seq., 219nt from 14536nt-14754nt in Shot-RE.
GACAAAATACACGATGAGGTCAAACGTCTGGTCATGCTGTGTACCTGCCGAC
AGAAGTTCCGTGTGTTCCAAGTTGGCGAGGGCAAGTACAGATTTGGAGAC
TCCCAGAAACTGCGCCTCGTTCGTATCCTTCGCAGCACTGTTATGGTGCG
CGTGGGTGGCGGTTGGGTTGCCCTGGATGAATTCCTGCAGAAGAACGATC
CTTGTCGCGCCAAAGGA

Comparison of:
(A) Gas2 domain                                                - 219 nt
(B) shot-RE-ATG-Stop                                           - 15606 nt

 100.0% identity in 219 nt overlap; score: 1095 E(10,000): 2.4e-82

               10        20        30        40        50        60
Gas2   GACAAAATACACGATGAGGTCAAACGTCTGGTCATGCTGTGTACCTGCCGACAGAAGTTC
       ::::::::::::::::::::::::::::::::::::::::::::::::::::::::::::
shot-R GACAAAATACACGATGAGGTCAAACGTCTGGTCATGCTGTGTACCTGCCGACAGAAGTTC
       14540     14550     14560     14570     14580     14590

               70        80        90       100       110       120
Gas2   CGTGTGTTCCAAGTTGGCGAGGGCAAGTACAGATTTGGAGACTCCCAGAAACTGCGCCTC
       ::::::::::::::::::::::::::::::::::::::::::::::::::::::::::::
shot-R CGTGTGTTCCAAGTTGGCGAGGGCAAGTACAGATTTGGAGACTCCCAGAAACTGCGCCTC
       14600     14610     14620     14630     14640     14650

              130       140       150       160       170       180
Gas2   GTTCGTATCCTTCGCAGCACTGTTATGGTGCGCGTGGGTGGCGGTTGGGTTGCCCTGGAT
       ::::::::::::::::::::::::::::::::::::::::::::::::::::::::::::
shot-R GTTCGTATCCTTCGCAGCACTGTTATGGTGCGCGTGGGTGGCGGTTGGGTTGCCCTGGAT
       14660     14670     14680     14690     14700     14710

              190       200       210
Gas2   GAATTCCTGCAGAAGAACGATCCTTGTCGCGCCAAAGGA
       :::::::::::::::::::::::::::::::::::::
shot-R GAATTCCTGCAGAAGAACGATCCTTGTCGCGCCAAAGGA
       14720     14730     14740     14750
```

```
>GAS2 binding peptide, 73aa from aa4846-aa4918 of Shot-PE.
DKIHDEVKRLVMLCTCRQKFRVFQVGEGKYRFGDSQKLRLVRILRSTVMV
RVGGGWVALDEFLQKNDPCRAKG

Comparison of:
(A) Gas2 peptide                                        - 73 aa
(B) shot-PE                                             - 5201 aa

 100.0% identity in 73 aa overlap; score:  502 E(10,000):  1e-37

               10        20        30        40        50        60
Gas2   DKIHDEVKRLVMLCTCRQKFRVFQVGEGKYRFGDSQKLRLVRILRSTVMVRVGGGWVALD
       ::::::::::::::::::::::::::::::::::::::::::::::::::::::::::::
shot-P DKIHDEVKRLVMLCTCRQKFRVFQVGEGKYRFGDSQKLRLVRILRSTVMVRVGGGWVALD
        4850      4860      4870      4880      4890      4900

               70
Gas2   EFLQKNDPCRAKG
       :::::::::::::
shot-P EFLQKNDPCRAKG
        4910
```

#### 6.10.7. EB1 domain

EB1 binding domain according to Slep et al.,2005 from aa5145- aa5191; see manuscript p.588. Behind this motif only 10aa remain to the Stop.

```
>EB1 domain, 142nt from 15434nt-15573nt in Shot-RE.
GCACTAACAGGCTTCGGCTTCAAACCAATTAGGCGAAACATCAGCGGTAG
CTCAACGCCCTCCGGGATGCAAACGCCGCGAAAGAGCTCAGCGGAGCCCA
CATTCAGCTCCACAATGAGACGCACTTCGCGGGGAACCACA


Comparison of:
(A) seq shot-R(E)-ATG_Stop                                - 15606 nt
(B) seq EB1-binding domain                                - 142 nt


          15440     15450     15460     15470     15480     15490
shot-R GCACTAACAGGCTTCGGCTTCAAACCAATTAGGCGAAACATCAGCGGTAGCTCAACGCCC
       ::::::::::::::::::::::::::::::::::::::::::::::::::::::::::::
EB1-bi GCACTAACAGGCTTCGGCTTCAAACCAATTAGGCGAAACATCAGCGGTAGCTCAACGCCC
               10        20        30        40        50        60
---- to ----
          15560     15570
shot-R CGCACTTCGCGGGGAACCACA
       ::::::::::::::::::::
EB1-bi CGCACTTCGCGGGGAACCACA
              130       140
```

```
>EB1 binding sequence: aa5145-aa5191 of shot-PE:
ALTGFGFKPIRRNISGSSTPSGMQTPRKSSAEPTFSSTMRRTSRGTT


Comparison of:
(A) seq EB1 binding motif                                 - 47 aa
(B) seq shot-PE                                           - 5201 aa

               10        20        30        40
EB1    ALTGFGFKPIRRNISGSSTPSGMQTPRKSSAEPTFSSTMRRTSRGTT
       ::::::::::::::::::::::::::::::::::::::::::::::::
shotPE ALTGFGFKPIRRNISGSSTPSGMQTPRKSSAEPTFSSTMRRTSRGTT
         5150      5160      5170      5180      5190
```

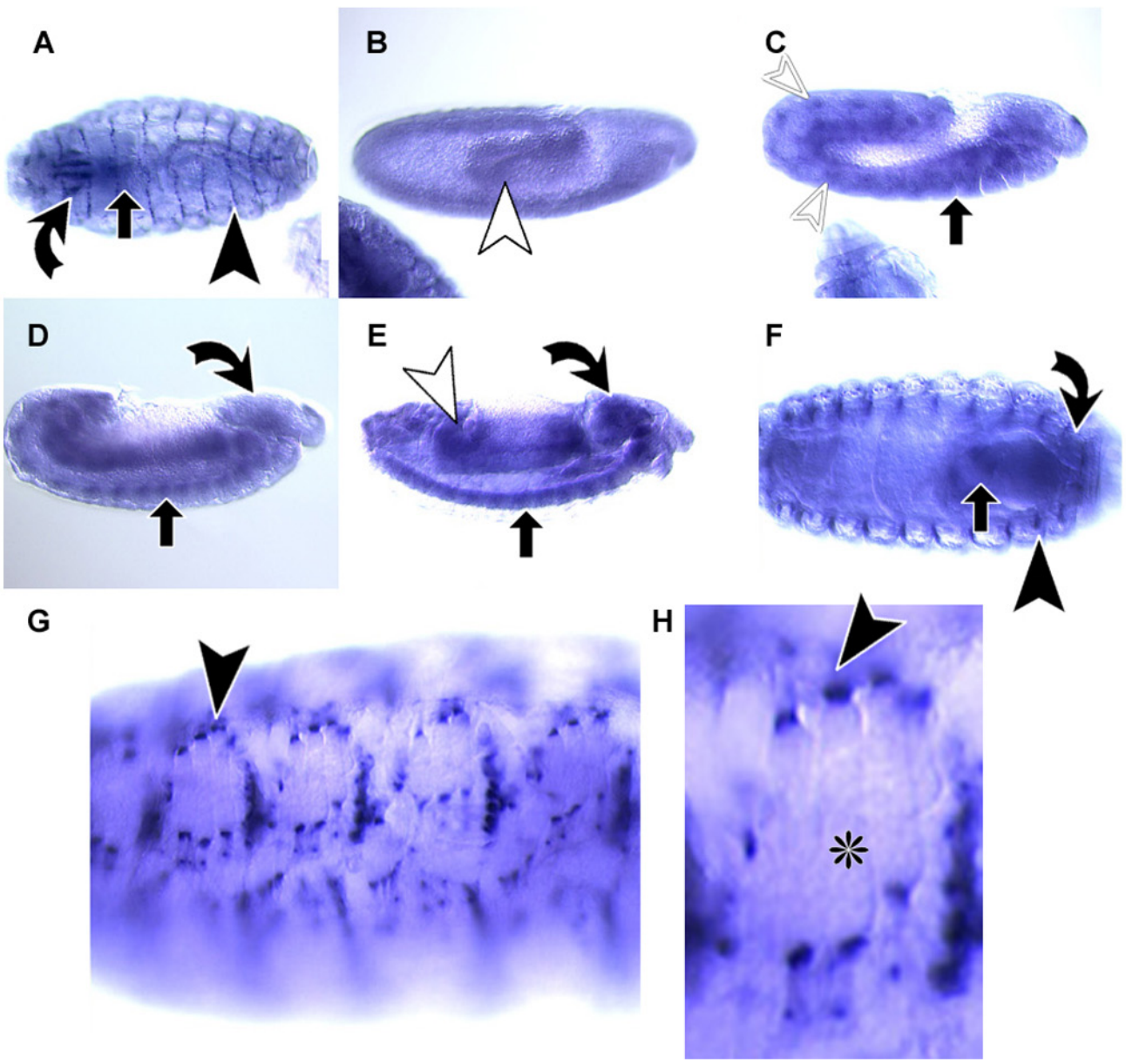
A
B
C
D
E
F
G
H

### 6.11. *In-situ* hybridisation reveals no tissue specific *shot* domain expression on the RNA level (Fig.23)

I generated DNA and RNA probes against four different *shot* domain: The actin binding domain, the plakin domain, the spectrin repeat rod domain and the Gas2 domain. For details see Materials and methods 2.6. and 2.7. and Appendix. 6.9.14. for the primers used. The original intention was to reveal differential transcription patterns of individual *shot* isoforms/domains in various tissues. Easy to handle Dig labelled DNA probes were generated successfully first (Materials and methods 2.7) but their sensitivity was too low (not shown). Subsequently highly sensitive Dig labelled RNA probes were generated (Materials and methods 2.6.) and applied successfully. Widespread staining in various tissues was detected but all four probes showed no tissues specific differences. This is consistent with published findings where also probes directed against the ABD (actin binding domain) and the Gas2 domain show no tissue specific differences (Roper and Brown, 2003).

Since stainings of all four generated probes resemble each other, only staining of one Dig-RNA probe is shown (*anti-plakin*). Different developmental stages are shown: stage.17 (A,F,G,H); stage.11 (B); stage 12-13 (C), stage 14-15 (D); stage 16 (F). Widespread staining was detected with elevated levels in tendon cells (black arrowhead), The CNS (black arrow), the brain (curved black arrow), midgut (white arrowhead) and tracheal pits (open white arrowhead). Muscles are shown (*). (G,H) Show surface views of stg.17 embryos. Tendon cells can be seen and muscles which attach to them (*).

## 7. References

**Adams, M. D., S. E. Celniker, R. A. Holt, C. A. Evans, J. D. Gocayne, P. G. Amanatides, S. E. Scherer, P. W. Li, R. A. Hoskins, R. F. Galle, et al.,** (2000). "The genome sequence of *Drosophila melanogaster*." Science **287**(5461): 2185-95.

**Andra, K., B. Nikolic, M. Stocher, D. Drenckhahn and G. Wiche** (1998). "Not just scaffolding: plectin regulates actin dynamics in cultured cells." Genes Dev **12**(21): 3442-51.

**Aronstein, K., V. Auld and R. Ffrench-Constant** (1996). "Distribution of two GABA receptor-like subunits in the Drosophila CNS." Invert Neurosci **2**(2): 115-20.

**Bate, M. and A. Martínez-Arias** (1993). The development of *Drosophila melanogaster* (2 Vol.). Cold Spring Harbor, New York, Cold Spring Harbor Laboratory Press.

**Bateman, A., E. Birney, L. Cerruti, R. Durbin, L. Etwiller, S. R. Eddy, S. Griffiths-Jones, K. L. Howe, M. Marshall and E. L. Sonnhammer** (2002). "The Pfam protein families database." Nucleic Acids Res **30**(1): 276-80.

**Bedford, F. K., J. T. Kittler, E. Muller, P. Thomas, J. M. Uren, D. Merlo, W. Wisden, A. Triller, T. G. Smart and S. J. Moss** (2001). "GABA(A) receptor cell surface number and subunit stability are regulated by the ubiquitin-like protein Plic-1." Nat Neurosci **4**(9): 908-16.

**Bernier, G., A. Brown, G. Dalpe, Y. De Repentigny, M. Mathieu and R. Kothary** (1995). "Dystonin expression in the developing nervous system predominates in the neurons that degenerate in dystonia musculorum mutant mice." Mol Cell Neurosci **6**(6): 509-20.

**Bernier, G., M. Mathieu, Y. De Repentigny, S. M. Vidal and R. Kothary** (1996). "Cloning and characterization of mouse ACF7, a novel member of the dystonin subfamily of actin binding proteins." Genomics **38**(1): 19-29.

**Bettencourt da Cruz, A., M. Schwarzel, S. Schulze, M. Niyyati, M. Heisenberg and D. Kretzschmar** (2005). "Disruption of the MAP1B-related protein FUTSCH leads to changes in the neuronal cytoskeleton, axonal transport defects, and progressive neurodegeneration in Drosophila." Mol Biol Cell **16**(5): 2433-42.

**Bhattacharya, S., C. G. Bunick and W. J. Chazin** (2004). "Target selectivity in EF-hand calcium binding proteins." Biochim Biophys Acta **1742**(1-3): 69-79.

**Bosher, J. M., B. S. Hahn, R. Legouis, S. Sookhareea, R. M. Weimer, A. Gansmuller, A. D. Chisholm, A. M. Rose, J. L. Bessereau and M. Labouesse** (2003). "The Caenorhabditis elegans vab-10 spectraplakin isoformsro." J Cell Biol **161**(4): 757-68.

**Bossy, B., M. Ballivet and P. Spierer** (1988). "Conservation of neural nicotinic acetylcholine receptors from Drosophila to vertebrate central nervous systems." Embo J **7**(3): 611-8.

**Brand, A. H. and E. L. Dormand** (1995). "The GAL4 system as a tool for unravelling the mysteries of the Drosophila nervous system." Curr Opin Neurobiol **5**(5): 572-8.

**Brand, A. H. and N. Perrimon** (1993). "Targeted gene expression as a means of altering cell fates and generating dominant phenotypes." Development **118**(2): 401-15.

Broadie, K. S. (2000). Electrophysiological approaches to the neuromusculature. *Drosophila* Protocols. W. Sullivan, M. Ashburner and R. S. Hawley. Cold Spring Harbor, New York, Cold Spring Harbor Laboratory Press**:** 273-295.

**Brose, K., K. S. Bland, K. H. Wang, D. Arnott, W. Henzel, C. S. Goodman, M. Tessier-Lavigne and T. Kidd** (1999). "Slit proteins bind Robo receptors and have an evolutionarily conserved role in repulsive axon guidance." Cell **96**(6): 795-806.

**Brown, A., G. Bernier, M. Mathieu, J. Rossant and R. Kothary** (1995). "The mouse dystonia musculorum gene is a neural isoform of bullous pemphigoid antigen 1." Nat Genet **10**(3): 301-6.

**Brown, N. H. and F. C. Kafatos** (1988). "Functional cDNA libraries from Drosophila embryos." J Mol Biol **203**(2): 425-37.

**Brunner, A. and C. J. O'Kane** (1997). "The fascination of the Drosophila NMJ." Trends Genet **13**(3): 85-7.

**Budnik, V.** (1996). "Synapse maturation and structural plasticity at Drosophila neuromuscular junctions." Curr Opin Neurobiol **6**(6): 858-67.

**Budnik, V., Y. H. Koh, B. Guan, B. Hartmann, C. Hough, D. Woods and M. Gorczyca** (1996). "Regulation of synapse structure and function by the Drosophila tumor suppressor gene dlg." Neuron **17**(4): 627-40.

**Burgoyne, R. D., D. W. O'Callaghan, B. Hasdemir, L. P. Haynes and A. V. Tepikin** (2004). "Neuronal Ca2+-sensor proteins: multitalented regulators of neuronal function." Trends Neurosci **27**(4): 203-9.

**Byers, T. J., A. H. Beggs, E. M. McNally and L. M. Kunkel** (1995). "Novel actin crosslinker superfamily member identified by a two step degenerate PCR procedure." FEBS Lett **368**(3): 500-4.

**Calver, A. R., M. J. Robbins, C. Cosio, S. Q. Rice, A. J. Babbs, W. D. Hirst, I. Boyfield, M. D. Wood, R. B. Russell, G. W. Price, et al.,** (2001). "The C-terminal domains of the GABA(b) receptor subunits mediate intracellular trafficking but are not required for receptor ignalling." J Neurosci **21**(4): 1203-10.

**Campbell, R. E., O. Tour, A. E. Palmer, P. A. Steinbach, G. S. Baird, D. A. Zacharias and R. Y. Tsien** (2002). "A monomeric red fluorescent protein." Proc Natl Acad Sci U S A **99**(12): 7877-82.

**Campbell, R. E., O. Tour, A. E. Palmer, P. A. Steinbach, G. S. Baird, D. A. Zacharias and R. Y. Tsien** (2002). "A monomeric red fluorescent protein 10.1073/pnas.082243699." PNAS **99**(12): 7877-7882.

**Campos-Ortega, J. A. and V. Hartenstein** (1997). The embryonic development of *Drosophila melanogaste*r. Berlin, Springer, New York.

**Chan, Y., H. Q. Tong, A. H. Beggs and L. M. Kunkel** (1998). "Human skeletal muscle-specific alpha-actinin-2 and -3 isoforms form homodimers and heterodimers in vitro and in vivo." Biochem Biophys Res Commun **248**(1): 134-9.

**Clark, I. E., L. Y. Jan and Y. N. Jan** (1997). "Reciprocal localization of Nod and kinesin fusion proteins indicates microtubule polarity in the Drosophila oocyte, epithelium, neuron and muscle." Development **124**(2): 461-70.

**Connolly, C. N., J. T. Kittler, P. Thomas, J. M. Uren, N. J. Brandon, T. G. Smart and S. J. Moss** (1999). "Cell surface stability of gamma-aminobutyric acid type A receptors. Dependence on protein kinase C activity and subunit composition." J Biol Chem **274**(51): 36565-72.

**Connolly, C. N., B. J. Krishek, B. J. McDonald, T. G. Smart and S. J. Moss** (1996). "Assembly and cell surface expression of heteromeric and homomeric gamma-aminobutyric acid type A receptors." J Biol Chem **271**(1): 89-96.

**Cross, R. A., M. Stewart and J. Kendrick-Jones** (1990). "Structural predictions for the central domain of dystrophin." FEBS Lett **262**(1): 87-92.

**Djinovic-Carugo, K., M. Gautel, J. Ylanne and P. Young** (2002). "The spectrin repeat: a structural platform for cytoskeletal protein assemblies." FEBS Lett **513**(1): 119-23.

**Dowling, J., Y. Yang, R. Wollmann, L. F. Reichardt and E. Fuchs** (1997). "Developmental expression of BPAG1-n: insights into the spastic ataxia and gross neurologic degeneration in dystonia musculorum mice." Dev Biol **187**(2): 131-42.

**DrosDel** An isogenic deficiency kit for Drosophila melanogaster.

**Drysdale, R. A. and M. A. Crosby** (2005). "FlyBase: genes and gene models." Nucleic Acids Res **33**(Database issue): D390-5.

**Duchen, L. W.** (1976). "Dystonia musculorum–an inherited disease of the nervous system in the mouse." Adv Neurol **14**: 353-65.

**Duffy, J. B.** (2002). "GAL4 system in Drosophila: a fly geneticist's Swiss army knife." Genesis **34**(1-2): 1-15.

**Elliott, S. L., C. F. Cullen, N. Wrobel, M. J. Kernan and H. Ohkura** (2005). "EB1 is essential during Drosophila development and plays a crucial role in the integrity of chordotonal mechanosensory organs." Mol Biol Cell **16**(2): 891-901.

**Entchev, E. V., A. Schwabedissen and M. Gonzalez-Gaitan** (2000). "Gradient formation of the TGF-beta homolog Dpp." Cell **103**(6): 981-91.

**Evan, G. I., G. K. Lewis, G. Ramsay and J. M. Bishop** (1985). "Isolation of monoclonal antibodies specific for human c-myc proto-oncogene product." Mol Cell Biol **5**(12): 3610-6.

**Ffrench-Constant, R. H.** (1993). "Cloning of a putative GABAA receptor from cyclodiene-resistant Drosophila: a case study in the use of insecticide-resistant mutants to isolate neuroreceptors." Exs **63**: 210-23.

**Ffrench-Constant, R. H. and R. T. Roush** (1991). "Gene mapping and cross-resistance in cyclodiene insecticide-resistant Drosophila melanogaster (Mg.)." Genet Res **57**(1): 17-21.

**Finney, N., F. Walther, P.-Y. Mantel, D. Stauffer, G. Rovelli and K. K. Dev** (2003). "The Cellular Protein Level of Parkin Is Regulated by Its Ubiquitin-like Domain 10.1074/jbc.C300051200." J. Biol. Chem. **278**(18): 16054-16058.

**FlyBase** (1998). FlyBase: the *Drosophila* Database.

**FlyMove**.

**Fly-Pushing** "Fly Pushing : The Theory and Practice of Drosophila Genetics; Ralph Greenspan."

**Foisner, R. and G. Wiche** (1991). "Intermediate filament-associated proteins." Curr Opin Cell Biol **3**(1): 75-81.

**Fontao, L., B. Favre, S. Riou, D. Geerts, F. Jaunin, J. H. Saurat, K. J. Green, A. Sonnenberg and L. Borradori** (2003). "Interaction of the bullous pemphigoid antigen 1 (BP230) and desmoplakin with intermediate filaments is mediated by distinct sequences within their COOH terminus." Mol Biol Cell **14**(5): 1978-92.

**Fontao, L., D. Geerts, I. Kuikman, J. Koster, D. Kramer and A. Sonnenberg** (2001). "The interaction of plectin with actin: evidence for cross-linking of actin filaments by ignalling n of the actin-binding domain of plectin." J Cell Sci **114**(Pt 11): 2065-76.

**Frambach, I., W. Rossler, M. Winkler and F. W. Schurmann** (2004). "F-actin at identified synapses in the mushroom body neuropil of the insect brain." J Comp Neurol **475**(3): 303-14.

**Frambach, I. and F. W. Schurmann** (2004). "Separate distribution of deutocerebral projection neurons in the mushroom bodies of the cricket brain." Acta Biol Hung **55**(1-4): 21-9.

**Fuchs, E. and D. W. Cleveland** (1998). "A structural scaffolding of intermediate filaments in health and disease." Science **279**(5350): 514-9.

**Gao, F. B., J. E. Brenman, L. Y. Jan and Y. N. Jan** (1999). "Genes regulating dendritic outgrowth, branching, and routing in Drosophila." Genes Dev **13**(19): 2549-61.

**Geerts, D., L. Fontao, M. G. Nievers, R. Q. Schaapveld, P. E. Purkis, G. N. Wheeler, E. B. Lane, I. M. Leigh and A. Sonnenberg** (1999). "Binding of integrin alpha6beta4 to plectin prevents plectin association with F-actin but does not interfere with intermediate filament binding." J Cell Biol **147**(2): 417-34.

**Gimona, M., K. Djinovic-Carugo, W. J. Kranewitter and S. J. Winder** (2002). "Functional plasticity of CH domains." FEBS Lett **513**(1): 98-106.

**Gimona, M. and R. Mital** (1998). "The single CH domain of ignalli is neither sufficient nor necessary for F-actin binding." J Cell Sci **111 ( Pt 13)**: 1813-21.

**Gimona, M. and S. J. Winder** (1998). "Single ignalli homology domains are not actin-binding domains." Curr Biol **8**(19): R674-5.

**Gomez, T. M., E. Robles, M. Poo and N. C. Spitzer** (2001). "Filopodial calcium transients promote substrate-dependent growth cone turning." Science **291**(5510): 1983-7.

Goodman, C. S. and C. Q. Doe (1993). Embryonic development of the Drosophila central nervous system. The Development of Drosophila melanogaster. M. B. a. A. M. n. Arias. Cold Spring Harbor, NY, Cold Spring Harbor Laboratory Press**:** 1131-1206.

**Goriounov, D., C. L. Leung and R. K. Liem** (2003). "Protein products of human Gas2-related genes on chromosomes 17 and 22 (hGAR17 and hGAR22) associate with both microfilaments and microtubules." J Cell Sci **116**(Pt 6): 1045-58.

**Greenspan, R. J.** (1997). Fly pushing: The theory and practice of *Drosophila* genetics. Cold Spring Harbor New York, Cold Spring Harbor Laboratory Press.

**Gregory, S. L. and N. H. Brown** (1998). "kakapo, a gene required for adhesion between and within cell layers in Drosophila, encodes a large cytoskeletal linker protein related to plectin and dystrophin." J Cell Biol **143**(5): 1271-82.

**Guo, L., L. Degenstein, J. Dowling, Q. C. Yu, R. Wollmann, B. Perman and E. Fuchs** (1995). "Gene targeting of BPAG1: abnormalities in mechanical strength and cell migration in stratified epithelia and neurologic degeneration." Cell **81**(2): 233-43.

**Halpern, M. E., A. Chiba, J. Johansen and H. Keshishian** (1991). "Growth cone ignallin underlying the development of stereotypic synaptic connections in Drosophila embryos." J Neurosci **11**(10): 3227-38.

**Hartwig, J. H.** (1994). "Actin-binding proteins 1: spectrin superfamily." Protein Profile **1**(7): 706-78.

**Hedwig, B. and M. Burrows** (1996). "Presynaptic inhibition of sensory neurons during kicking movements in the locust." J Neurophysiol **75**(3): 1221-32.

**Hirai, H. and S. Matsuda** (1999). "Interaction of the C-terminal domain of delta glutamate receptor with spectrin in the dendritic spines of cultured Purkinje cells." Neurosci Res **34**(4): 281-7.

**Hopkinson, S. B. and J. C. Jones** (2000). "The N terminus of the transmembrane protein BP180 interacts with the N-terminal domain of BP230, thereby mediating keratin cytoskeleton anchorage to the cell surface at the site of the ignalling n s." Mol Biol Cell **11**(1): 277-86.

**Hummel, T., T. Menne, H. Scholz, S. Granderath, K. Giesen and C. Klambt** (1997). "CNS midline development in Drosophila." Perspect Dev Neurobiol **4**(4): 357-68.

**Ishimoto, H. and T. Tanimura** (2004). "Molecular neurophysiology of taste in Drosophila." Cell Mol Life Sci **61**(1): 10-8.

**Jainchill, J. L., S. A. Aaronson and G. J. Todaro** (1969). "Murine sarcoma and ignallin viruses: assay using clonal lines of contact-inhibited mouse cells." J Virol **4**(5): 549-53.

**Jan, Y. N. and L. Y. Jan** (1994). "Neuronal cell fate specification in Drosophila." Curr Opin Neurobiol **4**(1): 8-13.

**Jefferis, G. S., E. C. Marin, R. J. Watts and L. Luo** (2002). "Development of neuronal connectivity in Drosophila antennal lobes and mushroom bodies." Curr Opin Neurobiol **12**(1): 80-6.

**Jefferson, J. J., C. L. Leung and R. K. Liem** (2004). "Plakins: goliaths that link cell junctions and the cytoskeleton." Nat Rev Mol Cell Biol **5**(7): 542-53.

**Kahana, E., G. Flood and W. B. Gratzer** (1997). "Physical properties of dystrophin rod domain." Cell Motil Cytoskeleton **36**(3): 246-52.

**Karakesisoglou, I., Y. Yang and E. Fuchs** (2000). "An epidermal plakin that integrates actin and microtubule networks at cellular junctions." J Cell Biol **149**(1): 195-208.

Kater, S. B. (1985). Dynamic regulators of neuronal form and conductivity in the adult snail *Helisoma*. Model neural networks and ignallin. A. I. Selverston. New Zork, Plenum**:** 191-209.

**Kawasaki, H. and R. H. Kretsinger** (1995). "Calcium-binding proteins 1: EF-hands." Protein Profile **2**(4): 297-490.

**Keesey, J.** (2000). "Epitope Tagging Basic Laboratory Methods. Roche Diagnostics Corporation Technical Manuals. F. Hoffmann-La Roche Ltd. Available from URL:http://biochem.roche.com/prodinfo_fst.htm?/prod_inf/manuals/epitope/epi_toc.htm."

**Kidd, T., K. S. Bland and C. S. Goodman** (1999). "Slit is the midline repellent for the robo receptor in Drosophila." Cell **96**(6): 785-94.

**Klagges, B. R., G. Heimbeck, T. A. Godenschwege, A. Hofbauer, G. O. Pflugfelder, R. Reifegerste, D. Reisch, M. Schaupp, S. Buchner and E. Buchner** (1996). "Invertebrate synapsins: a single gene codes for several isoforms in Drosophila." J Neurosci **16**(10): 3154-65.

**Klambt, C., T. Hummel, T. Menne, E. Sadlowski, H. Scholz and A. Stollewerk** (1996). "Development and function of embryonic central nervous system glial cells in Drosophila." Dev Genet **18**(1): 40-9.

**Klueg, K. M., D. Alvarado, M. A. Muskavitch and J. B. Duffy** (2002). "Creation of a GAL4/UAS-coupled inducible gene expression system for use in Drosophila cultured cell lines." Genesis **34**(1-2): 119-22.

**Knust, E.** (2002). "Regulation of epithelial cell shape and polarity by cell-cell adhesion (Review)." Mol Membr Biol **19**(2): 113-20.

**Kodama, A., I. Karakesisoglou, E. Wong, A. Vaezi and E. Fuchs** (2003). "ACF7: an essential integrator of microtubule dynamics." Cell **115**(3): 343-54.

**Konur, S. and A. Ghosh** (2005). "Calcium ignalling and the control of dendritic development." Neuron **46**(3): 401-5.

**Korenbaum, E. and F. Rivero** (2002). "Calponin homology domains at a glance." J Cell Sci **115**(Pt 18): 3543-5.

**Koster, J., D. Geerts, B. Favre, L. Borradori and A. Sonnenberg** (2003). "Analysis of the interactions between BP180, BP230, plectin and the integrin alpha6beta4 important for ignalling n s assembly." J Cell Sci **116**(Pt 2): 387-99.

**Kozak, M.** (1987). "An analysis of 5'-noncoding sequences from 699 vertebrate messenger RNAs." Nucleic Acids Res **15**(20): 8125-48.

**Kretsinger, R. H. and C. E. Nockolds** (1973). "Carp muscle calcium-binding protein. II. Structure determination and general description." The Journal Of Biological Chemistry **248**(9): 3313-3326.

**Lambert de Rouvroit, C. and A. M. Goffinet** (2001). "Neuronal migration." Mech Dev **105**(1-2): 47-56.

**Landgraf, M., N. Sanchez-Soriano, G. M. Technau, J. Urban and A. Prokop** (2003). "Charting the Drosophila neuropile: a strategy for the standardised characterisation of genetically amenable neurites." Dev Biol **260**(1): 207-25.

**Lee, H. J., T. Rocheleau, H. G. Zhang, M. B. Jackson and R. H. ffrench-Constant** (1993). "Expression of a Drosophila GABA receptor in a baculovirus insect cell system. Functional expression of insecticide susceptible and resistant GABA receptors from the cyclodiene resistance gene Rdl." FEBS Lett **335**(3): 315-8.

**Lee, S., K. L. Harris, P. M. Whitington and P. A. Kolodziej** (2000). "short stop is allelic to kakapo, and encodes rod-like cytoskeletal-associated proteins required for axon extension." J Neurosci **20**(3): 1096-108.

**Lee, S. and P. A. Kolodziej** (2002). "The plakin Short Stop and the RhoA GTPase are required for E-cadherin-dependent apical surface ignalling during tracheal tube fusion." Development **129**(6): 1509-20.

**Lee, S. and P. A. Kolodziej** (2002). "Short Stop provides an essential link between F-actin and microtubules during axon extension." Development **129**(5): 1195-204.

**Lee, T. and L. Luo** (1999). "Mosaic analysis with a repressible neurotechnique cell marker for studies of gene function in neuronal morphogenesis." Neuron **22**(3): 451-461.

**Letunic, I., L. Goodstadt, N. J. Dickens, T. Doerks, J. Schultz, R. Mott, F. Ciccarelli, R. R. Copley, C. P. Ponting and P. Bork** (2002). "Recent improvements to the SMART domain-based sequence annotation resource." Nucleic Acids Res **30**(1): 242-4.

**Leung, C. L., K. J. Green and R. K. Liem** (2002). "Plakins: a family of versatile cytolinker proteins." Trends Cell Biol **12**(1): 37-45.

**Leung, C. L., D. Sun, M. Zheng, D. R. Knowles and R. K. Liem** (1999). "Microtubule actin cross-linking factor (MACF): a hybrid of dystonin and dystrophin that can interact with the actin and microtubule cytoskeletons." J Cell Biol **147**(6): 1275-86.

**Leung, C. L., M. Zheng, S. M. Prater and R. K. Liem** (2001). "The BPAG1 locus: Alternative splicing produces multiple isoforms with distinct cytoskeletal linker domains, including predominant isoforms in neurons and muscles." J Cell Biol **154**(4): 691-7.

**Lewit-Bentley, A. and S. Rety** (2000). "EF-hand calcium-binding proteins." Curr Opin Struct Biol **10**(6): 637-43.

**Lin, C. M., H. J. Chen, C. L. Leung, D. A. Parry and R. K. Liem** (2005). "Microtubule actin crosslinking factor 1b: a novel plakin that localizes to the Golgi complex." J Cell Sci **118**(Pt 16): 3727-38.

**Littleton, J. T., H. J. Bellen and M. S. Perin** (1993). "Expression of synaptotagmin in Drosophila reveals transport and localization of synaptic vesicles to the synapse." Development **118**(4): 1077-88.

**Liu, J. J., J. Ding, A. S. Kowal, T. Nardine, E. Allen, J. D. Delcroix, C. Wu, W. Mobley, E. Fuchs and Y. Yang** (2003). "BPAG1n4 is essential for retrograde axonal transport in sensory neurons." J Cell Biol **163**(2): 223-9.

**Lohr, R., T. Godenschwege, E. Buchner and A. Prokop** (2002). "Compartmentalization of central neurons in Drosophila: a new strategy of mosaic analysis reveals localization of presynaptic sites to specific segments of neurites." J Neurosci **22**(23): 10357-67.

**Maatta, A., T. DiColandrea, K. Groot and F. M. Watt** (2001). "Gene targeting of envoplakin, a cytoskeletal linker protein and precursor of the epidermal cornified envelope." Mol Cell Biol **21**(20): 7047-53.

**Matthews, K. A., T. C. Kaufman and W. M. Gelbart** (2005). "Research resources for Drosophila: the expanding universe." Nat Rev Genet **6**(3): 179-93.

**Meier, J., C. Meunier-Durmort, C. Forest, A. Triller and C. Vannier** (2000). "Formation of glycine receptor clusters and their accumulation at synapses." J Cell Sci **113 ( Pt 15)**: 2783-95.

**Mende, M.** (2004). Analysing the Role of Short Stop during the Formation of Synaptic Terminals in Drosophila melanogaster. Institute of Genetics and Cell Biology. Mainz, Johannes Gutenberg-Universität Mainz.

**Michno, K., D. van de Hoef, H. Wu and G. L. Boulianne** (2005). "Modeling Age-Related Diseases in Drosophila: Can this Fly?" Curr Top Dev Biol **71**: 199-223.

**Minoshima, S., M. Amagai, J. Kudoh, R. Fukuyama, T. Hashimoto, T. Nishikawa and N. Shimizu** (1991). "Localization of the human gene for 230-kDal bullous pemphigoid autoantigen (BPAG1) to chromosome 6pter----q15." Cytogenet Cell Genet **57**(1): 30-2.

**Nelson, M. R. and W. J. Chazin** (1998). "Structures of EF-hand Ca(2+)-binding proteins: diversity in the organization, packing and response to Ca2+ binding." Biometals: An International Journal On The Role Of Metal Ions In Biology, Biochemistry, And Medicine **11**(4): 297-318.

**Palmucci, L., C. Doriguzzi, T. Mongini, G. Restagno, L. Chiado-Piat and M. Maniscalco** (1994). "Unusual expression and very mild course of Xp21 muscular dystrophy (Becker type) in a 60-year-old man with 26 percent deletion of the dystrophin gene." Neurology **44**(3 Pt 1): 541-3.

**Peters, A., S. Palay and H. Webster** (1991). The fine structure of the nervous system. Oxford, New York, Oxford University Press.

**Prokop, A.** (1999). "Integrating bits and pieces – synapse formation in *Drosophila* embryos." Cell Tissue Res. **297**(2): 169-186.

**Prokop, A., S. Bray, E. Harrison and G. M. Technau** (1998). "Homeotic regulation of segment-specific differences in neuroblast numbers and proliferation in the Drosophila central nervous system." Mech Dev **74**(1-2): 99-110.

**Prokop, A., M. Landgraf, E. Rushton, K. Broadie and M. Bate** (1996). "Presynaptic development at the Drosophila neuromuscular junction: assembly and localization of presynaptic active zones." Neuron **17**(4): 617-26.

**Prokop, A., J. Uhler, J. Roote and M. Bate** (1998). "The kakapo mutation affects terminal ignalling n and central dendritic sprouting of Drosophila motorneurons." J Cell Biol **143**(5): 1283-94.

**Prout, M., Z. Damania, J. Soong, D. Fristrom and J. W. Fristrom** (1997). "Autosomal mutations affecting adhesion between wing surfaces in Drosophila melanogaster." Genetics **146**(1): 275-85.

**Rastelli, L., C. S. Chan and V. Pirrotta** (1993). "Related chromosome binding sites for zeste, suppressors of zeste and Polycomb group proteins in Drosophila and their dependence on Enhancer of zeste function." Embo J **12**(4): 1513-22.

**Reuter, J. E., T. M. Nardine, A. Penton, P. Billuart, E. K. Scott, T. Usui, T. Uemura and L. Luo** (2003). "A mosaic genetic screen for genes necessary for Drosophila mushroom body neuronal morphogenesis." Development **130**(6): 1203-13.

**Rigaut, G., A. Shevchenko, B. Rutz, M. Wilm, M. Mann and B. Seraphin** (1999). "A generic protein purification method for protein complex characterization and proteome exploration." Nat Biotechnol **17**(10): 1030-2.

**Rogers, S. L., G. C. Rogers, D. J. Sharp and R. D. Vale** (2002). "Drosophila EB1 is important for proper assembly, dynamics, and positioning of the mitotic spindle." J Cell Biol **158**(5): 873-84.

**Rohrbough, J. and K. Broadie** (2002). "Electrophysiological analysis of synaptic transmission in central neurons of Drosophila larvae." J Neurophysiol **88**(2): 847-60.

**Rohrbough, J., S. Pinto, R. M. Mihalek, T. Tully and K. Broadie** (1999). "latheo, a Drosophila gene involved in learning, regulates functional synaptic plasticity." Neuron **23**(1): 55-70.

**Roper, K. and N. H. Brown** (2003). "Maintaining epithelial integrity: a function for gigantic spectraplakin isoforms in adherens junctions." J Cell Biol **162**(7): 1305-15.

**Roper, K. and N. H. Brown** (2004). "A spectraplakin is enriched on the fusome and organizes microtubules during oocyte specification in Drosophila." Curr Biol **14**(2): 99-110.

**Roper, K., S. L. Gregory and N. H. Brown** (2002). "The 'spectraplakins': cytoskeletal giants with characteristics of both spectrin and plakin families." J Cell Sci **115**(Pt 22): 4215-25.

**Rosenberg, M., J. Meier, A. Triller and C. Vannier** (2001). "Dynamics of glycine receptor insertion in the neuronal plasma membrane." J Neurosci **21**(14): 5036-44.

**Rubin, G. M. and A. C. Spradling** (1982). "Genetic transformation of Drosophila with transposable element vectors." Science **218**(4570): 348-53.

**Ruhrberg, C. and F. M. Watt** (1997). "The plakin family: versatile organizers of cytoskeletal architecture." Curr Opin Genet Dev **7**(3): 392-7.

**Sambrook, J., E. F. Fritsch and T. Maniatis** (1989). "Molecular cloning: a laboratory manual. Cold Spring Harbour, N.Y., Cold Spring Harbour Laboratory."

**Sanchez-Soriano, N., W. Bottenberg, A. Fiala, U. Haessler, A. Kerassoviti, E. Knust, R. Lohr and A. Prokop** (2005). "Are dendrites in Drosophila homologous to vertebrate dendrites?" Dev Biol **288**(1): 126-38.

**Sanchez-Soriano, N. and A. Prokop** (2005). "The influence of pioneer neurons on a growing motor nerve in Drosophila requires the neural cell adhesion molecule homolog FasciclinII." J Neurosci **25**(1): 78-87.

Santamaria, P. (1986). Injecting eggs.. In *Drosophila*: a practical approach. D.B.Roberts. Washington, DC**:** 159-173.

**Sherrington, C.** (1906). The integrative action of the nervous system. New Haven, Yale University Press.

**Slep, K. C., S. L. Rogers, S. L. Elliott, H. Ohkura, P. A. Kolodziej and R. D. Vale** (2005). "Structural determinants for EB1-mediated recruitment of APC and spectraplakins to the microtubule plus end." J Cell Biol **168**(4): 587-98.

**St Johnston, D.** (2002). "The art and design of genetic screens: Drosophila melanogaster." Nat Rev Genet **3**(3): 176-88.

**Stepanova, T., J. Slemmer, C. C. Hoogenraad, G. Lansbergen, B. Dortland, C. I. De Zeeuw, F. Grosveld, G. van Cappellen, A. Akhmanova and N. Galjart** (2003).

"Visualization of Microtubule Growth in Cultured Neurons via the Use of EB3-GFP (End-Binding Protein 3-Green Fluorescent Protein)." J. Neurosci. **23**(7): 2655-2537.

**Stradal, T., W. Kranewitter, S. J. Winder and M. Gimona** (1998). "CH domains revisited." FEBS Lett **431**(2): 134-7.

**Strumpf, D. and T. Volk** (1998). "Kakapo, a novel cytoskeletal-associated protein is essential for the restricted localization of the neuregulin-like factor, vein, at the muscle-tendon junction site." J Cell Biol **143**(5): 1259-70.

**Strynadka, N. C. and M. N. James** (1989). "Crystal structures of the helix-loop-helix calcium-binding proteins." Annual Review Of Biochemistry **58**: 951-998.

**Subramanian, A., A. Prokop, M. Yamamoto, K. Sugimura, T. Uemura, J. Betschinger, J. A. Knoblich and T. Volk** (2003). "Shortstop recruits EB1/APC1 and promotes microtubule assembly at the muscle-tendon junction." Curr Biol **13**(13): 1086-95.

**Sun, D., C. L. Leung and R. K. Liem** (2001). "Characterization of the microtubule binding domain of microtubule actin crosslinking factor (MACF): identification of a novel group of microtubule associated proteins." J Cell Sci **114**(Pt 1): 161-172.

**Suter, D. M. and P. Forscher** (1998). "An emerging link between cytoskeletal dynamics and cell adhesion molecules in growth cone guidance." Curr Opin Neurobiol **8**(1): 106-16.

**Svitkina, T. M., A. B. Verkhovsky and G. G. Borisy** (1996). "Plectin sidearms mediate interaction of intermediate filaments with microtubules and other components of the cytoskeleton." J Cell Biol **135**(4): 991-1007.

**Thomas, J. B., M. J. Bastiani, M. Bate and C. S. Goodman** (1984). "From grasshopper to Drosophila: a common plan for neuronal development." Nature **310**(5974): 203-7.

**Thomas, U., S. Ebitsch, M. Gorczyca, Y. H. Koh, C. D. Hough, D. Woods, E. D. Gundelfinger and V. Budnik** (2000). "Synaptic targeting and localization of discs-large is a stepwise process controlled by different domains of the protein." Curr Biol **10**(18): 1108-17.

**Turner, C. E.** (2000). "Paxillin interactions." J Cell Sci **113 Pt 23**: 4139-40.

**Vactor, D. V., H. Sink, D. Fambrough, R. Tsoo and C. S. Goodman** (1993). "Genes that control neuromuscular specificity in Drosophila." Cell **73**(6): 1137-53.

**Van Troys, M., J. Vandekerckhove and C. Ampe** (1999). "Structural modules in actin-binding proteins: towards a new classification." Biochim Biophys Acta **1448**(3): 323-48.

**Volk, T.** (1999). "Singling out Drosophila tendon cells: a dialogue between two distinct cell types." Trends Genet **15**(11): 448-53.

**Von Bergen, M., S. Barghorn, J. Biernat, E. M. Mandelkow and E. Mandelkow** (2005). "Tau aggregation is driven by a transition from random coil to beta sheet structure." Biochim Biophys Acta **1739**(2-3): 158-66.

**Wagh, D. A., T. M. Rasse, E. Asan, A. Hofbauer, I. Schwenkert, H. Durrbeck, S. Buchner, M. C. Dabauvalle, M. Schmidt, G. Qin, et al.,** (2006). "Bruchpilot, a protein with homology to ELKS/CAST, is required for structural integrity and function of synaptic active zones in Drosophila." Neuron **49**(6): 833-44.

**Walsh, E. P. and N. H. Brown** (1998). "A screen to identify Drosophila genes required for integrin-mediated adhesion." Genetics **150**(2): 791-805.

**Wiche, G.** (1998). "Role of plectin in cytoskeleton organization and dynamics." J Cell Sci **111 ( Pt 17)**: 2477-86.

**Yanagawa, S., J. S. Lee and A. Ishimoto** (1998). "Identification and characterization of a novel line of Drosophila Schneider S2 cells that respond to wingless ignalling." J Biol Chem **273**(48): 32353-9.

**Yang, Y., C. Bauer, G. Strasser, R. Wollman, J. P. Julien and E. Fuchs** (1999). "Integrators of the cytoskeleton that stabilize microtubules." Cell **98**(2): 229-38.

**Yang, Y., J. Dowling, Q. C. Yu, P. Kouklis, D. W. Cleveland and E. Fuchs** (1996). "An essential cytoskeletal linker protein connecting actin microfilaments to intermediate filaments." Cell **86**(4): 655-65.

**Young, K. G., M. Pool and R. Kothary** (2003). "Bpag1 localization to actin filaments and to the nucleus is regulated by its N-terminus." J Cell Sci **116**(Pt 22): 4543-55.

# 8 Abbreviations

| | |
|---|---|
| ABD | Actin binding domain |
| aCC | anterior corner cell |
| ACF7 | Actin and microtubule crosslinking factor 7 |
| AP | alkaline phosphatase |
| APG | Actin Plakin GFP |
| B&B | Broadie and Bate buffer |
| BCIP | 5-bromo-4-chloro-3-indolyl phosphate |
| BPAG1 | Bullous pemphigoid 1 |
| cDNA | complementary DNA |
| CH1 | Calponin homology domain 1 |
| CH2 | Calponin homology domain 2 |
| CIAP | calf intestine alkaline phosphatase |
| CNS | central nervous system |
| DAB | diaminobenzidine |
| ddNTPs | dideoxynucleotides |
| *Df* | deficiency |
| DGRC | *Drosophila* genome research center |
| DNA | deoxyribonucleotide acid |
| DO | dorsal oblique |
| DPxn | *Drosophila* Paxillin |
| dsRNA | double stranded RNA |
| EB1 | End-binding protein 1 |
| eGFP | enhanced green fluorescent protein |
| EGG | EF Gas2 |
| *elaV* | *embryonic lethal, abnormal vision* |
| *eve* | *even skipped* |
| FasII | Fasciclin II |
| GFP | green fluorescent protein |
| GT | TAP-tagged Gas2 homology protein domain of Shot |
| HA | Haemagglutinin |
| HRP | horse radish peroxydase |
| iPCR | Inverse PCR |
| IPTG | isopropyl-B-D-thiogalactoside |
| ISN | intersegmental nerve |
| Kak | Kakapo |
| Kbp | Kilo base pairs |
| kDA | kilo Dalton |
| MACF1 | human microtubule and actin crosslinking factor 1 (formerly ACF7) |
| mACF7 | mouse actin and microtubule crosslinking factor 7 |
| mRFP | Monomeric red fluorescent protein |
| mRNA | messenger RNA |
| MT | Microtubules |
| MTJ | Muscle tendon junction |
| *mys* | *myspheroid* |
| NBT | nitro blue tetrazolium chloride |
| N-CAM | neural cell adhesion molecule |
| NMJ | neuromuscular junction |
| ORF | open reading frame |
| pax | paxillin |
| PBS | phosphate buffered saline |
| PBT | PBS with Tween-20 |
| PCR | polymerase chain reaction |
| PSD | Postsynaptic density |
| PT | Plakin GFP |
| RNA | ribonucleotide acid |
| RNAi | RNA interference |
| sePCR | sePCR |
| Shot | Short stop |
| Syt | synaptotagmin |
| TAE | Tris-Acetate-EDTA buffer |
| *Taq* | *Thermus aquaticus* |
| TBS | Tris buffered saline |
| TE | Tris-EDTA buffer |
| Tris | Tris Hydroxymethylaminoethane |
| Tris | Tris Hydroxymethylaminoethane |
| tub | tubulin |
| UAS | upstream activating site |
| *VUM* | *ventral unpaired median* |

# Versicherungsgemäß §11 Abs. 3d der Promotionsordnung vom 22.12.2002

1) Ich habe die jetzt als Dissertation vorgelegte Arbeit selbst angefertigt und alle benutzten Hilfsmittel (Literatur, Apparaturen, Material) in der Arbeit angegeben.

2) Ich habe und hatte die jetzt als Dissertation vorgelegte Arbeit nicht als Prüfungsarbeit für eine staatliche oder andere wissenschaftliche Prüfung eingereicht.

3) Ich hatte weder die jetzt als Dissertation vorgelegte Arbeit noch Teile einer Abhandlung davon bei einer anderen Fakultät bzw. einem anderen Fachbereich als Dissertation eingereicht.

---

Mainz, den (Wolfgang Bottenberg)

# 9 Published Work related to this thesis

## Publication

Natalia Sánchez-Soriano, **Wolfgang Bottenberg**, André Fiala, Ulrike Haessler, Afroditi Kerassoviti, Elisabeth Knust, Robert Löhr and Andreas Prokop. **"**Are dendrites in *Drosophila* homologous to vertebrate dendrites?". *Dev.Biol*., 2005

## Abstracts (Conferences)

Prokop, A., **Bottenberg, W**., Haessler, U., Küppers-Munther, B., Löhr, R., Sánchez-Soriano, N. (2005) "Compartmentalization of central neurons in *Drosophila* studied by a new transplantation-based mosaic analysis strategy". (Proc. 6th meeting German Neurosci. Soc.)2005

**Bottenberg, W.**, Mende, M., Kolodziej, P., Prokop, A. "Dissecting the role of Short Stop during the de-novo formation of dendrites and neuromuscular terminals in *Drosophila melanogaster*". Intl. Meet. Dros. Neurobiol. (Neuchatel, Sept 4-8), 2004.

Sanchez-Soriano , N., Löhr , R., **Bottenberg,** W., Kerassoviti, A., Knust, E., Fiala, A., Prokop, A. „Dendrites in arthropods? Insights from *Drosophila* motorneurons". Intl. Meet. Dros. Neurobiol. (Neuchatel, Sept 4-8), 2004.

Sánchez-Soriano, N., Küppers-Munther, B., Löhr, R., **Bottenberg, W.**, Landgraf, M., Haessler, U., Prokop, A. (2004) "Exploring the formation of neuro-neuronal synapses in the *Drosophila* embryo". Intl. Meet. Dros. Neurobiol. (Neuchatel, Sept 4-8), 2004.

**Wolfgang Bottenberg**, Barbara Küppers, Johannes Letzkus, Robert Löhr, Natalia Sánchez-Soriano, Andreas Prokop "From the NMJ into the CNS - essential steps towards structural and functional analyses of neuro-neuronal synapses", EDRC (European Drosophila Research Conference) 2003; Göttingen, Germany, 2003.

# 11 Summary

The nervous system is the most complex organ in animals and the ordered interconnection of neurons is an essential prerequisite for normal behaviour. Neuronal connectivity requires controlled neuronal growth and differentiation. Neuronal growth essentially depends on the actin and microtubule cytoskeleton, and it has become increasingly clear, that crosslinking of these cytoskeletal fractions is a crucial regulatory process. The *Drosophila* Spectraplakin family member Short stop (Shot) is such a crosslinker and is crucial for several aspects of neuronal growth. Shot comprises various domains: An actin binding domain, a plakin-like domain, a rod domain, calcium responsive EF-hand motifs, a microtubule binding Gas2 domain, a GSR motif and a C-terminal EB1*aff* domain. Amongst other phenotypes, *shot* mutant animals exhibit severely reduced dendrites and neuromuscular junctions, the subcellular compartmentalisation of the transmembrane protein Fasciclin2 is affected, but it is also crucially required in other tissues, for example for the integrity of tendon cells, specialised epidermal cells which anchor muscles to the body wall. Despite these striking phenotypes, Shot function is little understood, and especially we do not understand how it can carry out functions as diverse as those described above.

To bridge this gap, I capitalised on the genetic possibilities of the model system *Drosophila melanogaster* and carried out a structure-function analysis in different neurodevelopmental contexts and in tendon cells. To this end, I used targeted gene expression of existing and newly generated Shot deletion constructs in *Drosophila* embryos and larvae, analyses of different *shot* mutant alleles, and transfection of Shot constructs into S2 cells or cultured fibroblasts. My analyses reveal that a part of the Shot C-terminus is not essential in the nervous system but in tendon cells where it stabilises microtubules. The precise molecular mechanism underlying this activity is not yet elucidated but, based on the findings presented here, I have developed three alternative testable hypothesis. Thus, either binding of the microtubule plus-end tracking molecule EB1 through an EB1*aff* domain, microtubule-bundling through a GSR rich motif or a combination of both may explain a context-specific requirement of the Shot C-terminus for tendon cell integrity. Furthermore, I find that the calcium binding EF-hand motif in Shot is exclusively required for a subset of neuronal functions of Shot but not in the epidermal tendon cells. These findings pave the way for complementary studies studying the impact of $[Ca^{2+}]$ on Shot function.

Besides these differential requirements of Shot domains I find, that most Shot domains are required in the nervous system and tendon cells alike. Thus the microtubule Gas2 domain shows no context specific requirements and is equally essential in all analysed cellular contexts. Furthermore, I could demonstrate a partial requirement of the large spectrin-repeat rod domain of Shot in neuronal and epidermal contexts. I demonstrate that this domain is partially required in processes involving growth and/or tissue stability but dispensable for cellular processes where no mechanical stress resistance is required. In addition, I demonstrate that the CH1 domain a part of the N-terminal actin binding domain of Shot is only partially required for all analysed contexts.

Thus, I conclude that Shot domains are functioning different in various cellular environments. In addition my study lays the base for future projects, such as the elucidation of Shot function in growth cones. Given the high degree of conservation between Shot and its mammalian orthologues MACF1/ACF7 and BPAG1, I believe that the findings presented in this study will contribute to the general understanding of spectraplakins across species borders.